The role of RAD16 and elongin A/C homologs in *Arabidopsis* UV tolerance and growth

by

Linda Alrayes

A thesis submitted to the Faculty of Graduate Studies of

The University of Manitoba

in partial fulfillment of the requirements of the degree of

DOCTOR OF PHILOSOPHY

Department of Biological Sciences

University of Manitoba

Winnipeg

Abstract

UV-B and UV-C can damage DNA by generating DNA photoproducts such as cyclobutane pyrimidine dimers (CPDs), pyrimidine 6-4 pyrimidone (6-4 PPs) and its Dewar isomers (Dewar PP). These DNA photoproducts inhibit DNA transcription and replication, and cause mutations. Thus, DNA photoproducts must be repaired. Plants use two different mechanisms to repair these DNA photoproducts: light-dependent repair via photolyase and light-independent repair via nucleotide excision repair (NER). The NER mechanism in plants is similar to that elucidated in yeast and mammalian models. In yeast systems, the global genomic NER (GG-NER) damage recognition complex RAD7/RAD16/ELOC/ CUL3 recognizes the damaged DNA in the non-transcribed regions of the genome. The mammalian Elongin A/B/C/CUL5 /RBX2 and the yeast Elongin A/C/CUL3/RBX1 complexes target the large subunit of the lesion stalled RNAPII on the transcribed strand for ubiqitination and degradation. *Arabidopsis* has two RAD16 homologs: *AtRAD16* and *AtRAD16b*. In this thesis, I characterized the role of *AtRAD16* and *AtRAD16b* in plant UV tolerance and growth using loss of function and gain of function analysis. *Atrad16* and *Atrad16b* null mutants exhibited increased UV sensitivity, early flowering time and short silique length. *AtRAD16* overexpression increased UV resistance, and YFP-tagged RAD16 is localized in the nucleus. In addition, AtRAD16 physically interacts with AtRAD7, all these results indicate that the role of AtRAD16 in GG-NER is conserved with its yeast counterpart. I also identified *Arabidopsis* ELOA homolog, ELOA, and characterized the role of both *Arabidopsis* ELOA and ELOC homologs in plant UV tolerance and growth. *Ateloa* and *Ateloc* null mutants exhibited increased UV sensitivity in seedlings and adult plants. AtELOA was found to physically and genetically interact with AtELOC. AtELOA is nuclear localized, whereas AtELOC localized in the nuclei and the cytosol. ELOA overexpression increases hypocotyl UV resistance and ELOA/ELOC overexpression increases the silique length and seed number. Thus, *Arabidopsis* RAD16, ELOA, and ELOC are implicated in UV tolerance and development.

Acknowledgments

I would like to express my sincere gratitude to the late Dr. Schroeder for her help and dedicated support during my PhD study. Working under her supervision was a fantastic learning experience. I always enjoyed working with her and learned a lot through it. Dr. Schroeder was a constant source of encouragement, and she was always willing to help. She provided me with insightful suggestions and comments, even while she was battling cancer. I would also like to thank my advisor, Dr. Stout, for his assistance and help during my research and writing process. Without Dr. Stout's help, I would not have been able to complete this work. I am also most grateful to my advisory committee members Dr. Renault and Dr. Ayele for their guidance and support.

I would like to thank and acknowledge Dr. Marcus for his continuous help and unconditional support during all the stages of my PhD study. I would like to extend my thanks to Dr. Court for letting me use her lab and equipment, as well as Ravinder Sidhu for assisting me with microscopic imaging. I would like to thank Dr. Schroeder's students who worked with us during the summer: Haya Izhar for helping me with some lab duties, Adam Carter and Ashley Bell for doing some of the research experiments.

Thank you to the University of Manitoba for providing financial assistance in the form of a Faculty of Science Scholarship, an International Graduate Student Scholarship, Graduate Enhancement of Tri-Council Stipends (GETS), and Dalgarno Graduate Fellowship. I would also like to extend my thanks to the dedicated office staff workers at the Department of Biological Sciences for their help.

Special thanks to you my beloved kids Ghassan, Yazan, Dana, and Danny for tolerating my long hours of work at the lab and my absence from many of your activities. Your love motivates me and provides me with the strength to continue forward in life and deal with difficult situations positively. I would also like to express my gratitude to my spouse Salem for bearing with me throughout this long process. Thank you for your love and support. Finally, I would like to thank my parents, Mr. Naem Shawahneh and Mrs. Zarifa Shawahneh, who always encourage me to pursue my dreams.

Dedication

This work is dedicated to my beloved family; Salem, Ghassan, Yazan, Dana, and Danny, my source of strength and inspiration. I love you to the moon and back.

List of Abbreviations

6-4 PPs	Pyrimidine 6-4 pyrimidone photoproducts
ABF1	Autonomously replicating sequence-binding factor 1
BER	Bear excision repair
CEN	Centrin
CNS	The COP9 signalosome
Col	*Arabidopsis thaliana* Ecotype Columbia
CPDs	Cyclobutane pyrimidine dimers
CSA/B	Cockayne syndrome A and B
CUL	Cullin
DAPI	4′,6-diamidino-2-phenylindole
DDB1/2	Damaged DNA binding protein 1 and 2
Dewar PP	Dewar isomers
DIC	Differential interference contrast
DSB	Double strand break
DSBR	Double strand break repair
DWD	DDB I -binding WD40 proteìn
ELOA	Elongin A
ELOB	Elongin B
ELOC	Elongin C
GG-NER	Global genomic nucleotide excision repair
h	Hours
HMGN1	High mobility group nucleosome-binding domain-containing protein 1
HR	Homologous recombination
IR	Ionizing radiation
J. m^{-2}	Joule per square meter
MFD	Mutation Frequency Decline protein
min	Minutes

MMR	Mismatch repair
MS medium	Murashige and Skooog medium
NER	Nucleotide excision repair
NHEJ	Nonhomologous end-joining
PCNA	proliferating cell nuclear antigen
PCR	Polymerase chain reaction
POL	DNA polymerase
RAD	Radiation sensitive
RBX	Ring-box protein
RNAi	RNA interference
RNAP	RNA polymerase
ROS	Reactive oxygen species
RPA	Recruitment protein A
SE	Standard error
SOCS	Suppressor of Cytokine Signaling
SSB	Single strand break
TC-NER	Transcription coupled nucleotide excision repair
T-DNA	Transferred DNA
UV	Ultraviolet radiation
UV-B	Ultraviolet class B
UV-C	Ultraviolet class C
uvh	UV-hypersensitivity
VHL	Von Hippel-Lindau tumor suppressor
XP	Xeroderma pigmentosum
YFP	Yellow fluorescence protein

Table of contents

List of Figures

List of Tables

Chapter 1. Literature Review

1.1 Introduction

Natural sunlight is the main source of light and energy for living organisms. It also enhances the production of vitamin D, which is required to maintain calcium homeostasis in humans (Wacker & Holick 2013). However, sunlight is also a source of harmful radiation such as gamma rays, X-rays, and ultraviolet rays. Gamma rays and X-rays are ionizing radiation (IR) with highly energetic photons. In contrast, UV-rays are less energetic, and most UV-rays are not ionizing. Harmful UV radiation represents the most common danger that most living beings are exposed to consistently. Excessive exposure to UV radiation causes various harmful effects on all living organisms including prokaryotic bacteria, fungi, plants, and mammals (Strzałka et al. 2020). UV radiation is divided into three main types: UVC (100-280 nm), UVB (280-315 nm), and UVA (315- 400 nm). UVC has the highest energy; therefore, its effects on living systems are extremely dangerous. UVB has a wide range of negative effects on living organisms. Whereas UVA is the least energetic and thus imposes the least risk of damage (Banaś et al. 2020).

The stratospheric ozone layer protects Earth from UV radiation. All the incoming UVC radiation is filtered out by the stratospheric ozone layer, so it does not reach the Earth's surface. However, most UVA and some UVB are transmitted through the ozone layer and reach Earth's surface (Yagura 2011). Between these two UV wavelengths that reach Earth's surface, UVB represents the highest threat to living systems due to it possessing the highest energy of daylight spectrum. UV radiation can cause a variety of damaging effects to many biological macromolecules, including proteins, lipids, and DNA. Cellular DNA is affected the most by UV radiation (Schuch et al. 2017). The damaging effects of UVB radiation on cellular DNA are extremely dangerous as DNA absorbs UVB directly and this causes direct excitation of DNA molecule resulting in the formation of cyclobutane pyrimidine dimers (CPDs) and pyrimidine 6-4 pyrimidone (6-4 PPs; Cadet & Douki 2018). In contrast, DNA does not directly absorb UVA and thus UVA does not directly damage DNA. Instead, UVA excites non-DNA chromophores, producing reactive oxygen species (ROS) that can interact with DNA and cause DNA

damage (Sinha & Häder 2002). Both direct and indirect UV- induced DNA damage impairs genome stability and causes deleterious effects on all living organisms ranging from prokaryotes to higher eukaryotes.

To protect cellular DNA from UV radiation, living organisms produce UV-absorbing pigments. However, because these UV-absorbing pigments cannot completely protect native DNA from UV-induced damage there was strong selective pressure on all living systems ranging from bacteria to humans to protect and repair DNA. Thus, various DNA repair mechanisms including light-dependent repair (known as photoreactivation or light repair), light-independent repair (known as dark repair), double and single strand break repair, mismatch repair, and other repair mechanisms have arisen throughout evolution. These DNA repair mechanisms efficiently remove lesions and repair damaged DNA (Sinha & Häder 2002; Rastogi et al. 2010).

The release of ozone-depleting substances such as chlorofluorocarbons (CFCs) and halons led to a depletion of the ozone layer. Ozone layer depletion together with climate change and anthropogenic activities results in more UV-B radiation reaching the earth's surface. Thus, understanding the damaging effects of UV radiation on living systems and the mechanisms that organisms use to repair UV-damaged DNA and maintain genomic integrity is much more important today than ever before (Dotto & Casati 2017). In this review, I discuss various types DNA lesions including the UV-induced DNA photoproducts and the related repair mechanisms in different evolutionary branches.

1.2 DNA Damage

DNA damage can occur spontaneously or as a consequence of induced environmental mutagenesis (Chatterjee & Walker 2017). Both spontaneous and environmental DNA damage has a direct impact on genome integrity and is a key factor in developing mutations, cancers, and triggering programmed cell death. Spontaneous DNA damage arises during endogenous cellular processes such as DNA metabolism and replication (Papamichos & Peterson 2013), whereas environmental DNA damage occurs when the genomes of living organisms are exposed to various chemical and/or physical agents such as ionizing radiation, UV radiation, alkylating agents, or toxicants

(Tuteja et al. 2001; Yousefzadeh et al. 2021). DNA damaging agents produce different types of DNA lesions. These DNA lesions include mismatched bases, single-strand breaks (SSBs), double strand breaks (DSBs), protein-protein cross links, protein-DNA cross links, and UV photoproducts such as CPDs and 6-4 PPs (Cagney et al. 2006; Jackson & Bartek 2009). The toxic and or mutagenic effects of these lesions on the cell vary depending on the nature of the lesion.

1.2.1 UV-induced DNA photoproducts

Excessive exposure to UV radiation causes indirect and direct damage to cellular DNA. UVA can cause indirect DNA damage through the absorption of UVA by non-DNA chromophores such as quinones and riboflavin. This generates ROS that can damage DNA molecules indirectly by generating mutations in DNA bases (Brem & Karran 2012). One of the most prevalent lesions caused by ROS is 8-oxoguanine (8-oxoG) lesion that hinders guanine-cytosine pairing and causes G-T transversion (Tubbs & Nussenzweig 2017). In addition, UVA-induced ROS may also cause single and double-strand breaks (Johann To Berens & Molinier 2020; Schuch et al. 2017).

Direct DNA damage occurs when a DNA molecule directly absorbs UVB or UVC radiation. Absorption of either UVB or UVC by a DNA molecule results in photo transformation in the DNA molecule that generates photoproducts through the formation of covalent bonds between two neighboring pyrimidines within a DNA strand. There are two main classes of DNA photoproducts: CPDs and 6-4 PPs (Figure 1.1). CPDs are a four-member cyclic structure that involves C5 and C6 of the neighboring pyrimidine bases, whereas in 6-4 PPs a non-cyclic bond is formed between C6 at the 5’ and C4 at 3’ of the neighbor pyrimidines (Rastogi et al. 2010; Yagura et al. 2011). CPDs and 6-4 PPs constitute around 75% and 25% of the total UV-induced DNA lesions, respectively (Pathak et al. 2019). While CPDs are stable photoproducts, 6-4 PPS are not stable, and they convert to 6-4pp Dewar isomers upon further irradiation with UVA or UVB (Figure 1.1). As a result, a considerable portion of 6-4PPs are projected to be in their Dewar isomers (Dewar PP) under normal conditions (Taylor 1995; Weber 2005).

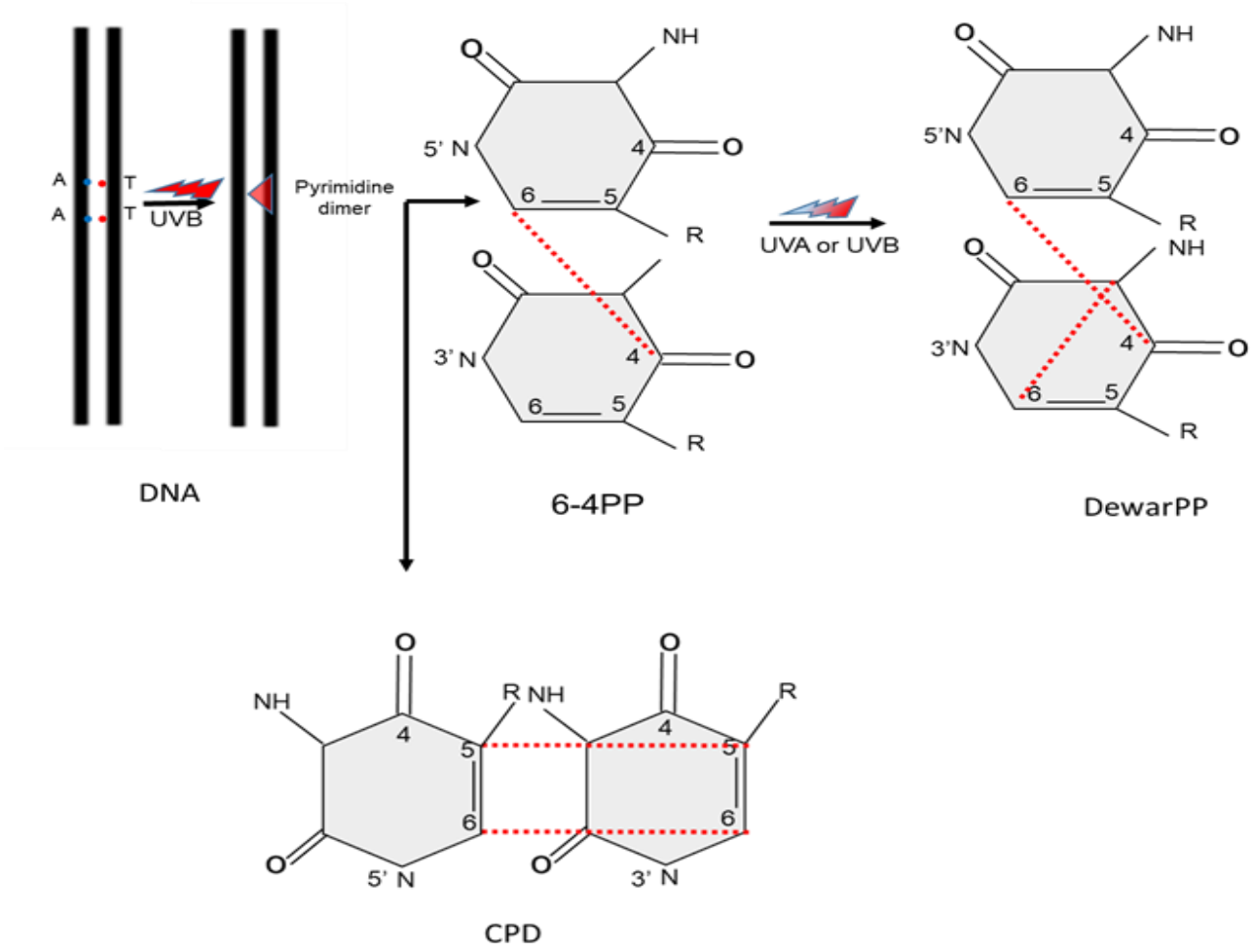

Figure 1.1 UV induced pyrmidine dimers

Cyclobutane pyrimidine dimers (CDP), pyrimidine 6-4 pyrimidone (6-4 PPs), and 6-4PP Dewar isomers (DewarPP)

The type of DNA photoproducts induced by UV radiation is determined by the structure and the sequence of the DNA (Rastogi et al. 2010; Sinha & Häder 2002). For example, CPDs are rarely formed when DNA bends toward small grooves, but they form at a high quantity at the flexible ends of poly (dA)-(dT) and in single -stranded DNA (Rastogi et al. 2010; Sinha & Häder 2002). In contrast, 6-4PPs are formed preferentially where the DNA is twisted (Rastogi et al. 2010). Both CPDs and 6-4PPs distort the DNA helical structure by inducing bends of 9^{o} and 44^{o} respectively (Kim & Choi 1995).

The biological effects of CPDs and 6-4PPs have been thoroughly investigated in many living systems including microorganisms and mammals (Schuch et al. 2017; Yasui et al. 1998). Pyrimidine dimers were found to block DNA transcription and replication through inhibiting DNA and/or RNA polymerases' progress; they were also found to cause mutations if transcription continues past the dimer's area (Brégeon & Doetsch 2011). Accumulation of these DNA photoproducts can lead to cell death (De Zio et al. 2013). Therefore, the repair of DNA photoproducts is crucial.

1.3 DNA Repair Mechanisms

Maintaining genomic integrity is essential for precise DNA transcription and replication as well as for organism survival. To maintain genomic integrity, living systems evolved various DNA repair mechanisms to counteract and repair spontaneous and environmental DNA damage. In the following section, I will introduce some of the DNA repair mechanisms that living systems utilize to repair spontaneous and indirectly UV-induced DNA damage such as mismatch repair (MMR), base excision repair (BER), and recombination repair. Then, I will focus specifically on the two main mechanisms that living organisms utilize to repair CPD and 6-4 PP photoproducts: photoreactivation, and nucleotide excision repair (NER; Giglia-Mari & Vermeulen 2011).

1.3.1 DNA mismatch repair

DNA mismatch repair (MMR) is an important repair pathway that is responsible for maintaining genome integrity in Archaea, Bacteria, and Eukarya. MMR is an important post-replicative repair pathway that is responsible for correcting mismatched bases and insertion/deletion loop (IDL) mispairs that occur because of DNA replication

errors (Elez 2021). The MMR system corrects the mismatched bases incorporated in the newly synthesized DNA strand by recognizing, excising, and replacing them with the correct bases. MMR mechanism is conserved in nearly all living beings, with the exception of Mollicutes and Actinobacteria, and many archaea (Elez 2021; Sachadyn 2010).

The genetic and molecular basis of *Escherichia coli* (*E. coli)* MMR pathway has been well studied and characterized. Therefore, *E. coli* MMR is a useful model for understanding both eukaryotic and prokaryotic MMR (Li 2008). The *E. coli* MMR system requires three key proteins: MutS, MutL, and MutH (Elez 2021). MMR is initiated when the mismatch recognition protein (MutS) detects and binds to either a mismatched base or an IDL (Elez 2021). MutL physically interacts with the MutS-DNA and enhances mismatch recognition. Then MutL binds to MutH and activates MutH restriction endonuclease activity, which in turn facilitates the incision of the error-containing DNA. This in turn facilitates the recruitment of complex repair components to the error-containing DNA. Helicases and exonucleases remove the error-containing strand. Finally, DNA polymerase and DNA ligase complete the DNA synthesis and repair by filling the gap and sealing the nick (Elez 2021).

Defects in MMR mechanism increase mutation rate and result in genome instability. For example, inactivation of MMR in humans causes sporadic and hereditary cancers and confers resistance to some chemotherapeutic agents (Elez 2021). Similarly, inactivation of MMR core protein in plants results in altered expression of important cell cycle genes following DNA damage. MutS and MutL exist in most bacteria, and well-conserved MutS homologs MutSα (MSH2/MSH6) and MutSβ (MSH2/MSH3) and MutL homologs MutLα (MLH1/PMS2) have been identified in eukaryotes (Fukui 2010). MutLα is required for the restriction endonuclease activity (Fishel 2015; Fukui 2010). However, most bacteria and eukaryotes lack *E. coli* MutH homologs (Fishel 2015; Fukui 2010). In contrast, no homologs of *E. coli* MutS and MutL have been identified in most archaea. However, homologs of both MutS and MutL, have been found in some halophilic archaea but mutational studies showed that these two proteins are not required for maintaining a low incidence mutation (Busch & DiRuggiero 2010), suggesting that the MMR pathway in archaea does not follow the conserved

MMR identified in prokaryotes and eukaryotes. Similarly, all cyanobacteria possess MutS homologs and lack MutH homologs, whereas only some cyanobacteria strains possess MutL homologs (Cassier-Chauvat et al. 2016).

1.3.2 Base excision repair

Base excision repair (BER) pathway protects the cell from mutations and cell death by correcting DNA lesions including methylated, alkylated, deaminated, oxidized, and incorrect bases arising from exogenous agents, intracellular metabolism, or by ROS generated by UV radiation (Bennett & Demple 2013; Rastogi et al. 2010). BER also has the ability to repair DNA single-strand break (SSBs). There are two forms of BER, short patch BER (SP-BER) and long patch BER (LP-BER). SP-NER has the ability to repair one damaged nucleotide, whereas LP-NER can repair up to 13 nucleotides (Pathak et al. 2019; Roldán-Arjona et al. 2019).

BER is a conserved repair pathway that exists in all three domains of life. It involves five major steps. Starting with recognition and removal of the affected base by DNA glycosylases to generate an apurinic or apyrimidinic (AP) site with the sugar-phosphate backbone intact. Different evolutionary branches evolved a variety of different DNA glycosylases that are responsible for recognizing and removing different types of modified bases. These DNA glycosylases are classified into five structural superfamilies. Uracil DNA glycosylase (UDG) is the first superfamily, and it targets uracil base and removes it from the DNA strand. UDG includes six different families that exist in prokaryotes and eukaryotes. For example, *E. coli* Ung represents the first UDG family, homologs of *E. coli* Ung exist in humans, plants, and the yeast *S. cerevisiae*. UDG second family is represented by *E. coli* Mug and human TDG, while the third UDG family is represented by vertebrate SMUG1, and the last two families exist only in thermophiles bacteria and Archaea (Roldán-Arjona et al. 2019; Schormann et al. 2014). The second DNA glycosylase superfamily is alkyladenine DNA glycosylase (AAG), members of this superfamily are responsible for recognizing and removing alkylated purines and ethanopurines. AAG genes exist in plants and mammals (Roldán-Arjona et al. 2019). The third superfamily is the helix-hairpin–helix (HhH-GPD), and enzymes in this superfamily recognize and remove lesions generated by oxidation, hydrolytic or

alkylation damage. Genes of HhH-GPD exist in plants, yeast, mammals, and *E. coli* (Huffman et al. 2005; Roldán-Arjona et al. 2019). The helix–two-turn–helix (H2TH) is the fourth DNA glycosylase superfamily. Members of H2TH recognize and remove oxidized bases and damaged pyrimidines, genes of this superfamily exist in prokaryotes, mammals, and plants (Huffman et al. 2005; Roldán-Arjona et al. 2019). The last superfamily of DNA glycosylase is the HEAT-like repeat (HLR). Members of this superfamily exist only in prokaryotes, and they are responsible for recognizing and removing alkylated bases (Dalhus et al. 2009; Roldán-Arjona et al. 2019). DNA glycosylases are either monofunctional or bifunctional. Monofunctional DNA glycosylases have only glycosylase activity, whereas bifunctional DNA glycosylases possess an additional activity that breaks the phosphodiester backbone generating a single-strand break (Fortini et al. 1999).

The second step after creating the AP site by DNA glycosylases is the AP site incision by AP endonucleases or AP lyase. In humans, there are two types of AP endonucleases named APE1 and APE2. Orthologs of human AP endonucleases exist in prokaryotes and eukaryotes. For example, Apn2p, Xth, are the human APE1 orthologs in *S. cerevisiae*, *E. coli*, respectively, and APR, APE1L are the two *Arabidopsis* orthologs of human APE1 (Roldán-Arjona et al. 2019). The third step is the removal of the AP site by phosphodiesterase or lyase. The fourth and fifth steps are the DNA synthesis by a DNA polymerase and nick sealing by ligases including Lig1, Lig III, and XRCC1. Homologs of DNA polymerase and ligase exist in prokaryotes and eukaryotes including *S. cerevisiae*, *E. coli*, and *Arabidopsis* (Corfield (invalid date); Kim & Wilson 2012; Roldán-Arjona et al. 2019). Homologs of *E. coli* BER pathway genes were also found in cyanobacteria, suggesting that BER pathway exists in cyanobacteria (Pathak et al. 2019).

BER mechanism is important to maintain genome stability, thus preventing death, premature aging, and diseases such as cancer. Defects in BER proteins can cause cancer in humans, a short life cycle in yeast, embryo lethality in mice, and seed abortion in *Arabidopsis* (Grundy & Parsons 2020; Maclean et al. 2003; Murphy et al. 2009; Xanthoudakis et al. 1996).

1.3.3 Double strand break repair (DSBR) mechanisms

DNA double-stranded breaks (DSBs) result from a plethora of exogenous and endogenous DNA damaging agents including IR, radiomimetic chemicals, ROS generated by metabolic reactions, or replication-related errors (Ayora et al. 2011; Cromie et al. 2001; Shen & Nickoloff 2007). DSBs are the most deleterious DNA lesions because they can result in cellular death, mutagenesis, transcription and replication arrest that may induce apoptosis; thus, DSB repair is essential (Cox 2013). To avoid the cytotoxic and mutagenic effects of DSBs, living organisms evolved two main mechanisms that effectively detect and repair DSB damage: homologous recombination (HR) and nonhomologous end-joining (NHEJ; Featherstone & Jackson 1999; Shrivastav et al. 2008). In humans, defective responses to DSBs result in cancer predisposition, immunodeficiency, altered neurological functions, Ataxia-Telangiectasia (AT), and Nijmegen Breakage Syndrome (NBS; Sharma et al. 2020).

1.3.3.1 Homologous recombination (HR) repair

HR uses the undamaged sister chromatid or homologous chromosome as a template for DNA polymerase to accurately repair the damaged DNA, therefore HR is an error-free repair pathway (Darmon et al. 2014; McKinnon & Caldecott 2007). HR is a multistep repair pathway that is highly conserved throughout evolution. The biochemical and genetic factors of HR are well understood in *E. coli*, therefore *E. coli* HR is a valuable framework for understanding HR (Cromie 2001). *E. coli* HR pathway starts with creating a 5'-3' cut, this step is carried out by RecBCD enzyme. Humans and *S. cerevisiae* do not possess homologs of *E. coli* RecBCD, so this step is carried out by hMRN (Mre11/Rad50/Nbs1) and scMRX (Mre11/Rad50/ XrS2) complexes (Cromie et al. 2001). After creating the 3' single strand overhang, homology search and strand exchange are performed by RecA protein in *E. coli* and RAD51 in humans and *S. cerevisiae*. Finally, *E. coli* RecG and RuvABC proteins facilitate strand invasion and recombination, both RAD52 and RAD54 proteins regulate this step in humans and *S. cerevisiae* (Cromie et al. 2001). Genetic analysis shows that plants have orthologues of yeast and human HR proteins. The HR pathway is also conserved in archaea; archaea have homologs of eukaryotic HR repair proteins Mre11 and Rad50. Archaea also have

unique archaeal HR repair proteins such as Hjc, NurA and HerA (Marshall & Santangelo 2020; White 2011). In cyanobacteria, RecA and RecG proteins are highly conserved, whereas RecBCD proteins are less conserved, and in some strains, RecB and RecC are replaced by AddA and AddB, respectively (Cassier-Chauvat et al. 2016). The mammalian MRN complex is not only involved in HR response, but is also required for NHEJ, telomere repair, and cell cycle checkpoint activation (Niida & Nakanishi 2006).

In humans, a *mre11* hypomorphic mutation causes ataxia telangiectasia-like disorder (ATLD; Fernet et al. 2005), and hypomorphic mutation in the *NBS1* gene causes Nijmegen breakage syndrome (NBS; Ciapponi et al. 2006; Seemanová et al. 2006). Loss of function mutations of genes encoding the MRN complex result in early lethality in vertebrates (Ciapponi et al. 2006). In budding yeast, defects in either RAD51 or RAD54 proteins result in DNA damage sensitivities (Pâques & Haber 1999). Similarly, *Arabidopsis MRE11* and *RAD50* genes are critical for DSB repair, and inactivation of either gene results in hypersensitivity to DSB damage (Bundock & Hooykaas 2002; Gallego et al. 2001; Manova & Gruszka 2015). In bacteria, inactivation of either RecBCD or AddAB enzyme increases DNA damage sensitivity and decreases viability (Dillingham & Kowalczykowski 2008).

1.3.3.2 Nonhomologous end-joining (NHEJ) repair

In contrast to the error-free DSB repair pathway (HR), NHEJ is an error-prone repair mechanism that can repair DSB. NHEJ repairs DSB by ligating the two DNA broken ends together without the use of a homologous template (Davis & Chen 2013; Cromie et al. 2001). NHEJ repair pathway was initially studied in mammalian systems, and two major protein complexes - the DNA-dependent protein kinase complex (DNA-PK) and the DNA ligase IV / XRCC4 complex - were found to be required to rejoin the non-compatible broken DNA ends (Cromie et al. 2001). In the beginning, the DSB is recognized by the 70/80 heterodimer, which attaches to the DSB. After that, Ku facilitates the recruitment of DNA-PKs to the DNA ends. The DNA-PKs play an important role in holding the DNA ends and making them accessible to DNA ligase. Finally, the DNA ligase IV/ XRCC4 complex carries on the DNA ligation (Davis & Chen 2013; Strzałka et al. 2020; Weterings & Chen 2007).

The NHEJ core proteins have been identified in many living systems ranging from bacteria to yeast to humans, suggesting the existence of a conserved NHEJ repair process throughout evolution (Dudásová et al. 2004). For example, in the yeast *S. cerevisiae,* homologues of KU70/80, and DNA ligase IV/ Xrcc4, Hdf1/Hdf2, and Lig4/Lif1, have been identified. The structures and the functions of NHEJ core components in yeast appeared to be highly conserved (Cromie et al. 2001; Dudásová et al. 2004). Similarly, in *Arabidopsis*, homologs of Ku70, Ku80, XRCC4, and LIG IV have been also characterized, and biochemical analysis showed that *Arabidopsis* Ku70/80 forms a complex with DNA (Tamura et al. 2002). Moreover, expression analysis showed upregulated expression of the *Arabidopsis* homologs in the presence of DSBs, suggesting the involvement of these genes in DSB repair (Strzałka et al. 2020; Tamura et al. 2002; West et al. 2000; West et al. 2002). Plants also possess another NHEJ repair pathway known as bNHEJ that requires AtLIG1, AtWEX, AtXRCC1, and AtKu70. The involvement of these genes in DSB repair was proved experimentally (Charbonnel et al. 2010; Li et al. 2005; Strzałka et al. 2020). No *Arabidopsis* homologs of mammalian DNA-PKs have been identified yet (Strzałka et al. 2020).

In prokaryotes, homologues of eukaryotic DNA-PKs have been identified in some bacterial species, suggesting that NHEJ pathway exists in bacteria. NHEJ repair pathway was found to function in *B. subtilis*, where Ku protein and LigD are required for damage recognition and rejoining the broken ends (Ayora et al. 2011; Cassier-Chauvat et al. 2016; Cromie et al. 2001). Similarly, in some archaeal species, NHEJ pathway depends on Ku for damage recognition and exonuclease for DNA repair, however, the proteins involved in NHEJ in several archaeal clades were not defined yet (Marshall & Santangelo 2020).

NHEJ repair is critical for maintaining genomic integrity; mutations in NHEJ factors have been studied in mice. For example, cells deficient in DNA-PKs exhibit a sensitive phenotype to DNA damaging agents, genome instability, and chromosomal abnormalities (Matsumoto et al. 2021). Deficiencies in Ku70 or Ku80 negatively affect embryonic neuron development, increase premature cell death, and result in increased susceptibility to DSB-inducing agents (Gu et al. 2000). In humans, DNA-PKs missense mutation causes radiosensitive T-B- severe combined immunodeficiency (RS-SCID; van

der Burg et al. 2009). In *S. cerevisiae*, *hdf2* and *hdf1* single loss of function mutants showed increased sensitivity to DSBs damaging agents such as Bleomycin and methyl methanesulfonate (Feldmann et al. 1996). Similarly, *Arabidopsis ku80* loss of function mutant showed a hypersensitive phenotype to DSB damaging agents such as bleomycin and menadione (West et al. 2002). In *B. subtilis*, inactivation of the *Ku* gene results in slight sensitivity to DNA double strand break-inducing agents (Ayora et al. 2011).

1.3.4 Photoreactivation-light repair

Photoreactivation is a light-dependent repair process that is catalyzed by photolyase. Photolyase repairs UV-induced lesions, CPDs and 6-4PPs, by directly binding to them and converting them back to monomers using blue-light as a source of energy (Marizcurrena et al. 2020; Strzałka et al. 2020). Photolyase is substrate-specific; thus, photolyases are classified as CPD photolyase that repairs CPDs and 6-4 photolyase that repairs 6-4PPs (Marizcurrena et al. 2020). CPD photolyase is found in different kinds of living organisms including bacteria, archaea, fungi, plants, as well as some mammals (Rastogi et al. 2010). 6-4 photolyase is found only in specific organisms such as silkworm, *Xenopus laevis*, Drosophila, rattlesnakes, and plants, but it is absent in both yeast and *E. coli* (Rastogi et al. 2010; Sinha & Häder 2002; Thoma 1999). Placental mammals such as humans seem to lack photolyases (Todo 1999). However, many previous studies identified a human homolog that shares a 40% amino acid identity to Drosophila 6-4 photolyase, but the role of this putative human photolyase in photorepair process has not yet been identified (Hsu et al. 1996; Todo 1999). Thus, the repair of CPD and 6-4PPs in placental mammals is catalyzed by another repair mechanism known as dark repair or NER.

Photolyases are monomeric Flavin dependent (FAD) enzymes with (420-616) amino acid residues and a molecular weight ranging from 46 to 66 KDa, depending on the organism (Essen & Klar 2006). These enzymes consist of two co-factors, the photocatalyst, and the light-harvesting cofactors. In *Arabidopsis*, CPDs and 6-4PPs are repaired by CDP and 6-4 photolyases, respectively. To repair CPDs, the light-harvesting co-factor collects energy by absorbing the photoreactivating blue light photon, and then

this excitation energy is transferred to FAD to generate FADH. The reduced FADH co-factor then converts the CPD into monomeric bases by transferring the energy to CPD in the form of electrons, thus breaking the bonds between C5-C5 and C6-C6 in the cyclobutane dimer (Johann To Berens & Molinier, 2020; Kavakli et al. 2019; Kao et al. 2005). In contrast to the simple repair process of CPD photoproducts operating by CPD photolyases, the repair of 6-4 photoproducts using 6-4 photolyases appears to be more complex. Since the repair of 6-4 photoproducts requires converting the dimer to the oxetane intermediate first, then the oxetane intermediate is converted to monomeric pyrmidines by subsequent electron donation (Todo 1999).

1.3.5 Nucleotide Excision Repair (NER)-dark repair

In contrast to light-dependent repair, NER is a light-independent repair method that removes many types of lesions including CPD and 6-4 photoproducts. This process exists in many organisms including placental mammals. NER is a multistep enzymatic process that uses many proteins to recognize and remove DNA lesions. It involves five sequential steps: lesion recognition, double helix unwinding, dual incision and excision of the damaged DNA, gap filling by DNA polymerases, and finally ligation (Schuch et al. 2017). In eukaryotic systems, NER is highly conserved, and it uses around 30 different proteins to complete the repair (Table1.1). In prokaryotes, the biochemical mechanism of NER is similar to the eukaryotic NER mechanism. However, the number and nature of NER proteins used by prokaryotic systems are widely different from those used by eukaryotic organisms (Table S1.2; Rastogi et al. 2010).

In humans, mutations of NER genes result in clinical diseases, such as Xeroderma pigmentosum (XP), Cockayne syndrome (CS), Trichothiodystrophy (TTD), and Cerebro-oculo-facio-skeletal syndrome (COFS; Kobaisi et al. 2019). XPs patients are divided into eight complementation groups: XP (A-G), as well as XP variant. Each group is linked to an inherited defect in a specific gene involved in NER pathway. XP patients exhibit extreme skin sensitivity to UV light, which in turn results in hyperpigmentation and increased skin cancer risk. XP also increases the risk of developing neurological disorders and internal tumors, as well as premature skin aging arising from the accumulation of DNA lesions (Petruseva et al. 2014; Yu & Lee 2017).

Whereas CS and TTD patients are more prone to develop neurological disorders, but they do not have an elevated risk of cancers. CS is classified into two complementation groups, CSA and CSB. CSA and CSB are associated with defects in NER-related genes known as CSA, and CSB, respectively (Reid-Bayliss et al. 2016; Yu & Lee 2017). Mutations in NER-related genes also result in UV hypersensitivity in *Arabidopsis thaliana*, and radiation sensitivity in the yeast *S. cerevisiae* (Lahari et al. 2018; Liu et al. 2003; Rastogi et al. 2010).

NER operates via two sub-pathways: global genomic repair (GG-NER) which repairs damage in non-transcribed DNA strands across the entire genome, and transcription-coupled repair (TC-NER) which removes lesions from the transcriptionally active DNA (Kobaisi et al. 2019). GG-NER and TC-NER have two different damage recognition mechanisms, followed by the common core NER machinery. The TC-NER process is a specific repair process that recognizes the stalled RNA polymerase at the damaged site, thus it repairs the damage more rapidly than the nonspecific GG-NER process (Duan et al. 2020; Spivak 2015).

1.3.5.1 Eukaryotic GG-NER

In mammals, the GG-NER damage recognition factors UV-DDB (UV Damaged DNA Binding protein) complex and the Xeroderma pigmentosum complementation group C (XPC) complex work cooperatively to recognize UV-photoproducts. Following DNA damage, the UV-DDB complex recognizes CPD and/or 6-4pp and binds to them. In addition to the role of UV-DDB complex as a damage detector, it has the ability to form an E3 ubiquitin ligase complex that fine-tunes the GG-NER activity (Rüthemann et al. 2016). Following DNA damage detection by UV-DDB complex, the DDB2 subunit of the UV-DDB complex forms a cullin- type ligase complex that mediates histone ubiquitinations, thus allowing chromatin opening (Wang et al. 2006). The same cullin-type ligase complex also ubiquitinates the DDB2 itself as well as the XPC protein, thus facilitating the recruitment of core NER machinery (Wang et al. 2006; Rüthemann et al. 2016). The core NER machinery involves damage verification and double strand unwinding, incision and excision of the error containing oligonucleotide as well as replacing the excised oligonucleotide by repair synthesis and ligation.

1.3.5.1.1 UV-DDB complex

In mammals, the UV-DDB complex facilitates the recognition of DNA photoproducts (Figure 1.2). It has a particularly strong affinity for 6-4 PPs, and modest but considerable specificity for CDPs (Fujiwara et al. 1999). UV-DDB complex is a heterodimer complex consisting of DDB1 and DDB2. DDB1 and DDB2 belong to the WDR protein family; DDB1 has a conserved protein motif (the DWD box), whereas DDB2 has a WD40 repeat that is required for DDB1 binding and N-terminal (HLH) motif that is responsible for the interaction with damaged DNA (Scrima et al. 2008). UV-DDB complex itself is a part of an E3 ubiquitin ligase complex that includes CUL4 (Cullin 4A) and RING box protein-1 (RBX/ROC1; Groisman et al. 2003; Sugasawa 2011). The DDB2 subunit of the DDB complex is the first damage recognition factor that recognizes the DNA photoproducts and binds to them (Scrima et al. 2008; Figure 1.2). Stable binding of DDB2 to the damaged DNA site activates the ubiquitin E3 ligase activity of the UV-DDB-CUL4-ROC1 complex that binds to DDB2 via the adaptor protein DDB1 (Wang et al. 2006). Then, the UV-DDB-CUL4-ROC1 complex targets XPC and DDB2 for ubiquitination (Wang et al. 2006). XPC ubiquitination enhances its affinity for DNA (Hannss & Dubiel 2011), whereas DDB2 ubiquitination mediates its proteasomal degradation (Rapić-Otrin et al. 2002). DDB2 degradation facilitates the recruitment of the subsequent NER proteins to the damaged site to verify the damage and proceed with the repair (El-Mahdy et al. 2006). Under normal conditions (i.e. no UV exposure), the E3 ubiquitin ligase activity of the UV-DDB-CUL4-ROC1 complex is inactivated by the COP9 signalosome (CSN), which is associated with UV-DDB (Fischer et al. 2011).

In human fibroblast cells, mutations in the DDB2 protein that impair UV-DDB binding to DNA, resulting in xeroderma pigmentosum group E (XP-E) patients, due to the impaired removal of potential oncogenic CDPs via GG-NER (Hwang et al. 1999; Strzałka et al. 2020). In murine fibroblasts, DDB2 overexpression enhances the repair of both 6-4PPs and CDPs (Hwang et al. 1999). Orthologues of mammalian DDB1 and DDB2 exist in many vertebrates but are absent in many other “lower” eukaryotes.

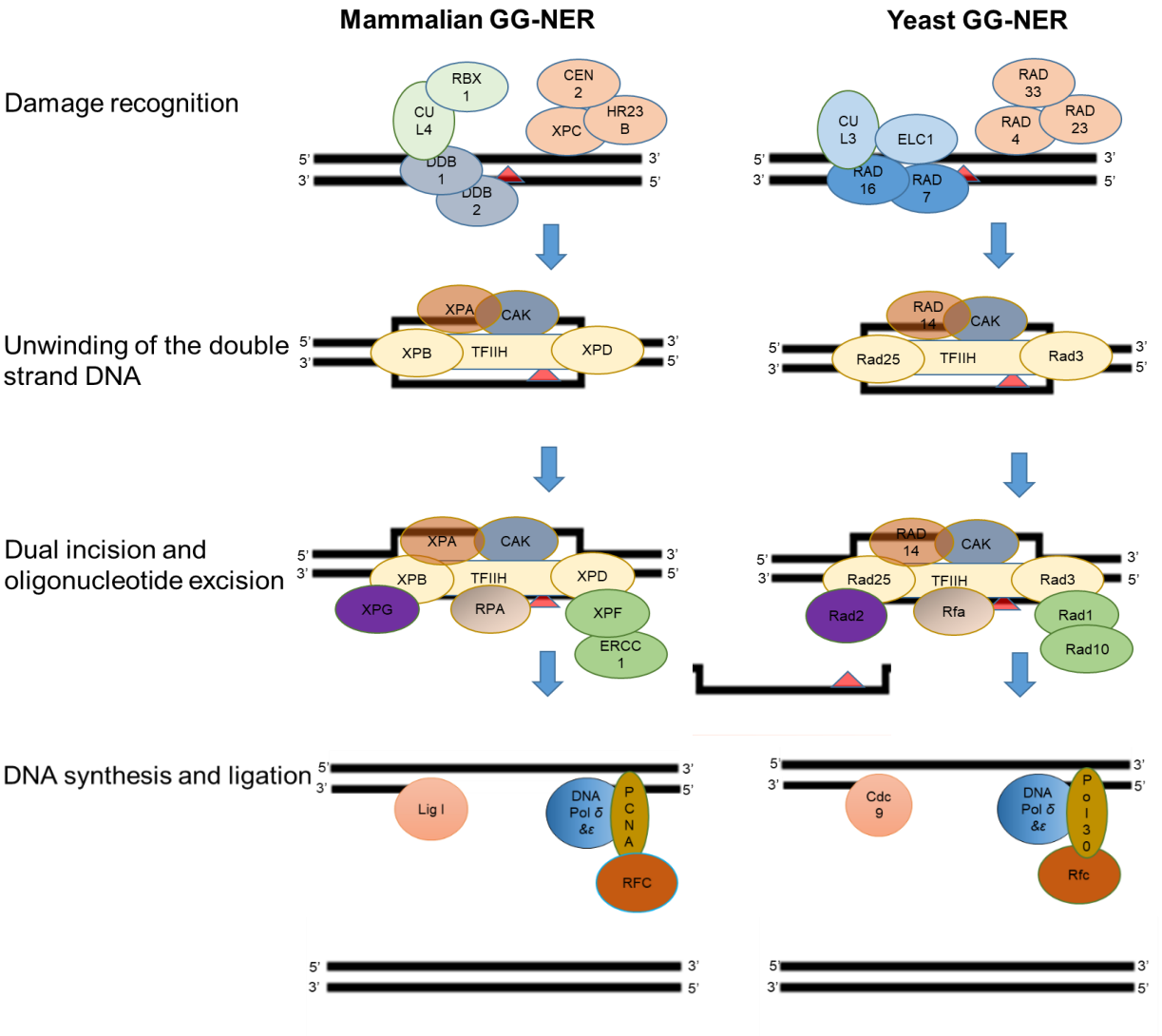

Figure 1.2 A schematic representation of GG-NER pathway in mammalian cells (human) and yeast cells (*Saccharomyces cerevisiae*)

The mammalian GG-NER, DDB1/2 complex detects the damaged DNA. In yeast GG-NER, the RAD7/16 complex recognizes the damage. After the damage recognition step conserved core NER proteins are recruited for unwinding the double strand around the lesion, excision of the damaged DNA, DNA synthesis and ligation. Proteins within the same complex and homologous proteins are color-coded, red triangle represents UV photoproducts. See text for details.

Homologues of mammalian DDB1 and DDB2 exist in plants, and the role of these two genes in plant UV tolerance and development has been studied in rice, tomato, and *Arabidopsis* (Shu & Yang 2017). In rice, exposure to UV radiation was found to increase the transcript levels of DDB2 mainly in root and shoot tips, and overexpression of *OsDDB2* enhances rice UV tolerance (Ishibashi et al. 2003; 2006). The *Arabidopsis* genome contains two homologs of mammalian *DDB1* known as *DDB1A*, and *DDB1B*, and one homolog of mammalian *DDB2*, *AtDDB2* (Schroeder et al. 2002). *Atddb1a* and *Atddb2* null mutants as well as *Atcul4* hypomorphic mutant exhibit UV sensitivity and reduction in the repair of UV photoproducts following UV irradiation (Molinier et al. 2008). Additionally, overexpression of *AtDDB1A* enhanced plant UV tolerance and UV lesions repair (Al Khateeb & Schroeder 2009). These results suggest that the CUL4-DDB1A-DDB2 E3 ligase complex is present in *Arabidopsis* and involved in the dark repair of UV photoproducts. In addition to the involvement of DDB factors in plant NER, they were found to be important for plant growth and development through their interactions with a variety of proteins (Ganpudi & Schroeder 2013; Manova & Gruszka 2015). For example, *atddb1b* null mutant was found to be lethal (Schroeder et al. 2002), and the tomato DDB1 protein was found to be important for fruit development and nutrient accumulation (Wang et al. 2019).

The yeast *S. cerevisiae* lacks DDB1 and DDB2 orthologues. Instead, it utilizes another damage recognition complex known as RAD7/16 complex (Reed et al. 2005; Figure 1.2).

1.3.5.1.2 Damaged DNA binding complex-XPC

In mammals, the XPC complex is a heterotrimeric complex consisting of Xeroderma pigmentosum complementation group C (XPC), the human homolog of yeast RAD23 (HR23B), and centrin 2 (CEN2; Figure 1.2). *In vitro*, XPC physically interacts with HR23B and CEN2 forming XPC-hHR23B-CEN2 complex (Araki et al. 2001). HR23B and CEN2 act cooperatively to stabilize XPC and promote its damage recognition activity, during the early stage of damage recognition, both *in vitro* and *in vivo*. (Bergink et al. 2012; Kobaisi et al. 2019; Nishi et al. 2005). XPC is the initiator of the GG-NER machinery, it facilitates the recruitment of a ten-subunit complex protein

transcription factor II H (TFIIH), to the damaged lesions through interacting with it (Rastogi et al. 2010). Two core TFIIH helicases XPB and XPD that have opposite polarities ((3'-5') and (5'-3'), respectively) open the DNA at both ends around the lesion in an ATP-dependent matter, creating a bubble structure. The XPC complex's bubble shape binds damaged DNA and facilitates damage verification by other TFIIH components before the initiation of the repair machinery (Johann To Berens & Molinier 2020).

The mammalian HR23B is a bifunctional protein; it is not only involved in DNA repair, but also in the control of many biological processes through the regulation of intracellular protein recycling (Dantuma et al. 2009; Sakai et al. 2020). Aside from the HR23B XPC- binding domain, HR23B possesses three other domains: a Ubiquitin-like domain (UBL), a Ubiquitin associated domain 1 (UBA1), and a Ubiquitin associated domain 2 (UBA2). These three domains are involved in shuttling polyubiquitinated proteins to the proteasome for degradation (Chen et al. 2011; Sakai et al. 2020).

The yeast *S. cerevisiae* has orthologues of mammalian XPC, HR23b, and CEN2, named RAD4, RAD23, and RAD33, respectively, and their roles in GG-NER seem to be highly conserved. RAD4 along with RAD23 recognizes the DNA lesion and destabilizes the double-strand DNA around the lesion (Min & Pavletich 2007; Table 1.1). The RAD4/RAD23 complex, named NER Factor 2 (NEF2), interacts with the RAD7/16 complex named NEF4. This physical interaction enhances NEF2 damage recognition ability (Prakash & Parkash 2000). The Rad33's involvement in the Rad4-Rad23 complex is similar to Centrin2's role in the XPC-HHR23B complex, as it interacts with the RAD4-RAD23 complex and enhances RAD4 damage recognition activity (den Dulk et al. 2008). Yeast RAD23 plays a dual role in NER; it stabilizes cellular RAD4 levels and enhances its damage recognition and binding activity. Following damage recognition, the NEF4 complex interacts with other NER factors to form a cullin-based E3 ubiquitin ligase complex that targets RAD4 for degradation, which facilitates the recruitment of other NER components to the damaged site (Gillette et al. 2006). In addition to the RAD4-binding domain, RAD23 possesses other three binding domains similar to those identified in the mammalian RAD23, suggesting that yeast RAD23 is not

only NER protein but also involved in other cellular functions (Xie et al. 204; Gillette et al. 2006).

GG-NER is also conserved in plants, and homologs of mammalian XPC, HR23b, and CEN2, (RAD4, RAD23, CEN2), have been identified in many plants, and their roles in plant UV tolerance have been studied in *Arabidopsis* (Lahari et al. 2017; Molinier et al. 2004; Table 1.1). AtRAD4 interacts with AtCEN2, AtRAD23b, as well as with HEMERA (HMR), a protein that is structurally similar to AtRAD23 (Lahari et al. 2017; Liang et al. 2006). AtRAD4 overexpression significantly increases *Arabidopsis* UV tolerance (Lahari et al. 2017). Similarly, AtCEN2 also plays a role in NER. Following UV-C irradiation, AtCEN2 protein concentration significantly increased and exhibited nuclear localization (Liang et al. 2006), and Atcen2 RNAi transgenic lines exhibited mild UV-C sensitivity. Transcriptional profiling of the same RNAi lines showed a remarkable change in the expression of DNA repair factors including NER components (Molinier et al. 2004). Similarly, AtRAD23 and AtHMR were found to play a role in plant UV tolerance and DNA repair, *Athmr* partial loss of function mutant exhibited increased UV sensitivity (Lahari et al. 2017)

Like mammalian and yeast, AtRAD23 is not only involved in plant UV tolerance and/or GG-NER, but it is also involved in translocating ubiquitylated proteins to the proteasome for degradation (Farmer et al. 2010). *Arabidopsis* has four isoforms of RAD23: RAD23A, B, C, and D. Genetic analysis of *Arabidopsis* RAD23s showed that this protein family regulates the degradation of several regulatory proteins, which is critical for plant growth and development (Farmer et al. 2010). For example, irradiating the *Atrad23d* mutant, that severely impaired for RAD23d expression, with UV-B light resulted in a significant increase in seed abortion and reduction in pollen grain development (Li et al. 2012), and *Atrad23a-c* single null mutants are sensitive to UV radiation (Lahari et al. 2017).

Table 1.1 Core NER components in humans, *S. cerevisiae*, and *Arabidopsis thaliana* and their functions

GG-NER damage recognition components			
Human protein	*S. cerevisiae* (homolog)	*Arabidopsis* (homolog)	Function
DDB1	n/a	AtDDB1A, AtDDB1B	DNA damage recognition
DDB2	n/a	AtDDB2	DNA damage recognition
CUL4	n/a	CUL4	E3 ubiquitin ligase complex backbone
n/a	ScRad7	AtRAD7A, AtRAD7B, AtRAD7C	DNA damage recognition
n/a	ScRad16	AtRAD16, AtRAD16B	DNA damage recognition
n/a	Abf1	n/a	DNA binding activity
ElonginC	ScELOC1	AtELOC	Complexes with RAD7-RAD16
XPC	ScRad4	AtRAD4	DNA damage recognition
HR23B	ScRad23b	AtRAD23A, AtRAD23B, AtRAD23C, AtRAD23D	Together with XPC/RAD4 bind damaged DNA and recruit other NER factors
CEN2	Rad33	ATCEN2	Stabilizes XPC and promotes its damage recognition activity
TC-NER damage recognition components			
CSA	Rad28	AtCSA1A, AtCSA1B	Ubiquitin ligase factor
CSB	Rad26	AtCSB/CHR8	DNA binding with ATPase/helicase activities.
USP7	ScUbp15	AtUBP12, UBP13	Ubiquitin ligase activity
UVSSA	n/a	AtUVSSA	Recruited by CSA to the damaged DNA
XAB2	Syf1	AtXAB2	Pre-mRNA processing
HMGN1	n/a	n/a	Chromatin modification
TFIIS	ScTFIIS	AtTFIIS/RDO2	Involved in transcription elongation
Down stream repair components for both (GG-NER and TC-NER)			
XPB	Rad25/SSL2	AtXPB1, AtXPB2	3’-5’ helicase
XPD	Rad3	AtXPD/UVH6	5’-3’ helicase
P62	Tfb1	AtTF2H1-1,AtTF2H1-2	TFIIH core complex
P44	Ssl1	AtTF2H2	
P34	Tfb4	AtTF2H3	

P52	Tfb2	AtTF2H4	
P8	Tfb5	AtTF2H5-1, AtTF2H5-2	
CDK7	Kin28	ATCDK D;1 ATCDK D;2 ATCDK D;3	THIIH CAK complex
MAT1	Tfb3	AtMAT1	
Cyclin H	Ccl1	At CYCH;1	
XPA	Rad14	n/a	Stabilizes the opened DNA structure via binding the damged site at ssDNA
RPA70	Rfa1	AtRPA70A, AtRPA70B, AtRPA70C, AtRPA70D, AtRPA70E	Stabilizes opened DNA structure and recruits nucleases
RPA32	Rfa2	AtRPA32A, AtRPA32B	
RPA14	Rfa3	AtRPA14A, AtRPA14B	
DNA excision components (nucleases)			
ERCC1	Rad10	AtERCC1/UVR7	Catalyzes the incision at 5'ssDNA
XPF	Rad1	AtRAD1/UVH1	
XPG	Rad2	AtRAD2/UVH3	Catalyzes the incision at 3'ssDNA
Repair synthesis components (DNA polymerases and ligases)			
RFC1,RFC2, RFC3,RFC4, RFC5	Rfc1,Rfc2, Rfc3,Rfc4, Rfc5	AtRFC1, AtRFC2, AtRFC3, AtRFC4, AtRFC5	Recruits PCNA to the damaged DNA (Involved in DNA repair and replication)
PCNA	Pol30	AtPCNA1, AtPCNA2	Stimulates DNA polymerase
DNA Pol *δ*	ScDNA Pol *δ*	*At1g09815* *At2g42120* *At5g63960*	Repair synthesis
DNA Pol *ε*	ScDNA Pol *ε*	At1g08260 At2g27120 At5g22110	
Ligase I	Cdc9	At1g08130 At1g49250	Ligation of ssDNA gap
Ligase III	n/a	n/a	
XRCC1	n/a	Exists but not involved	Forms a ligation complex with DNA Ligase III

1.3.5.1.3 RAD7/16 damage recognition complex

In *S. cerevisiae*, RAD7 and RAD16 proteins are involved in early damage recognition (Figure 1.2). RAD7 and RAD16 are structurally different from mammalian DDB1 and DDB2, however, the RAD7/16 complex and the mammalian UV-DDB complex have functional similarities (Reed 2005). Yeast RAD16 is required for GG-NER and mutations in RAD16 result in a radiation-sensitive phenotype (Bang et al. 1992). RAD16 is a member of SWI/SNF-related ATPase family that displays chromatin remodeling activity (Lettieri et al. 2008). RAD7 together with RAD16 form a stoichiometric complex (RAD7/16) known as NEF4. The NEF4 complex is the first complex that recognizes the UV damage binds to it in an ATP dependent manner, then NEF4 physically interacts with NEF2 (another damage recognition complex consisting of RAD23 and RAD4; Figure 1.2), and both complexes work synergistically to enhance the damaged DNA binding (Guzder et al.1999). After damage recognition, RAD7/16 complex forms an E3 ubiquitin ligase complex via its interaction with Elongin C (ELOC1), and Cullin3 (CUL3; Gillette et al. 2006). This E3 ligase complex targets RAD4 for degradation to facilitate the recruitment of core NER machinery (Shuck et al. 2008). The Autonomously Replicating Sequence-Binding Factor 1 (ABF1) is another protein that is associated with RAD7/16 complex and enhances GG-NER efficiency following UV radiation (Yu et al. 2009). In the absence of UV radiation, the heterotrimeric complex, RAD7/RAD16/ABF1, inhibits histone acetylation and chromatin remodeling (Waters et al. 2015). *S. cerevisiae* ELOC1 is an orthologue of mammalian ELOC.

Following DNA damage, the yeast ELOC1 together with RAD7/16 and CUL3 functions as an E3 ubiquitin ligase complex. This complex facilitates the recruitment of core NER components to the damaged site via RAD4 ubiquitination (Ramsey et al. 2004; Ribar et al. 2006). Thus, yeast ELOC1 is required for GG-NER. In addition, yeast ELOC1 itself is also a part of another ubiquitin ligase complex that includes ELOA, CUL3 and RING-box protein 1 (RBX1); this complex targets the large subunit of the stalled RNAP II (Rpb1) for ubiquitination and degradation in response to DNA damage (Ribar et al. 2006), implicating the involvement of ScELOC1 in the repair of transcriptionally active DNA. Thus, *S. cerevisiae* ELOC1 is involved in both GG-NER and TC-NER.

In plants, orthologues of *S. cerevisiae* GG-NER damage recognition factors are present (Table 1.1). For example, the model plant *Arabidopsis thaliana* has three homologues of yeast RAD7 (RAD7A, RAD7b, and RAD7c). It also has two Cul3 homologs known as CUL3a, and CUL3b (Thomann et al. 2005), two RAD16 homologs encoded by At1g05120 and At1g02670 (Shaked et al. 2006), and one ELOC homolog (At5g59140; Risseeuw et al. 2003). In this thesis, I have characterized the roles of *Arabidopsis* ELOC homolog (At5g59140) and RAD16 homologs (At1g05120, At1g02670) in plant UV tolerance and growth and investigated their interaction with other NER components. I also identified an *Arabidopsis* ELOA homolog encoded by At2g42780 and characterized its role in plant UV tolerance and growth.

1.3.5.1.4 Damage verification and DNA unwinding

Damage verification is the next step after damage recognition. This step is performed by the TFIIH complex that is recruited by XPC/RAD4 to the damaged site. In humans, TFIIH complex is a multi-subunit complex composed of a core complex of P62, p52, p44, p34, p8, XPD, and XPB, in addition to three Cdk-activating-kinase CAK proteins: CDK7, MAT1, and CyclinH (Greber et al. 2019; Strzałka et al. 2020) (Table 1.1). XPC recruits TFIIH to the damaged DNA via its interaction with XPB and P62. Then the two DNA helicases XPB (3'-5') and XPD (5'-3') unwind the double helix around the lesion in an ATP-dependent process, generating single-stranded regions of approximately 25 nucleotides (Evans et al. 1997; Rüthemann et al. 2016).

In *S. cerevisiae*, the TFIIH complex is also involved in damage verification during NER. The yeast TFIIH consists of the core TFIIH complex (Rad25/SSL2), Rad3, Tfb1, Tfb2, Ssl1, Tfb4, Tfb5 along with three CAK kinase subunits (Boiteux & Jinks-Robertson 2013; Table 1.1). RAD25 and RAD3 are the yeast homologues of mammalian XPB and XPD, respectively (Rastogi et al. 2010). Thus, RAD25 and RAD3 are DNA-dependent ATPases with (3'-5') and (5'-3') helicase activities, respectively. The ATPase/helicase activities of these two proteins are required for helix opening around the lesions (Guzder et al.1999).

In plant systems, homologues of some yeast and mammalian TFIIH components were identified via sequence similarity. For example, *Arabidopsis* has two gene copies

for *XPB*/*Rad25*, *AtXPB1*, and *AtXPB2*, one homolog of *XPD*/*Rad3* (*AtXPD*), two copies of each *P62* and *P8* as well as one homolog of each *P44*, *P34*, and *P52* (Spampinato 2017; Costa et al. 2001; Vonarx et al. 2006). The roles of these components in *Arabidopsis* NER and development have been studied using genetic analyses. The *Atxpb1* nonsense mutant does not exhibit increased UV sensitivity, possibly due to functional redundancy between AtXPB1 and AtXPB2 that share 95% amino acid identity. *AtXPB2* complements the UV-sensitive phenotype exhibited by the yeast *rad25* terminal deletion mutant (Morgante et al. 2005; Costa et al. 2001). The *Atxpd* missense mutant (called *uvh6-1*) shows a significant decrease in *Arabidopsis* UV tolerance along with growth defects, and the *Atxpd* null mutant (*uvh6-2)* was found to be lethal (Liu et al. 2003). Moreover, AtTF2H2 was found to physically interact with AtXPD, and complement the UV-sensitivity of yeast *ssl1* loss of function mutant (Vonarx et al. 2006). These results suggest a conserved function of TFIIH components in the plant GG-NER pathway, in addition to the involvement of AtXPD in plant development. The rice homolog of TFB5, OsREX1-S has also been characterized. *OsREX1-S* overexpression *in Arabidopsis* increased *Arabidopsis* UV tolerance and reduced CPD incidence following UV-B exposure (Kunihiro et al. 2014).

1.3.5.1.5 NER endonucleases recruitment

In mammals, after damage verification and the formation of an opened DNA structure by TFIIH components, three additional proteins (XPA, Replication Protein A (RPA), and XPG) are recruited and together form the preincision complex (Fagbemi et al. 2011; Alekseev & Coin 2015). XPA binds to TFIIH and to RPA to stabilize the opened DNA structure. It also promotes the recruitment of the XPF-ERCC1 complex to DNA damage sites and enhances the complex endonuclease activity (Krasikova et al. 2018). XPF-ERCC1 carries out the incision at the 5’ end of the opened DNA structure (the bubble) and the initiation of the repair synthesis by adding one hanging hydroxyl group to the 3’ end, whereas XPG carries out the incision at the 3’end and complete the DNA fragment excision. XPG also enhances efficient repair synthesis via its interaction with Proliferating Cell Nuclear Antigen (PCNA; Gary et al. 1997).

In *S. cerevisiae*, Rad14, Rad10, Rad1, and Rad2 are the yeast homologues mammalian XPA, ERCC1, XPF, and XPG, respectively (Table 1.1). The single stranded nuclease Rad10 forms a heterodimer complex with Rad1 that is recruited by Rad14 to the opened DNA structure. The Rad10-Rad1 complex, together with the other endonuclease Rad2, carry out the dual incision at the 5′ and 3′ ends of the opened DNA structure and complete the cleavage of lesion containing sites (Sarangi et al. 2014; Wood 1997).

In plant systems, orthologues of human ERCC1, XPF, XPG, and RPA have been reported, however, no plant homolog of XPA/RAD14 has been identified. In *Arabidopsis*, UV REPAIR DEFICIENT 7 (UVR7), AtRAD1/UVH1 (ultraviolet hypersensitive 1), and UVH3 are homologs of ERCC1/RAD10, XPF/RAD1, XPG/RAD2, respectively. A splice junction mutation in the *UVH1* gene results in UV sensitivity and defective NER, and expression of wild-type *AtUVH1* rescues the UV sensitivity and repair defects exhibited by *Atuvh1* mutant (Fidantsef et al. 2000; Liu et al. 2000). Similarly, *Atuvh3*, and *Atuvr7* nonsense mutants were also identified in UV- sensitivity screens (Bray & West 2005; Liu et al. 2001). Taken together, these data suggest conserved roles of *Arabidopsis* UVH1, UVH3, and UVR7 in dark repair. An XPG/RAD2 orthologue also exists in rice, and UV radiation was found to induce the expression of rice *XPG*, *OsSEND1,* suggesting the involvement of this protein in DNA repair (Furukawa et al. 2003). Similarly, RPA homologs have been identified in *Arabidopsis* and rice. *Arabidopsis* possesses five *RPA70* genes and two paralogs of each of RPA32 and RPA14, whereas rice has three copies each of *RPA70* and *RPA32* and one *RPA14* gene (Shultz et al. 2007; Ishibashi et al. 2006). OsRPA70a is essential for DNA repair and plant fertility (Chang et al. 2009), and the *Atrpa70a* null mutant is sensitive to mutagenic agents and defective in telomere length regulation (Takashi et al. 2009).

1.3.5.1.6 DNA re-synthesis and ligation

In mammals, DNA repair synthesis is executed by the coordinated action of DNA polymerase epsilon/delta (Pol *ε*/*δ*), and factors including PCNA, RPA, and Replication Factor C (RFC; Kobaisi et al. 2019). Interaction between the ATP-dependent RFC complex and PCNA facilitates the loading of PCNA near the 3’OH of the DNA

(Petruseva et al. 2014). The ring-shaped structure PCNA moves along the DNA and binds to the DNA polymerase to start the DNA synthesis. RPA facilitates the recruitment of PCNA and RFC to the ssDNA. Finally, either DNA ligase 1 or XRCC1– DNA ligase 3 seals the generated nick (Gillette et al. 2006).

S. cerevisiae has one PCNA homolog, named POL30. Yeast PCNA maintains the ring-shaped structure during DNA repair, comparable to mammalian PCNA (Chakraborty et al. 2016). It also plays a role in recruiting repair components to damage sites for repair (Halmai et al. 2016). DNA synthesis is performed by Polδ or Polε (Wu et al. 2001), and DNA ligation is executed by the yeast orthologue of mammalian DNA ligase I, Cdc9 (Wu et al. 1999).

In plants systems, homologues of mammalian RFC and PCNA, and DNA polymerases δ, and ε have been identified. *Arabidopsis* possesses five RFC homologues, two PCNA homologues, PCNA1 and PCNA2, three orthologues of each Polδ and Polε, and two DNA ligase I orthologues (Spampinato 2017). Both RFC and PCNA are involved in DNA replication and DNA repair (Chen et al. 2018). AtPCNA2 performs a function similar to its yeast counterpart in response to DNA damage, and its role in DNA repair is more critical than AtPCNA1 (Xue et al. 2015).

1.3.5.2 Prokaryotic GG-NER

In *E. coli*, two proteins known as UvrA and UvrB (XPC and HTFII in humans) carry out the damage recognition and verification step (Figure 1.3). UvrA is a member of the ATP-binding cassette (ABC) superfamily and thus possesses ATPase/GTPase activity (Sancar 1996). UvrB belongs to the SF2 helicase family of proteins. UvrA and UvrB form a heterodimeric complex that recognizes the damage and binds to it. UvrB can interact with UvrA and other NER factors. After damage recognition, UvrA dissociates from UvrB, which enhances the DNA unwinding around the lesion and damage verification by UvrB. Following damage verification, DNA incision at the 5’ and 3’ends flanking the lesion is carried out by the endonuclease UvrC (Figure 1.3). The DNA helicase II UvrD completes the excision of the damaged oligonucleotide. Then, DNA polymerase I fills the resultant gap, while DNA ligase I seals the nick (Kisker et al. 2013). In Archaea, NER pathway has not been as well defined. However, the majority of

archaea have homologs of both bacterial and eukaryotic NER proteins including Uvrs, XPB/XPD, and XPF (Marshall & Santangelo. 2020). Similarly, in many cyanobacterial genomes, orthologues of *E. coli* NER genes *UvrABCD* are present. These genes are clustered with other core DNA repair genes such as Photolyase (*phr*) or *recN* (Cassier-Chauvat et al. 2016). Moreover, transcriptome analysis of the radiation-tolerant cyanobacterium *Arthrospira* PCC 8005, showed that the expressions of *UvrBCD* genes are induced after gamma radiation (Badri et al. 2015).

1.3.5.3 Eukaryotic TC-NER

In contrast to GG-NER that directly detects the damage in the non-transcribed DNA strand, TC-NER recognizes the damage in the transcribed strand indirectly via sensing the lesion-stalled RNAPII. The stalled RNAP II initiates the TC-NER by recruiting TC-NER specific components including Cockayne Syndrome proteins CSA and CSB, UV-Stimulated Scaffold protein A (UVSSA), Ubiquitin-Specific-Processing Protease 7 (USP7) to form a functional repair complex (Marteijn et al. 2014). During the TC-NER process, CSB (a nuclear protein that belongs to the SWI/SNF family) interacts with the stalled RNA polymerase and changes the local chromatin structure to facilitate the recruitment of CSA and other repair factors to the lesion (Schwertman et al. 2013). Then, UVSSA interacts with RNAPII and stabilizes CSB by transporting USP7 to TC-NER complex (Melis et al. 2013). CSA together with CSB facilitates the recruitment of high mobility group nucleosome-binding domain-containing protein 1 (HMGN1), XPA-binding protein 2 (XAB2), and TFIIS (Spivak 2016). TFIIS is involved in nascent RNA cleavage at the site of the damage and resuming the transcription after the removal of the lesion (Fousteri & Mullenders 2008). After that, analogous to DDB2 function in GG-NER, the WD-repeat protein CSA, together with DDB1-CUL4-RBX1, form the CSA- E3-ubiquitin ligase complex that interacts with RNAPII and ubiquitinates CSB mediating its proteasomal degradation (Figure 1.4; Kobaisi et al. 2019; Nakazawa et al. 2020). As a result, CSB and UVSSA are subjected to proteasomal degradation and the TC-repair complex is destabilized, stimulating the recruitment of the core TFIIH complex to the damaged site (Johann To Berens & Molinier 2020). Although the damage recognition proteins required for the recruitment of TFIIH differ for TC-NER and GG-NER, the

subsequent steps including TFIIH recruitment machinery, damage verification, dual incision, and repair synthesis are similar for both pathways (Spivak 2015; Okuda et al. 2017). TC-NER mechanism is also conserved in yeast, and it is important for the removal of lesion-stalled RNAP II from the transcriptionally active gene. The yeast homologues of mammalian CSB and CSA are RAD26 and RAD28, respectively (Peng et al. 2011; Figure 1.4). RAD26 is a member of the SWI2/SNF2 family with an ATP-dependent chromatin remodeling activity that is required for TC-NER (Duan et al. 2020). Inactivation of the RAD26 gene does not result in a significant increase in yeast UV sensitivity. However, inactivation of RAD26 together with either RAD16 or RAD7 (the GG-NER specific factors) results in increased sensitivity to UV radiation compared to *rad16* and *rad7* single null mutants (Li 2015). Similarly, *rad28* null mutants do not exhibit a detectable UV sensitivity, but *rad28 rad16*, and *rad28 rad7* double null mutants are more vulnerable to UV radiation than *rad16* and *rad7* single null mutants (Bhatia et al. 1996). The moderate effects of RAD26 and RAD28 on yeast UV sensitivity may be explained by the efficient GG-NER in yeast that compensates for the defects in TC-NER. SYF1 and UBP15 are the yeast orthologues of mammalian XAB2 and USP7 (Ben-Yehuda et al. 2000; Peng et al. 2011). *S. cerevisiae* UBP15 is involved in the processing of proteolytic cleavage of precursor proteins and SYF1 was found to play a role in pre-RNA splicing (Amerik et al. 2000; Ben-Yehuda et al. 2000).

In plant systems, similarly to mammalian and yeast systems, TC-NER repair that selectively repairs DNA damage-induced transcription stalling plays a critical role in preventing transcription arrest and enabling gene expression (Fidantsef et al. 2012). In the *Arabidopsis* genome, homologs of most mammalian TC-NER proteins have been identified (Table 1.1). *Arabidopsis* possesses two orthologues of mammalian CSA, AtCSA1A and AtCSA1B, and one homolog of mammalian CSB, AtCSB, also named Chromatin Remodelling 8 (CHR8; Shaked et al. 2006; Zhang et al. 2010). AtCSAs are WD40 repeat proteins that assemble with the DDB1-CUL4A-E3 complex in the nucleus, whereas AtCSB (CHR8) is a SWI2/SNF2 chromatin remodeler protein family with ATPase/helicase activities (Zhang et al. 2010). Knockdown of *Arabidopsis* CSB results in increased UV sensitivity; however, this UV sensitivity was observed under light and dark conditions, suggesting the involvement of AtCHR8 in light-dependent and

independent repair (Al Khateeb et al. 2019). Similarly, *Atcsa1a* and *Atcsa1b* null mutants exhibit enhanced UV sensitivity and reduction in the removal of UV-induced lesions (Al Khateeb et al. 2019; Zhang et al. 2010). AtXAB2 is the mammalian XAB2 homolog, it contains tetratricopeptide repeats which are expected to be involved in pre-mRNA splicing. However, the role of AtXAB2 in NER has yet to be studied (Kunz et al. 2005). *Arabidopsis* also possesses two USP7 homologs, Ubiquitin like proteases 12 and 13 (AtUBP12, AtUBP13), one UVSSA homolog, AtUVSSA, and one TFIIS homolog, the Reduced Dormancy 2 (AtRDO2; Derkacheva et al. 2016; Al Khateeb et al. 2019). Both UBP12/13 possess ubiquitin-specific protease activity and have been implicated in flowering regulation and stress response (Cui et al. 2013; Zhou et al. 2017). *Arabidopsis* UBP12 is hypothesized to be involved in UVSSA deubiquitination (Al Khateeb et al. 2019), whereas AtRDO2 promotes RNAPII elongation and regulates seed dormancy (Grasser et al. 2009). *Uvssa, ubp12,* and *rod2* loss of function mutant plants are hypersensitive to UV radiation under dark conditions, suggesting the involvement of these proteins in TC-NER (Al Khateeb et al. 2019).

1.3.5.4 Prokaryotic TC-NER

In contrast to eukaryotic TC-NER, in prokaryotes the Mutation Frequency Decline protein (Mfd) binds the stalled RNA polymerase (RNAP) in an ATP-dependent manner and initiates prokaryotic TC-NER. Mfd/RNAP binding promotes RNAP displacement from the damaged site that facilitates the recruitment of bacterial NER factors (UvrA, UvrB, and UvrC) to the damaged site (Figure 1.3). After that, TC-NER follows the same subsequent steps discussed in GG-NER previously (Peng et al. 2011; Kisker et al. 2013). Alternatively, a Mfd independent TC-NER mechanism also exists in some bacteria. In this alternative repair pathway, UvrD helicase interacts with the lesion stalled RNAP and together with the elongation factor, NusA promotes RNAP backtracking. RNAP backtracking allows the remainder of the bacterial NER components to reach the damaged site and repair it (Epshtein et al. 2014; Figure 1.3).

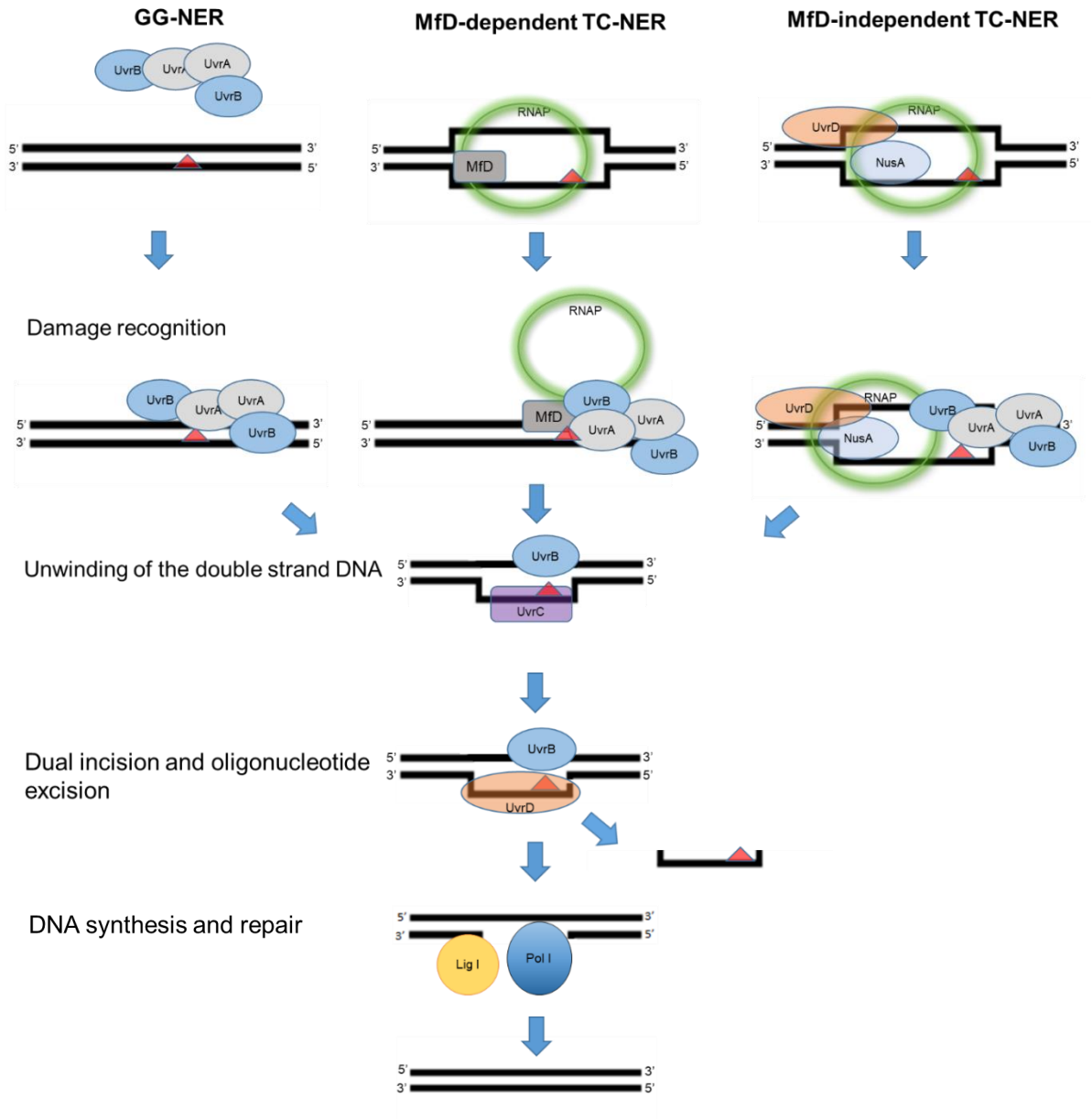

Figure 1.3 A schematic representation of GG-NER and TC-NER pathways in prokaryotic cells (*Escherichia coli*)

In procaryotic GG-NER, UvrA and UvrB detect the damaged DNA, whereas in TC-NER, the Mfd or the UvrD and NusA recognize the lesion stalled RNAPII. After the damage recognition step both TC-NER and GG-NER have a common pathway for unwinding the double strand around the lesion, excision of the damaged DNA, DNA synthesis and ligation. Red triangles represent UV photoproducts. See text for details.

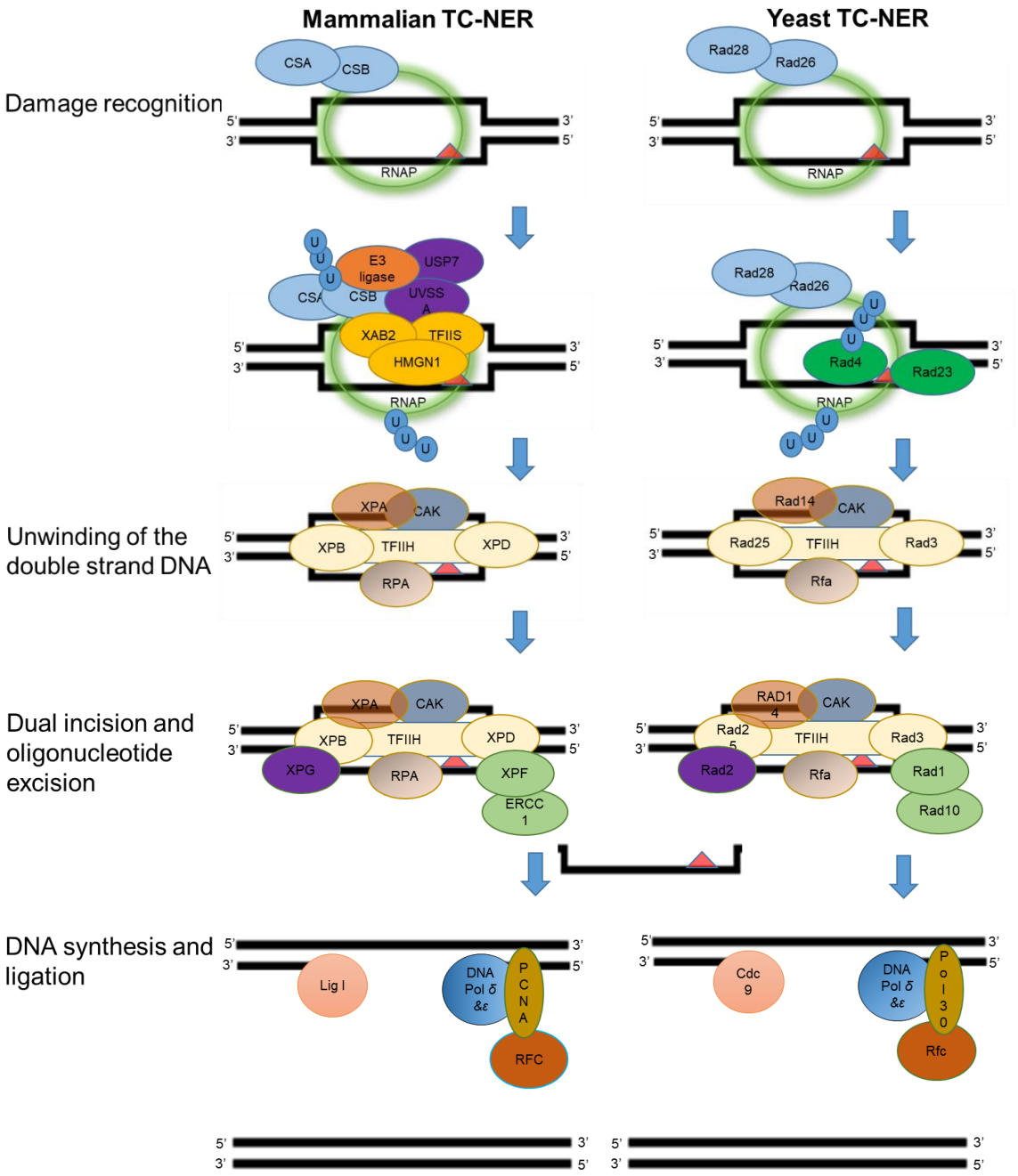

Figure 1.4 A schematic representation of TC-NER pathway in mammalian cells (human) and yeast cells (*Saccharomyces cerevisiae*)

In TC-NER, mammalian CSA/CSB or yeast RAD28/RAD26 complexes recognize the lesion stalled RNAPII. After the damage recognition step, conserved core NER proteins are recruited for unwinding the double strand around the lesion, excision of the damaged DNA, DNA synthesis and ligation. Proteins within the same complex and homologous proteins are color-coded, red triangle represents UV photoproducts. See text for details.

1.4 Conclusions

Thus, NER is a highly conserved mechanism that carries out the repair of UV-induced DNA photoproducts in both prokaryotes and eukaryotes. In eukaryotes, NER is a multistep repair process with homologous proteins in mammals, plants, and yeast. Recognition of UV-damaged DNA during NER is via two subpathways: TC-NER if the lesion is in a transcriptionally active strand and GG-NER if it is in non-transcribed DNA strands across the entire genome. One of the few aspects of NER that varies between organisms is the recognition of damaged DNA during GG-NER. In mammalian GG-NER, UV-damaged DNA is recognized by the Damaged DNA Binding protein (DDB) 1 and 2 / Cullin 4 (CUL4) E3 ubiquitin ligase complex (Sugasawa 2016). In the yeast *S. cerevisiae*, a distinct complex consisting of RAD7, RAD16, Elongin C (ELOC), and CUL3 recognizes UV-damaged DNA (Gillette et al. 2006).

ELOC was originally identified in mammals as being part of the Elongin complex, consisting of Elongin A, B, and C that Promotes transcript elongation by acting on RNAPII (Aso et al. 1995). In addition, Elongin C, along with Elongin A and B in mammals or Elongin A in yeast, facilitates the ubiquitination and degradation of the large subunit of RNAP II after UV irradiation (Ribar et al. 2007; Okumara et al. 2012). Thus, in yeast, ELOC is involved in GG-NER and ELOC/ELOA complex is involved in RNAP II degradation. In mammals, ELOC/ELOA complex is implicated in transcript elongation and RNAPII degradation.

Nucleotide excision repair in plants has been studied in *Arabidopsis* and the *Arabidopsis* homologs of mammalian GG-NER factors DDB1, DDB2, CUL4, CEN2, and RAD23 were found to be involved in *Arabidopsis* GG-NER (Molinier et al. 2004; Molinier et al. 2008; Al Khateeb & Schroeder 2009; Li et al. 2012; Ganpudi & Schroeder 2013). While this evidence suggests that NER in plants follows the mammalian model, bioinformatics analysis has revealed the presence of three homologs of yeast RAD7, two homologs of RAD16, two homologs of CUL3, and one Elongin C homolog in the *Arabidopsis* genome (Lahari et al. 2018; Weber et al. 2005; Shaked et al. 2006). No *Arabidopsis* ELOA homolog has been identified before this study and the roles of *Arabidopsis* ELOC and RAD16 homologs in NER have yet to be elucidated.

1.5 Thesis Objectives

The goals of my thesis were to identify a potential ELOA homolog and characterize the roles of *Arabidopsis* RAD7/RAD16/ELOC and ELOA/ELOC complexes in plant UV tolerance and growth. To achieve these goals, I divided my thesis into two main streams.

In the first stream of my thesis (chapter 2), I asked whether *Arabidopsis* RAD16 homologs, RAD16 and RAD16b, are implicated in plant UV tolerance and growth. Since bioinformatics analysis indicates that the complete components of the yeast RAD7/16 complex are present in *Arabidopsis*, I hypothesized that both DDB1/2 (the mammalian type) and RAD7/16 (the yeast type) complexes are likely to be involved in *Arabidopsis* GG-NER and/or UV tolerance. To test my hypothesis, I examined the effects of genetic loss of function alleles of both *Arabidopsis RAD16* and *RAD16b* and gain of function of RAD16 on plant UV tolerance and growth. Then, I examined the subcellular localization of *Arabidopsis* RAD16 protein and the physical interactions between *Arabidopsis* RAD16 and other NER proteins. After that, I investigated the relative contributions of the DDB1/2 and RAD7/16 complexes to *Arabidopsis* GG-NER. Finally, I assessed the relative contribution of TC-NER and GG-NER to plant UV tolerance.

High throughput yeast-two hybrid analysis (Braun et al. 2011) indicates that *Arabidopsis* ELOC homolog interacts with the protein product of At2g42780. This protein appears to be *Arabidopsis* ELOA homolog, providing evidence that both ELOA and ELOC homologs exist in *Arabidopsis* genome. Thus, in the second stream of my thesis (chapter 3), I asked whether *Arabidopsis* ELOA and ELOC homologs are involved in plant UV tolerance and growth. Since *Arabidopsis* ELOA homolog is expected to interact with *Arabidopsis* ELOC homolog similar to their yeast and mammalian counterparts, I hypothesized that *Arabidopsis* ELOA and ELOC homologs might be involved in plant UV tolerance and development. To test the hypothesis, I assessed the effects of loss of function of *Arabidopsis ELOA* and *ELOC* homologs on UV tolerance and growth. Then, I examined the genetic and physical interactions between *Arabidopsis* ELOA and ELOC homologs. Next, I assessed the effects of gain of function of *Arabidopsis* ELOA and ELOC homologs on plant UV tolerance and

development. Finally, I examined the subcellular localization of *Arabidopsis* ELOA and ELOC homologs.

1.6 References

Al Khateeb, W. M., & Schroeder, D. F. (2009). Overexpression of *Arabidopsis* damaged DNA binding protein 1A (DDB1A) enhances UV tolerance. Plant molecular biology, 70(4), 371–383. https://doi.org/10.1007/s11103-009-9479-9

Al Khateeb, W. M., Sher, A. A., Marcus, J. M., & Schroeder, D. F. (2019). UVSSA, UBP12, and RDO2/TFIIS Contribute to *Arabidopsis* UV Tolerance. Frontiers in plant science, 10, 516. https://doi.org/10.3389/fpls.2019.00516

Alekseev, S., & Coin, F. (2015). Orchestral maneuvers at the damaged sites in nucleotide excision repair. Cellular and molecular life sciences: CMLS, 72(11), 2177–2186. https://doi.org/10.1007/s00018-015-1859-5

Amerik, A. Y., Li, S. J., & Hochstrasser, M. (2000). Analysis of the deubiquitinating enzymes of the yeast Saccharomyces cerevisiae. Biological chemistry, 381(9-10), 981–992. https://doi.org/10.1515/BC.2000.121

Araki, M., Masutani, C., Takemura, M., Uchida, A., Sugasawa, K., Kondoh, J., Ohkuma, Y., & Hanaoka, F. (2001). Centrosome protein centrin 2/caltractin 1 is part of the xeroderma pigmentosum group C complex that initiates global genome nucleotide excision repair. The Journal of biological chemistry, 276(22), 18665–18672. https://doi.org/10.1074/jbc.M100855200

Aso, T., Lane, W. S., Conaway, J. W., & Conaway, R. C. (1995). Elongin (SIII): A Multisubunit Regulator of Elongation by RNA Polymerase II. Science, 269(5229), 1439–1443. http://www.jstor.org/stable/2888734

Ayora, S., Carrasco, B., Cárdenas, P. P., César, C. E., Cañas, C., Yadav, T., Marchisone, C., & Alonso, J. C. (2011). Double-strand break repair in bacteria: a view from Bacillus subtilis. FEMS microbiology reviews, 35(6), 1055–1081. https://doi.org/10.1111/j.1574-6976.2011.00272.x

Badri, H., Monsieurs, P., Coninx, I., Wattiez, R., & Leys, N. (2015). Molecular investigation of the radiation resistance of edible cyanobacterium Arthrospira sp. PCC 8005. MicrobiologyOpen, 4(2), 187–207. https://doi.org/10.1002/mbo3.229

Bang, D. D., Verhage, R., Goosen, N., Brouwer, J., & van de Putte, P. (1992). Molecular cloning of RAD16, a gene involved in differential repair in Saccharomyces cerevisiae. Nucleic acids research, 20(15), 3925-3931

Bennett, R. A. O., & Demple, B. (2013). DNA Base Excision Repair Pathways. Encyclopedia of Biological Chemistry (Second Edition).

Ben-Yehuda, S., Dix, I., Russell, C. S., McGarvey, M., Beggs, J. D., & Kupiec, M. (2000). Genetic and physical interactions between factors involved in both cell cycle progression and pre-mRNA splicing in Saccharomyces cerevisiae. Genetics, 156(4), 1503–1517. https://doi.org/10.1093/genetics/156.4.1503

Bergink, S., Toussaint, W., Luijsterburg, M. S., Dinant, C., Alekseev, S., Hoeijmakers, J. H., Dantuma, N. P., Houtsmuller, A. B., & Vermeulen, W. (2012). Recognition of DNA damage by XPC coincides with disruption of the XPC-RAD23 complex. The Journal of cell biology, 196(6), 681–688. https://doi.org/10.1083/jcb.201107050

Bhatia, P. K., Verhage, R. A., Brouwer, J., & Friedberg, E. C. (1996). Molecular cloning and characterization of Saccharomyces cerevisiae RAD28, the yeast homolog of the human Cockayne syndrome A (CSA) gene. Journal of bacteriology, 178(20), 5977–5988. https://doi.org/10.1128/jb.178.20.5977-5988.1996

Boiteux, S., & Jinks-Robertson, S. (2013). DNA repair mechanisms and the bypass of DNA damage in Saccharomyces cerevisiae. Genetics, 193(4), 1025–1064. https://doi.org/10.1534/genetics.112.145219

Braun, B., Pfirrmann, T., Menssen ,R., Hofmann, K., Scheel, H., Wolf, D. H. (2011). Gid9, a second RING finger protein contributes to the ubiquitin ligase activity of the Gid complex required for catabolite degradation. FEBS Lett. 585:3856-61. doi: 10.1016/j.febslet

Bray, C. M., & West, C. E. (2005). DNA repair mechanisms in plants: crucial sensors and effectors for the maintenance of genome integrity. The New phytologist, 168(3), 511–528. https://doi.org/10.1111/j.1469-8137.2005.01548.x

Brégeon, D., & Doetsch, P. W. (2011). Transcriptional mutagenesis: causes and involvement in tumour development. *Nature reviews. Cancer*, *11*(3), 218–227. https://doi.org/10.1038/nrc3006

Brem, R., & Karran, P. (2012). Multiple forms of DNA damage caused by UVA photoactivation of DNA 6-thioguanine. Photochemistry and photobiology, 88(1), 5–13. https://doi.org/10.1111/j.1751-1097.2011.01043.x

Bundock, P., & Hooykaas, P. (2002). Severe developmental defects, hypersensitivity to DNA-damaging agents, and lengthened telomeres in *Arabidopsis* MRE11 mutants. The Plant cell, 14(10), 2451–2462. https://doi.org/10.1105/tpc.005959

Busch, C. R., & DiRuggiero, J. (2010). MutS and MutL are dispensable for maintenance of the genomic mutation rate in the halophilic archaeon Halobacterium salinarum NRC-1. PloS one, 5(2), e9045. https://doi.org/10.1371/journal.pone.0009045

Cadet, J., & Douki, T. (2018). Formation of UV-induced DNA damage contributing to skin cancer development. *Photochemical & Photobiological Sciences*, *17*(12), 1816-1841

Cagney, G., Alvaro, D., Reid, R. J., Thorpe, P. H., Rothstein, R., & Krogan, N. J. (2006). Functional genomics of the yeast DNA-damage response. Genome biology, 7(9), 233. https://doi.org/10.1186/gb-2006-7-9-233

Cassier-Chauvat, C., Veaudor, T., & Chauvat, F. (2016). Comparative Genomics of DNA Recombination and Repair in Cyanobacteria: Biotechnological Implications. Frontiers in microbiology, 7, 1809. https://doi.org/10.3389/fmicb.2016.01809

Chakraborty, U., George, C. M., Lyndaker, A. M., & Alani, E. (2016). A delicate balance between repair and replication factors regulates recombination between divergent DNA sequences in Saccharomyces cerevisiae. *Genetics*, *202*(2), 525-540

Chang, Y., Gong, L., Yuan, W., Li, X., Chen, G., Li, X., Zhang, Q., & Wu, C. (2009). Replication protein A (RPA1a) is required for meiotic and somatic DNA repair but is dispensable for DNA replication and homologous recombination in rice. Plant physiology, 151(4), 2162–2173. https://doi.org/10.1104/pp.109.142877

Charbonnel, C., Gallego, M. E., & White, C. I. (2010). Xrcc1-dependent and Ku-dependent DNA double-strand break repair kinetics in *Arabidopsis* plants. The Plant journal: for cell and molecular biology, 64(2), 280–290. https://doi.org/10.1111/j.1365-313X.2010.04331.x

Chatterjee, N., & Walker, G. C. (2017). Mechanisms of DNA damage, repair, and mutagenesis. Environmental and molecular mutagenesis, 58(5), 235–263. https://doi.org/10.1002/em.22087

Chen, Y. W., Tajima, T., & Agrawal, S. (2011). The crystal structure of the ubiquitin-like (UbL) domain of human homologue A of Rad23 (hHR23A) protein. Protein engineering, design & selection: PEDS, 24(1-2), 131–138. https://doi.org/10.1093/protein/gzq084

Chen, Y., Qian, J., You, L., Zhang, X., Jiao, J., Liu, Y., & Zhao, J. (2018). Subunit Interaction Differences Between the Replication Factor C Complexes in *Arabidopsis* and Rice. Frontiers in plant science, 9, 779. https://doi.org/10.3389/fpls.2018.00779

Ciapponi, L., Cenci, G., & Gatti, M. (2006). The Drosophila Nbs protein functions in multiple pathways for the maintenance of genome stability. Genetics, 173(3), 1447–1454. https://doi.org/10.1534/genetics.106.058081

Corfield, J. (Invalid Date). base excision repair. Encyclopedia Britannica. https://www.britannica.com/science/base-excision-repair

Costa, R. M., Morgante, P. G., Berra, C. M., Nakabashi, M., Bruneau, D., Bouchez, D., Sweder, K. S., Van Sluys, M. A., & Menck, C. F. (2001). The participation of AtXPB1, the XPB/RAD25 homologue gene from *Arabidopsis thaliana*, in DNA repair and plant development. The Plant journal : for cell and molecular biology, 28(4), 385–395. https://doi.org/10.1046/j.1365-313x.2001.01162.x

Cox, M. M. (2013). Proteins pinpoint double strand breaks. eLife, 2, e01561. https://doi.org/10.7554/eLife.01561

Cromie, G. A., Connelly, J. C., & Leach, D. R. (2001). Recombination at double-strand breaks and DNA ends: conserved mechanisms from phage to humans. Molecular cell, 8(6), 1163–1174. https://doi.org/10.1016/s1097-2765(01)00419-1

Cui, X., Lu, F., Li, Y., Xue, Y., Kang, Y., Zhang, S., Qiu, Q., Cui, X., Zheng, S., Liu, B., Xu, X., & Cao, X. (2013). Ubiquitin-specific proteases UBP12 and UBP13 act in circadian clock and photoperiodic flowering regulation in *Arabidopsis*. Plant physiology, 162(2), 897–906. https://doi.org/10.1104/pp.112.213009

Dalhus, B., Laerdahl, J. K., Backe, P. H., & Bjørås, M. (2009). DNA base repair--recognition and initiation of catalysis. FEMS microbiology reviews, 33(6), 1044–1078. https://doi.org/10.1111/j.1574-6976.2009.00188.x

Dantuma, N. P., Heinen, C., & Hoogstraten, D. (2009). The ubiquitin receptor Rad23: at the crossroads of nucleotide excision repair and proteasomal degradation. DNA repair, 8(4), 449–460. https://doi.org/10.1016/j.dnarep.2009.01.005

Darmon, E., Eykelenboom, J. K., Lopez-Vernaza, M. A., White, M. A., & Leach, D. R. (2014). Repair on the go: E. coli maintains a high proliferation rate while repairing a chronic DNA double-strand break. PLoS One, 9(10), e110784.

Davis, A. J., & Chen, D. J. (2013). DNA double strand break repair via non-homologous end-joining. Translational cancer research, 2(3), 130–143. https://doi.org/10.3978/j.issn.2218-676X.2013.04.02

De Zio, D., Cianfanelli, V., & Cecconi, F. (2013). New insights into the link between DNA damage and apoptosis. Antioxidants & redox signaling, 19(6), 559–571. https://doi.org/10.1089/ars.2012.4938

den Dulk, B., van Eijk, P., de Ruijter, M., Brandsma, J. A., & Brouwer, J. (2008). The NER protein Rad33 shows functional homology to human Centrin2 and is involved in modification of Rad4. DNA repair, 7(6), 858–868. https://doi.org/10.1016/j.dnarep.2008.02.004

Derkacheva, M., Liu, S., Figueiredo, D. D., Gentry, M., Mozgova, I., Nanni, P., ... & Hennig, L. (2016). H2A deubiquitinases UBP12/13 are part of the *Arabidopsis* polycomb group protein system. Nature plants, 2(9), 1-10

Dillingham, M. S., & Kowalczykowski, S. C. (2008). RecBCD enzyme and the repair of double-stranded DNA breaks. Microbiology and molecular biology reviews : MMBR, 72(4), 642–671. https://doi.org/10.1128/MMBR.00020-08

Dotto, M., & Casati, P. (2017). Developmental reprogramming by UV-B radiation in plants. Plant science : an international journal of experimental plant biology, 264, 96–101. https://doi.org/10.1016/j.plantsci.2017.09.006

Duan, M., Selvam, K., Wyrick, J. J., & Mao, P. (2020). Genome-wide role of Rad26 in promoting transcription-coupled nucleotide excision repair in yeast chromatin. Proceedings of the National Academy of Sciences of the United States of America, 117(31), 18608–18616. https://doi.org/10.1073/pnas.2003868117

Dudásová, Z., Dudás, A., & Chovanec, M. (2004). Non-homologous end-joining factors of Saccharomyces cerevisiae. FEMS microbiology reviews, 28(5), 581–601. https://doi.org/10.1016/j.femsre.2004.06.001

Elez, M. (2021). Mismatch Repair: From Preserving Genome Stability to Enabling Mutation Studies in Real-Time Single Cells. Cells, 10(6), 1535. https://doi.org/10.3390/cells10061535

El-Mahdy, M. A., Zhu, Q., Wang, Q. E., Wani, G., Prætorius-Ibba, M., & Wani, A. A. (2006). Cullin 4A-mediated proteolysis of DDB2 protein at DNA damage sites regulates in vivo lesion recognition by XPC. The Journal of biological chemistry, 281(19), 13404–13411. https://doi.org/10.1074/jbc.M511834200

Epshtein, V., Kamarthapu, V., McGary, K., Svetlov, V., Ueberheide, B., Proshkin, S., Mironov, A., & Nudler, E. (2014). UvrD facilitates DNA repair by pulling RNA polymerase backwards. Nature, 505(7483), 372–377. https://doi.org/10.1038/nature12928

Essen, L. O., & Klar, T. (2006). Light-driven DNA repair by photolyases. Cellular and molecular life sciences : CMLS, 63(11), 1266–1277. https://doi.org/10.1007/s00018-005-5447-y

Evans, E., Fellows, J., Coffer, A., & Wood, R. D. (1997). Open complex formation around a lesion during nucleotide excision repair provides a structure for cleavage by human XPG protein. The EMBO journal, 16(3), 625–638. https://doi.org/10.1093/emboj/16.3.625

Fagbemi, A. F., Orelli, B., & Schärer, O. D. (2011). Regulation of endonuclease activity in human nucleotide excision repair. DNA repair, 10(7), 722–729. https://doi.org/10.1016/j.dnarep.2011.04.022

Farmer, L. M., Book, A. J., Lee, K. H., Lin, Y. L., Fu, H., & Vierstra, R. D. (2010). The RAD23 family provides an essential connection between the 26S proteasome and ubiquitylated proteins in *Arabidopsis*. The Plant Cell, 22(1), 124-142

Featherstone, C., & Jackson, S. P. (1999). DNA double-strand break repair. Current biology : CB, 9(20), R759–R761. https://doi.org/10.1016/S0960-9822(00)80005-6

Feldmann, H., Driller, L., Meier, B., Mages, G., Kellermann, J., & Winnacker, E. L. (1996). HDF2, the second subunit of the Ku homologue from Saccharomyces cerevisiae. The Journal of biological chemistry, 271(44), 27765–27769. https://doi.org/10.1074/jbc.271.44.27765

Fernet, M., Gribaa, M., Salih, M. A., Seidahmed, M. Z., Hall, J., & Koenig, M. (2005). Identification and functional consequences of a novel MRE11 mutation affecting 10 Saudi Arabian patients with the ataxia tELOAngiectasia-like disorder. Human molecular genetics, 14(2), 307–318. https://doi.org/10.1093/hmg/ddi027

Fidantsef, A. L., Mitchell, D. L., & Britt, A. B. (2000). The *Arabidopsis* UVH1 gene is a homolog of the yeast repair endonuclease RAD1. Plant physiology, 124(2), 579–586. https://doi.org/10.1104/pp.124.2.579

Fischer, E. S., Scrima, A., Böhm, K., Matsumoto, S., Lingaraju, G. M., Faty, M., Yasuda, T., Cavadini, S., Wakasugi, M., Hanaoka, F., Iwai, S., Gut, H., Sugasawa, K., & Thomä, N. H. (2011). The molecular basis of CRL4DDB2/CSA ubiquitin ligase architecture, targeting, and activation. Cell, 147(5), 1024–1039. https://doi.org/10.1016/j.cell.2011.10.035

Fishel, R. (2015). Mismatch repair. J. Biol. Chem. 290, 26395–26403. doi: 10.1074/jbc.R115.660142

Fortini, P., Parlanti, E., Sidorkina, O. M., Laval, J., & Dogliotti, E. (1999). The type of DNA glycosylase determines the base excision repair pathway in mammalian cells. The Journal of biological chemistry, 274(21), 15230–15236. https://doi.org/10.1074/jbc.274.21.15230.

Fousteri, M., & Mullenders, L. H. (2008). Transcription-coupled nucleotide excision repair in mammalian cells: molecular mechanisms and biological effects. Cell research, 18(1), 73–84. https://doi.org/10.1038/cr.2008.6

Fujiwara, Y., Masutani, C., Mizukoshi, T., Kondo, J., Hanaoka, F., & Iwai, S. (1999). Characterization of DNA recognition by the human UV-damaged DNA-binding protein. The Journal of biological chemistry, 274(28), 20027–20033. https://doi.org/10.1074/jbc.274.28.20027

Fukui, K. (2010). DNA mismatch repair in eukaryotes and bacteria. Journal of nucleic acids, 2010, 260512. https://doi.org/10.4061/2010/260512

Furukawa, T., Kimura, S., Ishibashi, T., Mori, Y., Hashimoto, J., & Sakaguchi, K. (2003). OsSEND-1: a new RAD2 nuclease family member in higher plants. Plant molecular biology, 51(1), 59–70. https://doi.org/10.1023/a:1020789314722

Gallego, M. E., Jeanneau, M., Granier, F., Bouchez, D., Bechtold, N., & White, C. I. (2001). Disruption of the *Arabidopsis* RAD50 gene leads to plant sterility and MMS sensitivity. The Plant journal : for cell and molecular biology, 25(1), 31–41. https://doi.org/10.1046

Ganpudi, A. L., & Schroeder, D. F. (2013). Genetic interactions of *Arabidopsis thaliana* damaged DNA binding protein 1B (DDB1B) with DDB1A, DET1, and COP1. G3 (Bethesda, Md.), 3(3), 493–503. https://doi.org/10.1534/g3.112.005249

Gary, R., Ludwig, D. L., Cornelius, H. L., MacInnes, M. A., & Park, M. S. (1997). The DNA repair endonuclease XPG binds to proliferating cell nuclear antigen (PCNA) and shares sequence elements with the PCNA-binding regions of FEN-1 and cyclin-dependent kinase inhibitor p21. The Journal of biological chemistry, 272(39), 24522–24529. https://doi.org/10.1074/jbc.272.39.24522

Giglia-Mari, G., Zotter, A., & Vermeulen, W. (2011). DNA damage response. Cold Spring Harbor perspectives in biology, 3(1), a000745. https://doi.org/10.1101/cshperspect.a000745
Gillette, T. G., Yu, S., Zhou, Z., Waters, R., Johnston, S. A., & Reed, S. H. (2006). Distinct functions of the ubiquitin-proteasome pathway influence nucleotide excision repair. The EMBO journal, 25(11), 2529–2538. https://doi.org/10.1038/sj.emboj.7601120
Grasser, M., Kane, C. M., Merkle, T., Melzer, M., Emmersen, J., & Grasser, K. D. (2009). Transcript elongation factor TFIIS is involved in *Arabidopsis* seed dormancy. Journal of molecular biology, 386(3), 598–611. https://doi.org/10.1016/j.jmb.2008.12.066
Greber, B. J., Toso, D. B., Fang, J., & Nogales, E. (2019). The complete structure of the human TFIIH core complex. eLife, 8, e44771. https://doi.org/10.7554/eLife.44771
Groisman, R., Polanowska, J., Kuraoka, I., Sawada, J., Saijo, M., Drapkin, R., Kisselev, A. F., Tanaka, K., & Nakatani, Y. (2003). The ubiquitin ligase activity in the DDB2 and CSA complexes is differentially regulated by the COP9 signalosome in response to DNA damage. Cell, 113(3), 357–367. https://doi.org/10.1016/s0092-8674(03)00316-7
Grundy, G. J., & Parsons, J. L. (2020). Base excision repair and its implications to cancer therapy. *Essays in biochemistry*, *64*(5), 831–843. https://doi.org/10.1042/EBC20200013
Gu, Y., Sekiguchi, J., Gao, Y., Dikkes, P., Frank, K., Ferguson, D., Hasty, P., Chun, J., & Alt, F. W. (2000). Defective embryonic neurogenesis in Ku-deficient but not DNA-dependent protein kinase catalytic subunit-deficient mice. Proceedings of the National Academy of Sciences of the United States of America, 97(6), 2668–2673. https://doi.org/10.1073/pnas.97.6.2668
Guzder, S. N., Sung, P., Prakash, L., & Prakash, S. (1999). Synergistic interaction between yeast nucleotide excision repair factors NEF2 and NEF4 in the binding of ultraviolet-damaged DNA. The Journal of biological chemistry, 274(34), 24257–24262. https://doi.org/10.1074/jbc.274.34.24257
Halmai, M., Frittmann, O., Szabo, Z., Daraba, A., Gali, V. K., Balint, E., & Unk, I. (2016). Mutations at the Subunit Interface of Yeast Proliferating Cell Nuclear Antigen Reveal a Versatile Regulatory Domain. PloS one, 11(8), e0161307. https://doi.org/10.1371/journal.pone.0161307
Hannss, R., & Dubiel, W. (2011). COP9 signalosome function in the DDR. *FEBS letters*, *585*(18), 2845–2852. https://doi.org/10.1016/j.febslet.2011.04.027
Hsu, D. S., Zhao, X., Zhao, S., Kazantsev, A., Wang, R. P., Todo, T., Wei, Y. F., & Sancar, A. (1996). Putative human blue-light photoreceptors hCRY1 and hCRY2 are flavoproteins. Biochemistry, 35(44), 13871–13877. https://doi.org/10.1021/bi962209o
Huffman, J. L., Sundheim, O., & Tainer, J. A. (2005). DNA base damage recognition and removal: new twists and grooves. Mutation research, 577(1-2), 55–76. https://doi.org/10.1016/j.mrfmmm.2005.03.012
Hwang, B. J., Ford, J. M., Hanawalt, P. C., & Chu, G. (1999). Expression of the p48 xeroderma pigmentosum gene is p53-dependent and is involved in global genomic

repair. Proceedings of the National Academy of Sciences of the United States of America, 96(2), 424–428. https://doi.org/10.1073/pnas.96.2.424
Ishibashi, T., Kimura, S., FURUKAWA, T., & Sakaguchi, K. (2006). DNA repair mechanisms in UV-B tolerant plants. Japan Agricultural Research Quarterly: JARQ, 40(2), 107-113
Ishibashi, T., Kimura, S., Yamamoto, T., Furukawa, T., Takata, K., Uchiyama, Y., Hashimoto, J., & Sakaguchi, K. (2003). Rice UV-damaged DNA binding protein homologues are most abundant in proliferating tissues. Gene, 308, 79–87. https://doi.org/10.1016/s0378-1119(03)00447-5
Jackson, S. P., & Bartek, J. (2009). The DNA-damage response in human biology and disease. Nature, 461(7267), 1071–1078. https://doi.org/10.1038/nature08467
Johann To Berens, P., & Molinier, J. (2020). Formation and Recognition of UV-Induced DNA Damage within Genome Complexity. International journal of molecular sciences, 21(18), 6689. https://doi.org/10.3390/ijms21186689
Kao, Y. T., Saxena, C., Wang, L., Sancar, A., & Zhong, D. (2005). Direct observation of thymine dimer repair in DNA by photolyase. Proceedings of the National Academy of Sciences of the United States of America, 102(45), 16128–16132. https://doi.org/10.1073/pnas.0506586102
Kavakli, I. H., Ozturk, N., & Gul, S. (2019). DNA repair by photolyases. Advances in protein chemistry and structural biology, 115, 1–19. https://doi.org/10.1016/bs.apcsb.2018.10.003
Kim, J. K., Patel, D., & Choi, B. S. (1995). Contrasting structural impacts induced by cis-syn cyclobutane dimer and (6-4) adduct in DNA duplex decamers: implication in mutagenesis and repair activity. Photochemistry and photobiology, 62(1), 44–50. https://doi.org/10.1111/j.1751-1097.1995.tb05236.x
Kim, Y. J., & Wilson, D. M., 3rd (2012). Overview of base excision repair biochemistry. Current molecular pharmacology, 5(1), 3–13. https://doi.org/10.2174/1874467211205010003
Kisker, C., Kuper, J., & Van Houten, B. (2013). Prokaryotic nucleotide excision repair. Cold Spring Harbor perspectives in biology, 5(3), a012591. https://doi.org/10.1101/cshperspect.a012591
Kobaisi, F., Fayyad, N., Rezvani, H. R., Fayyad-Kazan, M., Sulpice, E., Badran, B., Fayyad-Kazan, H., Gidrol, X., & Rachidi, W. (2019). Signaling Pathways, Chemical and Biological Modulators of Nucleotide Excision Repair: The Faithful Shield against UV Genotoxicity. Oxidative medicine and cellular longevity, 2019, 4654206. https://doi.org/10.1155/2019/4654206
Krasikova, Y. S., Rechkunova, N. I., Maltseva, E. A., & Lavrik, O. I. (2018). RPA and XPA interaction with DNA structures mimicking intermediates of the late stages in nucleotide excision repair. PloS one, 13(1), e0190782. https://doi.org/10.1371/journal.pone.0190782
Kunihiro, S., Kowata, H., Kondou, Y., Takahashi, S., Matsui, M., Berberich, T., ... & Kusano, T. (2014). Overexpression of rice OsREX1-S, encoding a putative component of the core general transcription and DNA repair factor IIH, renders plant cells tolerant to cadmium-and UV-induced damage by enhancing DNA excision repair. Planta, 239(5), 1101-1111.

Kunz, B. A., Anderson, H. J., Osmond, M. J., & Vonarx, E. J. (2005). Components of nucleotide excision repair and DNA damage tolerance in *Arabidopsis thaliana*. Environmental and molecular mutagenesis, 45(2-3), 115–127. https://doi.org/10.1002/em.20094

Lahari, T., Lazaro, J., & Schroeder, D. F. (2017). RAD4 and RAD23/HMR Contribute to *Arabidopsis* UV Tolerance. Genes, 9(1), 8. https://doi.org/10.3390/genes9010008

Lahari, T., Lazaro, J., Marcus, J. M., & Schroeder, D. F. (2018). RAD7 homologues contribute to *Arabidopsis* UV tolerance. Plant science: an international journal of experimental plant biology, 277, 267–277. https://doi.org/10.1016/j.plantsci.2018.09.017

Lettieri, T., Kraehenbuehl, R., Capiaghi, C., Livingstone-Zatchej, M., & Thoma, F. (2008). Functionally distinct nucleosome-free regions in yeast require Rad7 and Rad16 for nucleotide excision repair. DNA repair, 7(5), 734–743. https://doi.org/10.1016/j.dnarep.2008.01.016

Li, B., Conway, N., Navarro, S., Comai, L., & Comai, L. (2005). A conserved and species-specific functional interaction between the Werner syndrome-like exonuclease atWEX and the Ku heterodimer in *Arabidopsis*. Nucleic acids research, 33(21), 6861–6867. https://doi.org/10.1093/nar/gki984

Li, G. M. (2008). Mechanisms and functions of DNA mismatch repair. Cell research, 18(1), 85–98. https://doi.org/10.1038/cr.2007.115

Li, S. (2015). Transcription coupled nucleotide excision repair in the yeast Saccharomyces cerevisiae: The ambiguous role of Rad26. DNA repair, 36, 43–48. https://doi.org/10.1016/j.dnarep.2015.09.006

Li, X., Guo, X., Zhao, L., Zhang, J., Tang, D., Zhao, X., & Liu, X. (2012). *Arabidopsis* rad23-4 gene is required for pollen development under UV-B light. African Journal of Biotechnology, 11(44), 10161-10169

Liang, L., Flury, S., Kalck, V., Hohn, B., & Molinier, J. (2006). CENTRIN2 interacts with the *Arabidopsis* homolog of the human XPC protein (AtRAD4) and contributes to efficient synthesis-dependent repair of bulky DNA lesions. Plant molecular biology, 61(1-2), 345–356. https://doi.org/10.1007/s11103-006-0016-9

Liu, Z., Hall, J. D., & Mount, D. W. (2001). *Arabidopsis* UVH3 gene is a homolog of the Saccharomyces cerevisiae RAD2 and human XPG DNA repair genes. The Plant journal: for cell and molecular biology, 26(3), 329–338. https://doi.org/10.1046/j.1365-313x.2001.01031.x

Liu, Z., Hong, S. W., Escobar, M., Vierling, E., Mitchell, D. L., Mount, D. W., & Hall, J. D. (2003). *Arabidopsis* UVH6, a homolog of human XPD and yeast RAD3 DNA repair genes, functions in DNA repair and is essential for plant growth. Plant physiology, 132(3), 1405–1414. https://doi.org/10.1104/pp.103.021808

Liu, Z., Hossain, G. S., Islas-Osuna, M. A., Mitchell, D. L., & Mount, D. W. (2000). Repair of UV damage in plants by nucleotide excision repair: *Arabidopsis* UVH1 DNA repair gene is a homolog of Saccharomyces cerevisiae Rad1. The Plant journal : for cell and molecular biology, 21(6), 519–528. https://doi.org/10.1046/j.1365-313x.2000.00707.x

Maclean, M. J., Aamodt, R., Harris, N., Alseth, I., Seeberg, E., Bjørås, M., & Piper, P. W. (2003). Base excision repair activities required for yeast to attain a full chronological life span. *Aging cell*, *2*(2), 93-104

Manova, V., & Gruszka, D. (2015). DNA damage and repair in plants - from models to crops. Frontiers in plant science, 6, 885. https://doi.org/10.3389/fpls.2015.00885
Marizcurrena, J. J., Acosta, S., Canclini, L., Hernández, P., Vallés, D., Lamparter, T., & Castro-Sowinski, S. (2020). A natural occurring bifunctional CPD/(6-4)-photolyase from the Antarctic bacterium Sphingomonas sp. UV9. Applied microbiology and biotechnology, 104(16), 7037–7050. https://doi.org/10.1007/s00253-020-10734-5
Marshall, C. J., & Santangelo, T. J. (2020). Archaeal DNA Repair Mechanisms. Biomolecules, 10(11), 1472. https://doi.org/10.3390/biom10111472
Marteijn, J. A., Lans, H., Vermeulen, W., & Hoeijmakers, J. H. (2014). Understanding nucleotide excision repair and its roles in cancer and ageing. Nature reviews Molecular cell biology, 15(7), 465-481
Matsumoto, Y., Asa, A., Modak, C., & Shimada, M. (2021). DNA-Dependent Protein Kinase Catalytic Subunit: The Sensor for DNA Double-Strand Breaks Structurally and Functionally RELOAted to Ataxia TELOAngiectasia Mutated. Genes, 12(8), 1143. https://doi.org/10.3390/genes12081143
McKinnon, P. J., & Caldecott, K. W. (2007). DNA strand break repair and human genetic disease. Annual review of genomics and human genetics, 8, 37–55. https://doi.org/10.1146/annurev.genom.7.080505.115648
Melis, J. P., van Steeg, H., & Luijten, M. (2013). Oxidative DNA damage and nucleotide excision repair. Antioxidants & redox signaling, 18(18), 2409–2419. https://doi.org/10.1089/ars.2012.5036
Min, J. H., & Pavletich, N. P. (2007). Recognition of DNA damage by the Rad4 nucleotide excision repair protein. Nature, 449(7162), 570–575. https://doi.org/10.1038/nature06155
Molinier, J., Lechner, E., Dumbliauskas, E., & Genschik, P. (2008). Regulation and role of *Arabidopsis* CUL4-DDB1A-DDB2 in maintaining genome integrity upon UV stress. PLoS genetics, 4(6), e1000093. https://doi.org/10.1371/journal.pgen.1000093
Molinier, J., Ramos, C., Fritsch, O., & Hohn, B. (2004). CENTRIN2 modulates homologous recombination and nucleotide excision repair in *Arabidopsis*. The Plant cell, 16(6), 1633–1643. https://doi.org/10.1105/tpc.021378
Morgante, P. G., Berra, C. M., Nakabashi, M., Costa, R. M., Menck, C. F., & Van Sluys, M. A. (2005). Functional XPB/RAD25 redundancy in *Arabidopsis* genome: characterization of AtXPB2 and expression analysis. Gene, 344, 93–103. https://doi.org/10.1016/j.gene.2004.10.006
Murphy, T. M., Belmonte, M., Shu, S., Britt, A. B., Hatteroth, J. (2009). Requirement for abasic endonuclease gene homologues in *Arabidopsis* seed development. PLoS One 4 (1), e4297. doi: 10.1371/journal.pone.0004297
Nakazawa, Y., Hara, Y., Oka, Y., Komine, O., van den Heuvel, D., Guo, C., Daigaku, Y., Isono, M., He, Y., Shimada, M., Kato, K., Jia, N., Hashimoto, S., Kotani, Y., Miyoshi, Y., Tanaka, M., Sobue, A., Mitsutake, N., Suganami, T., Masuda, A., … Ogi, T. (2020)). Ubiquitination of DNA Damage-Stalled RNAPII Promotes Transcription-Coupled Repair. Cell, 180(6), 1228–1244.e24. https://doi.org/10.1016/j.cell.2020.02.010
Niida, H., & Nakanishi, M. (2006). DNA damage checkpoints in mammals. Mutagenesis, 21(1), 3–9. https://doi.org/10.1093/mutage/gei063

Nishi, R., Okuda, Y., Watanabe, E., Mori, T., Iwai, S., Masutani, C., Sugasawa, K., & Hanaoka, F. (2005). Centrin 2 stimulates nucleotide excision repair by interacting with xeroderma pigmentosum group C protein. Molecular and cellular biology, 25(13), 5664–5674. https://doi.org/10.1128/MCB.25.13.5664-5674.2005

Okuda, M., Nakazawa, Y., Guo, C., Ogi, T., & Nishimura, Y. (2017). Common TFIIH recruitment mechanism in global genome and transcription-coupled repair subpathways. Nucleic acids research, 45(22), 13043–13055. https://doi.org/10.1093/nar/gkx970

Okumura, F., Matsuzaki, M., Nakatsukasa, K., & Kamura, T. (2012). The Role of Elongin BC-Containing Ubiquitin Ligases. Frontiers in oncology, 2, 10. https://doi.org/10.3389/fonc.2012.00010

Papamichos-Chronakis, M., & Peterson, C. L. (2013). Chromatin and the genome integrity network. Nature reviews. Genetics, 14(1), 62–75. https://doi.org/10.1038/nrg3345

Pâques, F., & Haber, J. E. (1999). Multiple pathways of recombination induced by double-strand breaks in Saccharomyces cerevisiae. Microbiology and molecular biology reviews : MMBR, 63(2), 349–404. https://doi.org/10.1128/MMBR.63.2.349-404.1999

Pathak, J., Rajneesh, Singh, P., Häder, D., & Sinha, R. (2019). UV-induced DNA damage and repair: A cyanobacterial perspective. Plant Gene, 19, 100194.

Peng, Y., Wang, H., Santana-Santos, L., Kisker, C., & Houten, B. V. (2011). Nucleotide excision repair from bacteria to humans: Structure–function studies. In Chemical Carcinogenesis (pp. 267-296). Humana Press.

Petruseva, I. O., Evdokimov, A. N., & Lavrik, O. I. (2014). Molecular mechanism of global genome nucleotide excision repair. Acta naturae, 6(1), 23–34

Prakash, S., & Prakash, L. (2000). Nucleotide excision repair in yeast. Mutation research, 451(1-2), 13–24. https://doi.org/10.1016/s0027-5107(00)00037-3

Ramsey, K. L., Smith, J. J., Dasgupta, A., Maqani, N., Grant, P., & Auble, D. T. (2004). The NEF4 complex regulates Rad4 levels and utilizes Snf2/Swi2-rELOAted ATPase activity for nucleotide excision repair. Molecular and cellular biology, 24(14), 6362–6378. https://doi.org/10.1128/MCB.24.14.6362-6378.2004

Rapić-Otrin, V., McLenigan, M. P., Bisi, D. C., Gonzalez, M., & Levine, A. S. (2002). Sequential binding of UV DNA damage binding factor and degradation of the p48 subunit as early events after UV irradiation. *Nucleic acids research*, *30*(11), 2588-2598

Rastogi, R. P., Richa, Kumar, A., Tyagi, M. B., & Sinha, R. P. (2010). Molecular mechanisms of ultraviolet radiation-induced DNA damage and repair. Journal of nucleic acids, 2010, 592980. https://doi.org/10.4061/2010/592980

Reed, S. H. (2005). Nucleotide excision repair in chromatin: the shape of things to come. DNA repair, 4(8), 909-918

Reid-Bayliss, K. S., Arron, S. T., Loeb, L. A., Bezrookove, V., & Cleaver, J. E. (2016). Why Cockayne syndrome patients do not get cancer despite their DNA repair deficiency. Proceedings of the National Academy of Sciences of the United States of America, 113(36), 10151–10156. https://doi.org/10.1073/pnas.1610020113

Ribar, B., Prakash, L., & Prakash, S. (2006). Requirement of ELOC1 for RNA polymerase II polyubiquitylation and degradation in response to DNA damage in

Saccharomyces cerevisiae. Molecular and cellular biology, 26(11), 3999–4005. https://doi.org/10.1128/MCB.00293-06
Risseeuw, E. P., Daskalchuk, T. E., Banks, T. W., Liu, E., Cotelesage, J., Hellmann, H., Estelle, M., Somers, D. E., & Crosby, W. L. (2003). Protein interaction analysis of SCF ubiquitin E3 ligase subunits from *Arabidopsis*. The Plant journal : for cell and molecular biology, 34(6), 753–767. https://doi.org/10.1046/j.1365-313x.2003.01768.x
Roldán-Arjona, T., Ariza, R. R., & Córdoba-Cañero, D. (2019). DNA Base Excision Repair in Plants: An Unfolding Story With Familiar and Novel Characters. Frontiers in plant science, 10, 1055. https://doi.org/10.3389/fpls.2019.01055
Rüthemann, P., Balbo Pogliano, C., & Naegeli, H. (2016). Global-genome Nucleotide Excision Repair Controlled by Ubiquitin/Sumo Modifiers. Frontiers in genetics, 7, 68. https://doi.org/10.3389/fgene.2016.00068
Sachadyn, P. (2010). Conservation and diversity of MutS proteins. Mutation Research/Fundamental and Molecular Mechanisms of Mutagenesis, 694(1-2), 20-30
Sakai, W., Yuasa-Sunagawa, M., Kusakabe, M., Kishimoto, A., Matsui, T., Kaneko, Y., Akagi, J. I., Huyghe, N., Ikura, M., Ikura, T., Hanaoka, F., Yokoi, M., & Sugasawa, K. (2020). Functional impacts of the ubiquitin-proteasome system on DNA damage recognition in global genome nucleotide excision repair. Scientific reports, 10(1), 19704. https://doi.org/10.1038/s41598-020-76898-2
Sancar, A. (1996). DNA excision repair. Annual review of biochemistry, 65(1), 43-81.
Sarangi, P., Bartosova, Z., Altmannova, V., Holland, C., Chavdarova, M., Lee, S. E., Krejci, L., & Zhao, X. (2014). Sumoylation of the Rad1 nuclease promotes DNA repair and regulates its DNA association. Nucleic acids research, 42(10), 6393–6404. https://doi.org/10.1093/nar/gku300
Schormann, N., Ricciardi, R., & Chattopadhyay, D. (2014). Uracil-DNA glycosylases-structural and functional perspectives on an essential family of DNA repair enzymes. Protein science : a publication of the Protein Society, 23(12), 1667–1685. https://doi.org/10.1002/pro.2554
Schroeder, D. F., Gahrtz, M., Maxwell, B. B., Cook, R. K., Kan, J. M., Alonso, J. M., Ecker, J. R., & Chory, J. (2002). De-etiolated 1 and damaged DNA binding protein 1 interact to regulate *Arabidopsis* photomorphogenesis. Current biology: CB, 12(17), 1462–1472. https://doi.org/10.1016/s0960-9822(02)01106-5
Schuch, A. P., Moreno, N. C., Schuch, N. J., Menck, C., & Garcia, C. (2017). Sunlight damage to cellular DNA: Focus on oxidatively generated lesions. Free radical biology & medicine, 107, 110–124. https://doi.org/10.1016/j. freeradbiomed.2017. 01.029
Schul, W., Jans, J., Rijksen, Y.M., Klemann, K., Eker, A.P., de Wit, J., Nikaido, O., Nakajima, S., Yasui, A., Hoeijmakers, J.H., & van der Horst, G.T. (2002). Enhanced repair of cyclobutane pyrimidine dimers and improved UV resistance in photolyase transgenic mice. The EMBO Journal, 21.
Schwertman, P., Vermeulen, W., & Marteijn, J. A. (2013). UVSSA and USP7, a new couple in transcription-coupled DNA repair. Chromosoma, 122(4), 275–284. https://doi.org/10.1007/s00412-013-0420-2

Scrima, A., Konícková, R., Czyzewski, B. K., Kawasaki, Y., Jeffrey, P. D., Groisman, R., Nakatani, Y., Iwai, S., Pavletich, N. P., & Thomä, N. H. (2008). Structural basis of UV DNA-damage recognition by the DDB1-DDB2 complex. Cell, 135(7), 1213–1223. https://doi.org/10.1016/j.cell.2008.10.045

Seemanová, E., Sperling, K., Neitzel, H., Varon, R., Hadac, J., Butova, O., Schröck, E., Seeman, P., & Digweed, M. (2006). Nijmegen breakage syndrome (NBS) with neurological abnormalities and without chromosomal instability. Journal of medical genetics, 43(3), 218–224. https://doi.org/10.1136/jmg.2005.035287

Shaked, H., Avivi-Ragolsky, N., & Levy, A. A. (2006). Involvement of the *Arabidopsis* SWI2/SNF2 chromatin remodeling gene family in DNA damage response and recombination. Genetics, 173(2), 985–994. https://doi.org/10.1534/genetics.105.051664

Sharma, R., Lewis, S., & Wlodarski, M. W. (2020). DNA Repair Syndromes and Cancer: Insights Into Genetics and Phenotype Patterns. Frontiers in pediatrics, 8, 570084. https://doi.org/10.3389/fped.2020.570084

Shen, Z., & Nickoloff, J. A. (2007). Mammalian homologous recombination repair and cancer intervention. In DNA repair, genetic instability, and cancer (pp. 119-156)

Shrivastav, M., De Haro, L. P., & Nickoloff, J. A. (2008). Regulation of DNA double-strand break repair pathway choice. Cell research, 18(1), 134–147. https://doi.org/10.1038/cr.2007.111

Shu, K., & Yang, W. (2017). E3 Ubiquitin Ligases: Ubiquitous Actors in Plant Development and Abiotic Stress Responses. Plant & cell physiology, 58(9), 1461–1476. https://doi.org/10.1093/pcp/pcx071

Shuck, S. C., Short, E. A., & Turchi, J. J. (2008). Eukaryotic nucleotide excision repair: from understanding mechanisms to influencing biology. Cell research, 18(1), 64–72. https://doi.org/10.1038/cr.2008.2

Shultz, R. W., Tatineni, V. M., Hanley-Bowdoin, L., & Thompson, W. F. (2007). Genome-wide analysis of the core DNA replication machinery in the higher plants *Arabidopsis* and rice. Plant physiology, 144(4), 1697–1714. https://doi.org/10.1104/pp.107.101105

Sinha, R. P., & Häder, D. P. (2002). UV-induced DNA damage and repair: a review. Photochemical & photobiological sciences: Official journal of the European Photochemistry Association and the European Society for Photobiology, 1(4), 225–236. https://doi.org/10.1039/b201230h

Spampinato, C. P. (2017). Protecting DNA from errors and damage: an overview of DNA repair mechanisms in plants compared to mammals. Cellular and molecular life sciences : CMLS, 74(9), 1693–1709. https://doi.org/10.1007/s00018-016-2436-2

Spivak, G. (2015). Nucleotide excision repair in humans. DNA repair, 36, 13–18. https://doi.org/10.1016/j.dnarep.2015.09.003

Spivak, G. (2016). Transcription-coupled repair: an update. Archives of toxicology, 90(11), 2583–2594. https://doi.org/10.1007/s00204-016-1820-x

Strzałka, W., Zgłobicki, P., Kowalska, E., Bażant, A., Dziga, D., & Banaś, A. K. (2020). The Dark Side of UV-Induced DNA Lesion Repair. Genes, 11(12), 1450. https://doi.org/10.3390/genes11121450

Sugasawa, K. (2011). Multiple DNA damage recognition factors involved in mammalian nucleotide excision repair. Biochemistry. Biokhimiia, 76(1), 16–23. https://doi.org/10.1134/s0006297911010044
Sugasawa, K. (2016). Molecular mechanisms of DNA damage recognition for mammalian nucleotide excision repair. DNA repair, 44, 110–117. https://doi.org/10.1016/j.dnarep.2016.05.015
Takashi, Y., Kobayashi, Y., Tanaka, K., & Tamura, K. (2009). *Arabidopsis* replication protein A 70a is required for DNA damage response and telomere length homeostasis. Plant and cell physiology, 50(11), 1965-1976.
Tamura, K., Adachi, Y., Chiba, K., Oguchi, K., & Takahashi, H. (2002). Identification of Ku70 and Ku80 homologues in *Arabidopsis thaliana*: evidence for a role in the repair of DNA double-strand breaks. The Plant journal : for cell and molecular biology, 29(6), 771–781. https://doi.org/10.1046/j.1365-313x.2002.01258.x
Taylor, J. S. (1995). DNA, sunlight and skin cancer. Pure and applied chemistry, 67(1), 183-190
Thoma, F. (1999). Light and dark in chromatin repair: repair of UV-induced DNA lesions by photolyase and nucleotide excision repair. The EMBO journal, 18(23), 6585–6598. https://doi.org/10.1093/emboj/18.23.6585
Thomann, A., Brukhin, V., Dieterle, M., Gheyeselinck, J., Vantard, M., Grossniklaus, U., & Genschik, P. (2005). *Arabidopsis* CUL3A and CUL3B genes are essential for normal embryogenesis. The Plant journal: for cell and molecular biology, 43(3), 437–448. https://doi.org/10.1111
Todo, T. (1999). Functional diversity of the DNA photolyase/blue light receptor family. Mutation research, 434(2), 89–97. https://doi.org/10.1016/s0921-8777(99)00013-0
Tubbs, A., & Nussenzweig, A. (2017). Endogenous DNA Damage as a Source of Genomic Instability in Cancer. Cell, 168(4), 644–656. https://doi.org/10.1016/j.cell.2017.01.002
Tuteja, N., Singh, M. B., Misra, M. K., Bhalla, P. L., & Tuteja, R. (2001). Molecular mechanisms of DNA damage and repair: progress in plants. Critical reviews in biochemistry and molecular biology, 36(4), 337–397. https://doi.org/10.1080/20014091074219
van der Burg, M., Ijspeert, H., Verkaik, N. S., Turul, T., Wiegant, W. W., Morotomi-Yano, K., Mari, P. O., Tezcan, I., Chen, D. J., Zdzienicka, M. Z., van Dongen, J. J., & van Gent, D. C. (2009). A DNA-PKcs mutation in a radiosensitive T-B- SCID patient inhibits Artemis activation and nonhomologous end-joining. The Journal of clinical investigation, 119(1), 91–98. https://doi.org/10.1172/JCI37141
Vonarx, E. J., Tabone, E. K., Osmond, M. J., Anderson, H. J., & Kunz, B. A. (2006). *Arabidopsis* homologue of human transcription factor IIH/nucleotide excision repair factor p44 can function in transcription and DNA repair and interacts with AtXPD. The Plant journal: for cell and molecular biology, 46(3), 512–521. https://doi.org/10.1111/j.1365-313X.2006.02705.x
Wacker, M., & Holick, M. F. (2013). Sunlight and Vitamin D: A global perspective for health. Dermato-endocrinology, *5*(1), 51–108. https://doi.org/10.4161/derm.24494
Wang, A., Chen, D., Ma, Q., Rose, J., Fei, Z., Liu, Y., & Giovannoni, J. J. (2019). The tomato HIGH PIGMENT1/DAMAGED DNA BINDING PROTEIN 1 gene contributes

to regulation of fruit ripening. Horticulture research, 6, 15. https://doi.org/10.1038/s41438-018-0093-3
Wang, H., Zhai, L., Xu, J., Joo, H. Y., Jackson, S., Erdjument-Bromage, H., Tempst, P., Xiong, Y., & Zhang, Y. (2006). Histone H3 and H4 ubiquitylation by the CUL4-DDB-ROC1 ubiquitin ligase facilitates cellular response to DNA damage. Molecular cell, 22(3), 383–394. https://doi.org/10.1016/j.molcel.2006.03.035
Waters, R., van Eijk, P., & Reed, S. (2015). Histone modification and chromatin remodeling during NER. DNA repair, 36, 105–113. https://doi.org/10.1016/j.dnarep.2015.09.013
Weber, S. (2005). Light-driven enzymatic catalysis of DNA repair: a review of recent biophysical studies on photolyase. Biochimica et biophysica acta, 1707(1), 1–23. https://doi.org/10.1016/j.bbabio.2004.02.010
West, C. E., Waterworth, W. M., Jiang, Q., & Bray, C. M. (2000). *Arabidopsis* DNA ligase IV is induced by gamma-irradiation and interacts with an *Arabidopsis* homologue of the double strand break repair protein XRCC4. The Plant journal: for cell and molecular biology, 24(1), 67–78. https://doi.org/10.1046/j.1365-313x.2000.00856.x
West, C. E., Waterworth, W. M., Story, G. W., Sunderland, P. A., Jiang, Q., & Bray, C. M. (2002). Disruption of the *Arabidopsis* AtKu80 gene demonstrates an essential role for AtKu80 protein in efficient repair of DNA double-strand breaks in vivo. The Plant journal: for cell and molecular biology, 31(4), 517–528. https://doi.org/10.1046/j.1365-313x.2002.01370.x
Weterings, E., & Chen, D. J. (2007). DNA-dependent protein kinase in nonhomologous end joining: a lock with multiple keys?. The Journal of cell biology, 179(2), 183–186. https://doi.org/10.1083/jcb.200705106
White, M. F. (2011). Homologous recombination in the archaea: the means justify the ends. Biochemical Society transactions, 39(1), 15–19. https://doi.org/10.1042/BST0390015
Wood, R. D. (1997). Nucleotide excision repair in mammalian cells. The Journal of biological chemistry, 272(38), 23465–23468. https://doi.org/10.1074/jbc.272.38.23465
Wu, X., Braithwaite, E., & Wang, Z. (1999). DNA ligation during excision repair in yeast cell-free extracts is specifically catalyzed by the CDC9 gene product. Biochemistry, 38(9), 2628-2635.
Wu, X., Guo, D., Yuan, F., & Wang, Z. (2001). Accessibility of DNA polymerases to repair synthesis during nucleotide excision repair in yeast cell-free extracts. Nucleic acids research, 29(14), 3123–3130. https://doi.org/10.1093/nar/29.14.3123
Xanthoudakis, S., Smeyne, R. J., Wallace, J. D., Curran, T. (1996). The redox/DNA repair protein, Ref-1, is essential for early embryonic development in mice. Proc. Natl. Acad. Sci. U.S.A. 93 (17), 8919–8923. doi: 10.1073/pnas.93.17.8919
Xie, Z., Liu, S., Zhang, Y., & Wang, Z. (2004). Roles of Rad23 protein in yeast nucleotide excision repair. Nucleic acids research, 32(20), 5981–5990. https://doi.org/10.1093/nar/gkh934
Xue, C., Liang, K., Liu, Z., Wen, R., & Xiao, W. (2015). Similarities and differences between *Arabidopsis* PCNA1 and PCNA2 in complementing the yeast DNA

damage tolerance defect. DNA repair, 28, 28–36. https://doi.org/10.1016/j.dnarep.2015.02.003
Yagura, T., Makita, K., Yamamoto, H., Menck, C. F., & Schuch, A. P. (2011). Biological sensors for solar ultraviolet radiation. Sensors (Basel, Switzerland), 11(4), 4277–4294. https://doi.org/10.3390/s110404277
Yasui, A., & McCready, S. J. (1998). Alternative repair pathways for UV-induced DNA damage. BioEssays : news and reviews in molecular, cellular and developmental biology, 20(4), 291–297. https://doi.org/10.1002/(SICI)1521-1878(199804)20:4<291::AID-BIES5>3.0.CO;2-T
Yousefzadeh, M., Henpita, C., Vyas, R., Soto-Palma, C., Robbins, P., & Niedernhofer, L. (2021). DNA damage-how and why we age? eLife, 10, e62852. https://doi.org/10.7554/eLife.62852
Yu, S. L., & Lee, S. K. (2017). Ultraviolet radiation: DNA damage, repair, and human disorders. Molecular & Cellular Toxicology, 13(1), 21-28.
Yu, S., Smirnova, J. B., Friedberg, E. C., Stillman, B., Akiyama, M., Owen-Hughes, T., Waters, R., & Reed, S. H. (2009). ABF1-binding sites promote efficient global genome nucleotide excision repair. The Journal of biological chemistry, 284(2), 966–973. https://doi.org/10.1074/jbc.M806830200
Zhang, C., Guo, H., Zhang, J., Guo, G., Schumaker, K. S., & Guo, Y. (2010). *Arabidopsis* cockayne syndrome A-like proteins 1A and 1B form a complex with CULLIN4 and damage DNA binding protein 1A and regulate the response to UV irradiation. The Plant cell, 22(7), 2353–2369. https://doi.org/10.1105/tpc.110.073973
Zhou, H., Zhao, J., Cai, J., & Patil, S. B. (2017). UBIQUITIN-SPECIFIC PROTEASES function in plant development and stress responses. Plant Molecular Biology, 94(6), 565-576

Chapter 2. *Arabidopsis* RAD16 homologues are involved in UV tolerance and growth

Alrayes LN, Stout J, Schroeder DF. Manuscript in preparation.

2.1 Abstract

In plants, prolonged exposure to ultraviolet (UV) radiation causes harmful DNA lesions. NER is an important DNA repair mechanism that operates via two pathways: Transcription coupled repair (TC-NER) and global genomic repair (GG-NER). In plants and mammals, TC-NER is initiated by the Cockayne Syndrome A and B (CSA/CSB) complex; whereas GG-NER is initiated by the DAMAGED DNA BINDING PROTEIN 1/2 (DDB1/2) complex. In the yeast *S. cerevisiae*, GG-NER is initiated by RADIATION SENSITIVE 7 and 16, (RAD7/16) complex. *Arabidopsis* has two homologues of yeast RAD16, At1g05120 and At1g02670, I named these AtRAD16 and AtRAD16b, respectively. In this study, I characterized the roles of AtRAD16 and AtRAD16b. *Arabidopsis rad16* and *rad16b* null mutants exhibited increased UV sensitivity, showed early flowering time, and short silique lengths. Moreover, AtRAD16 overexpression increased plant UV tolerance. Thus, AtRAD16 and AtRAD16b contribute to plant UV tolerance and growth. Additionally, I found physical interaction between AtRAD16 and AtRAD7. Thus, the *Arabidopsis* RAD7/16 complex is functional in plant NER. Furthermore, AtRAD16 makes a significant contribution to *Arabidopsis* UV tolerance compared to the DDB1/2 and the CSB pathways.

2.2 Introduction

Plants are sessile organisms that must adapt and respond to their environment to successfully survive. Sunlight is an important part of a plant's environment, it contains both useful visible light that plants use for growth and development and harmful ultraviolet (UV) light. UV light has pleiotropic effects on plant development and can damage cellular structures including DNA. UV-induced DNA damage can alter transcription, replication, and cause genome instability (Mullenders 2018). Plants utilize two different repair mechanisms to repair UV- damaged DNA and maintain genome

integrity: light repair via photolyases (Essen & Klar 2006), and dark repair via nucleotide excision repair (NER). NER is a five step process consisting of initial recognition of UV-damaged DNA, helicase activity to open the double-helix, excision of the damaged base, incorporation of the correct base-paired nucleotide, and the final ligation of the repaired strand. NER is a well conserved repair process across both prokaryotes and eukaryotes. Defects in NER and failure to remove lesions from the genome cause xeroderma pigmentosa (UV-sensitivity with increased skin cancer risk) in humans (Petruseva et al. 2014), UV hypersensitivity (*uvh*) in *Arabidopsis* (Ganpudi & Schroeder 2011), and radiation sensitivity (*rad*) in the yeast *S. cerevisiae* (Rastogi et al. 2010).

NER utilizes two distinct sub-pathways: transcription-coupled repair (TC-NER) and global genomic repair (GG-NER), which are responsible for the repair of transcriptionally active areas and transcriptionally silent areas, respectively (Spampinato 2017; Rastogi et al. 2010; Shuck et al. 2008). In mammalian TC-NER, the Cockayne Syndrome A and B proteins (CSA and CSB), as well as the UV-stimulated scaffold protein A (UVSSA), are required to displace the stalled RNA polymerase from the damaged site to allow NER proteins access to the lesion to proceed with the repair (Vermeulen & Fousteri 2013; Henning et al.1995). In yeast, TC-NER is initiated by RAD28 and RAD26, the yeast homologues of mammalian CSA and CSB (Spivak 2016). The downstream repair components are also well conserved between mammals and yeast (Tatum & Li 2011).

In mammals, the damage recognition complex that initiates GG-NER is comprised of DDB1, DDB2, CULLIN4 (CUL4), and RING-BOX1 (RBX1) (Shuck et al. 2008; Sugasawa 2016). This complex has E3 ubiquitin ligase activity that targets core histone proteins for chromatin modification, resulting in recruitment and ubiquitination of Xeroderma Pigmentosa C (XPC) (Wang et al. 2006; El-Mahdy et al. 2006). Then XPC, together with HR23B and CENTRIN2 (CEN2) proteins form another complex that recruits the NER machinery (Nishi et al. 2005; Ganpudi & Schroeder 2011). *S. cerevisiae* has homologues of human XPC and HR23B named as ScRAD4 and ScRAD23, respectively, and their roles in the NER pathway are well conserved (Rastogi et al. 2010). However, no homologues of the initial damage recognition complex DDB1, DDB2 and CUL4 exist in yeast (Reed 2005). Instead, another complex consisting of

RADIATION SENSITIVE 7 (RAD7), RAD16, ELONGIN C (ELOC1), and CULLIN3 (CUL3) plays similar recognition roles in yeast, such as chromatin modification and RAD4 recruitment (Gillette et al. 2006). Although RAD7 and RAD16 have the same function as DDB1 and DDB2, respectively, these proteins are not direct homologs.

Nucleotide excision repair in plants has been studied in *Arabidopsis* and the overall process appears to be well conserved (Ganpudi & Schroeder 2011). Current understanding of this process is that it follows the mammalian model of GG-NER, given that mutations in the homologs of the core downstream NER components CEN2 and RAD23 result in UV sensitivity (Lahari et al. 2017; Molinier et al. 2004). Loss of function mutations in genes encoding the components of DNA damage recognition (DDB1, DDB2, CUL4) also results in UV sensitivity (Ganpudi & Schroeder 2013; Li et al. 2012; Al Khateeb & Schroeder 2009; Molinier et al. 2008). However, the *Arabidopsis* genome contains homologs of the yeast DNA damage recognition machinery: three homologs of RAD7, two homologs of RAD16, two homologs of CUL3, and one Elongin C homologue (Lahari et al. 2018; Shaked et al. 2006; Weber et al. 2005). The presence of RAD16, RAD7, ELOC, and DDB1/2 homologues in the *Arabidopsis* genome provide a unique opportunity to examine the role and interaction of both the mammalian homologs DDB1/2 and yeast homologs RAD7/16 in DNA damage recognition in a single system.

RAD16 is a member of the SWI/SNF family. This family possesses ATPase/helicase activity to initiate chromatin remodeling and increase the accessibility of DNA to machinery such as DNA repair (Shaked et al. 2006; Flaus & Owen-Hughes 2011). The chromatin remodeling includes DNA translocase activity together with ATPase activity (Narlikar et al. 2013). In *S. cerevisiae*, UV damage in untranscribed genomic regions is recognized by the RAD7/16 complex that possesses DNA translocase activity. Together, RAD7 and RAD16 form a complex called Nucleotide Excision Repair Factor 4 (NEF4) to bind UV-induced DNA damage in an ATP dependent manner, then NEF4 physically interacts with NEF2 (another damage recognition complex consisting of RAD23 and RAD4). The NEF2 complex enhances the binding to the damaged DNA and facilitates the recruitment of other NER component to the damaged site (Guzder et al. 1999). Loss of function studies indicate that the RAD7/16 complex is required for yeast GG-NER, where it recruits NER factors to the

damaged site (Verhage et al. 1994). RAD7/16 complex activities include recognizing and binding the damaged DNA, modifying chromatin, and subsequent recruitment of RAD4 to the damaged site. After that, RAD4 is subjected to degradation and core NER activity is recruited; this process requires a cullin-based E3 ligase. The RAD7/16 complex interacts with Elongin C (ELOC) and CUL3 for RAD4 ubiquitination and degradation (Gillette et al. 2006). Thus, RAD16 is essential for GG-NER as it displays an affinity for binding UV lesions and additionally is involved in the degradation of RAD4 (Ribar et al. 2006). Additionally, RAD16 together with RAD7 and ABFI form a complex that facilitates lesion recognition during yeast GG-NER (Boiteux & Jinks-Robertson 2013). Yeast RAD16 is also required for normal growth and development (Mastro & Forsburg 2014).

Homologs of yeast *S. cerevisiae* RAD16 exist in the model plant *Arabidopsis thaliana*, At1g05120, and At1g02670. However, it is not known whether *Arabidopsis* RAD16 homologs play a role in the plant NER pathway. Thus, the goal of this study is to characterize the roles of the *Arabidopsis* RAD16 homologues in UV tolerance and growth, address potential redundancy between *AtRAD16* homologs, and to investigate the relative contribution of AtRAD16 to plant UV tolerance compared to AtDDB1/2 and AtCSB/CSA repair pathways. Furthermore, I sought to detect physical interactions within *Arabidopsis* RAD7/16 complex and between AtRAD16 and other NER proteins. I used genetic loss of function mutants to characterize AtRAD16 and AtRAD16b individually. Genetic gain of function was used to examine the effects of AtRAD16 overexpression on seedling and adult UV tolerance and microscopy utilizing florescence from the YFP tag was used to examine AtRAD16 subcellular localization. To address potential redundancy between *AtRAD16* and *AtRAD16b*, A*trad16 Atrad16b* double mutant was generated and assessed for UV tolerance. To examine the relative contribution of AtRAD16 to plant UV tolerance compared to AtDDB1/2 and AtCSB/CSA repair pathways, *Atrad16 Atddb2*, *Atrad16 Atcsb*, and *Atrad16 Atuvssa* double null mutant plants were generated and assessed for UV tolerance. To examine the genetic interaction within *Arabidopsis* RAD7/16 complex, *Atrad7a Atrad7c* and *Atrad7a Atrad16* double null mutant plants were generated and assessed for UV tolerance. Finally, I used yeast two-hybrid assay to identify the proteins that physically interact with AtRAD16. This

is the first study of the roles and interactions of DDB1/2, RAD7/16, and CSA/CSB components in a single system.

2.3 Materials and Methods

2.3.1 Sequence analysis

Amino acid sequences for RAD16 homologs were downloaded from public databases. The Pfam database online was used to obtain the protein domains. Publicly-available expression databases were obtained from http://bar.utoronto.ca/interactions/cgibin/*Arabidopsis*_interactions_viewer.cgi to determine tissue-specific and stress-responsive expression in *Arabidopsis*.

2.3.2 Plant materials and growth conditions

All T-DNA insertion alleles and the wild type control (Col-0) used in this study were ordered from the *Arabidopsis* Biological Resource Center (ABRC): *rad7a-3* (SALK_107725 in At2g06040), *rad7c-1* (SALK_025534 in At5g21900), *ddb2-1* (SALK_040408 in At5g58760), *uvssa-2* (SALK_061538 in At3g61800), *csb-1* (SALK_000799 in At2g18760*),* and *rad23b-1* (SALK_076360 in At1g79650) were previously analyzed (Al Khateeb et al. 2019; Al Khateeb & Schroeder 2007; Lahari et al. 2018). *rad16-2* (SALK_130522.34.85x in At1g05120), *rad16b-1* (SALK_147762 in At1g02670) were analyzed in this study. All insertion mutant lines were genotyped using allele-specific primers along with the T-DNA-specific primer LBb1.3 (Table S2.1). Seeds were surface sterilized and spread on Linsmaier and Skoog (LS) media with 0.86% phytoblend and 0.6% sucrose. Following stratification at 4 ^{o}C for two days, the plates were transferred to 20 ^{o}C under fluorescent lights (100 µM photons m^{-2} s^{-1}) at 50% relative humidity. Seedlings were transplanted after 14 days into Sunshine mix #1 (SunGro). Both seedlings and adults were grown at 20 ^{o}C under long day conditions (16h light/8h dark).

2.3.3 RNA extraction and RT-PCR

Total RNA from 50 seven-day-old whole seedlings/genotype were extracted using the E.Z.N.A. Plant RNA Kit (Omega Bio-tek) according to manufacturer instructions, which included a DNase treatment. The Maxima First Strand cDNA synthesis kit (Fermentas, Waltham, MA, USA) was used to generate cDNA. For semi-quantitative RT-PCR, *RAD16* and *RAD16b* transcript abundance was estimated by PCR amplification for 25 cycles using gene-specific primers (Table S2.1). PCR cycling was run using initial denaturation for two minutes at 94 ^{o}C, denaturation for one minute at 94 ^{o}C, primer annealing for one minute at 60 ^{o}C, primer extension for one minute at 72 ^{o}C, and final extension for seven minutes at 72 ^{o}C. The loading control actin was used and amplified for 24 cycles using the primers listed in (Table S2.1). SsoFast EvaGreen Supermix (Bio-Rad, Hercules, CA, USA) was used to perform RT-PCR using RAD16 cDNA specific primers listed in (Table S2.1). The CFX ConnectReal-time PCR detection system (Bio-Rad, Hercules, CA, USA) was used for analysis. The *EF1α* gene (At5g60390) was used as a control to normalize the RT-q*PCR* data (Jain et al. 2006; Hossain et al. 2012). qPCR was performed using three biological replicates per genotype and each biological replicate was performed in three technical replicates. The mean Ct values of three technical replicates per each biological replicate were calculated and *RAD16* transcript level was expressed as the average of 2^-ΔΔCt of the three biological replicates compared to the mean values of the *EF1α* gene. RT-PCR cycling was as follows: initial denaturation for three minutes at 95 ^{o}C, primer annealing for 30 second at 55 ^{o}C, primer extension for 30 second at 72 ^{o}C.

2.3.4 UV sensitivity assays

For hypocotyl and root UV sensitivity assays, seeds were surface sterilized and spread on LS media with 0.86% phytoblend and 0.6% sucrose, stratified for two days at 4 °C, and grown vertically for four days at 20 ^{o}C before being irradiated with either 0, 500, or 1000 J m^{-2} UV-C emitted by a shortwave UV lamp XX-15S (UV Products). After that, to avoid photoreactivation, irradiated plates were wrapped in aluminum foil, then rotated 90^{o} and incubated vertically on either light or dark conditions for two or three

days. Plates were scanned and new root growth and hypocotyl length were measured using ImageJ (1.36b NIH, USA).

For adult plants UV sensitivity assays,14 day-old-seedlings were transferred to soil. After 21 days of growth, the plants were irradiated with either 0, 300, 500, or 600 J m^{-2} UV-C. After incubation in the dark for three days, the plants were then returned to standard growth conditions (16h light/8h dark). After four days of growth under standard growth conditions, leaf damage was scored. Any leaf exhibiting brown or yellow colouration was scored as a damaged leaf, and the percent of undamaged leaves (undamaged leaves-green) / undamaged and damaged leaves-green and brown or yellow) was computed for twelve plants of each genotype and each treatment.

2.3.5 Adult growth and developmental parameters

Seedlings were grown for two weeks on LS media then transferred to Sunshine Mix Number 1 soil (SunGro,Bellevue, WA), and 12 plants per line were used to collect the following data: flowering time-days (number of days it took for buds to appear), flowering time-leaves (the number of rosette and cauline leaves at flowering), rosette diameter was measured at 28 days of growth. Apical dominance (number of stems), plant height, and silique length were measured at seven weeks of growth.

2.3.6 Generation of RAD16 overexpression lines

A *RAD16* cDNA in pCMV SPORT6.1 vector was obtained from the French Institut National de la Recherche Agronomie. The cDNA was PCR-amplified with primers that added Sfil inkers, and cloned into the pENTR223.1-Sfi vector. Then, LR recombinase was used to clone the *RAD16* cDNA into pEarleyGate100 (CaMV 35S promoter) and pEarleyGate104 (CaMV 35S promoter with an N-terminal yellow florescent protein ((YFP) tag; Earley et al. 2006). The overexpression vectors were then transformed into *Agrobacterium tumefaciens* GV3101strain and flowering wild type (Col-0) and *Atrad16-2* were sprayed with *Agrobacterium* (Weigel & Glazebrook 2006). Basta selection was used to screen the transformed T1 as well as to screen for T2 lines carrying a single-copy transgene insertion (heterozygous T2 plants). Homozygous T3 plants were used for subsequent experiments. A full-length RAD16b clone is not

available in public collections accessed via online resources, thus I did not generate RAD16b overexpression lines.

2.3.7 Protein subcellular localization

YFP-tagged RAD16 seeds were plated on LS media, incubated at 4 ^{o}C for two days, then exposed to light for 6 hrs at 20 ^{o}C. Following light treatment, plates were wrapped in two layers of foil and returned to the incubator for three days. Three seedlings were placed on a slide; a drop of distilled water is added, observed using a Zeiss AXIO Imager Z1 Microscope equipped with AxioVision 4.8 software, using YFP (Filter Set YFP-2427B-000, Semrock Inc), and DAPI (Zeiss Filter Set 02 (488002-9901-000) filters. A nuclei (blue-fluorescent) Hoechst 33342 staining was used to visualize the nucleus (Bucevičius et al. 2018). 5 µg/mL Hoechst staining was prepared, and seedlings were immersed in the prepared staining for 30 min and imaged. For UV treatment, seedlings were treated with 1000 J m^{-2} UV-C, some were incubated in the dark for one hour and some for two hours then observed.

2.3.8 Yeast two-hybrid screening

The GAL-4 Matchmaker gold yeast two-hybrid system (Clontech, Mountian View, CA, USA) was used to investigate *Arabidopsis* RAD16 protein interactions with other *Arabidopsis* GG-NER components (RA7a, RAD7b, RAD7c, RAD4, RAD23b, ELOC, and DDB2). *Arabidopsis RAD16*, and *RAD7a* cDNAs were PCR-amplified with primers that added Sfil inkers and cloned into the pENTR223.1-Sfi entry vector using T4 ligase. Subsequent clones were produced using LR recombinase to clone each gene into pGADT7-DEST (Leu selection) prey vector and pGBKT7-DEST (Trp selection) bait vector (Lu et al. 2010). These clones were then transformed into haploid yeast strains Y2HGold and Y187 using electroporation. pGBKT7-DEST and pGADT7-DEST vectors were kindly provided by Yuhai Cui (Agriculture and Agri-Food Canada, London, ON). RAD7b, RAD7c, RAD4, RAD23b, ELOC, and DDB2 expressing strains were previously prepared by other students in our lab. Haploid yeast cells were mated to generate diploid strains as follows; *AtRAD16* pGADT7 was mated with *AtRAD7a* pGBKT7, *AtRAD7b* pGBKT7, *AtRAD4* pGBKT7, *AtRAD7c* pGBKT7, *AtDDB2* pGBKT7, *AtELOC*

pGBKT7, and *AtRAD23b* pGBKT7. *AtRAD16* pGBKT7 was mated with *AtRAD7a* pGADT7, *AtRAD7b* pGADT7, *AtRAD7c* pGADT7, *AtRAD4* pGADT7, *AtDDB2* pGADT7, *AtELOC* pGADT7, and *AtRAD23b* pGADT7.

Interaction between proteins in diploid yeast were detected by selecting on quadruple drop-out medium (–ade, –his, –leu, –trp), and double drop-out (-trp -leu) medium was used as a control. p53/T (murine p53/ SV40 large T-antigen) and Lam/T (Lamin/ SV40 large T-antigen) were used as the positive and negative controls, respectively. Protein/protein interaction induces the expression of *ADE2* and *HIS3* reporters which allows for growth on quadruple drop-out selection medium (-ade –his –leu -trp).

2.3.9 Generating of double mutant plants

Double mutant plants were generated by crossing their corresponding homozygous single parental mutants to generate F1 heterozygotes. After selfing, the F2 generation was genotyped to identify double loss of function mutants. Homozygous F3 plants were used for subsequent experiments.

2.3.10 Statistical analysis

All analyses were performed using a two-tailed student's *t*-test in Microsoft Excel. Probabilities of 0.05 or less were used to assess statistical significance. All experiments were repeated at least twice.

2.4 Results

2.4.1 *Arabidopsis* RAD16 proteins are homologous to yeast RAD16 proteins

Two homologues of yeast RAD16 exist in *Arabidopsis thaliana* encoded by At1g05120 and At1g02670 (Shaked et al. 2006). An amino acid sequence alignment with *S. cerevisiae* RAD16 and *S. pombe* 16 homologue RHP16 was used to identify functional similarities between *Arabidopsis* RAD16 and yeast RAD16 proteins. Our results show that, despite (400) million years of evolutionary separation between plants and fungi, extensive homology exists between these proteins (Delwiche & Cooper 2015)

(Figure S2.1). The protein encoded by At1g05120 is 40% identical to both ScRAD16 and SpHRP16, whereas the protein encoded by At1g02670 is 34% and 35% identical to the same proteins (respectively; Table S2.2); thus I refer to At1g05120 and At1g02670 as AtRAD16 and AtRAD16b, respectively. AtRAD16 and AtRAD16b are 61% identical at the amino acid level. In agreement with the homology of these sequences, the Princeton Protein Orthology Database groups At1g05120 and At1g02670 with *S. cerevisiae* RAD16 and *S. pombe* RHP16 in several phylogenic trees (Heinicke et al. 2007; data was not shown).

Our Pfam domain analysis shows that ScRAD16 has ATPase domains, the C3HC4-Ring domain, and the C-terminal helicase domain (Mistry et al. 2021). In ScRAD16, the ATPase domains and the C3HC4-Ring domain are required for efficient DNA repair following UV damage (Yu et al. 2016). These functional domains exist in both *S. pombe* RAD16 and AtRAD16, however, AtRAD16b lacks the C3HC4-Ring domain (Figure 2.1).

2.4.2 *Arabidopsis RAD16*s are expressed during development and in response to UV radiation

AtGenExpress data was used to examine the mRNA abundance levels of *Arabidopsis RAD16* and *RAD16b* throughout the growth as well the expression in response to UV radiation (Schmid et al. 2005). These data show that both *AtRAD16* and *AtRAD16b* are expressed throughout development, but *AtRAD16* is expressed at higher levels than *AtRAD16b* during all developmental stages (Figure S2.2). Public gene expression data (Kilian et al. 2007) also indicated that UV-B treatment induces the expression of *AtRAD16b* in aerial tissue >3 fold after both 30 min and six hours treatments, while *AtRAD16b* levels drop slightly in roots under these experimental conditions (Figure S2.3). In contrast, *AtRAD16* level does not appear to be significantly induced in either roots or aerial tissues following UV-B treatment (Figure S2.3).

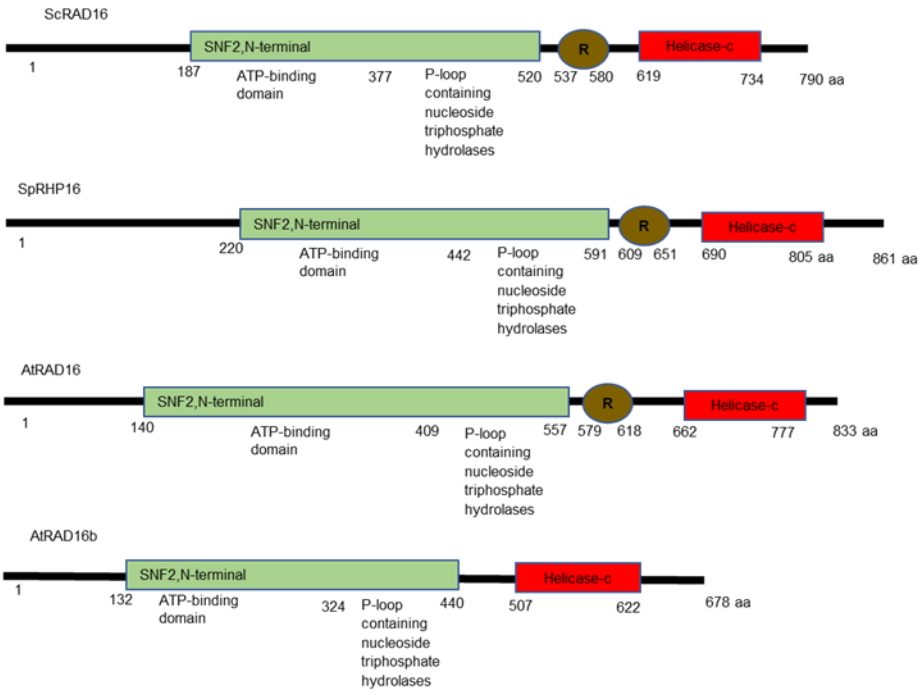

Figure 2.1 Illustration of the conserved domains and their organization in yeast RAD16 proteins and their *Arabidopsis* homologs

The SNF2, N-terminal helicase ATP binding domain is indicated in green, R represents the C3HC4-zinc finger ring-type and indicated in brown, followed by the helicase-C terminal domain in red.

2.4.3 *Arabidopsis rad16 and rad16b* mutants exhibit increased UV sensitivity

The role of *S. cerevisiae* RAD16 and *S. pombe RAD16* in GG-NER has been reported (Lombaerts et al.1999; Yu et al. 2016), and the *S. cerevisiae rad16* mutant was found to exhibit a UV sensitive phenotype (Bang et al. 1995). In this study, our protein sequence analysis results provide evidence that *Arabidopsis* RAD16 proteins are true homologs of *cerevisiae* RAD16 and *S. pombe RAD16*, suggesting a possible conserved role of *Arabidopsis* RAD16s in plant GG-NER and/or UV tolerance. Thus, I sought to perform UV sensitivity assays to examine the effects of *Arabidopsis RAD16* loss of function on plant UV sensitivity.Two T-DNA insertion mutants were ordered from ABRC. The T-DNA insertion line used for *Atrad16* (SALK_130522.34.85x, *Atrad16-2*) is in the eleventh exon, whereas the insertion line used for *Atrad16b* (SALK_147762, *Atrad16b-*

1) is in the first intron (Figure 2.2a). Both *Atrad16-2* and *Atrad16b-1* loss of function alleles are RNA nulls (Figure 2.2b&c).

UV sensitivity assays were performed using *Atrad16-2* and *Atrad16b-1* single and double mutants. Both single and double mutants exhibited increased seedlings and adult UV sensitivity. Following a 1000 J m^{-2} UV treatment, four day-old seedlings exhibited a significant reduction in root and hypocotyl growth of both single mutants relative to wild type, and double mutant relative to *Atrad16-2* (Figure 2.3a&c). Mutant adult plants also exhibited a UV sensitive phenotype as indicated by a significant increase in leaf damage in both single mutants relative to wild type, and the double mutant relative to *Atrad16-2* (Figure 2.3d). Thus, *Atrad16* and *Atrad16b* single and double loss of function mutant seedlings and adults are sensitive to UV radiation.

2.4.4 *Arabidopsis rad16 and rad16b* UV sensitivity is dark-specific

There are two DNA repair mechanisms in plants; light repair via photolyase, and dark repair via NER. I expect *Arabidopsis* RAD16 to be involved in NER. Thus, in order to confirm that *Atrad16* UV sensitivity is dark specific, after UV irradiation I incubated one set of the UV-treated seedlings in the dark (to avoid photolyase activity) and the other set in the light. The seedlings that were incubated in the dark after UV treatment showed a significant decrease in the root length for both single and double mutants (Figure 2.3a). However, the seedlings of both single and the double mutant that were incubated in light after UV treatment did not exhibit any significant decrease in the root length compared to the wild type (Figure 2.3b), suggesting that *Atrad16* and *Atrad16b* UV sensitivity is dark repair specific, consistent with its hypothesized role in NER.

2.4.5 Lacking either AtRAD16 or AtRAD16b results in early flowering time and short silique length

Based on the observation that *Arabidopsis RAD16* and *RAD16b* are expressed throughout plants development, I sought to study the role of *AtRAD16* genes in plant growth and development. I examined the effect of *Atrad16* and *Atrad16b* single and double loss of function mutants on adult growth parameters such as flowering time (in days to bolting and leaf count), height, apical dominance, silique length, and rosette

width. Both *Atrad16-2* and *Atrad16b-1* single mutants showed early flowering time with respect to both days and the number of leaves (Figure S2.4a&b). Both mutant lines also exhibited a short silique length phenotype compared to wild type (Col-0; Figure S2.4e). These results suggest the involvement of *Arabidopsis* RAD16s in the regulation of important growth parameters.

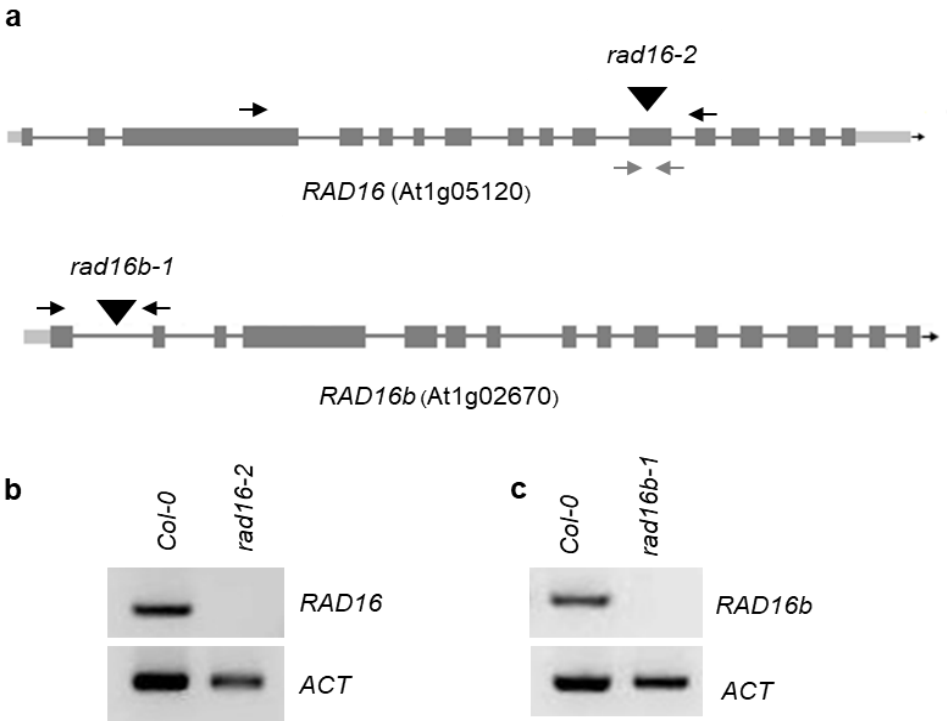

Figure 2.2 *Arabidopsis* RAD16 homologues null alleles

(**a**) Gene structures of *RAD16* (At1g05120) and *RAD16b* (At1g02670). Introns are shown as lines and exons as boxes. TDNA insertion lines *rad16-2* (SALK_130522.34.85x) and *rad16b-1* (SALK_147762), sites of T-DNA insertions are shown as triangles, primer pairs used in semi-quantitative and quantitative RT-PCR are shown in black and grey arrows, respectively. (**b**) Semi-quantitative RT-PCR showing *RAD16* expression in the wild type (Col-0) and *rad16-2* (**c**) Semi-quantitative RT-PCR showing *RAD16b* expression in the wild type (Col-0) and *rad16-2*. *ACTIN* was used as a control.

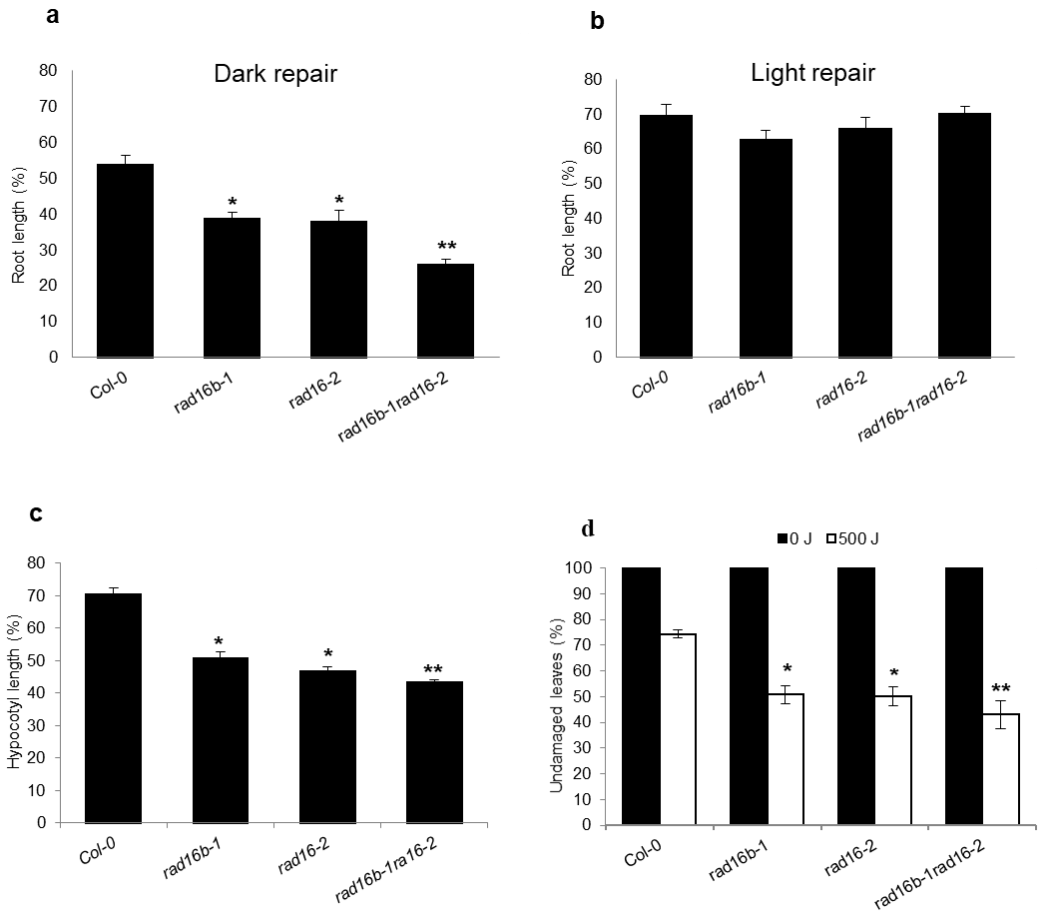

Figure 2.3 *Arabidopsis rad16* and *rad16b* single and double null mutants exhibit a UV sensitive phenotype that is dark-specific

(**a**) Relative root length of single and double mutant seedlings exposed to 1000 J m^{-2} UV-C radiation and incubated in the dark for two days (n=40). (**b**) Relative root length of single and double mutant seedlings exposed to 1000 J m^{-2} UV-C radiation and incubated in the light for two days (n=40).(**c**) Relative hypocotyl length of single and double mutant seedlings exposed to 1000 J m^{-2} UV-C radiation and incubated for three days in the dark (n=40). (**d**) Percentage of undamaged leaves exposed to 500 J m^{-2} UV-C irradiation, incubated in the dark for three days, followed by four days incubation (16h light/8h dark; n=12). For a-c, root and hypocotyl growth are presented as the treated relative to non-treated controls. Values are means ± SE, * = $p \leq 0.05$ of single mutant vs wild type, and ** = $p \leq 0.05$ of double mutants vs *rad16-2*.

2.4.6 AtRAD16 overexpression rescues the UV-sensitivity and adult developmental phenotypes exhibited by *Atrad16* null mutant and increases UV tolerance

To verify that the observed UV-sensitive phenotypes in both seedlings and adults and the early flowering time and short silique length phenotypes in adults were due to null insertion mutations in *Atrad16*, I carried out genetic complementation experiments. Wild-type *AtRAD16* was introduced into two overexpression vectors: pEarleygate 100 (pEG100) which produces a tagless version of AtRAD16, and pEarleygate 104 (pEG104) which produces a AtRAD16 product with an N-terminal YFP tag. In both cases, ubiquitous overexpression is driven by the CaMV 35S promoter. These constructs were transformed into the *Atrad16-2* null background using *Agrobacterium* mediated transformation. Tagless AtRAD16 overexpression lines; *35S:RAD16* in the *Atrad16-2* background rescued seedlings and adults UV sensitivity exhibited by the *Atrad16-2* null mutant (Figure 2.4b&c). Similarly, YFP-tagged AtRAD16 overexpression in its respective mutant; *35S:YFP-RAD* in the *Atrad16-2* background rescued seedlings and adults UV sensitivity exhibited by the *Atrad16-2* loss of function mutant (Figure 2.5b&c). These overexpression lines also rescued the early flowering time and short silique length in adult *Atrad16-2* plants (Figure S2.5 a,b,&e; Figure S2.6 a,b,&e). These results indicate that the UV sensitivity and adult developmental phenotypes exhibited by the *AtRAD16* loss of function mutant are due to a defect in *AtRAD16* gene, and it is unlikely that the YFP tag disrupts AtRAD16 function.

To examine the effects of AtRAD16 overexpression on seedling and adult UV tolerance, both *35S:RAD16* and *35S:YFP-RAD16* overexpression constructs were transformed into the wild type (Col-0). Both the tagless and YFP-tagged AtRAD16 overexpression in the wild-type background exhibited a significant increase in seedling and adult UV tolerance compared to the wild type (Figure 2.4b&c; Figure 2.5b&c). The expression level of *AtRAD16* in all the transgenic plants (tagless and YFP-tagged RAD16 overexpression lines) was higher than that in wild type plants (Figure 2.4a; Figure 2.5a). These results indicate that AtRAD16 overexpression is sufficient to increase UV tolerance in seedlings and adults, and that the YFP epitope tag did not disrupt AtRAD16 function.

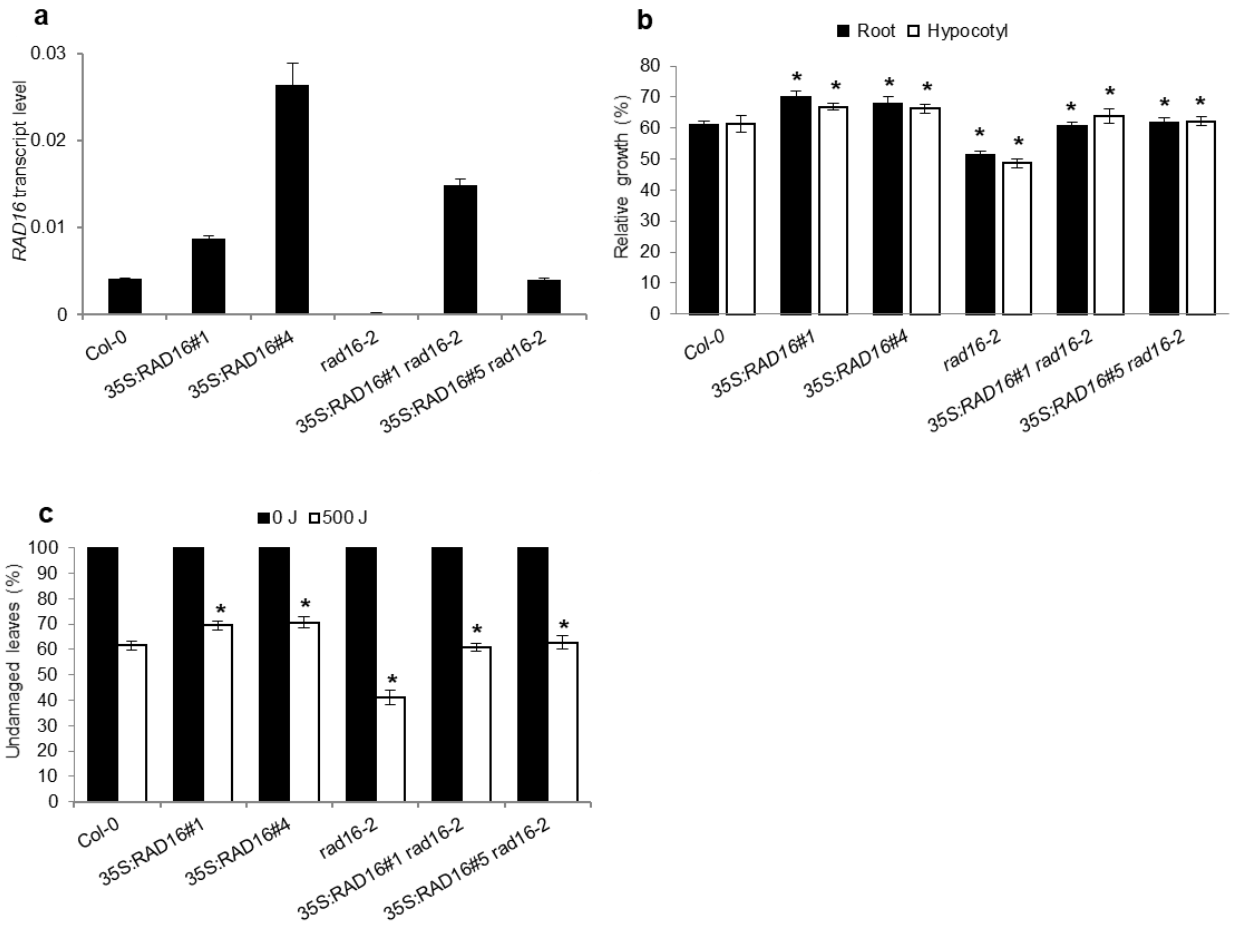

Figure 2.4 *Arabidopsis* RAD16 overexpression complements adult and seedling UV sensitive phenotypes and increases UV tolerance

(**a**) *RAD16* transcript level in Col-0 (wild type), *35S: RAD16*, *rad16-2*, and *35S: RAD16 rad16-2*. The *EF1α* gene was used to normalize the values. Error bars represent SE of the mean. (**b**) Lengths of root and hypocotyl in seedlings incubated in the dark for three days following 1000 J m^{-2} UV-C treatment, for each genotype, data are shown as relative to non-treated control (n=40). (**c**) Percentage of undamaged leaves exposed to 500 J m^{-2} UV-C radiation, incubated in dark conditions for three days, followed by four days incubation at 16h light/8h dark (n=12). For (b) and (c) values are means ± SE, * = $p \leq 0.05$ of *35S: RAD16* and *rad16-2* vs Col-0, and *35S: RAD16 rad16-2* vs *rad16-2*.

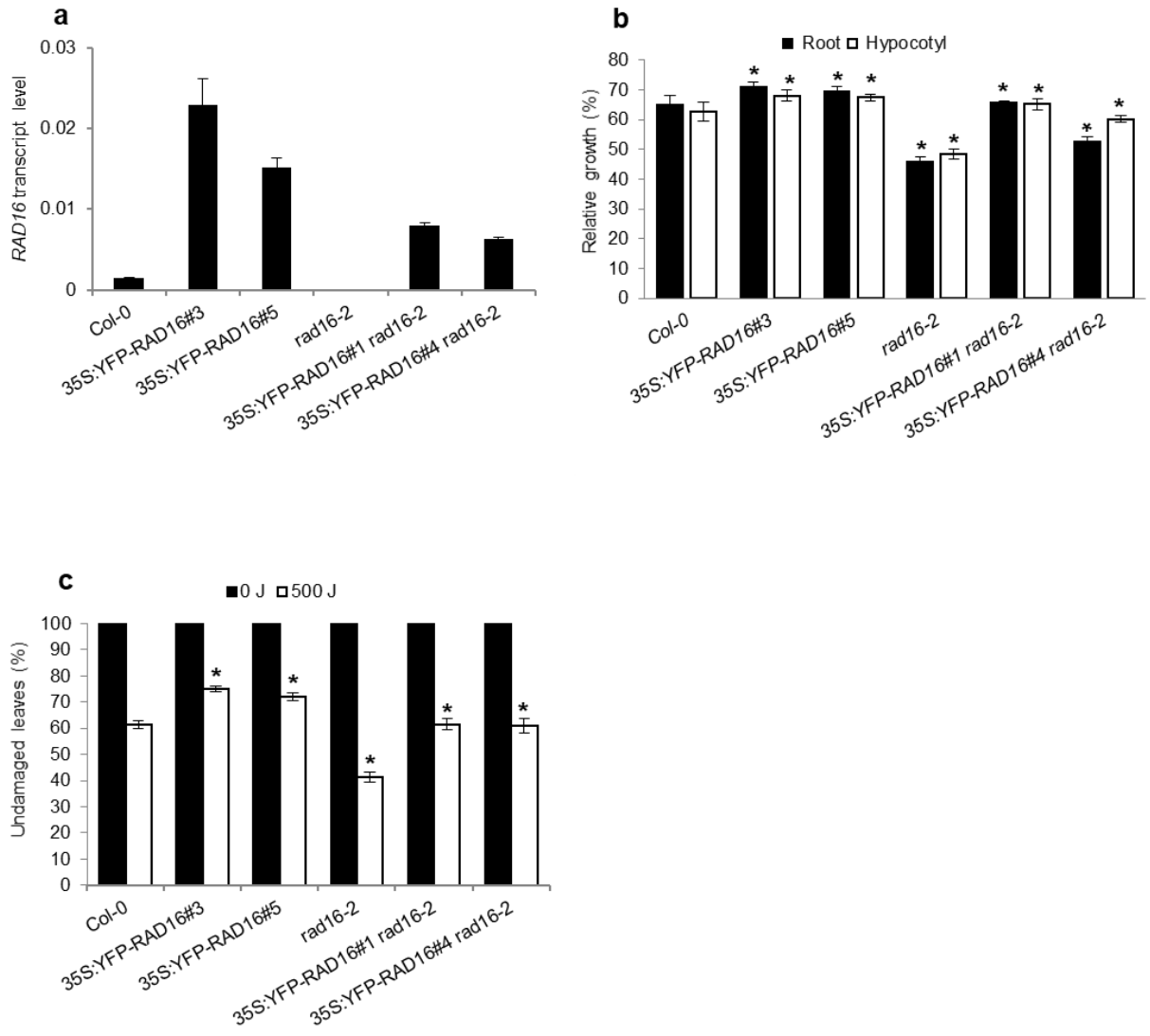

Figure 2.5 *Arabidopsis* YFP-RAD16 overexpression complements adult and seedling UV sensitive phenotype and increases UV tolerance

(**a**) *RAD16* transcript level in Col-0 (wild type), *35S:YFP-RAD16*, *rad16-2*, and *35S:YFP-RAD16 rad16-2*. The *EF1α* gene was used to normalize the values. Error bars represent SE of the mean. (**b**) Lengths of root and hypocotyl in seedlings incubated in the dark for three days following 1000 J m^{-2} UV-C treatment, for each genotype, data are shown as relative to non-treated control (n=40). (**c**) Percentage of undamaged leaves exposed to 500 J m^{-2} UV-C radiation, incubated in dark conditions for three days, followed by four days incubation at 16h light/8h dark (n=12). For (b) and (c) values are means ± SE, * = $p \leq 0.05$ of *35S: RAD16* and *rad16-2* vs Col-0, and *35S: RAD16 rad16-2* vs *rad16-2*.

2.4.7 *Arabidopsis* RAD16 exhibits nuclear localization that is not changed by UV treatment

Arabidopsis NER proteins are either localized to the nucleus or are relocalized to the nucleus from the cytoplasm in response to DNA damage (Lahari et al. 2017). Given that *Arabidopsis* RAD16 is expected to be involved in NER, I sought to examine AtRAD16 cellular localization before and after UV treatment. In order to examine AtRAD16 cellular localization, 35S:YFP-RAD16 #3 overexpression line in Col-0 background was examined for YFP fluorescence. Non-UV treated plants exhibited YFP fluorescence in the nucleus, and no YFP fluorescence was observed in the cytosol of YFP-tagged RAD16 plants. This observation suggests that YFP tagged RAD16 is localized exclusively throughout the nucleus, as verified with Hoechst staining (Figure 2.6). In order to examine the effects of UV radiation on AtRAD16 nuclear localization, cellular localization of the same YFP tagged overexpression line was examined following UV treatment. AtRAD16 nuclear localization was not altered following UV treatment (Figure 2.7).

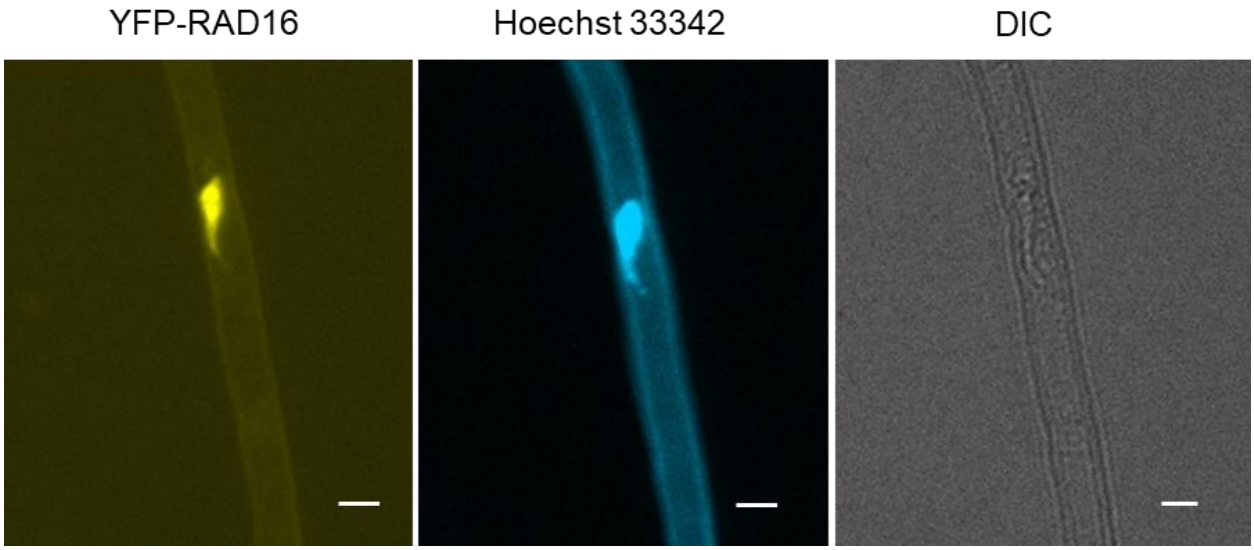

Figure 2.6 *Arabidopsis* YFP-RAD16 localizes in the nucleus

AtRAD16 localization in root hair of YFP-tagged RAD16 seedlings grown in the dark for three days was examined under the Zeiss AXIO Imager Microscope. YFP fluorescence, Hoechst 33342 dye, and differential interference contrast (DIC) are shown separately. Scale bar represents 20μm.

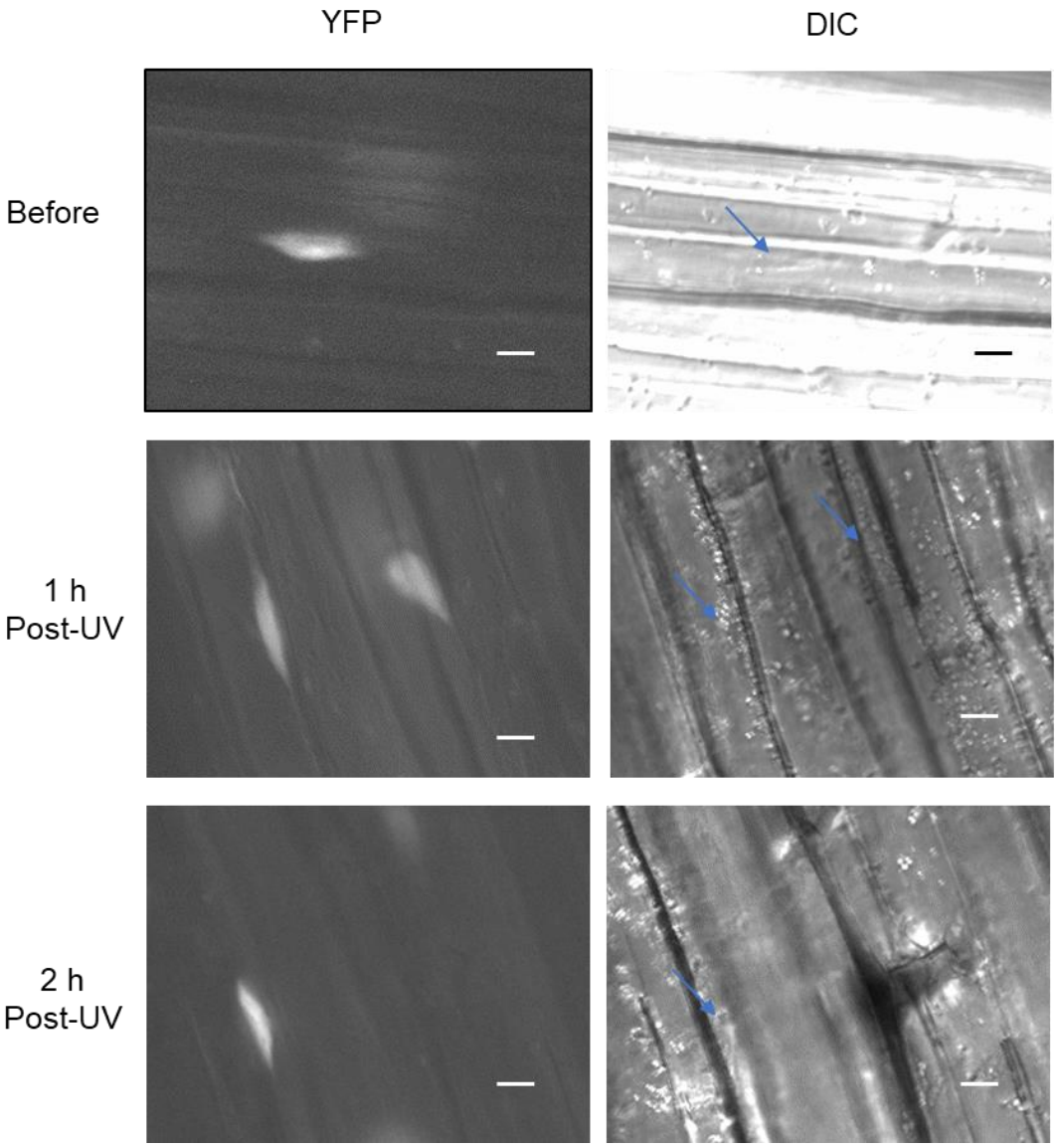

Figure 2.7 UV treatment does not alter *Arabidopsis* RAD16 nuclear localization

AtRAD16 localization in hypocotyl cells of YFP-tagged RAD16 seedlings grown in the dark for three days was examined before and after one and two hours following UV treatment for YFP fluorescence, and differential interference contrast (DIC). Scale bar represents 10μm.

2.4.8 *Arabidopsis* RAD16 physically interacts with *Arabidopsis* RAD7a and RAD7c

The *Arabidopsis* Interaction Viewer identified two previously characterized *Arabidopsis* RAD7 homologues: RAD7a encoded by At2g06040 and RAD7b encoded by At4g15475 (Lahari et al. 2018). Also identified an ELOC homologue encoded by At5g59140 (AtELOC) as potential interaction partners of AtRAD16, based on the interactions of the homologous proteins in yeast (Geisler-Lee et al. 2007). The Genemania prediction server (Warde-Farley et al. 2010), which is used to identify the potential interaction partners of proteins based on publicity available databases, also predicts interactions between AtRAD16 and each of AtRAD7a, At5g21900 (RAD7c), and AtELOC. In order to determine whether *Arabidopsis* RAD16 interacts as the predicted yeast model or if it has additional interaction partners, I sought using yeast two-hybrid analysis to examine physical interactions of AtRAD16 with other GG-NER proteins (AtRAD7a, AtRAD7b, AtRAD7c, AtELOC, and AtDDB2), as well as with other NER components such as AtRAD4, and AtRAD23.

In the yeast two-hybrid systems, the interaction was tested by growing diploid stains on quadruple drop-out selective medium (-leu –trp –his –ade). The diploid yeast strain that has *Arabidopsis RAD16* as bait and *AtRAD7a* as a prey grew on the selective media, indicating that AtRAD16 interacts with AtRAD7a and induces the expression of the *ADE2* and *HIS3* reporters which allow the diploid yeast to grow on the selection media. This interaction was seen between AtRAD16 bait/AtRAD7a prey and vice versa (Figure 2.8a&b). Moreover, AtRAD16 and AtRAD7a did not form homodimers (Figure S2.7a&b). AtRAD16 pGBKT7 (bait) was also found to interact with AtRAD7c pGADT7 (prey; Figure 2.9). However, I could not examine the interaction between AtRAD16 pGADT7 (prey) and AtRAD7c pGBKT7 (bait) as AtRAD7c pGBKT7(bait) was found to auto-activate. No interaction was detected between *Arabidopsis* RAD16 and each of AtRAD7b, AtRAD4, AtDDB2, AtELOC, or AtRAD23b (Figures S2.8-S2.12).

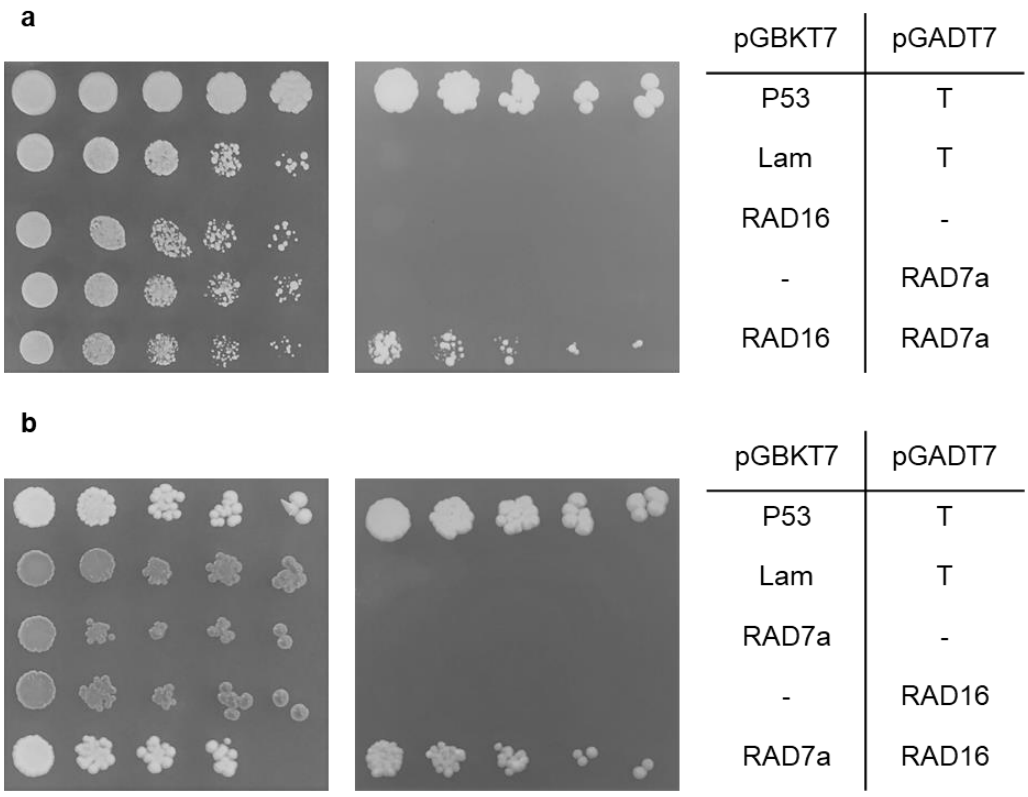

Figure 2.8 Yeast two-hybrid screening for *Arabidopsis* RAD16/RAD7a interaction.

RAD16 interacts with RAD7a. Each of *RAD16* and *RAD7a* were cloned into pGBKT7 (bait) and pGADT7 (prey) vectors and transformed into haploid yeast cells, then mated. Five fold dilutions of the mated diploid strain; (**a**) RAD16 bait/RAD7a prey and (**b**) RAD7a bait/RAD16 prey were spotted on (-leu -trp) non-selective plates (left) and on selective plates (-leu –trp –ade -his) (right). P53/T and Lam/T are the positive and negative controls respectively, as P53 interacts with T, whereas Lam does not interact with T.

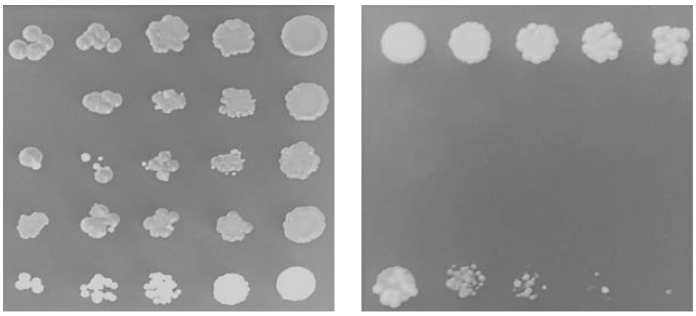

pGBKT7	pGADT7
P53	T
Lam	T
RAD16	-
-	RAD7C
RAD16	RAD7C

Figure 2.9 Yeast two-hybrid screening for *Arabidopsis* RAD16/RAD7c interaction

RAD16 interacts with RAD7c. *RAD16* and *RAD7c* were cloned into pGBKT7 (bait) and pGADT7 (prey) vectors (respectively) and transformed into haploid yeast cells, and then mated. Five fold dilutions of the mated diploid strain; RAD16 bait/RAD7c prey were spotted on (-leu -trp) non-selective plates (left) and on selective plates (-leu –trp –ade -his) (right). P53/T and Lam/T are the positive and negative controls respectively, as P53 interacts with T, whereas Lam does not interact with T.

2.4.9 *Arabidopsis rad16 rad7a* and *rad7a rad7c* double null mutant plants are more sensitive to UV radiation than single mutants

The results of this study show that a defect in the *Arabidopsis RAD16* gene results in increased UV sensitivity (Figure 2.3a,c &d), and AtRAD16 physically interacts with AtRAD7a and AtRAD7c providing evidence that *Arabidopsis* RAD7/16 complex is required for plant UV tolerance. Therefore, I decided to examine the genetic interactions within the AtRAD7/16 complex. To examine the interaction within AtRAD7/16 complex, I generated *Atrad7a Atrad7c* and *Atrad16 Atrad7a* double mutants. Then I assessed the effects of double loss of function on *Arabidopsis* UV tolerance and growth. Both *Atrad7a Atrad7c* and *Atrad16 Atrad7a* double mutants exhibited a significant decrease in roots and hypocotyls length compared to *Atrad7a* and *Atrad16* single mutants respectively (Figure 2.10a&b). Also, *Atrad7a Atrad7c* and *Atrad16 Atrad7a* adult plants exhibited a significant increase in the percentage of UV-damaged leaves compared to *Atrad7a* and *Atrad16* single mutants (Figure 2.10c&d). The increased UV sensitivity exhibited by the double mutants; *Atrad7a Atrad7c* and *Atrad16 Atrad7a* may reflect the additive UV sensitivity exhibited by single mutants in each double. Compared to single mutants,

neither *Atrad7a Atrad7c* nor *Atrad16 Atrad7a* has a significant effect on adult growth parameters such as flowering time in days and leaf counts, height, apical dominance, silique length, and rosette diameter (Figures S2.13 & S2.14).

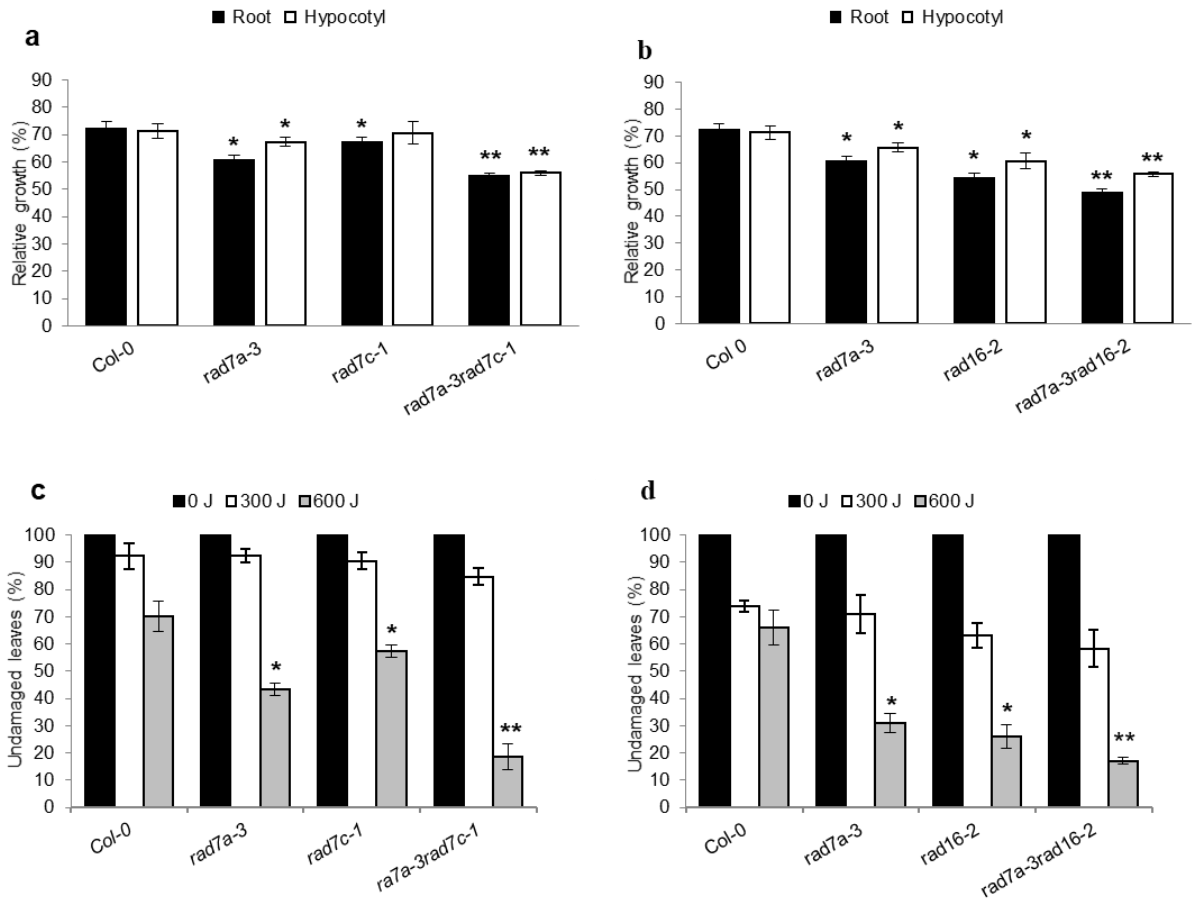

Figure 2.10 Double loss of function mutation in *Arabidopsis RAD7a*/*RAD7c* and *RAD7a*/*RAD16* increase UV sensitivity

Lengths of root and hypocotyl in *rad7a rad7c* **(a)** and *rad7a rad16* **(b)** seedlings incubated in the dark for three days following 1000 J m^{-2} UV-C treatment, for each genotype, data are shown as relative to non-treated control (n=40). Percentage of undamaged leaves in *rad7a rad7c* (**c**) and *rad7a rad16* (**d**) adults exposed to varying doses of UV-C radiation, incubated in dark conditions for three days, followed by four days incubation at 16h light/8h dark (n=12). Values are means ± SE, * = $p \leq 0.05$ of single mutant vs wild type, and ** = $p \leq 0.05$ of double mutants vs single mutant.

2.4.10 Lacking both *Arabidopsis RAD16* and *RAD23b* results in embryo lethality

To examine the genetic interaction between AtRAD7/16 complex and *Arabidopsis* NEF2 complex (RAD23/RAD4), which is also involved in DNA damage recognition and facilitating the recruitment of NER components to the damaged site, I attempted to generate *Atrad16 Atrad23b* double mutants. However, no *Atrad16 Atrad23b* homozygous double mutants were ever recovered from this cross. I was able to grow plants that were heterozygous for one gene and homozygous for the other (*Atrad16 Atrad23b*/+, and *Atrad16*/+ *Atrad23b*). Siliques of these lines were screened for the presence of defective seeds. Approximately 22% of the seeds were deformed suggesting tha*t Atrad16 Atrad23b* double mutants result in embryo lethality. Thus I hypothesized that the number of deformed seeds in each of *Atrad16 Atrad23b*/+ and *Atrad16*/+ *Atrad23b* will be 25% of the total number of seeds. To validate our hypothesis I performed Chi-square statistical analysis. Chi-square statistical values were as follows: *Atrad16 Atrad23b*/+, X^2 =1.5122e-28, df=1, P-value=1 and for *Atrad16*/+ *Atrad23b,* X^2 =2.003, df=1, P-value=.157. The chi-square calculated values are less than the critical values that are required to reject our stated hypothesis.

2.4.11 RAD7/16 damage recognition module makes a significant contribution to *Arabidopsis* NER compared to the DDB1/2 module

Arabidopsis contains both mammalian and yeast homologs that participate in DNA damage recognition, which provides a unique opportunity to clarify the individual contributions and the genetic interactions between DDB1/2 and RAD7/16 (homologs of mammalian and yeast GG-NER damage recognition factors, respectively) in a single system. To do so, I generated a *Atrad16 Atddb2* double loss of function mutant and assessed the effects of lacking both potential damage recognition pathways on *Arabidopsis* UV tolerance. The double mutant exhibited enhanced UV sensitivity compared to single mutants in seedlings and adults, following treatment with 1000 and 600J, respectively (Figure 2.11). This suggest that both the yeast-like GG-NER damage recognition factors RAD7/16 the mammalian-like GG-NER damage recognition factors DDB1/2 are important to wild-type UV tolerance and/or GG-NER. With respect to plant

developmental phenotypes, I did not observe any significant differences between the double and single mutants.

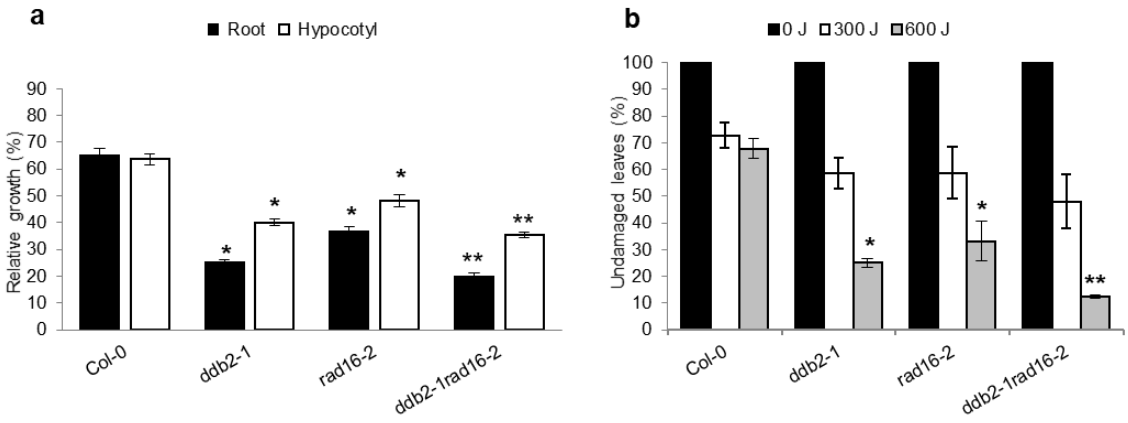

Figure 2.11 Double loss of function mutation in *Arabidopsis DDB2*/*RAD16* increases UV sensitivity

(a) Root and hypocotyl lengths of single and double-mutants seedlings incubated in the dark for three days following 1000 J m^{-2} UV-C treatment. For each genotype, data are shown as relative to non-treated control (n=40). (**b**) Percentage of undamaged leaves in adult plants exposed to varying doses of UV-C radiation, incubated in dark conditions for three days, followed by four days incubation at 16h light/8h dark (n=12). Values are means ± SE, * = p ≤ 0.05 of single mutant vs wild type, and ** = p ≤ 0.05 of double mutant vs *ddb2-1*mutant.

2.4.12 The RAD7/16 pathway makes a significant contribution to *Arabidopsis* NER compared to the CSB pathway

In the *Arabidopsis* genome, homologs of both mammalian TC-NER proteins and yeast GG-NER proteins have been identified. In this study, I characterized the role of the yeast GG-NER homologs (RAD7/16 complex) in plant GG-NER. The role of the mammalian TC-NER homologs (CSB/UVSSA) have been previously studied (Al khateeb et al. 2019; Shaked et al. 2006). Thus, I sought to assess the relative contribution of the yeast GG-NER homologs (RAD7/16) and the mammalian TC-NER homologs (CSB/UVSSA) to *Arabidopsis* UV tolerance. I generated double mutants with the TC-NER specific components *AtCSB* and *AtUVSSA* and *AtRAD16* and assessed the genetic effects of simultaneous null mutations in these complexes on UV tolerance. Both the *Atrad16-2 Atcsb-1* and the *Atrad16-2 Atuvssa-2* double mutants exhibited

increased UV sensitivity in seedlings; this sensitivity resulted in reduction in roots and hypocotyl length following 500J UV treatment compared to single mutants (Figure 2.12a &b). Also, *Atrad16-2 Atcsb-1* and *Atrad16-2 Atuvssa-2* exhibited an increase adult UV sensitivity compared to the single mutants (Figure 2.12c&d). These results indicate that both the RAD7/16 pathway and the CSB pathway are important to the dark repair process. In addition, these results suggest that the role of CSB pathway is more crucial to plant NER compared to DDB1/2 and Rad7/RAD16 pathways. Since *Atrad7a Atrad16* double loss of function results in ~80% leaf damage compared to ~70% and ~ 60% leaf damage in *Atrad7a*, *Atrad16* single null mutants, respectively (Figure 2.10 d). *Atddb2 Atrad16* double loss of function results in ~85% leaf damage compared to ~75% and ~ 65% leaf damage exhibited by *Atddb-2* and *Atrad16* single loss of function mutants, respectively (figure 2.11b). Whereas *Atcsb Atrad16* and *Atuvssa Atrad16* double loss of function resulted in ~95% and ~ 97% leaf damage, respectively, compared to ~85% leaf damage exhibited by each of *Atuvssa* and *Atcsb* single loss of function mutants and ~ 65% exhibited by *Atrad16* single null mutant.(Figure 2.11c&d). Similarly, the seedling UV sensitivity was observed even with a low UV dosage (500J). The reduction in root and hypocotyl lengths exhibited by *Atcsb Atrad16* and *Atuvssa Atrad16* double loss of function following irradiating with 500 J was almost the same as the reduction exhibited by *Atrad7a Atrad16* and *Atddb2 Atrad16* loss of function mutants following 1000J UV treatment (Figure 2.10b, Figure 2.11a, & Figure 2.12a&b). With respect to plant developmental phenotypes, I did not observe any statistical differences between the *Atrad16-2 Atcsb-1* and the *Atrad16-2 Atuvssa-2* double mutants and the single mutats (Figures S2.15 & S2.16).

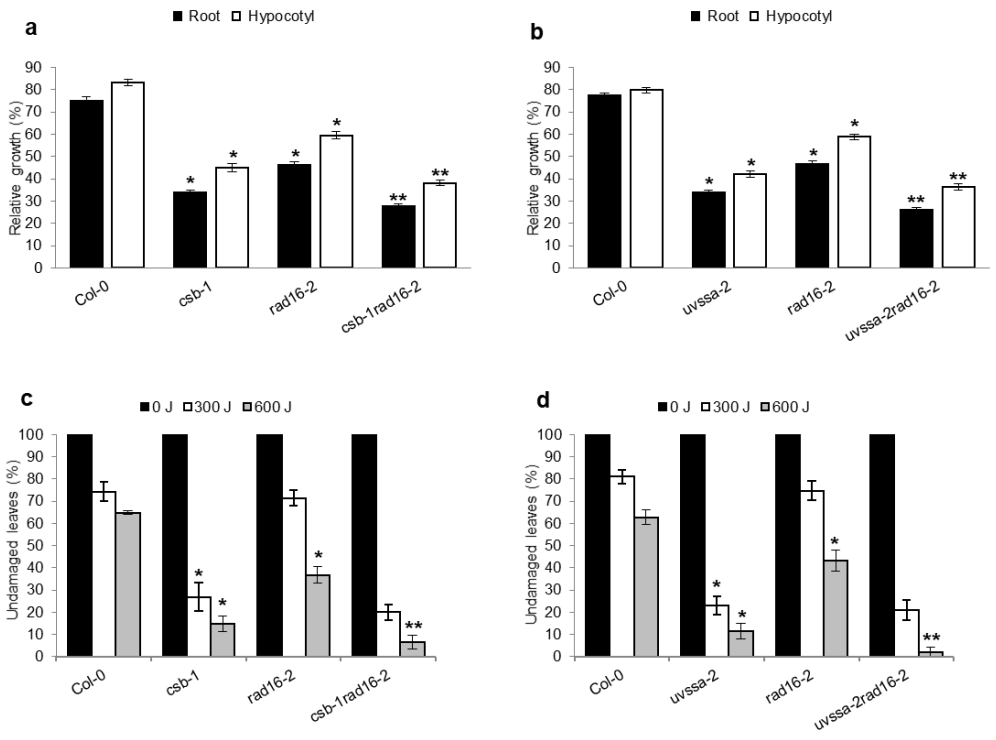

Figure 2.12 Double loss of function mutations in *Arabidopsis CSB*/*RAD16* and *UVSSA*/*RAD16* increase UV sensitivity

Lengths of root and hypocotyl in **(a)** *csb rad16* and **(b)** *uvssa rad16* seedlings incubated in the dark for three days following 500 J m^{-2} UV-C treatment. For each genotype, data are shown as relative to non-treated control (n=40). Percentage of undamaged leaves in **(c)** *csb rad16* and **(d)** *uvssa rad16* adults exposed to varying doses of UV-C radiation, incubated in dark conditions for three days, followed by four days incubation at 16h light/8h dark; n=12). For (a-d), values are means ± SE, * = $p \leq 0.05$ of single mutant vs wild type, and ** = $p \leq 0.05$ of double mutants vs single mutants.

2.5 Discussion

In mammals, GG-NER is initiated by the damage recognition complex DDB1/2. In the yeast *S. cerevisiae*, GG-NER is initiated by the RAD7/16 complex, which performs many of the same functions as DDB1/2. Like mammalian complex, the RAD7/16 complex is an E3 ubiquitin ligase complex that causes chromatin modification, ubiquitinating ScRAD4 as well as subsequent recruitment of conserved downstream core NER activities (Reed 2005). *S. cerevisiae* RAD16 and *S. pombe* RAD16 homolog

(rhp16), as members of this complex, are required for GG-NER (Li et al. 2007; Lombaerts et al. 1999; Mastro et al. 2014). In plant systems, the DDB1/2 complex have been shown to be necessary for GG-NER (Al khateeb & Schroeder 2009; Molinier et al. 2008)

In this thesis, I characterized the roles of the two *Arabidopsis* RAD16 homologs in plant UV tolerance and growth. Findings from this study have demonstrated for the first time the involvement of AtRAD16 and AtRAD16b in plant UV tolerance. I also have shown the involvement of these homologs in plant growth and development.

2.5.1 Suggested conserved function of *Arabidopsis* RAD16 proteins in DNA repair

Our protein sequence analysis results show that AtRAD16 and AtRAD16b are more related to each other than to yeast RAD16 (Table S2.2), suggesting that both *AtRAD16* and *AtRAD16b* have evolved through gene duplication. Protein functional analysis shows that ScRAD16 has SNF2 related domain and the C3HC4-Ring domain (Figure 2.1). AtRAD16 also has these two domains. In ScRAD16, the ATPase activity of the SNF2 related domain and the E3 ubiquitin ligase activity of the RING domain are required for efficient GG-NER since both affect RAD16 distribution during GG-NER. Individually mutating these domains results in a mild UV sensitivity and reduction in the DNA repair rates (Yu et al. 2016). Inactivation of both domains results in increased UV sensitivity resembles that exhibited by the *scrad16* null mutant (Yu et al. 2016).Thus both domains are required for efficient GG-NER in yeast.

The GG-NER components in mammals and yeast, DDB1/DDB2/CUL4 and RAD7/RAD16/ELOC/CUL3, have E3 ubiquitin ligase activities (Gillette et al. 2006; Sugasawa 2016).Thus *S. cerevisiae* RAd7/16 complex interacts with CUL3 and ELOC forming a CUL3-type ubiquitin ligase complex. Since AtRAD16 also possesses the ring domain, it is possible that AtRAD16 has the ability to form a Cullin-based E3 ubiquitin ligase complex. If so, it will be compelling to identify the components of the E3 ubiquitin ligase complex that AtRAD16 might form. AtRAD16b lacks the ring domain but it has the SNF2 domain (Figure 2.1), therefore I expect AtRAD16b to play a partial redundant function with AtRAD16 in plant GG-NER. These results provide evidence that *Arabidopsis* RAD16 homologs may have a conserved role in plant GG-NER.

2.5.2 *Arabidopsis* RAD16s are required for GG-NER (dark repair)

The role of RAD7/16 damage recognition factors in GG-NER has been studied in the yeast system (Guzder et al.1998). *Arabidopsis* has two homologs of yeast RAD16 (AtRAD16 and AtRAD16b) and in this study I found these homologs to be involved in *Arabidopsis* GG-NER /or UV tolerance. Both *Atrad16* and *Atrad16b* single and double null mutants exhibited a significant increase in seedling and adult UV sensitivity (Figure 2.3a,c&d). I found that the UV sensitivity exhibited by both null alleles is dark-specific (Figure 2.3a &b), which indicates that *Arabidopsis* RAD16 and RAD16b are involved in the dark repair pathway (GG-NER) rather than the light repair pathway of UV induced DNA photoproducts. Even though AtRAD16b was not predicted to interact with other AtRAD7 complex members (Geisler-Lee et al. 2007; Warde-Farley et al. 2010), *AtRAD16b* expression was found to be induced in response to UV-B radiation (Kilian et al. 2007) in the wild type plants. Thus, AtRAD16b may perform a partially redundant function with AtRAD16, and this may account for the additive increased UV-sensitivity observed in the *Atrad16 Atrad16b* double mutant compared to both the *Atrad16* and *Atrad16b* single mutants (Figure 2.3a,c&d). Consistent with my results, *S. cerevisiae rad16* loss of function mutant exhibits increased UV sensitivity (Bang et al. 1995) and ScRAD16 was found to contribute to GG-NER (Li et al. 2007). Similarly, the *S. pombe* RAD16 homologue (rhp16) is also required for GG-NER (Lombaerts et al.1999; Mastro & Forsburg 2014). The UV-sensitivity of *Arabidopsis rad16* and *rad16b* single and double null mutants provides further evidence in support of the involvement of AtRAD16 and AtRAD16b in GG-NER (dark repair).

2.5.3 Regulation of developmental processes

S. pombe RAD16 is required for normal chromosome segregation and loss of function of *ScRAD16* resulted in a reduction in spore viability. In yeast vegetative cells, RAD16 is required for maintaining genome stability (Mastro & Forsburg 2014). In this study, I have shown the involvement of the *Arabidopsis* RAD16 homologs in plant growth and development. *Atrad16* and *atrad16b* single mutants showed early flowering time and short silique length compared to wild type (Figure S2.4a,b&d). Additionally, AtRAD16 overexpression rescued the early flowering time and short silique length

exhibited by *Atrad16* loss of function mutant (Figure S2.5 a,b&d); Figure S2.6a,b&d). These results suggest that AtRAD16s are important for flowering time regulation and silique development. Interestingly, *Atrad16* loss of function mutants exhibited the opposite flowering time phenotype (early) of that previously exhibited by the *Atcul3* null mutant (late; Figure 2.4a&b; Dieterle et al. 2005). This may indicate that AtRAD16s are negative regulators of AtCUL3 activity. It is also possible that *Arabidopsis* ELOC/RAD7/RAD16 and CUL3 form an E3 ligase complex that is required for flowering time regulation. Other classes of CUL3-based E3 ligases such as CUL3/LRB 1&2 also play a role in light signaling including flowering time regulation (Christians et al. 2012) to control flowering time. Thus, the role of AtRAD16 and AtRAD16b is not limited to DNA repair only but it extends to the regulation of important growth parameters.

2.5.4 Overexpression of NER components

Overexpression of AtRAD16 in wild type plants significantly increased adults and seedlings UV tolerance compared to the wild type. Moreover, overexpression of AtRAD16 in *Atrad16-2* null mutant complemented the UV sensitivity exhibited by *Atrad16-2* mutant (Figure 2.4b&c) and (Figure 2.5b&c). In *S. cerevisiae*, a purified RAD7/16 complex from cells overexpressing both proteins was found to bind to damaged DNA and promote the excision of damaged DNA fragment *in vitro* (Guzder et al.1997). Also, *ScRAD16* expression restored the UV-sensitive phenotype exhibited by the yeast *rad16* mutant (Bang et al. 1995). Thus, our results suggest that *Arabidopsis* RAD16 contributes to plant UV tolerance and or/GG-NER, and it is limiting. Consistent with my results, overexpression of GG-NER proteins such as AtRAD4, AtRAD7, AtCEN2, AtDDB2, and AtDDB1a resulted in increased UV tolerance in *Arabidopsis* (Lahari et al. 2018; Lahari et al. 2017; Liang et al. 2006; Molinier et al. 2008). My findings together with the previous findings from *Arabidopsis* and yeast GG-NER studies support my hypothesis, which states that *Arabidopsis* RAD16 is is a component GG-NER.

2.5.5 Cellular localization of NER components

I analyzed AtRAD16 subcellular localization using YFP-tagged RAD16 seedlings. AtRAD16 was found to localize throughout the nucleus (Figure 2.6). The PSI (Plant Subcellular localization integrative predictor; liu et al. 2013) and the consensus algorithm SUBAcon (Hooper et al. 2017) predict AtRAD16 to localize to the nucleus with scores of 0.959 and 1.000, respectively. Additionally, the cNLS mapper predicts AtRAD16 to have classical monopartite NLSs (Kosug et al. 2009). Thus, my AtRAD16 nuclear localization result was consistent with the results obtained by *in silico* prediction tools. AtRAD16 nuclear location was not affected by UV treatment (Figure 2.7).

AtRAD16 nuclear localization is consistent with the role of AtRAD16 in NER that takes place in the nucleus after UV damage. This nuclear localization is also consistent with the dark-specific UV sensitivity exhibited by *Atrad16* loss of function mutant (Figure2.3a,c,&d), and the increased UV tolerance exhibited by AtRAD16 overexpression (Figure 24.b&c; Figure 2.5b&c) which all suggest the involvement of AtRAD16 in UV tolerance and/or GG-NER.

Like AtRAD16, other *Arabidopsis* NER proteins such as AtRAD7, AtRAD4 and AtDDB2 are nuclear localized (Lahari et al. 2018; Lahari et al. 2017; Molinier et al. 2008). GFP-tagged AtCSA, a TC-NER protein also exhibited nuclear localization (Biedermann and Hellmann 2010). However, the *Arabidopsis* homolog of mammalian NER factor CEN2 (AtCEN2) exhibited cytoplasmic localization under unstressed conditions and is shuttled to the nucleus upon UV treatment (Liang et al. 2006). Similarly, *Arabidopsis* DDB1 (a homolog of mammalian DDB1 damage recognition factor) was found to relocalize from the cytosol to the nucleus following UV treatment (Molinier et al. 2008). These results suggest that NER proteins that are located in the cytosol under unstressed conditions, shuttled to the nucleus following UV radiation. Whereases, those are located in the nucleus remain there.

Consistent with my results, GFP tagged ScRAD16 was found to be localized in the nucleus, and treatment with methyl methanesulfonate and hydroxyurea, DNA damaging agents, did not change this pattern (Tkach et al. 2012). *S. pombe* RAD16 homolog rhp16 is also predicted to be localized to the nucleus as predicted by the eukaryotic protein subcellular localization predictor (Almagro Armenteros et al. 2019).

2.5.6 Suggested role for *Arabidopsis* RAD7/16 complex in GG-NER

I used yeast two-hybrid assay to identify the proteins that physically interact with AtRAD16. My results showed physical interactions between the following protein pairs: AtRAD16 with AtRAD7a (Figure2.8), and AtRAD16 with AtRAD7c (Figure 2.9). This result is consistent with the Genemania prediction server, which predicts an interaction between AtRAD16 and AtRAD7a, as well as between AtRAD16 and AtRAD7c. However, no interaction was detected between AtRAD16 and AtRAD7b, this result contradicts the AIV prediction model that predicts an interaction between AtRAD16 and AtRAD7b (Figure S2.8). Protein sequence analysis of *Arabidopsis* RAD7a, RAD7b, and RAD7c shows that AtRAD7a and AtRAD7c are more closely related to each other than to AtRAD7b, as they share 43% amino acid identity. However, AtRAD7b shares only 27% and 24% amino acid identity with AtRAD7a & AtRAD7c respectively, which may explains the lack of interaction between AtRAD16 and AtRAD7b.

Consistent with my results, in *S. cerevisiae* an interaction between ScRAD16 and ScRAD7 has been detected in yeast two-hybrid assays (Wang et al. 1997). ScRAD16 interacts with ScRAD7 and forms the yeast GG-NER initiation complex known as NEF4 in response to UV- damaged DNA. This complex recognizes UV damaged DNA, binds to it, and recruits other NER components to the damaged DNA. The interaction between ScRAD16 and ScRAD7 is required for the repair of transcriptionally inactive DNA *in vivo* (Ramsey et al. 2004). Therefore, the interaction between AtRAD16 and AtRAD7 suggests that the yeast GG-NER initiation complex RAD7/16 is active in *Arabidopsis.*

AtRAD16 did not physically interact with each of AtELOC (Figure S2.11), and AtRAD23 (Figure S2.12). Consistent with my results, no interaction between ScRAD16 and ScELOC1 or ScRAD23 has been demonstrated in yeast. Nevertheless, physical interaction between ScRAD16 and ScELOC1 was determined by using co-purification techniques (Gillette et al. 2006), and genetic interaction was detected between ScRAD16 and ScRAD23 (Ramsey et al. 2004). My results also showed genetic interaction between *AtRAD16* and *AtRAD23*. No physical interaction was detected between AtRAD16 and AtRAD4 (Figure S2.9). Similarly, ScRAD16 was found not to physically interact with ScRAD4 using yeast two-hybrid assay (Wang et al. 1997).

2.5.7 AtRAD16 and AtRAD7 are involved in UV tolerance

Arabidopsis rad7 and *rad16* single loss of function mutants exhibited enhanced UV sensitivity in both seedlings and adults compared to the wild type (Figure 2.10b&d), and *Arabidopsis rad7 rad16* double loss of function mutant plants are more sensitive to UV radiation than the single null mutants. Consistent with our results, loss of function studies of the yeast *S. cerevisiae* showed that ScRAD7 and ScRAD16 are required for the repair of the untranscribed regions of the genome, and loss of either gene resulted in a moderate UV sensitivity (Ramsey et al. 2004, Lettieri et al. 2008, Guzder et al.1998). However, yeast *rad7 rad16* double loss of function mutant exhibited UV sensitivity resemble that of single mutants (Verhage et al.1994; Wang et al. 1997).Thus, my results suggest that both *Arabidopsis* RAD7 and RAD16 are required for plant UV tolerance. Moreover, the role of *Arabidopsis* RAD7and/or RAD16 extends the damage recognition pathway identified in yeast to other NER pathways. Additionally, The UV sensitivity exhibited by the *Atrad7a Atrad16* double null mutant plants resembles that exhibited by *Atra7a Atrad7c* double null mutant plants. This result my account for the partial redundancy between *AtRAD7a* and *AtRAD7c*, thus AtRAD7c might partially complement *Atrad7a* loss of function in the *Atrad7a Atrad16* double null mutant.

2.5.8 *Arabidopsis* RAD16 and RAD23 are required for embryo development

I examined the genetic interaction between *AtRAD16* and *AtRAD23b* and found that loss of both *AtRAD16* and *AtRAD23b* resulted in embryo lethality. This suggests that AtRAD16 acts with AtRAD23b regulate growth and development. In the *S. cerevisiae*, RAD4 alone is expected to be intrinsically unstable and RAD23 binding to RAD4 was found to stabilize RAD4 levels in unstressed cells (Xie et al. 2004). Additionally, ScRad23 is functionally redundant with one of the ScRAD16 biochemical activities (Ramsey et al. 2004), so it is possible that ScRAD16 is also involved in stabilizing the ScRAD4 level. In *Arabidopsis*, it is possible that both AtRAD23 and AtRAD16 are also involved in stabilizing AtRAD4 level and preventing its degradation like their yeast counterparts. Thus, loss of function of both AtRAD16 and AtRAD23b may result in AtRAD4 instability and degradation. Since the loss of function mutation of AtRAD4 was found to be lethal (Lahari et al. 2018), my finding may indicate that the

embryo lethality of the *Arabidopsis rad16 rad23b* double mutant is an indirect effect of the reduced or unstable AtRAD4 levels in the double mutant.

Alternatively, given that *Atrad23b* loss of function mutant exhibited mild sterility defect (Farmer et al. 2010) and *Atrad16* loss of function mutation resulted in short silique length and early flowering time. Thus, it is possible that both *AtRAD16* and *AtRAD23* are involved in the regulation of important growth parameters, thus loss of both *At RAD23* and *AtRAD16* results in defect in embryo development.

2.5.9 Both RAD7/16 and DDB1/2 damage recognition modules contribute to *Arabidopsis* UV tolerance

The role of AtDDB2 (a homolog of the mammalian GG-NER damage recognition factor DDB2) in plant UV tolerance has been reported (Koga et al. 2006). The *Atddb2* single null mutant exhibits increased UV sensitivity (Molinier et al. 2008), and in this research, *the Atrad16* single mutant also exhibited increased UV sensitivity (Figure 2.3). Thus, both AtRAD16 and AtDDB2 contribute to plant UV tolerance and/or DNA repair. I also showed that the UV sensitivity exhibited by *Atddb2* null mutant is more than 10% higher than the UV sensitivity exhibited by *Atrad16* null mutant. In addition, UV sensitivity of *Atrad16 Atddb2* double null mutant plants is significantly higher than than that exhibited by the *Atrad16* and the *Atddb2* single null mutants (Figure 2.11). The enhanced UV sensitivity exhibited by *Atrad16 Atddb2* double mutant reflects the additive UV sensitivity exhibited by single mutants, and indicates that both the yeast homolog (RAD7/16 complex) and the mammalian homolog (DDB1/2 complex) are required for plant GG-NER. This result is consistent with my plant GG-NER model, as I expect homologs of both yeast and mammalian GG-NER damage recognition factors to contribute to plant GG-NER via forming two different complexes.

2.5.10 Both *Arabidopsis* RAD16 and CSB/UVSSA contribute to plant UV tolerance and CSB/UVSSA pathway is more essential at early developmental stages

In *Arabidopsis*, CSB and UVSSA (the homologs of mammalian TC-NER factors), were found to be involved in TC-NER. Inactivation of either AtCSB or AtUVSSA results in increased UV sensitivity (Alkhateeb et al. 2019; Shaked et al. 2006). Findings from

this study demonstrated that *Atcsb Atrad16* and *Atuvssa Atrad16* double null mutants are UV radiation sensitive compared to single mutants in both seedlings and adults (Figure 2.12). The adult UV sensitivity exhibited by *Atcsb Atrad16* and *Atuvssa Atrad16* mutants was more severe than the adult UV sensitivity exhibited by *rad7 rad16* and *ddb2 rad16* double mutants. Additionally, irradiating *Atcsb Atrad16* and *Atuvssa Atrad16* double loss of function mutant seedlings with 1000 J resulted in a sever reduction in seedlings growth to a degree that prevents me from detecting seedlings UV sensitivity, which may indicate that the role that TC-NER component play during NER is more significant than that of GG-NER components at early developmental stages.

Taken together, these results suggest that the *Arabidopsis* RAD7/16 (the yeast-like GG-NER path) makes a significant contribution to plant NER compared to CSB/UVSSA and DDB1/2 pathways. These data agree with my plant NER model in which I hypothesized AtRAD16, AtDDB2, and AtCSB/UVSSA to contribute to GG-NER and NER pathways, respectively (Figure S2.17).

2.6 References

Al Khateeb, W. M., & Schroeder, D. F. (2009). Overexpression of *Arabidopsis* damaged DNA binding protein 1A (DDB1A) enhances UV tolerance. Plant molecular biology, 70(4), 371–383. https://doi.org/10.1007/s11103-009-9479-9

Al Khateeb, W. M., Sher, A. A., Marcus, J. M., & Schroeder, D. F. (2019). UVSSA, UBP12, and RDO2/TFIIS Contribute to *Arabidopsis* UV Tolerance. Frontiers in plant science, 10, 516. https://doi.org/10.3389/fpls.2019.00516

Almagro Armenteros, J. J., Salvatore, M., Emanuelsson, O., Winther, O., von Heijne, G., Elofsson, A., & Nielsen, H. (2019). Detecting sequence signals in targeting peptides using deep learning. Life science alliance, 2(5), e201900429. https://doi.org/10.26508/lsa.201900429

Bang, D. D., Timmermans, V., Verhage, R., Zeeman, A. M., van de Putte, P., & Brouwer, J. (1995). Regulation of the Saccharomyces cerevisiae DNA repair gene RAD16. Nucleic acids research, 23(10), 1679–1685. https://doi.org/10.1093/nar/23.10.1679

Biedermann, S., & Hellmann, H. (2010). The DDB1a interacting proteins ATCSA-1 and DDB2 are critical factors for UV-B tolerance and genomic integrity in *Arabidopsis thaliana*. The Plant journal : for cell and molecular biology, 62(3), 404–415. https://doi.org/10.1111/j.1365-313X.2010.04157.x

Boiteux, S., & Jinks-Robertson, S. (2013). DNA repair mechanisms and the bypass of DNA damage in Saccharomyces cerevisiae. Genetics, 193(4), 1025–1064. https://doi.org/10.1534/genetics.112.145219

Bucevičius, J., Lukinavičius, G., & Gerasimaitė, R. (2018). The use of Hoechst dyes for DNA staining and beyond. Chemosensors, 6(2), 18.
Christians, M. J., Gingerich, D. J., Hua, Z., Lauer, T. D., & Vierstra, R. D. (2012). The light-response BTB1 and BTB2 proteins assemble nuclear ubiquitin ligases that modify phytochrome B and D signaling in *Arabidopsis*. Plant physiology, 160(1), 118–134. https://doi.org/10.1104/pp.112.199109
Delwiche, C. F., & Cooper, E. D. (2015). The Evolutionary Origin of a Terrestrial Flora. Current biology : CB, 25(19), R899–R910. https://doi.org/10.1016/j.cub.2015.08.029
Dieterle, M., Thomann, A., Renou, J. P., Parmentier, Y., Cognat, V., Lemonnier, G., Müller, R., Shen, W. H., Kretsch, T., & Genschik, P. (2005). Molecular and functional characterization of *Arabidopsis* Cullin 3A. The Plant journal : for cell and molecular biology, 41(3), 386–399. https://doi.org/10.1111/j.1365-313X.2004.02302.x
Earley, K. W., Haag, J. R., Pontes, O., Opper, K., Juehne, T., Song, K., & Pikaard, C. S. (2006). Gateway-compatible vectors for plant functional genomics and proteomics. The Plant journal : for cell and molecular biology, 45(4), 616–629. https://doi.org/10.1111/j.1365-313X.2005.02617.x
El-Mahdy, M. A., Zhu, Q., Wang, Q. E., Wani, G., Prætorius-Ibba, M., & Wani, A. A. (2006). Cullin 4A-mediated proteolysis of DDB2 protein at DNA damage sites regulates in vivo lesion recognition by XPC. The Journal of biological chemistry, 281(19), 13404–13411. https://doi.org/10.1074/jbc.M511834200
Essen, L. O., & Klar, T. (2006). Light-driven DNA repair by photolyases. Cellular and molecular life sciences : CMLS, 63(11), 1266–1277. https://doi.org/10.1007/s00018-005-5447-y
Farmer, L. M., Book, A. J., Lee, K. H., Lin, Y. L., Fu, H., & Vierstra, R. D. (2010). The RAD23 family provides an essential connection between the 26S proteasome and ubiquitylated proteins in *Arabidopsis*. The Plant cell, 22(1), 124–142. https://doi.org/10.1105/tpc.109.072660
Flaus, A., & Owen-Hughes, T. (2011). Mechanisms for ATP-dependent chromatin remodelling: the means to the end. The FEBS journal, 278(19), 3579–3595. https://doi.org/10.1111/j.1742-4658.2011.08281.x
Ganpudi, A. L., & Schroeder, D. F. (2011). UV Damaged DNA Repair & Tolerance in Plants. In (Ed.), Selected Topics in DNA Repair. IntechOpen. https://doi.org/10.5772/22138
Ganpudi, A. L., & Schroeder, D. F. (2013). Genetic interactions of *Arabidopsis thaliana* damaged DNA binding protein 1B (DDB1B) with DDB1A, DET1, and COP1. G3 (Bethesda, Md.), 3(3), 493–503. https://doi.org/10.1534/g3.112.005249
Geisler-Lee, J., O'Toole, N., Ammar, R., Provart, N. J., Millar, A. H., & Geisler, M. (2007). A predicted interactome for *Arabidopsis*. Plant physiology, 145(2), 317–329. https://doi.org/10.1104/pp.107.103465
Gillette, T. G., Yu, S., Zhou, Z., Waters, R., Johnston, S. A., & Reed, S. H. (2006). Distinct functions of the ubiquitin-proteasome pathway influence nucleotide excision repair. The EMBO journal, 25(11), 2529–2538. https://doi.org/10.1038/sj.emboj.7601120

Guzder, S. N., Sung, P., Prakash, L., & Prakash, S. (1997). Yeast Rad7-Rad16 complex, specific for the nucleotide excision repair of the nontranscribed DNA strand, is an ATP-dependent DNA damage sensor. *The Journal of biological chemistry*, *272*(35), 21665–21668. https://doi.org/10.1074/jbc.272.35.21665

Guzder, S. N., Sung, P., Prakash, L., & Prakash, S. (1998). The DNA-dependent ATPase activity of yeast nucleotide excision repair factor 4 and its role in DNA damage recognition. The Journal of biological chemistry, 273(11), 6292–6296. https://doi.org/10.1074/jbc.273.11.6292

Heinicke, S., Livstone, M. S., Lu, C., Oughtred, R., Kang, F., Angiuoli, S. V., White, O., Botstein, D., & Dolinski, K. (2007). The Princeton Protein Orthology Database (P-POD): a comparative genomics analysis tool for biologists. PloS one, 2(8), e766. https://doi.org/10.1371/journal.pone.0000766

Henning, K. A., Li, L., Iyer, N., McDaniel, L. D., Reagan, M. S., Legerski, R., Schultz, R. A., Stefanini, M., Lehmann, A. R., Mayne, L. V., & Friedberg, E. C. (1995). The Cockayne syndrome group A gene encodes a WD repeat protein that interacts with CSB protein and a subunit of RNA polymerase II TFIIH. Cell, 82(4), 555–564. https://doi.org/10.1016/0092-8674(95)90028-4

Hooper, C. M., Castleden, I. R., Tanz, S. K., Aryamanesh, N., & Millar, A. H. (2017). SUBA4: the interactive data analysis centre for *Arabidopsis* subcellular protein locations. Nucleic acids research, 45(D1), D1064–D1074. https://doi.org/10.1093/nar/gkw1041

Hossain, Z., Amyot, L., McGarvey, B., Gruber, M., Jung, J., & Hannoufa, A. (2012). The translation elongation factor eEF-1Bβ1 is involved in cell wall biosynthesis and plant development in *Arabidopsis thaliana*. PloS one, 7(1), e30425. https://doi.org/10.1371/journal.pone.0030425

Jain, M., Nijhawan, A., Tyagi, A. K., & Khurana, J. P. (2006). Validation of housekeeping genes as internal control for studying gene expression in rice by quantitative real-time PCR. Biochemical and biophysical research communications, 345(2), 646–651. https://doi.org/10.1016/j.bbrc.2006.04.140

Kilian, J., Whitehead, D., Horak, J., Wanke, D., Weinl, S., Batistic, O., D'Angelo, C., Bornberg-Bauer, E., Kudla, J., & Harter, K. (2007). The AtGenExpress global stress expression data set: protocols, evaluation and model data analysis of UV-B light, drought and cold stress responses. The Plant journal : for cell and molecular biology, 50(2), 347–363. https://doi.org/10.1111/j.1365-313X.2007.03052.x

Koga, A., Ishibashi, T., Kimura, S., Uchiyama, Y., & Sakaguchi, K. (2006). Characterization of T-DNA insertion mutants and RNAi silenced plants of *Arabidopsis thaliana* UV-damaged DNA binding protein 2 (AtUV-DDB2). Plant molecular biology, 61(1-2), 227–240. https://doi.org/10.1007/s11103-006-6408-z

Kosugi, S., Hasebe, M., Tomita, M., and Yanahawa, H. (2009). Systematic identification of cell cycle-dependent yeast nucleocytoplasmic shuttling proteins by prediction of composite motifs. Proc. Natl. Acad. Sci. U.S.A. 106, 10171–10176. doi: 10.1073/pnas.0900604106

Lahari, T., Lazaro, J., & Schroeder, D. (2017). RAD4 and RAD23/HMR Contribute to *Arabidopsis* UV Tolerance. Genes, 9(1), 8. doi:10.3390/genes9010008

Lahari, T., Lazaro, J., Marcus, J. M., & Schroeder, D. F. (2018). RAD7 homologues contribute to *Arabidopsis* UV tolerance. Plant science : an international journal of

experimental plant biology, 277, 267–277. https://doi.org/10.1016/j.plantsci.2018.09.017
Lettieri, T., Kraehenbuehl, R., Capiaghi, C., Livingstone-Zatchej, M., & Thoma, F. (2008). Functionally distinct nucleosome-free regions in yeast require Rad7 and Rad16 for nucleotide excision repair. DNA repair, 7(5), 734–743. https://doi.org/10.1016/j.dnarep.2008.01.016
Li, S., Ding, B., LeJeune, D., Ruggiero, C., Chen, X., & Smerdon, M. J. (2007). The roles of Rad16 and Rad26 in repairing repressed and actively transcribed genes in yeast. DNA repair, 6(11), 1596–1606. https://doi.org/10.1016/j.dnarep.2007.05.005
Li, X., Guo, X., Zhao, L., Zhang, J., Tang, D., Zhao, X., & Liu, X. (2012). *Arabidopsis* rad23-4 gene is required for pollen development under UV-B light. African Journal of Biotechnology, 11(44), 10161-10169.
Liang, L., Flury, S., Kalck, V., Hohn, B., & Molinier, J. (2006). CENTRIN2 interacts with the *Arabidopsis* homolog of the human XPC protein (AtRAD4) and contributes to efficient synthesis-dependent repair of bulky DNA lesions. Plant molecular biology, 61(1-2), 345–356. https://doi.org/10.1007/s11103-006-0016-9
Liu, L., Zhang, Z., Mei, Q., & Chen, M. (2013). PSI: a comprehensive and integrative approach for accurate plant subcellular localization prediction. PloS one, 8(10), e75826. https://doi.org/10.1371/journal.pone.0075826
Lombaerts, M., Peltola, P. H., Visse, R., den Dulk, H., Brandsma, J. A., & Brouwer, J. (1999). Characterization of the rhp7(+) and rhp16(+) genes in Schizosaccharomyces pombe. Nucleic acids research, 27(17), 3410–3416. https://doi.org/10.1093/nar/27.17.3410
Lu, Q., Tang, X., Tian, G., Wang, F., Liu, K., Nguyen, V., Kohalmi, S. E., Keller, W. A., Tsang, E. W., Harada, J. J., Rothstein, S. J., & Cui, Y. (2010). *Arabidopsis* homolog of the yeast TREX-2 mRNA export complex: components and anchoring nucleoporin. The Plant journal : for cell and molecular biology, 61(2), 259–270. https://doi.org/10.1111/j.1365-313X.2009.04048.x
Mastro, T. L., & Forsburg, S. L. (2014). Increased meiotic crossovers and reduced genome stability in absence of Schizosaccharomyces pombe Rad16 (XPF). Genetics, 198(4), 1457–1472. https://doi.org/10.1534/genetics.114.171355
Molinier, J., Lechner, E., Dumbliauskas, E., & Genschik, P. (2008). Regulation and role of *Arabidopsis* CUL4-DDB1A-DDB2 in maintaining genome integrity upon UV stress. PLoS genetics, 4(6), e1000093. https://doi.org/10.1371/journal.pgen.1000093
Molinier, J., Ramos, C., Fritsch, O., & Hohn, B. (2004). CENTRIN2 modulates homologous recombination and nucleotide excision repair in *Arabidopsis*. The Plant cell, 16(6), 1633–1643. https://doi.org/10.1105/tpc.021378
Mullenders L., (2018). Solar UV damage to cellular DNA: from mechanisms to biological effects. Photochemical & photobiological sciences : Official journal of the European Photochemistry Association and the European Society for Photobiology, 17(12), 1842–1852. https://doi.org/10.1039/c8pp00182k
Narlikar, G. J., Sundaramoorthy, R., & Owen-Hughes, T. (2013). Mechanisms and functions of ATP-dependent chromatin-remodeling enzymes. Cell, 154(3), 490–503. https://doi.org/10.1016/j.cell.2013.07.011

Nishi, R., Okuda, Y., Watanabe, E., Mori, T., Iwai, S., Masutani, C., Sugasawa, K., & Hanaoka, F. (2005). Centrin 2 stimulates nucleotide excision repair by interacting with xeroderma pigmentosum group C protein. Molecular and cellular biology, 25(13), 5664–5674. https://doi.org/10.1128/MCB.25.13.5664-5674.2005

Petruseva, I. O., Evdokimov, A. N., & Lavrik, O. I. (2014). Molecular mechanism of global genome nucleotide excision repair. Acta naturae, 6(1), 23–34.

Ramsey, K. L., Smith, J. J., Dasgupta, A., Maqani, N., Grant, P., & Auble, D. T. (2004). The NEF4 complex regulates Rad4 levels and utilizes Snf2/Swi2-rELOAted ATPase activity for nucleotide excision repair. Molecular and cellular biology, 24(14), 6362–6378. https://doi.org/10.1128/MCB.24.14.6362-6378.2004

Rastogi, R. P., Richa, Kumar, A., Tyagi, M. B., & Sinha, R. P. (2010). Molecular mechanisms of ultraviolet radiation-induced DNA damage and repair. Journal of nucleic acids, 2010, 592980. https://doi.org/10.4061/2010/592980

Reed, S. H. (2005). Nucleotide excision repair in chromatin: the shape of things to come. DNA repair, 4(8), 909–918. https://doi.org/10.1016/j.dnarep.2005.04.009

Ribar, B., Prakash, L., & Prakash, S. (2006). Requirement of ELOC1 for RNA polymerase II polyubiquitylation and degradation in response to DNA damage in Saccharomyces cerevisiae. Molecular and cellular biology, 26(11), 3999–4005. https://doi.org/10.1128/MCB.00293-06

Schmid, M., Davison, T. S., Henz, S. R., Pape, U. J., Demar, M., Vingron, M., Schölkopf, B., Weigel, D., & Lohmann, J. U. (2005). A gene expression map of *Arabidopsis thaliana* development. Nature genetics, 37(5), 501–506. https://doi.org/10.1038/ng1543

Shaked, H., Avivi-Ragolsky, N., & Levy, A. A. (2006). Involvement of the *Arabidopsis* SWI2/SNF2 chromatin remodeling gene family in DNA damage response and recombination. Genetics, 173(2), 985–994. https://doi.org/10.1534/genetics.105.051664

Shuck, S. C., Short, E. A., & Turchi, J. J. (2008). Eukaryotic nucleotide excision repair: from understanding mechanisms to influencing biology. Cell research, 18(1), 64–72. https://doi.org/10.1038/cr.2008.2

Spampinato C. P. (2017). Protecting DNA from errors and damage: an overview of DNA repair mechanisms in plants compared to mammals. Cellular and molecular life sciences : CMLS, 74(9), 1693–1709. https://doi.org/10.1007/s00018-016-2436-2

Spivak, G. (2016). Transcription-coupled repair: an update. Archives of toxicology, 90(11), 2583–2594. https://doi.org/10.1007/s00204-016-1820-x

Sugasawa, K. (2016). Molecular mechanisms of DNA damage recognition for mammalian nucleotide excision repair. DNA repair, 44, 110–117. https://doi.org/10.1016/j.dnarep.2016.05.015

Tatum, D. and S. Li (2011). Nucleotide excision repair in S. cerevisiae. DNA Repair / Book 1. F. Storici, InTech Open Access Publisher: 97-122.

Tkach, J. M., Yimit, A., Lee, A. Y., Riffle, M., Costanzo, M., Jaschob, D., Hendry, J. A., Ou, J., Moffat, J., Boone, C., Davis, T. N., Nislow, C., & Brown, G. W. (2012). Dissecting DNA damage response pathways by analysing protein localization and abundance changes during DNA replication stress. Nature cell biology, 14(9), 966–976. https://doi.org/10.1038/ncb2549

Verhage, R., Zeeman, A. M., de Groot, N., Gleig, F., Bang, D. D., van de Putte, P., & Brouwer, J. (1994). The RAD7 and RAD16 genes, which are essential for pyrimidine dimer removal from the silent mating type loci, are also required for repair of the nontranscribed strand of an active gene in Saccharomyces cerevisiae. Molecular and cellular biology, 14(9), 6135–6142. https://doi.org/10.1128/mcb.14.9.6135-6142.1994

Vermeulen, W., & Fousteri, M. (2013). Mammalian transcription-coupled excision repair. Cold Spring Harbor perspectives in biology, 5(8), a012625. https://doi.org/10.1101/cshperspect.a012625

Wang, H., Zhai, L., Xu, J., Joo, H. Y., Jackson, S., Erdjument-Bromage, H., Tempst, P., Xiong, Y., & Zhang, Y. (2006). Histone H3 and H4 ubiquitylation by the CUL4-DDB-ROC1 ubiquitin ligase facilitates cellular response to DNA damage. Molecular cell, 22(3), 383–394. https://doi.org/10.1016/j.molcel.2006.03.035

Wang, Z., Wei, S., Reed, S. H., Wu, X., Svejstrup, J. Q., Feaver, W. J., Kornberg, R. D., & Friedberg, E. C. (1997). The RAD7, RAD16, and RAD23 genes of Saccharomyces cerevisiae: requirement for transcription-independent nucleotide excision repair in vitro and interactions between the gene products. Molecular and cellular biology, 17(2), 635–643. https://doi.org/10.1128/MCB.17.2.635

Warde-Farley, D., Donaldson, S. L., Comes, O., Zuberi, K., Badrawi, R., Chao, P., Franz, M., Grouios, C., Kazi, F., Lopes, C. T., Maitland, A., Mostafavi, S., Montojo, J., Shao, Q., Wright, G., Bader, G. D., & Morris, Q. (2010). The GeneMANIA prediction server: biological network integration for gene prioritization and predicting gene function. Nucleic acids research, 38(Web Server issue), W214–W220. https://doi.org/10.1093/nar/gkq537

Weber, H., Bernhardt, A., Dieterle, M., Hano, P., Mutlu, A., Estelle, M., Genschik, P., & Hellmann, H. (2005). *Arabidopsis* AtCUL3a and AtCUL3b form complexes with members of the BTB/POZ-MATH protein family. Plant physiology, 137(1), 83–93. https://doi.org/10.1104/pp.104.052654

Weigel, D., & Glazebrook, J. (2006). Vectors and agrobacterium hosts for *Arabidopsis* transformation. CSH protocols, 2006(7), pdb.ip29. https://doi.org/10.1101/pdb.ip29

Xie, Z., Liu, S., Zhang, Y., & Wang, Z. (2004). Roles of Rad23 protein in yeast nucleotide excision repair. Nucleic acids research, 32(20), 5981–5990. https://doi.org/10.1093/nar/gkh934

Yu, S., Evans, K., van Eijk, P., Bennett, M., Webster, R. M., Leadbitter, M., Teng, Y., Waters, R., Jackson, S. P., & Reed, S. H. (2016). Global genome nucleotide excision repair is organized into domains that promote efficient DNA repair in chromatin. Genome research, 26(10), 1376–1387. https://doi.org/10.1101/gr.209106.116

Chapter Bridge

Throughout this thesis, I characterized the role of *Arabidopsis* RAD16 and ELOC homologs in plant UV tolerance and growth. I also identified an *Arabidopsis* ELOA homolog and characterized its role in plant UV tolerance and growth. In the first stream, I characterized the role of *Arabdopsis* RAD16 homolog in plant UV tolerance and growth and examined its physical and genetic interactions with other NER components. In the second stream, I identified a *Arabidopsis* ELOA homolog and characterized its role in plant UV tolerance and growth. I also characterized the role of *Arabidopsis* ELOC homolog in plant UV tolerance and growth and investigated its physical and genetic interactions with *Arabidopsis* ELOA homolog.

Chapter 3. Characterization of Elongin homologues in *Arabidopsis thaliana*

Alrayes LN, Bell A, Carter A, Stout J, Schroeder DF. Manuscript in preparation

3.1 Abstract

Elongins A (ELOA), B (ELOB), and C (ELOC) were originally identified in mammals as transcription elongation complex. In addition to this transcript elongation activity, the three mammalian elongins are involved in E3 ligase complex that targets the large subunit of the stalled RNA polymerase II for degradation following DNA damage. *S.cerevisiae* also possesses ELOA and ELOC homologs but no ELOB. *S. cerevisiae* ELOA and ELOC also forms an E3 ligase complex that targets the large subunit of the stalled RNA polymerase II for degradation following DNA damage. The function of yeast ELOA and ELOC seems to be conserved with their mammalian counterparts, as yeast ELOC can enhance mammalian ELOA transcript elongation via interacting with it, but the yeast ELOA/C complex alone does not promote yeast transcriptional elongation. The roles of these proteins in polyubiquitylation and degradation of RNA polymerase II following DNA damage have been well characterized. In this study, I identified *Arabidopsis* elongin A homologue (ELOA; At2g42780) and examined the role of the ELOA and elongin C homologue (ELOC; At5g59140) in plant UV tolerance and development using molecular and genetic analysis. YFP-ELOA was found to exhibit

nuclear localization and this pattern was not affected after UV treatment. However, YFP-ELOC was observed in both nuclei and apparent cytosol and the cytoplasmic localization decreased after UV treatment. Both *Ateloa-2* and *Ateloc-3* loss of function mutants exhibited enhanced UV-sensitive phenotypes in both seedlings and adults. In addition, ELOA overexpression enhanced hypocotyl UV tolerance. Yeast two-hybrid screening was used to confirm the interaction between *Arabidopsis* ELOA and ELOC as identified by previous high throughput results. Interestingly, ELOA and ELOC overexpression increased the silique length and seed number, and ELOC overexpression increased plant height. Therefore, my results indicate that ELOA and ELOC homologs are required for *Arabidopsis* UV tolerance and involved in plant development.

3.2 Introduction

Plants depend on solar radiation for energy, and beneficial visible light (425-780 nm) is crucial for plant growth and development. However, harmful ultraviolet (UV) in the (100-400 nm) range can damage DNA by generating cyclobutane pyrimidine dimer and 6-4 photoproducts that both inhibit DNA transcription and replication, and thus DNA repair mechanisms are crucial for maintaining cellular viability and DNA integrity (Donà & Mittelstein Scheid 2015). All cellular life on earth have evolved mechanisms to detect and repair these UV photoproducts, and as such many of the mechanisms that perform these functions are highly conserved across prokaryotic and eukaryotic lineages. Although there is overall conservation in the function of these repair pathways, there are differences in the individual component proteins that perform these functions with examples of non-homologous proteins serving similar functions in different evolutionary lineages.

In general, UV damaged DNA is repaired via two pathways: light-dependent repair (also called photoreactivation) which enzymatically repairs damaged bases, and the light-independent nucleotide excision repair (NER) which removes and replaces damaged bases. Steps in NER include damage recognition and verification, the unwinding of the double helix around the lesion, excision of the lesion, DNA synthesis using the undamaged strand as a template, and finally ligation of the new bases to the

DNA strand (Al Khateeb et al. 2019; Boiteux & Jinks-Robertson 2013; Lahari et al. 2018). There are two different mechanisms through which NER occurs. Transcription coupled NER (TC-NER) recognizes the damage in the template DNA strand when lesions interrupt RNA polymerase II (RNAP II) elongation (Johann To Berens & Molinier 2020; Mullenders 2018; Rastogi et al. 2010). In contrast, global genomic NER (GG-NER) detects the damage of nontranscribed regions throughout the genome. In human GG-NER, UV photoproducts are recognized by the Damaged DNA Binding protein (DDB) 1 and 2 / Cullin 4 (CUL4) E3 ubiquitin ligase complex (Ribeiro-Silva et al. 2020; Sugasawa 2016). In the yeast *S. cerevisiae*, the RAD7, RAD16, Elongin C (ELOC), and Cullin 3 (CUL3) also recognize UV-damaged DNA, yet these proteins are not directly homologous to the human proteins that have the same function (Boiteux & Jinks-Robertson 2013; Gillette et al. 2006). In both humans and yeast, the damage recognition by the DDB1/2 and RAD7/16 complexes (respectively) is followed by chromatin modification and ubiquitination of conserved components human XERODERMA PIGMENTOSA complementation groupC (HsXPC) and yeast RADIATION SENSITIVE 4 (ScRAD4). Then, XPC/RAD4 together with HR23B/RAD23 and CENTRIN2 (CEN2)/ScCDC31 recruits the core NER activities (Reed 2005; Shuck et al. 2008; Sugasawa 2016). Thus, the yeast E3 ligase complex ELOC/RAD7/RAD16/CUL3 is required for GG-NER. In mammalian systems, ELOC together with Elongin B forms multiple E3 ligase complexes through interacting with CUL2, Ring Box protein 1(RBX I), and VHL (von Hippel-Lindau tumor suppressor) protein, or with CUL5, Ring Box 2 (RBX2), and (Suppressor of Cytokine Signaling) SOCS box proteins (Mahrour et al. 2008; Okumura et al. 2012). Therefore, the mammalian ELOC also forms E3 ligase complexes but with different cullins other than CUL3. In *Arabidopsis*, no homologues of Cul2, Cul5, VHL, or SOCS type proteins have been identified. Nevertheless, *Arabidopsis* ELOC is well conserved, it shares more than 70% amino acid identity with ELOC homologs in other plants, 46% and 40% identity with human and yeast ELOC homologs, respectively (Yamasaki & Ohama 2011). ELOC consists of a single BTB domain that interacts with CUL3, but ELOC also shares 30% amino acid identity with SKP1 proteins that interact with CUL1 (Stogios et al. 2005). Thus, in plants, Elongins could interact with Cullin and Ring box protein to have E3 ligase activity. It will be compelling to determine if

the AtELOC protein can form a cullin-based E3 ligase complex and if so, with which proteins.

ELOC was originally identified in mammals as part of the Elongin heterotrimer consisting of Elongin A (ELOA), the large transcriptionally active subunit, ELOB, and ELOC (Bradsher et al.1993 a &b). Under unstressed conditions, ELOB and ELOC bind to the BC box motif of ELOA to form a heterotrimer that enhances the rate of RNAP II elongation and inhibits the enzyme transient pausing during transcription (Aso et al. 1995; Conaway & Conaway 2019; Kawauchi et al. 2013; Weems et al. 2015). However, after DNA damage, and when the damage is in transcriptionally active DNA, the three mammalian Elongins A/B/C interact with CUL5 and RBX2 to form another E3 ubiquitin ligase complex that ubiquitinates Rpb1, the large subunit of transcriptionally stalled RNAPol II at sites of DNA lesions (Conaway & Conaway 2019; Okumura et al. 2012; Weems et al. 2015; Yasukawa et al. 2008;). In *Saccharomyces cerevisiae*, sequence homologues of mammalian ELOA and ELOC have been identified, but no obvious Elongin B homologue is present in the genome (Aso & Conrad 1997; Koth et al. 2000). Yeast ELOA and ELOC homologs can form a stable dimer but is not involved in yeast transcript elongation during unstressed conditions (Koth et al. 2000). However, following DNA damage the yeast ELOA/ELOC complex interacts with CUL3 and RBX1 to form an E3 ligase complex that targets the large subunit of RNAP II for polyubiquitylation and degradation (Ribar et al. 2007). Therefore, ELOA/ELOC complexes are involved in both transcript elongation and RNAPol II degradation.

In plants, homologues of *S. cerevisiae* CUL3, as well as homologues of mammalian and yeast ELOC, have been identified. For example, *Arabidopsis* has two cullin3 homologs: CUL3a & CUL3b encoded by At1g25830 and At1g69670, respectively (Weber et al. 2005), and one ELOC homologue (At5g59140) (Risseeuw et al. 2003). In a previous report, *Arabidopsis eloc* null mutants did not exhibit abnormal phenotypes under standard growth conditions (long day /23 ^{o}C; Hua & Vierstra 2011). However, the roles of *Arabidopsis* ELOC in plant UV tolerance has not been previously studied. In this study, I identified the *Arabidopsis* ELOA homologue (At2g42780) and examined the roles of the *Arabidopsis* ELOA and ELOC in UV tolerance and development through the

analysis of null mutants and overexpression lines. I also examined the physical and genetic interactions between these two homologues.

3.3 Materials and Methods

3.3.1 Phylogenetic analysis

Amino acid sequences for Elongin homologs were downloaded from public databases and aligned using default parameters in the Muscle algorithm. The alignment was tested using the MEGA X software package to determine the best substitution model to use for the phylogenetic reconstruction. The evolutionary history was then inferred using the maximum likelihood method using the MEGA X software package and the JTT model. The bootstrap consensus tree was generated with 1000 bootstrap replicates, and the percentage of replicate trees in which the associated taxa clustered together in the bootstrap test (1000 replicates) are shown next to the branches (Felsenstein 1985).

3.3.2 Plant material and growth conditions

All *Arabidopsis thaliana* T-DNA insertion lines including *eloa-1* (At2g42780; SALK_134637), *eloa-2* (At2g42780; SALK_201710), *eloc-1* (At5g59140; SALK_017367), *eloc-3* (At5g59140; SAIL_418_A10), and wildtype controls were ordered from the *Arabidopsis* Biological Resource Center (ABRC). For the SALK alleles (Alonso et al. 2003) and overexpression lines, the *Arabidopsis* ecotype Columbia-0 (Col-0) was used as wildtype. The *Arabidopsis* ecotype Columbia-3 (Col-3) was used as the wildtype for the SAIL allele (Sessions et al. 2002). Genotyping loss of function alleles was performed using the T-DNA specific primers LBb1.3 (SALK lines) and LB3SAIL (SAIL line) together with allele-specific primers (Table S3.1). Seeds were sterilized and plated on Linsmaier and Skoog (LS) media containing 0.86% phytoblend and 0.6% sucrose, stratified at 4 ^{o}C for 2-3 days, then incubated at 20 ^{o}C with fluorescent lights providing 100 µM photons m^{-2} s^{-1} long day (16 h light / 8 h dark) illumination. For adult growth experiments, two week-seedlings were transferred to

Sunshine mix #1 (SunGro) and grown at 20 ºC in long day conditions. Double mutant plants were generated as described in Schroeder et al. (2002).

3.3.3 RNA extraction and RT-PCR

For RNA extraction, ~50 seven day old seedlings grown in long day conditions were collected per genotype and extracted using the E.Z.N.A. Plant RNA Kit (Omega Bio-tek), which included a DNase step. The Maxima First Strand cDNA synthesis kit (Fermentas) was used to generate cDNA from 1 µg RNA. For semi-quantitative RT-PCR, *ELOA* was amplified for 28 cycles, while *ELOC* and *Actin* were amplified for 25 cycles using the selected primer pairs shown in (Table S3.1). For real-time PCR, 40-fold diluted cDNA was used to perform qPCR using SsoFast EvaGreen Supermix (Bio-Rad) and the primers listed in (Table S3.1). An CFX Connect Real-time PCR detection system (Bio-Rad) was used for analysis. The *EF1α* reference gene (At5g60390) was used for normalizing sample loading (Jain et al. 2006; Hossain et al. 2012). For ELOC UV induction, four day old seedlings were treated with 1000 J m^{-2} UV-C, followed by immediate RNA extraction. For each genotype, qPCR was performed using three biological replicates each was preformed in three technical replicates and ΔΔCt method was used to calculate *ELOA/ELOC* transcript levels.

3.3.4 Generation of overexpression plants

ELOA (U15059) and *ELOC* (G10376) cDNAs in Gateway entry vectors obtained from the ABRC. cDNAs were cloned into pEarleygate vectors pEG100 (CaMV35S promoter) and pEG104 (CaMV 35S promoter with N-terminal YFP tag; Earley et al. 2006) using LR recombination enzyme mix (ThermoFisher). Overexpression constructs were introduced into *Agrobacterium tumefaciens* GV3101strain, and then used to transform *Arabidopsis* using floral spray method. Basta screening was used to identify T1 transformants, T2 were screened for heterozygous plants, and T3 (or later) homozygotes were identified and subsequently used in experiments.

3.3.5 Adult growth analysis

Seedlings were transferred to soil at two weeks and monitored for the emergence of the inflorescence meristem (flowering time – days), as well as the total number of rosette and cauline leaves (flowering time – leaves). Rosette diameter (the maximal distance between two points belonging to the rosette) was measured at four weeks and height, apical dominance (number of stems), silique length, and seed number determined at 6-7 weeks.

3.3.6 UV sensitivity assays

For seedling sensitivity assays, seeds were plated on square plates with LS media, 0.86% phytoblend and 0.6% sucrose then stratified for 2-3 days. Plates were then placed in a 20 ^{o}C long day incubator and grown in a vertical position. After four days of growth, plates were exposed in the dark to UV-C irradiation emitted by a shortwave UV lamp XX-15S (UV Products) at either 500, 1000, or 1500 J m^{-2} (dependent on the experiment). The plates were then wrapped in aluminum foil to avoid photolyase activity. Plates were then rotated 90^{o}, and grown vertically at 20 ^{o}C in the dark for another three days. Plates were scanned and either the entire hypocotyl or new root growth from the bend to the tip measured using the ImageJ software package. For adult UV sensitivity assays, seedlings were transferred to soil at two weeks then one week later exposed to UV-C in the indicated doses. Plants were incubated in the dark at 20 ^{o}C for 72 hours then returned to normal growth conditions (16 h light / 8 h dark). Four days later leaves were scored as either undamaged (green) or damaged (brown/yellow) and % of undamaged leaves (green/ total) calculated per plant.

3.3.7 Protein Localization

For protein localization, three day-old dark grown homozygous YFP-ELOA or YFP-ELOC seedlings were mounted in distilled water at 2-3 seedlings per slide and examined using a Zeiss AXIO Imager Z1 Microscope equipped with AxioVision 4.8 software, using YFP (Filter Set YFP-2427B-000, Semrock Inc) and DAPI (Zeiss Filter Set 02 (488002-9901-000)) filters. DAPI (Sigma-Aldrich Canada) staining (10 µg /mL) working solution was prepared from the stock solution, then seedlings were incubated in

the working solution for 30 min and imaged. For UV treatments, seedlings were treated with 1000 J m^{-2} UV-C and then observed at the indicated time.

3.3.8 Yeast two hybrid assay

ELOA and ELOC physical interactions were examined using the Matchmaker gold yeast two-hybrid system (Clontech). *ELOA* (U15059) and *ELOC* (G10376) cDNAs in Gateway entry vectors were cloned into Gateway-compatible bait (pGBKT7-DEST) and prey (pGADT7-DEST) vectors (Lu et al., 2010; kindly provided by Yuhai Cui, Agriculture and Agri-Food Canada, London, ON) and transformed into haploid yeast and crossed to obtain diploid strains. Diploid yeast strains were plated on both the control medium (-trp -leu) and the section medium (-ade –his –leu -trp). p53/T (murine p53/ SV40 large T-antigen) was used as a positive control and Lam/T (Lamin/ SV40 large T-antigen) as a negative control. Positive interaction between proteins result in the expression of ADE2 and HIS3 reporters which allow the growth on (-ade –his –leu -trp) selective medium.

3.3.9 Statistical analysis

The statistical significance was determined using two-tailed student's t-test in Microsoft Excel (p 0.05). All the experiments are repeated at least twice.

3.4 Results

In mammals, Elongin C plays roles in RNA polymerase elongation and nucleotide excision repair, whereas in yeast it has only been found to play a role in NER. These roles for Elongin C in plants have not yet been explored until this work. To date, the only role of Elongin C that has been identified in plants is in plant-microbe interactions. Sugarcane Elongin C (ScELOC) and Maize Elongin C (ZmELOC) were found to facilitate some viral infections through physically interacting with a viral protein (Zhu et al. 2014; Zhai et al. 2015). However, Elongin subunits also physically interact with each other while performing their basal functions. For example, in mammals, yeast two-hybrid experiment showed that ELOC interacts with ELOA and EOLB (Pause et al. 1999). Moreover, ScELOC was found to interact with rat ELOA and enhance its transcript

elongation (Aso & Conrad 1997). Less is known about these processes in plants. In the BioGRID high throughput yeast-two hybrid analysis (Braun et al. 2011), the *Arabidopsis* elongin C homologue (ELOC; At5g59140) was found to physically interact with the *Arabidopsis* elongin A homologue (ELOA; At2g42780). In this study, I confirmed this interaction using yeast two-hybrid analysis. AtELOC was found to interact with AtELOA in both prey/bait parings (Figure S3.1). In addition, also consistent with BioGRID results, no interaction was detected between AtELOA proteins, or between AtELOC proteins (Figure S3.2).

3.4.1 *Arabidopsis* ELOA is a true homolog of mammalian and yeast ELOA

To examine the evolutionary relationships of *Arabidopsis* ELOA protein and ELOA proteins from other organisms, I conducted a phylogenetic analysis. The consensus maximum likelihood tree showed that Elongin A is well conserved throughout evolution (Figure 3.1a). To identify conserved domains, I performed sequence alignments of *Arabidopsis* and other organisms' ELOA homologs, the alignments show that *Arabidopsis* ELOA is most orthologous to uncharacterized protein LOC112273302 (*Physcomitrella patens*) as *Arabidopsis* ELOA shares the highest amino acid identity (35%) with *Physcomitrella patens* ELOA. On the other hand, *Arabidopsis* ELOA shares 23% and 25% amino acid identity to *Drosophila melanogaster* and *Dictyostelium discoideum*, respectively. *Schizosaccharomyces pombe* and human ELOA have a higher identity (28%) than *Saccharomyces cerevisiae* and *Caenorhabditis elegans* (24%) to *Arabidopsis* ELOA. The mammalian Elongin A is a SOCS-box protein (Kile et al. 2002) with a BC-box (mediating Elongin B and C interactions) and a Cullin 5 interaction domain (Yasukawa et al. 2008). Our Pfam analysis indicates that AtELOA has an Elongin A domain (El-Gebali et al. 2019; Aso et al. 1995) as well as disordered regions in the C-termini (Figure 3.1b).

Arabidopsis Elongin A is also well conserved in the BC-box region with 40% and 30% amino acid identities with *S. cerevisiae* and human BC-box region, respectively, consistent with the elongin C interaction I observe (Figure 3.1b). AtELOA is also well conserved in the Cullin 5 interaction domain, as this domain also shares 35% and 40% amino acid identities to *S. cerevisiae* and human Cullin 5 interaction domain, which is

interesting since plants and fungi do not contain Cullin 5 homologues (Hua & Vierstra 2011; Sarikas et al. 2011). *S. cerevisiae* elongin C interacts with Cullin 3 instead of cullin 5 (Ribar et al. 2007; Finley et al. 2012), suggesting that perhaps AtELOA also utilizes an alternative cullin. Plant and fungal Elongin As lack the N-terminal Rpb1 interaction domain (mediating Med26 interactions) present in mammalian Elongin A. However, this domain is not required for E3 ligase or transcript elongation activity (Yasukawa et al.q 2012). ScELOA does not enhance transcript elongation (Koth et al. 2000) but does ubiquitinate RNAP II following DNA damage (Ribar et al. 2007).

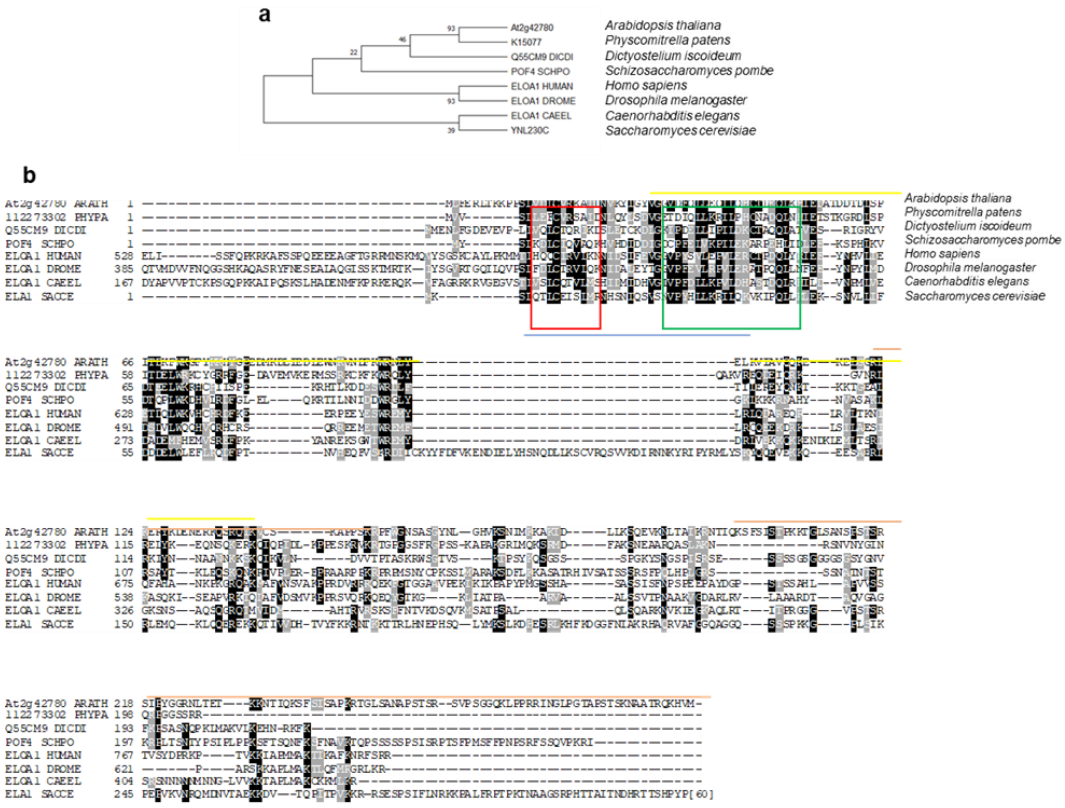

Figure 3.1 Elongin A analysis

Elongin A homologues were identified via P-POD: Princeton Protein Orthology Database (Heinicke et al., 2007) and/or KEGG (Kyoto Encyclopedia of Genes and Genomes) (http://www.kegg.jp/). (**a**) Phylogenic tree (species names are attached). (**b**) Protein alignment done in NCBI COBALT (Papadopoulos and Agarwala, 2007) and formatted using Boxshade. Amino acids showing similarity (gray) and identity (black) are shown. The elongin A domain is indicated in yellow, disordered domains in tan, SOCS-box in blue, BC-box in red, and cullin interaction domain in green.

3.4.2 *AtELOA* and *AtELOC* are expressed throughout many developmental stages and induced by DNA damaging agents

To examine the role of *Arabidopsis ELOA* and *ELOC* genes in plant development, as well as to examine the effect of DNA damaging agents on the expression of both genes, public gene expression data for *Arabidopsis ELOA* and *ELOC* was examined (Schmid et al. 2005; Winter et al. 2007). These data indicate that *Arabidopsis ELOA* and *ELOC* are expressed throughout development, with At*ELOC* levels higher in seed and *AtELOA* in pollen (Figure S3.3). In to response to DNA damaging agents, *AtELOC* is up-regulated ~75% 6 hrs after UV-B exposure in shoots, while *AtELOA* is induced ~50% 6 hr following UV-B exposure in root (Figure S3.4; Kilian et al. 2007). Gamma irradiation induced both *AtELOA* and *AtELOC* immediately (20 min) after treatment, followed by a drop at 3 hr, then a second peak at 6 hr (*AtELOA*) or 12 hr (*AtELOC*). For both *AtELOA* and *AtELOC*, the second peak is dependent on the presence of suppressor of gamma radiation 1 (SOG1; Figure S3.5; Bourbousse et al., 2018). Neither gene is induced by genotoxic (bleomycin and mitomycin C) treatment, showing that the differential expression is likely induced by radiation (Kilian et al. 2007).

3.4.3 *Ateloa* and *Ateloc* null mutants are sensitive to UV radaiation

In light of the observation that both *AtELOA* and *AtELOC* transcript levels rise in response to UV-B exposure, I sought to examine the role the *AtELOA* and *AtELOC* in *Arabidopsis* UV tolerance. I obtained T-DNA lines from the ABRC, bred these lines to be homozygous for the T-DNA insertions, and then used semi-quantitative RT-PCR to assess the effect of the insertions on *AtELOA* and *AtELOC* expression. Although the *Ateloa-1* line harbored the T-DNA in the first intron, this mutant still expressed *AtELOA* and thus this line was not used for subsequent analysis (data not shown). In *Ateloa-2* the T-DNA insertion is in the second exon and results in a null allele (Figure 3.2a&b). For *AtELOC*, the *Ateloc-3* allele is in the first exon, 3 bp 5’ of the start codon, and is also an RNA null (Figure 3.2a&c). The *Ateloc-1* allele is in the *AtELOC* promoter and is not a null allele (Figure 3.2a).To determine the molecular nature of *Ateloc-1* defect, I examined *AtELOC* transcript level in *Ateloc-1* mutant and wild type (Col-0) following UV treatment. Using qRT-PCR I determined that *AtELOC* transcript level was significantly

reduced by approximately 20% in *Ateloc-1* compared to the wild type (Figure 3.2d), indicating that T-DNA insertion interferes with *AtELOC* expression following UV treatment in *Ateloc-1*.

The identification of loss of function mutants in *AtELOA* and *AtELOC* allowed me to study the involvement of *Arabidopsis* ELOA and ELOC in UV tolerance. Using the *AtELOA* and *AtELOC* loss of function mutants I performed assays that measured the inhibition of root and shoot growth in UV-irradiated seedlings. *Ateloa-2* seedlings exhibited decreased growth in both hypocotyls and roots following a 1000 J m^{-2} UV treatment, with a larger difference in the root phenotype at day 3 (Figure 3.3a,b). Thus I chose to do subsequent analyses at day 3. Treatments at 1500 J m^{-2} at day 3 did not cause a notable increase in sensitivity (Figure 3.3c). The *Ateloc-3* null mutant also exhibits enhanced UV sensitivity in roots and hypocotyls following exposure to 1000 J m^{-2} UV-C (Figure 3.3d), whereas, *Ateloc-1* mutant that still expressed *AtELOC* did not show a significant increase in seedling UV sensitivity compared to the wild type (Figure 3.2d; Figure 3.3d). To discern any genetic interactions between these two genes I also examined the effects of *Ateloa-2 Ateloc-1* double mutants on seedling UV sensitivity. The *Ateloa-2 Ateloc-1* double mutants showed significantly reduced root and hypocotyl elongation compared to the *eloa-2* single mutant (Figure 3.3d). Given that the *eloc-1* mutant still expressed *AtELOC1* to some degree, together these data suggest that both *AtELOA* and *AtELOC* contribute to seedling UV tolerance in an additive manner.

Adult *Arabidopsis* leaves accumulate sinapoyl malate that functions as a UV-absorbent sunscreen (Fraser & Chapple 2011). Thus, I sought to assess whether adult *Ateloa-2* and *Ateloc-1* single and double mutants also exhibited a reduction in UV tolerance by measuring the percentage of undamaged leaves to the total number of leaves in 500 J m-2 UV-treated 21 day old plants. The *Ateloa-2* and *Ateloc-3* single mutants exhibited a significant increase in leaf damage compared to the wild type (Col-0) following treatment (Figure 3.3e). The *Ateloa-2 Ateloc-1* double mutant also exhibited significantly increased UV damage compared to *Ateloa-2* single mutant, while *Ateloc-1* didn't show a significant increase in UV sensitivity compared to the wild type (Figure 3.3e). Thus, the *Ateloa-2 Ateloc-1* double mutant exhibits enhanced UV-sensitive

phenotypes in both seedlings and adults. The observed pattern UV-sensitive in the adult mutants matches those observed in the seedlings.

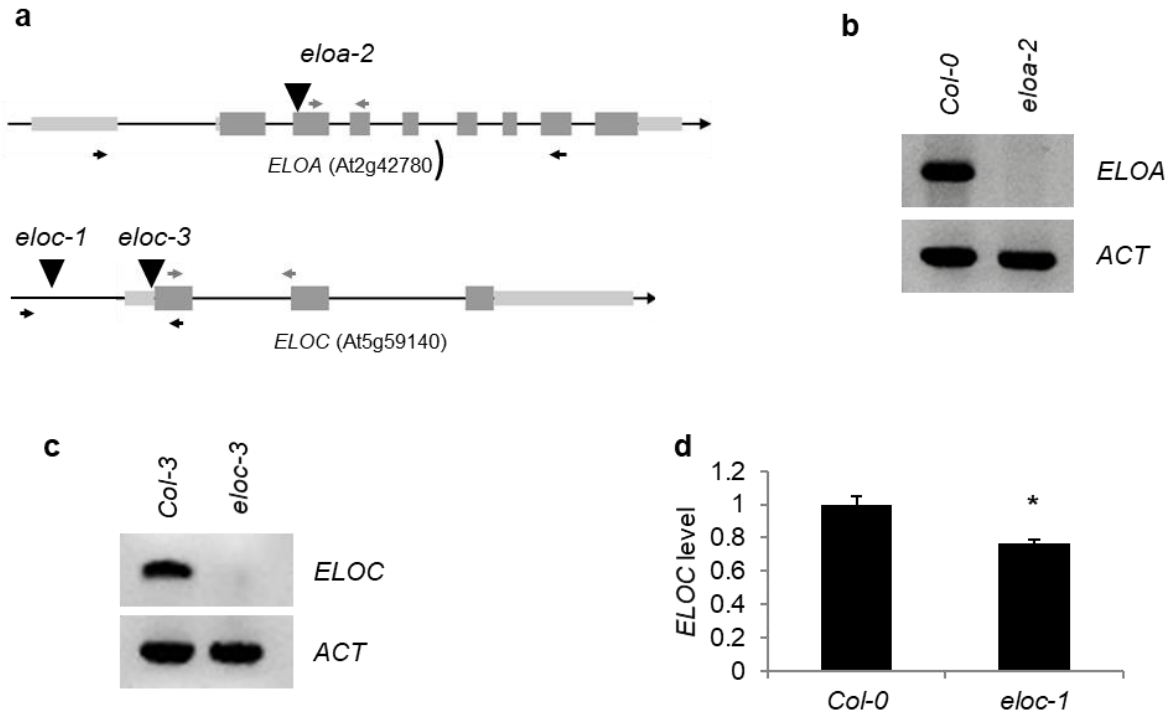

Figure 3.2 *Arabidopsis* Elongin A and C loss of function alleles

(**a**) Schematic of *ELOA* (At2g42780) and *ELOC* (At5g59140) genes. Introns are indicated as lines and exons as boxes, with untranslated regions shaded light gray and coding regions dark gray. T-DNA alleles *eloa-2* (SALK_201710), *eloc-1* (SALK_017367), and *eloc-3* (SAIL_418_A10) are presented as triangles. Black and gray arrows show primers used in semi-quantitative and quantitative RT-PCR analysis, respectively. (**b**) Semi-quantitative RT-PCR analysis of Col-0 wildtype and *eloa-2* with *ELOA* and *Actin* primers. (**c**) Semi-quantitative RT-PCR analysis of wildtype Col-3 and eloc-3 with ELOC and Actin primers. (**d**) RT-qPCR analysis of *ELOC* transcript level in wild type Col-0 and *eloc-1* after 1000 J M-2 UV-C treatment. *ELOC* level was normalized relative to *EF1α* gene.

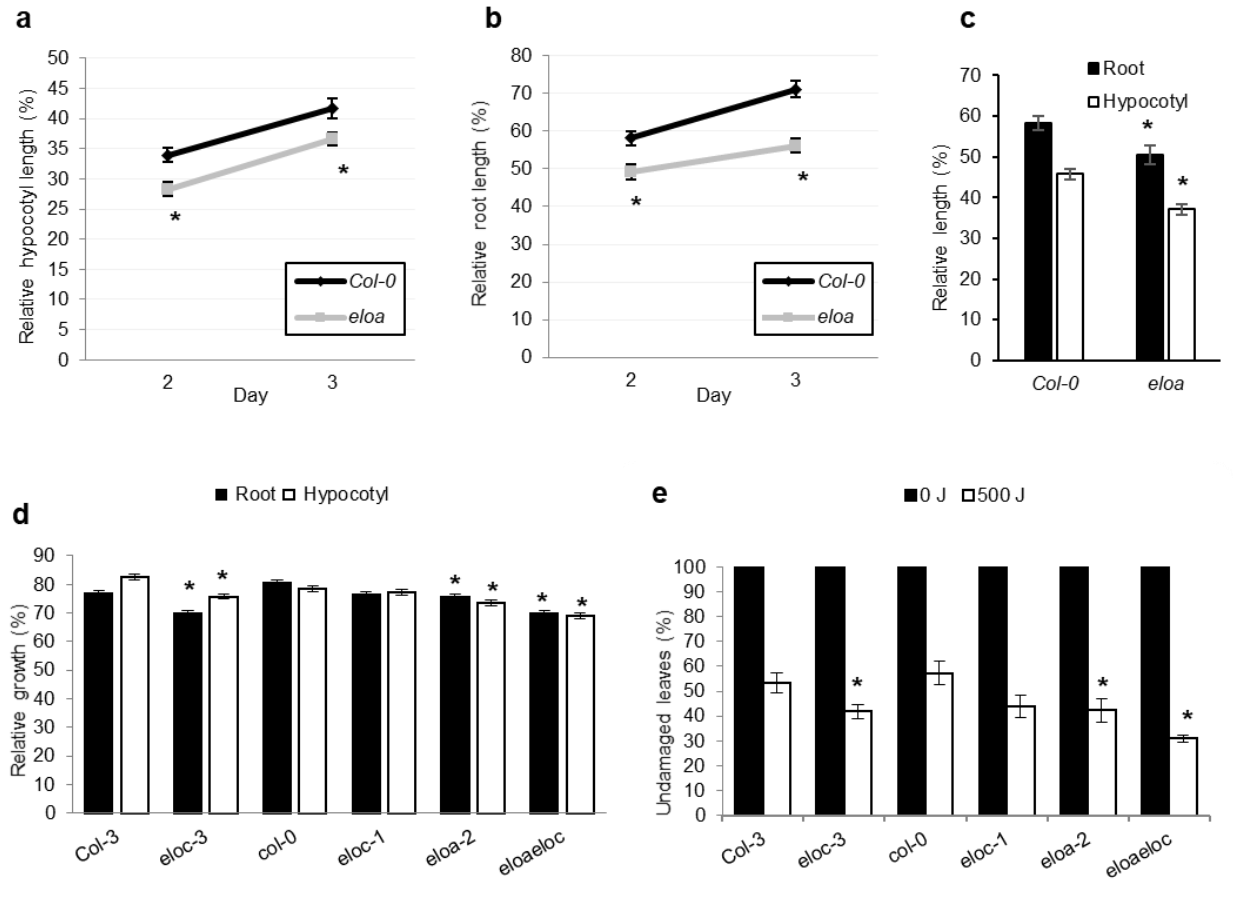

Figure 3.3 *Arabidopsis ELOA and ELOC* single and double mutant seedlings and adults exhibit decreased UV tolerance

(**a**) Root and (**b**) hypocotyl length of four-day-old seedlings exposed to UV stress (1000 J m^{-2} UV-C) then incubated under dark conditions for 48 or 72 hours. (**c**) and (**d**) Hypocotyl and root length of four-day-old seedlings exposed to UV stress (1500 and 1000 J m^{-2} UV-C, respectively), then incubated under dark conditions for 72 hours. (**e**) Percentage of undamaged leaves in 3-week- old plants exposed to UV stress (500 J m^{-2} UV-C), then incubated under dark conditions for 72 hours, (n=12). For a-d, data are represented as relative to unstressed controls of the same genotype (n=40). For a-e, values are means ± SE, * = p≤ 0.05 of single mutant vs wild type, and double mutants vs *eloa-2*.

3.4.4 AtELOA overexpression complements *Ateloa* UV-sensitivity

To verify that the seedling and adult UV sensitive phenotypes exhibited by the *Ateloa-2* loss of function mutant is due to the absence of AtELOA, I performed rescue experiments using AtELOA overexpression lines *35S:ELOA* and *35S:YFP-ELOA* in the *eloa-2* background. *AtELOA* cDNA was cloned into pEarleygate vectors pEG100 (CaMV35S promoter) and pEG104 (CaMV 35S promoter with N-terminal YFP tag (Earley et al. 2006). Then Agrobacterium-mediated transformation was used to transform these overexpression constructs into *Ateloa-2*. Basta-resistant plants harboring either the *35S:ELOA* or *35S:YFP-ELOA* construct showed more than 2-fold increase in *AtELOC* transcript abundance compared to *Ateloa-2* (Figure 3.4a; Figure 3.5a). The same *35S:ELOA* and *35S:YFP-ELOA* overexpression lines in *Ateloa-2* background rescued the seedlings UV sensitive growth reduction phenotype, and the adult UV sensitive leaf damage phenotype exhibited by *Ateloa-2* (Figure 3.4b&c; Figure3.5b&c). Thus, the UV sensitivity exhibited by *Ateloa-2* loss of function mutant is directly attributable to the T-DNA insert in *AtELOA* gene.

To test the hypothesis that *AtELOA* or *AtELOC* expression is limiting in *Arabidopsis*' ability to tolerate UV light, I examined the effect of overexpressing these genes in wild type backgrounds. Both tagless and YFP-tagged ELOA overexpression in the wild type background showed a significant increase in hypocotyl UV tolerance compared to the wild type (Figure 3.4b; Figure 3.5b). However, the same overexpression lines did not show a significant increase in roots and adults UV tolerance compared to the wild type (Figure 3.4b&c; Figure 3.5b&c). This indicates that the expression of *AtELOA* is limiting in *Arabidopsis's* ability to tolerate UV in aerial tissues during early growth.

On the other hand, neither *35S:ELOC* nor *35S:YFP-ELOC* increases adult or seedling UV tolerance phenotypes (Figure S3.6c-f). Suggesting that the expression of *AtELOC* is not limiting in *Arabidopsis* UV tolerance; the increased levels of the gene does not result in increased UV tolerance.

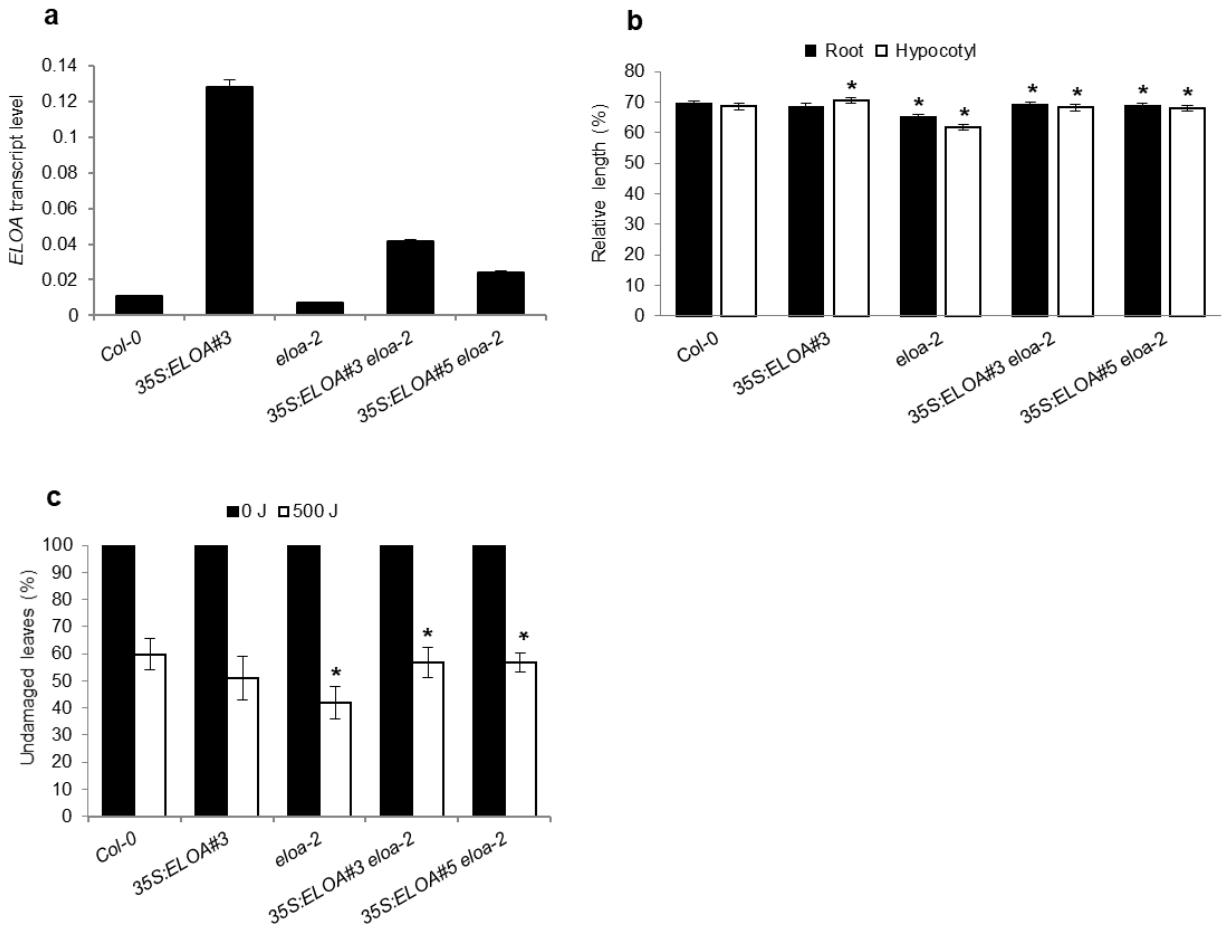

Figure 3.4 *Arabidopsis* 35S: ELOA overexpression rescues adult UV sensitivity and increases hypocotyl UV tolerance

(**a**) *ELOA* transcript level in Col-0, *35S: ELOA*, *ela-2*, and *35S: ELOA ela-2*. *EF1α* gene used as a control to normalize the values. Error bars represent SE of the mean. (**b**) Hypocotyl and root length of four-day-old seedlings exposed to UV stress (1000 J m^{-2} UV-C), then incubated under dark conditions for 72 hours, (n=40), data are represented as relative to unstressed controls of the same genotype. (**c**) Percentage of undamaged leaves in 3-week-old plants exposed to UV stress (500 J m^{-2} UV-C), then incubated under dark conditions for 72 hours, (n=12). Values are means ± SE,* = p≤ 0.05 of *eloa-2* and *35S: ELOA* vs wild type (Col-0)**,** and *35S: YFP-ELOA eloa-2* vs *eloa-2* mutant.

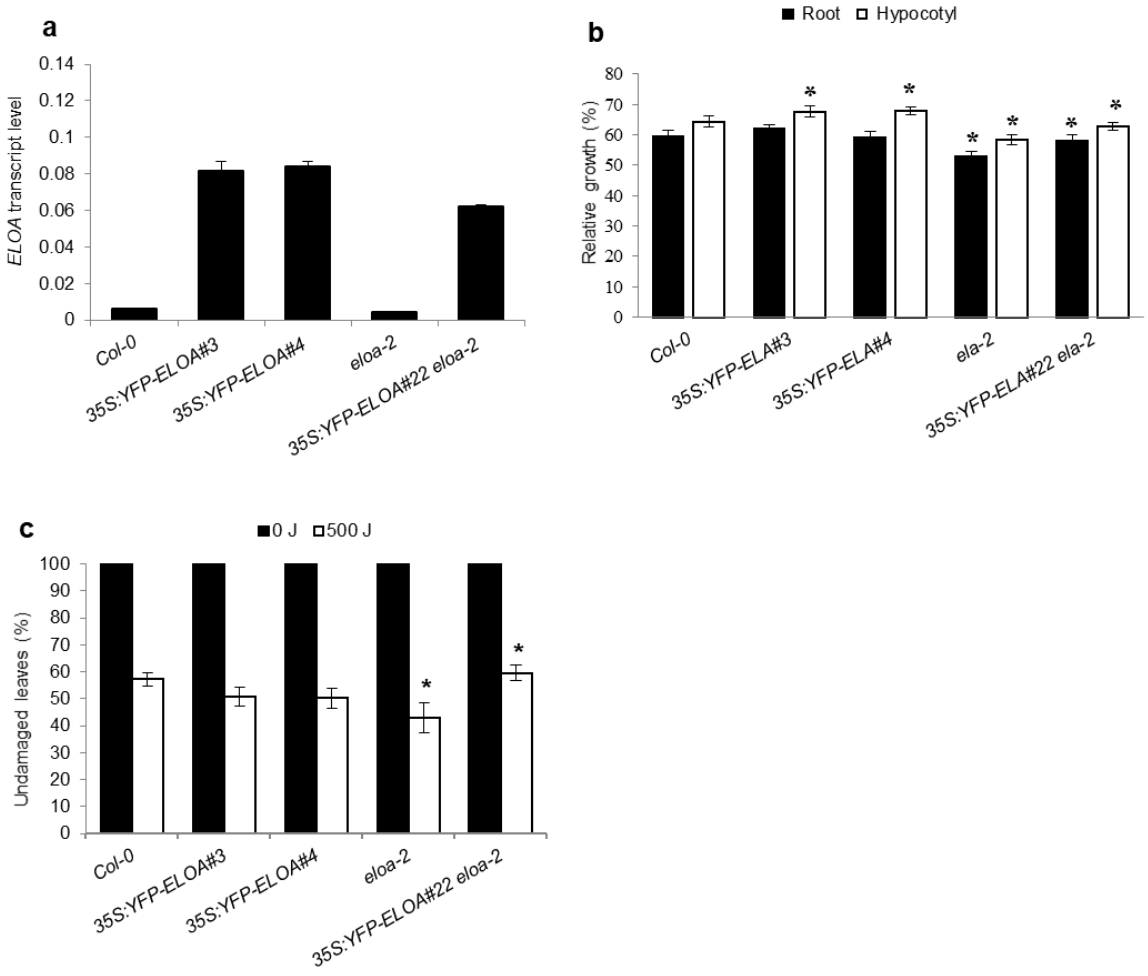

Figure 3.5 35S: YFP-ELOA overexpression rescues adult and seedling UV sensitivity and increases hypocotyl UV tolerance

(**a**) *ELOA* transcript level in Col-0, *35S: YFP-ELOA#3*, *35S: YFP-ELOA#4, ela-2*, and *35S: YFP-ELOA eloa-2*. *EF1α* gene used as a control to normalize the values. Error bars represent SE of the mean. (**b**) Hypocotyl and root length of four day old seedlings exposed to UV stress (1000 J m^{-2} UV-C) then incubated under dark conditions for 72 hours, (n=40). (**c**) Percentage of undamaged leaves in 3-week- old plants exposed to UV stress (500 J m^{-2} UV-C), then incubated under dark conditions for 72 hours, (n=12). For b, data are represented as relative to unstressed controls of the same genotype. For (a) and (c), values are means ± SE, * = p≤ 0.05 of *eloa-2* and *35S: YFP-ELOA* vs wild type (Col-0)**,** and *35S: YFP-ELOA ela-2* vs *eloa-2* mutant.

3.4.5 AtELOA and AtELOC subcellular localization

Other proteins that are involved in NER are either nuclear localized, or are transported from the cytosol into the nucleus upon genomic insult (Lahari et al. 2017; Liang et al. 2006; Molinier et al. 2008). I used fluorescent microscopy to determine the subcellular localization of AtELOA and AtELOC using the YFP-ELOA and YFP-ELOC overexpression lines. YFP-ELOA was found to co-localize with DAPI staining, consistent with nuclear localization (Figure 3.6). No fluorescent signal was detected in the cytosol of plant cells overexpressing this construct. Closer examination showed that YFP-ELOA exhibited punctuated fluorescence within the nuclei, suggesting that YFP-ELOA may be enriched in the nucleolus (Figure 3.7). The observed nuclear localization was not obviously altered by UV treatment (Figure 3.7). In contrast, YFP-ELOC was observed in both nuclei and apparent cytosol (Figure 3.8), consistent with its previous identification as a component of the *Arabidopsis* cytosol proteome (Ito et al. 2011).

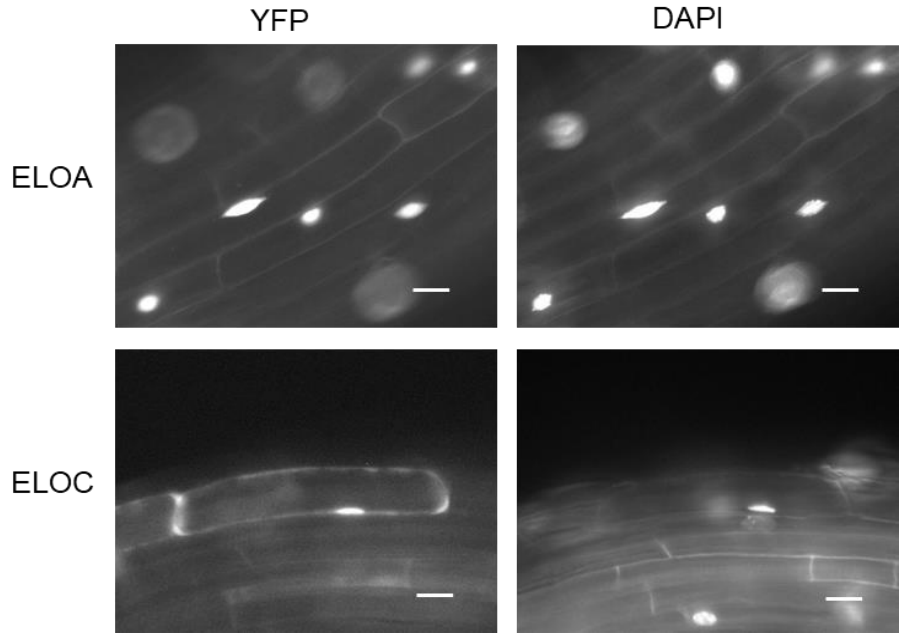

Figure 3.6 Cellular localization of *Arabidopsis* YFP-ELOA and YFP-ELOC

Localization of N-terminal YFP fusion ELOA and ELOC proteins in seedlings (grown in the dark for three days) was examined with YFP fluorescence and DAPI staining under 20X magnification. Scale bar represents 20 μm

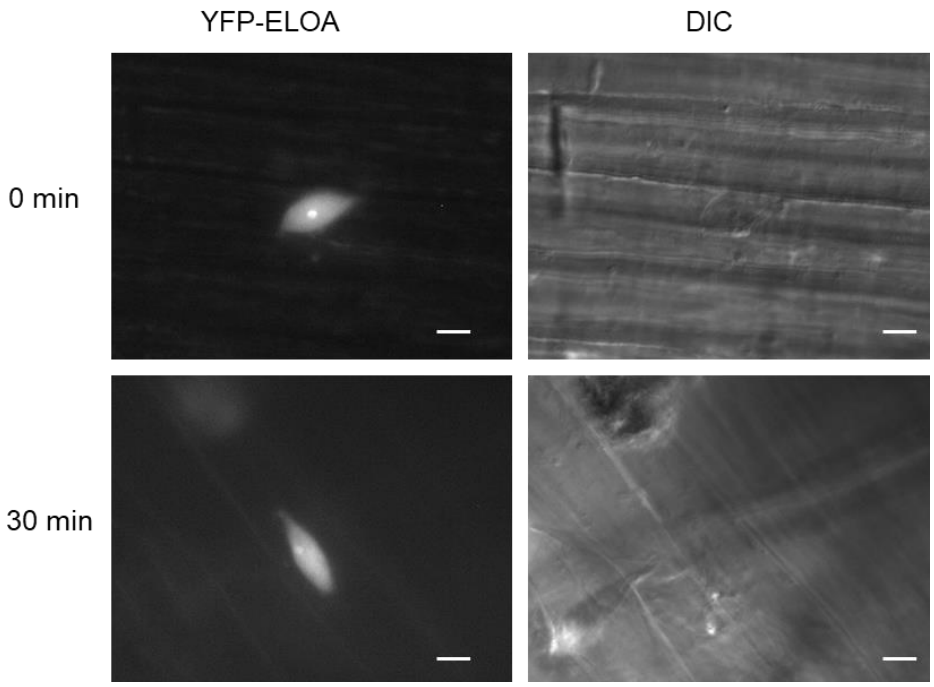

Figure 3.7 *Arabidopsis* YFP-ELOA nuclear localization is not altered by UV treatment

YFP-ELOA examined with YFP fluorescence and differential interference contrast (DIC) under 40X magnification in the absence of or 30 min after 1000 J m^{-2} UV-C treatment. Scale bar represents 10 μm

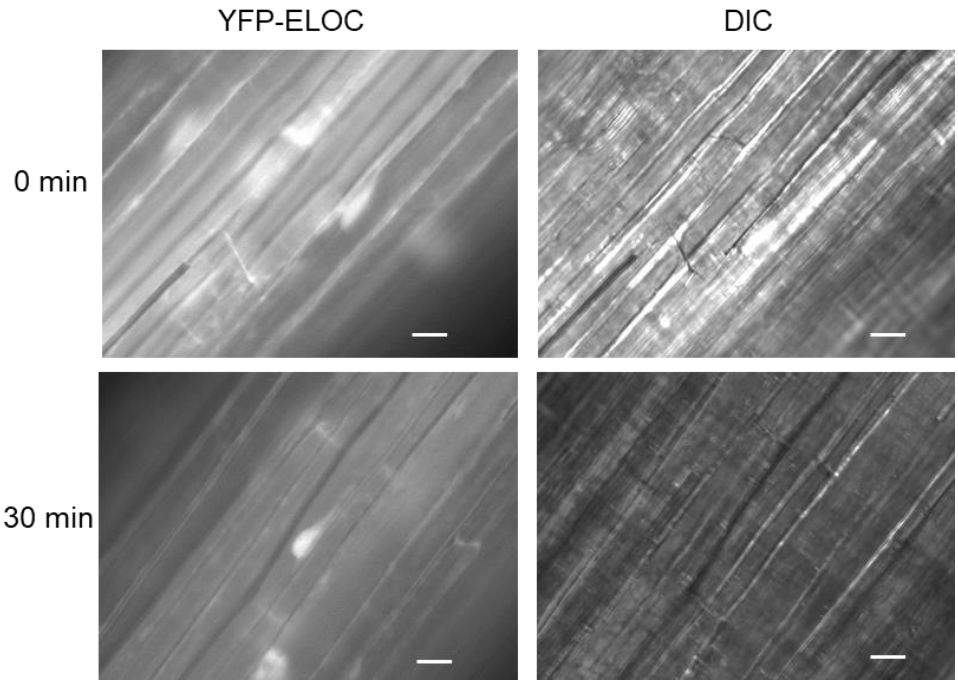

Figure 3.8 *Arabidopsis* YFP-ELOC cytoplasmic localization decreases following UV treatment

YFP- ELOC examined with YFP fluorescence and differential interference contrast (DIC) under 20X magnification in the absence of or 30 min after 1000 J m^{-2} UV-C treatment. Scale bar represents 20 μm

3.4.6 AtELOA and AtELOC overexpression increase silique length and seed count

Although overexpression experiments can lead to spurious conclusions, I sought to examine the effects of AtELOA and AtELOC overexpression on plant growth and development. Overexpression lines *35S:ELOA*/*ELOC* and *35S:YFP-ELOA*/*ELOC* in the wild type and mutant backgrounds were used to perform adult growth analysis experiments. All the three tagless and two out of three YFP-tagged ELOA overexpression lines exhibited significantly increased silique length and seed production compared to the wild type (Figure 3.9a-d). Similarly, both *35S:ELOC* and *35S:YFP-ELOC* in wild type background also result in a significant increase in both silique length and number of seeds per silique as well as increased plant height compared to wild type (Figure 3.10a-d; Figures S3.9d; S3.10d). However, AtELOA overexpression has no significant effects on plant height (Figures S3.7;S3.8). These results show that *AtELOA* and *AtELOC* overexpression are sufficient to increase the silique length and seed production and *AtELOC* overexpression also increases plant height. Thus, *AtELOC* and *AtELOA* transcript levels are limiting in same aspect of *Arabidopsis* growth and development. To further investigate the basis of this enhanced fertility, I examined similar stage flowers from both wild type and overexpression lines to detect any differences in the stamen length that might cause this phenotype. I examined this possibility since it has been reported that silique length is proportional to seed number, which is influenced by stamen length. Enhanced stamen growth relative to the pistil was found to facilitate the fertilization process (Al Khateeb & Schroeder 2007). However, I did not detect any differences between the wild type and overexpression lines. Further studies are still required to determine the basis of these growth phenotypes in the context of ELOA and ELOC overexpression.

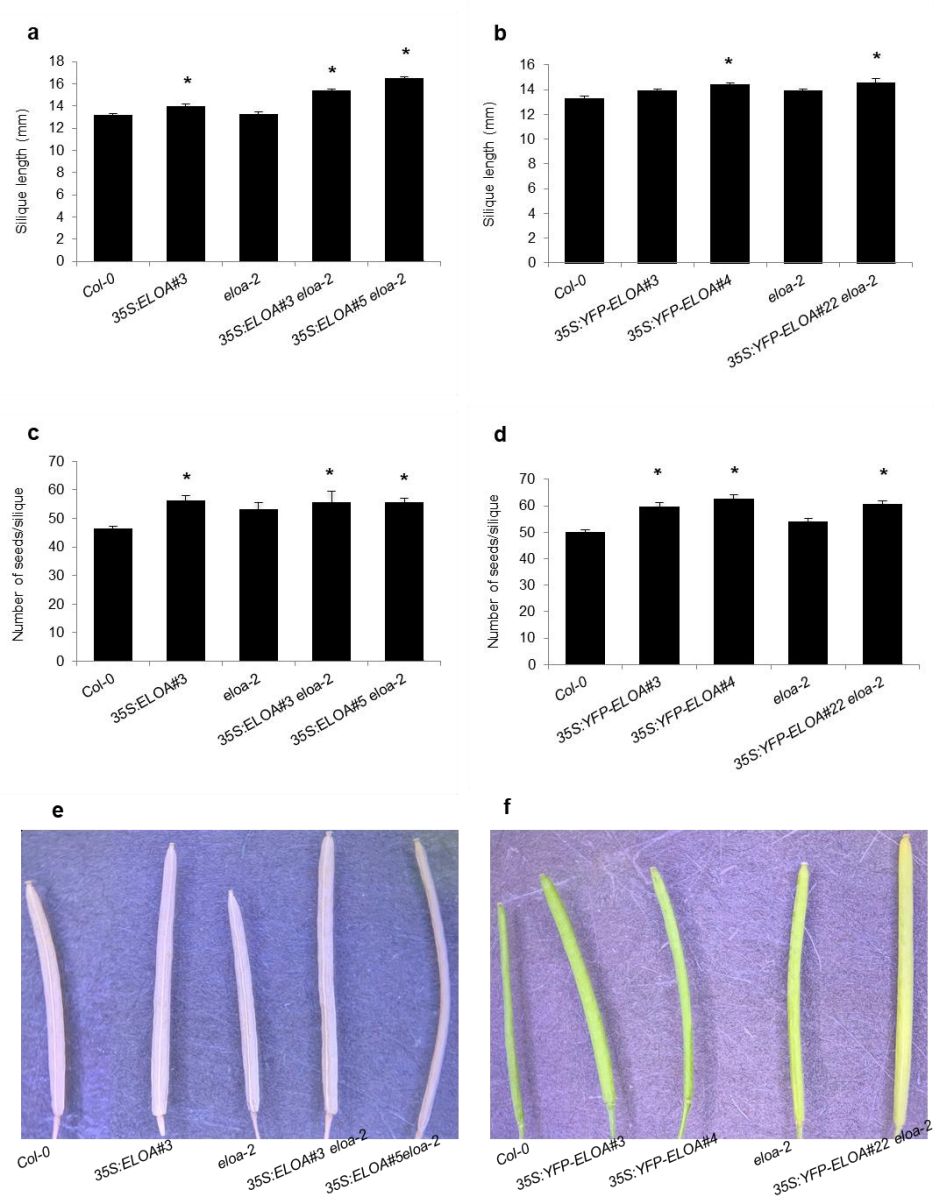

Figure 3.9 *Arabidopsis* ELOA overexpression results in increased silique length and seed number/silique

35S: ELOA overexpression lines in Col-0 and *eloa-2* background exhibited significantly increased silique length (**a**) and seed production (**c**). (**e**) Silique morphology of Col-0 ,*35S:ELOA* overexpression lines, and *eloa-2*. *35S: YFP-ELOA* overexpression lines in Col-0 and *eloa-2* background exhibited significantly increased silique length (**b**) and seed production (**d**). (**f**) Silique morphology of Col-0, *35S:YFP-ELOA* overexpression lines, and *eloa-2 .* For a-d, values are means ± SE, n=12, * = p≤ 0.05 of *eloa-2*, *35S:YFP-ELOA*, *35S:ELOA* vs wild type (Col-0) and *35S:YFP-ELOA eloa-2*, *35S:ELOA eloa-2* vs *eloa-2* mutant.

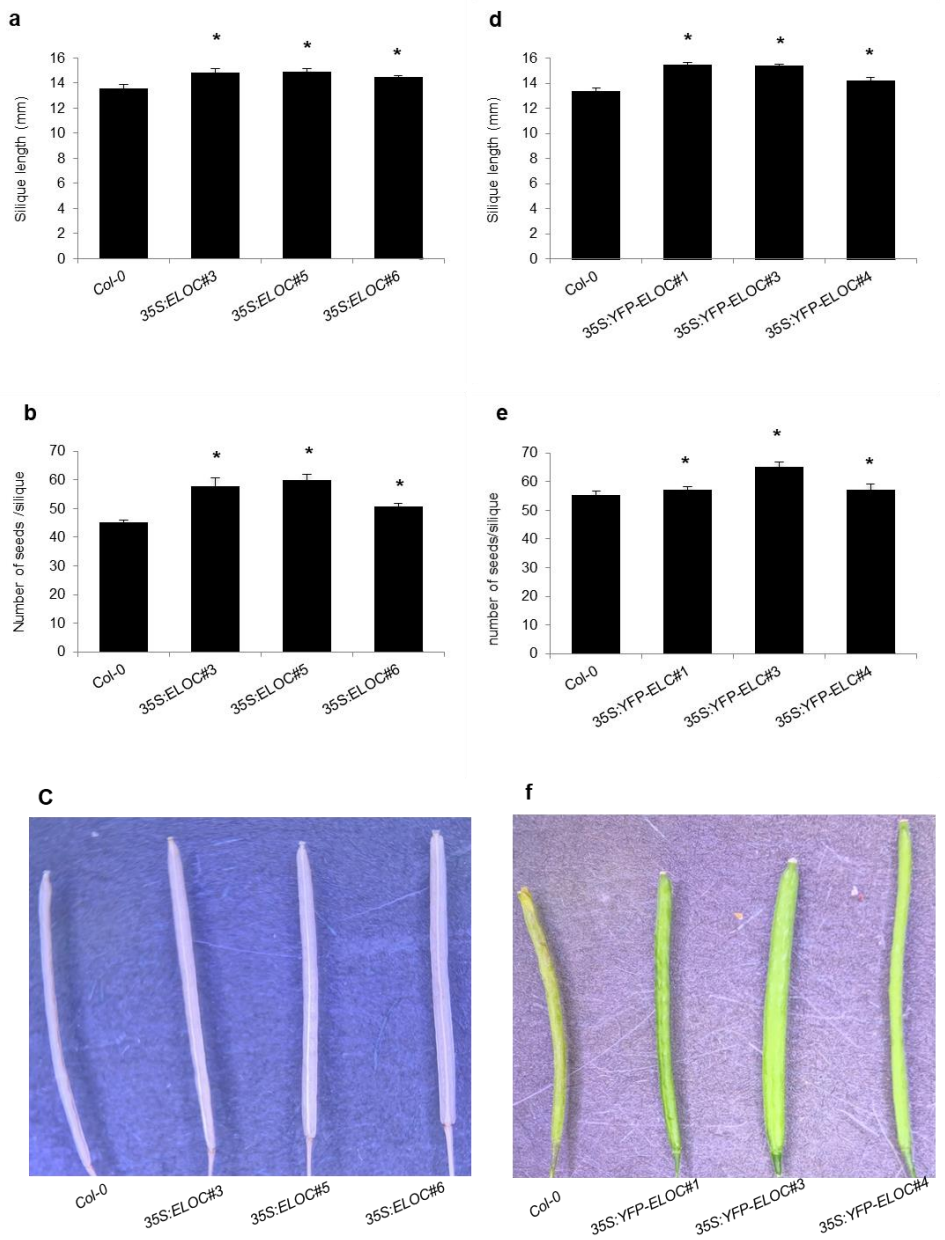

Figure 3.10 *Arabidopsis* ELOC overexpression results in increased silique length and seed number/silique

35S: ELOC overexpression lines in Col-0 background exhibited significantly increased silique length (**a**) and seed production (**c**). (**e**) Silique morphology of Col-0 and *35S: ELOC* overexpression lines. *35S:YFP-ELOC* overexpression lines in Col-0 background exhibited significantly increased silique length (**b**) and seed production (**d**). (**f**) Silique morphology of Col-0 and *35S:YFP-ELOC* overexpression lines. For a-d, values are means ± SE, n =12 * = p≤ 0.05 of *35S: ELOC* and *35S:YFP-ELOC* vs wild type (Col-0).

3.5 Discussion

3.5.1 *Arabidopsis* ELOA and ELOC appear to be dispensable for growth

In this research, I identified the *Arabidopsis ELOA* homolog and determined the roles of *Arabidopsis ELOA* and *ELOC* homologues *in planta* through examining loss of function and gain function mutants. Under normal growth conditions, no mutant developmental phenotypes were observed for either *Ateloc-1* or *Ateloa-2* single and double mutants. These observations are consistent with the only previous study that investigated the role of *ELOC* in *Arabidopsis* growth, which demonstrated that *Arabidopsis ELOC* is dispensable for wild-type plant growth and development (Hua & Vierstra 2011). Similarly in *Saccharomyces cerevisiae*, no detectable growth phenotype was observed in either *ELOA* or *ELOC* loss of function mutants compared to the wild type strain (Koth et al. 2000). In contrast, mammalian ELOA is required for cell viability *in vivo,* and loss of function ELOA mutations impairs neural development in mice (Conaway & Conaway 2019: Yasukawa et al. 2012). In *Drosophila*, ELOA (dELOA) was found to be required for proper development and loss of dELOA function appears to be lethal (Gerber et al. 2004). It is thus apparent that ELOA function has neofunctionalized in the different lineages of life. It is well established that ELOA also functions in transcriptional elongation in animals, and thus it is apparent that ELOA is required for cell viability (Aso et al. 1995).

3.5.2 *Arabidopsis* ELOA and ELOC are required for plant UV-tolerance

Arabidopsis eloa-2 and *eloc-3* are null alleles, whereas *eloc-1* harbors a T-DNA insert in the promoter and thus exhibits an approximate 20 percent reduction in *ELOC* transcript following UV exposure (Figure 3.2d). In the seedling UV sensitivity assays, *Ateloa-2* and *Ateloc-3* mutants exhibited a significant reduction in hypocotyl and root growth following a 1000 J m^{-2} dose of UV, demonstrating that both genes play a role in NER. However, *Ateloc-1* exhibits wild-type growth phenotypes after UV irradiation, suggesting that the reduction of *AtELOC* transcript abundance in the *Ateloc-1* mutant is not enough to cause UV sensitivity in this mutant. This is not surprising given the small 20 percent reduction in *AtELOA* transcript abundance in this mutant, and that

haploinsufficiency has not been reported with these genes in any phyla. The observation that the *Ateloa-2 Ateloc-3* double mutants showed significantly reduced root and hypocotyl elongation compared to the *Ateloa* single mutant suggests an additive genetic effect. In measuring UV-induced damage to adult leaves, *Ateloa-2* and *Ateloc-3* single mutants and *Ateloa-2 eloc-1* double mutants exhibited increased UV sensitivity. In mammals and yeast it has been shown that elongins participate in the E3 ligase complex that is responsible for the ubiquitylation and subsequent degradation the large subunit of RNAPII following DNA damage (Edenberg et al. 2014; Okumura et al. 2012; Ribar et al. 2007 & 2006; Weems et al. 2015; Yasukawa et al. 2008). The inability to degrade the stalled RNA polymerase at DNA lesions, in turn, prevents the DNA repair factors from accessing the lesion. In plants, it is currently unknown whether the E3 ligase complex operates the same at the biochemical level. However, my data showing the UV-sensitive phenotypes exhibited by the *Ateloa-2* and *Ateloc-3* mutants supports the involvement of AtELOA and AtELOC in the E3 ligase complex and thus in NER. Interestingly, in *Saccharomyces cerevisiae*, UV sensitivity was observed only on double mutant combinations, and no UV sensitive phenotypes were observed in *ELOA* or *ELOC* single mutants (Ribar et al. 2007 & 2006), suggesting the increased importance of plant ELOA and ELOC in response to UV damage compared to their yeast counterparts.

In yeast, ELOC is not only a component of E3 ligase complex that is involved in ubiquitination and degradation of RNAPII at sites of DNA damage, but it is also present in another ubiquitin ligase complex that is involved in GG-NER (Ribar et al. 2007 & 2006). In mammals, DNA damage following UV irradiation was found to induce the formation of ELOA ubiquitin ligase complex in vivo (Weems et al. 2017 & 2015), and to increase the interaction between Cockayne syndrome B (CSB; a TC-NER factor), and the ELOA ubiquitin ligase complex and recruit them to the damage site (Weems et al. 2017). In mammalian and yeast cells, mutation of *ELOA* or *ELOC* gene impair RNAPII degradation following DNA damage (Harreman et al. 2009; Kawauchi et al. 2013; Ribar et al. 2007 &2006; Weems et al. 2015; Yasukawa et al. 2008). Thus, the UV sensitivity exhibited by *Arabidopsis eloa* and *eloc* mutants suggests that *Arabidopsis* ELOA and ELOC are involved in responses to DNA damage.

3.5.3 AtELOA overexpression significantly increased hypocotyl UV tolerance

Despite the fact that overexpression experiments can lead to erroneous conclusions, my results show that YFP-tagged and tagless AtELOA overexpression significantly enhanced UV tolerance in seedling hypocotyls compared to the wild type. This may indicate that the role that AtELOA plays in UV repair is most critical for aerial parts in early growth stages. It is also possible that the genes are not equally overexpressed in all the tissues. In mammals, a purified complex from cells overexpressing ELOA-BC-Cul5/Rbx2 was found to increase the large subunit RNAPI ubiquitination in vitro (Yasukawa et al. 2008). Thus, overexpression of *Arabidopsis* ELOA may increase UV tolerance via increasing the degradation of the large subunit of the stalled RNAPII at the damaged site.

3.5.4 UV irradiation decreases AtELOC cytoplasmic localization

I used YFP-tagged proteins to analyze the subcellular localization of AtELOC and AtELOA and found that AtELOC exhibits cytoplasmic and nuclear localization under unstressed conditions, followed by a decrease in cytoplasmic localization after UV treatment. Consistent with our results, both a cytoplasmic and nuclear localization of ELOC homologs have been observed in maize, sugarcane, *S. cerevisiae*, and *S. pombe* (Huh et al. 2003; Matsuyama et al. 2006; Zhai et al. 2015; Zhu et al. 2014). The *Arabidopsis* YFP-tagged ELOA exhibited only nuclear localization and this nuclear localization was not obviously altered by UV treatment. DNA repair after UV radiation takes place in the nucleus therefore it is expected for NER proteins to exhibit nuclear localization following UV irradiation if these proteins are not already localized to the nucleus. This is consistent with human elongin A which has also been detected in the nucleolus in low- or high-throughput protein localization assays in the LOCATE Curated Protein Localization Annotations dataset (Sprenger et al. 2008). Similarly, ELOA homologs in *S. cerevisiae* and human HELOA cells were also found to be nuclear localized, whereas the *S. pombe* ELOA homolog has been observed to be both cytoplasmic and nuclear localized (Matsuyama et al. 2006; Tkach et al. 2012; Weems et al. 2015). Additionally, our ELOA and ELOC subcellular localization results are also consistent with the results obtained by SUBA4 consensus algorithm SUBAcon which

predicts cytosolic (0.996) and minimal nuclear (0.004) localization for AtELOC and nuclear localization for AtELOA (0.999; Hooper et al. 2014).

3.5.5 Suggested role for *Arabidopsis* ELOA and ELOC in NER

My yeast two-hybrid experiment confirms a previous high-throughput result which indicated an interaction between *Arabidopsis* ELOA and ELOC (Braun et al. 2011). Interaction between AtELOA and AtELOC was observed when AtELOA was used as both bait and prey (Figure S3.1). No self-interaction was detected in AtELOA and AtELOC (Figure S2). In mammals, ELOC interacts with ELOA and induces ELOA transcriptional activity (Aso et al.1995). In addition, mammalian ELOA interacts with mammalian elongin B/C along with CUL5 and RBX2 and targets the large subunit of RNAPII for ubiquitination and degradation following DNA damage (Yasukawa et al. 2008). In yeast, ELOC was found to assemble with ELOA and form Yeast ELOA/C complex, which interacts with CUL3 and RBX1 and also targets the large subunit of RNAPII for ubiquitination and degradation following DNA damage (Ribar et al. 2007). While yeast ELOA/C complex does not stimulate transcript elongation of yeast RNAPII (Koth et al. 2000), yeast ELOC was found to interact with mammalian ELOA and promote mammalian ELOA transcriptional activity (Aso & Conrad 1997). Together, these obsevations suggest that the function of yeast ELOA/ELOC is well conserved with their mammalian homologs. My yeast two-hybrid results provide evidence that Elongin A/C complex can similarly form in *Arabidopsis*, and thus this complex may be involved in the degradation of the large subunit of RNAPII following DNA damage and/or in promoting *Arabidopsis* transcript elongation activity. The interaction between *Arabidopsis* ELOA and ELOC suggests that the function of elongin A/C complex appears similar to the function of elongin A/C complex in mammals and yeast.

3.5.6 AtELOC and AtELOA overexpression plants exhibited enhanced silique length and seed count

Overexpression of either ELOA or ELOC results in increased silique length and the number of seeds per silique. In plants, the roles of transcript elongation factors are beginning to be assessed (Grasser 2005), and several elongation factors were found to

play roles in dormancy and seed production phenotypes. For example, the facilitates chromatin transcription complex (FACT) is one of the *Arabidopsis* transcript elongation factors that found to play a role in regulating a variety of developmental processes including silique formation and flowering induction. The FACT complex interacts with histone proteins and regulates gene expression (Lolas et al. 2010). During transcript elongation ELOC is paired with ELOA, and thus overexpression of either gene may enhance the transcript elongation activity of the complex. It is possible that ELOA/ELOC acts as a transcript elongation factor that enhances the transcription of specific genes involved in silique development and seed production. ELOA/ELOC overexpression may enhance the transcription of these specific genes either by directly increasing the rate of RNAPII transcription or by functionally interacting with transcription factors that activate the transcription of genes involved in silique and seed development. On the other hand, ELOC overexpression increased plant height, again the transcript elongation activity of ELOC may result in this phenotype by enhancing the transcription of stem elongation factors (Figure S3.11b).

AtELOC consists of a single BTB/POZ domain that interacts with CUL3 forming CRL3 complex. However, ELOC is also closely related to SKP1 proteins, and SKP1 together with F-box containing proteins interacts with CUL1 forming SCF complex (Choi et al. 2014; Stogios et al. 2005). Thus, ELOC has the ability to form different types of E3 ligase complexes that target specific proteins for proteasomal degradation. The ubiquitin proteasomal pathway plays an important role in many plant developmental stages including pollen tube elongation, seed dormancy, and flowering time (Chang et al. 2009; Shu & Yang 2017). Thus, the observed phenotypes exhibited by the overexpression line might be because of the ELOC involvement in ubiquitin ligase activities (Figure S3.11a).

3.6 References

Al Khateeb, W. M., Sher, A. A., Marcus, J. M., & Schroeder, D. F. (2019). UVSSA, UBP12, and RDO2/TFIIS Contribute to *Arabidopsis* UV Tolerance. Frontiers in plant science, 10, 516. https://doi.org/10.3389/fpls.2019.00516

Al Khateeb, W., & Schroeder, D.F. (2007). DDB2, DDB1A and DET1 Exhibit Complex Interactions During *Arabidopsis* Development. Genetics, 176, 231 - 242.

Alonso, J. M., Stepanova, A. N., Leisse, T. J., Kim, C. J., Chen, H., Shinn, P., Stevenson, D. K., Zimmerman, J., Barajas, P., Cheuk, R., Gadrinab, C., Heller, C., Jeske, A., Koesema, E., Meyers, C. C., Parker, H., Prednis, L., Ansari, Y., Choy, N., Deen, H., … Ecker, J. R. (2003). Genome-wide insertional mutagenesis of *Arabidopsis thaliana*. Science (New York, N.Y.), 301(5633), 653–657. https://doi.org/10.1126/science.1086391

Aso, T., and Conrad, M.N. (1997). Molecular cloning of DNAs encoding the regulatory subunits of elongin from Saccharomyces cerevisiae and Drosophila mELOAnogaster. Biochem. Biophys. Res. Commun. 241: 334-340

Aso, T., Lane, W. S., Conaway, J. W., & Conaway, R. C. (1995). Elongin (SIII): A Multisubunit Regulator of Elongation by RNA Polymerase II. Science, 269(5229), 1439–1443. http://www.jstor.org/stable/2888734

Boiteux, S., & Jinks-Robertson, S. (2013). DNA repair mechanisms and the bypass of DNA damage in Saccharomyces cerevisiae. Genetics, 193(4), 1025–1064. https://doi.org/10.1534/genetics.112.145219

Bourbousse, C., Vegesna, N., Law, J. A. (2018). SOG1 activator and MYB3R repressors regulate a complex DNA damage network in *Arabidopsis*. PNAS. 2018;115:E12453–E12462. doi: 10.1073/pnas.1810582115

Bradsher, J. N., Jackson, K. W., Conaway, R. C., & Conaway, J. W. (1993). RNA polymerase II transcription factor SIII. I. Identification, purification, and properties. The Journal of biological chemistry, 268(34), 25587–25593

Bradsher, J. N., Tan, S., McLaury, H.-J., Conaway, J. W., and Conaway,R. C. (1993) RNA polymerase II transcription factor SIII: II. Functionalproperties and role in RNA chain elongation.J. Biol. Chem.268,25594–25603

Braun, B., Pfirrmann, T., Menssen ,R., Hofmann, K., Scheel, H., Wolf, D. H. (2011). Gid9, a second RING finger protein contributes to the ubiquitin ligase activity of the Gid complex required for catabolite degradation. FEBS Lett. 585:3856-61. doi: 10.1016/j.febslet

Chang, L. C., Guo, C. L., Lin, Y. S., Fu, H., Wang, C. S., & Jauh, G. Y. (2009). Pollen-specific SKP1-like proteins are components of functional scf complexes and essential for lily pollen tube elongation. Plant & cell physiology, 50(8), 1558–1572. https://doi.org/10.1093/pcp/pcp100

Choi, C. M., Gray, W. M., Mooney, S., & Hellmann, H. (2014). Composition, roles, and regulation of cullin-based ubiquitin e3 ligases. The *Arabidopsis* book, 12, e0175. https://doi.org/10.1199/tab.0175

Conaway, R.C., Conaway, J.W. (2019). The hunt for RNA polymerase II elongation factors: a historical perspective. Nat Struct Mol Biol 26, 771–776. https://doi-org.uml.idm.oclc.org/10.1038/s41594-019-0283-1

Donà, M., & Mittelsten Scheid, O. (2015). DNA Damage Repair in the Context of Plant Chromatin. Plant physiology, 168(4), 1206–1218. https://doi.org/10.1104/pp.15.00538

Earley, K. W., Haag, J. R., Pontes, O., Opper, K., Juehne, T., Song, K., & Pikaard, C. S. (2006). Gateway-compatible vectors for plant functional genomics and proteomics. The Plant journal : for cell and molecular biology, 45(4), 616–629. https://doi.org/10.1111/j.1365-313X.2005.02617.x

Edenberg, E. R., Downey, M., & Toczyski, D. (2014). Polymerase stalling during replication, transcription and translation. Current biology : CB, 24(10), R445–R452. https://doi.org/10.1016/j.cub.2014.03.060

El-Gebali, S., Mistry, J., Bateman, A., Eddy, S. R., Luciani, A., Potter, S. C., Qureshi, M., Richardson, L. J., Salazar, G. A., Smart, A., Sonnhammer, E., Hirsh, L., Paladin, L., Piovesan, D., Tosatto, S., & Finn, R. D. (2019). The Pfam protein families database in 2019. Nucleic acids research, 47(D1), D427–D432. https://doi.org/10.1093/nar/gky995

Felsenstein, J. (1985). Confidence limits on phylogenies: An approach using the bootstrap. Evolution 39:783-791.

Finley, D., Ulrich, H. D., Sommer, T., & Kaiser, P. (2012). The ubiquitin-proteasome system of saccharomyces cerevisiae. Genetics, 192(2), 319-360. doi:10.1534/genetics.112.140467

Fraser, C. M., & Chapple, C. (2011). The phenylpropanoid pathway in *Arabidopsis*. *The Arabidopsis book*, *9*, e0152. https://doi.org/10.1199/tab.0152

Gerber, M., Eissenberg, J. C., Kong, S., Tenney, K., Conaway, J. W., Conaway, R. C., & Shilatifard, A. (2004). In vivo requirement of the RNA polymerase II elongation factor elongin A for proper gene expression and development. Molecular and cellular biology, 24(22), 9911–9919. https://doi.org/10.1128/MCB.24.22.9911-9919.2004

Gillette, T. G., Yu, S., Zhou, Z., Waters, R., Johnston, S. A., & Reed, S. H. (2006). Distinct functions of the ubiquitin-proteasome pathway influence nucleotide excision repair. The EMBO journal, 25(11), 2529–2538. https://doi.org/10.1038/sj.emboj.7601120

Grasser, K. D. (2005). Emerging role for transcript elongation in plant development. Trends in plant science, 10(10), 484–490. https://doi.org/10.1016/j.tplants.2005.08.004

Harreman, M., Taschner, M., Sigurdsson, S., Anindya, R., Reid, J., Somesh, B., Kong, S. E,, Banks, C. A. S., Conaway, R. C. ,Conaway, J. W., Svejstrup, J. Q. (2009). Distinct ubiquitin ligases act sequentially for RNA polymerase II polyubiquitylation. Proceedings of the National Academy of Sciences of the United States of America, 106(49), 20705-20710. doi:10.1073/pnas.0907052106

Heinicke, S., Livstone, M. S., Lu, C., Oughtred, R., Kang, F., Angiuoli, S. V., White, O., Botstein, D., & Dolinski, K. (2007). The Princeton Protein Orthology Database (P-POD): a comparative genomics analysis tool for biologists. PloS one, 2(8), e766. https://doi.org/10.1371/journal.pone.0000766

Hooper, C. M., Tanz, S. K., Castleden, I. R., Vacher, M. A., Small, I. D., & Millar, A. H. (2014). SUBAcon: a consensus algorithm for unifying the subcellular localization data of the *Arabidopsis* proteome. Bioinformatics (Oxford, England), *30*(23), 3356–3364. https://doi.org/10.1093/bioinformatics/btu550.

Hossain, Z., Amyot, L., McGarvey, B., Gruber, M., Jung, J., & Hannoufa, A. (2012). The translation elongation factor eEF-1Bβ1 is involved in cell wall biosynthesis and plant development in *Arabidopsis thaliana*. PloS one, 7(1), e30425. https://doi.org/10.1371/journal.pone.0030425

Hua, Z., & Vierstra, R. D. (2011). The cullin-RING ubiquitin-protein ligases doi:10.1146/annurev-arplant-042809-112256 Retrieved from www.scopus.com

Huh, W. K., Falvo, J. V., Gerke, L. C., Carroll, A. S., Howson, R. W., Weissman, J. S., & O'Shea, E. K. (2003). Global analysis of protein localization in budding yeast. Nature, 425(6959), 686–691. https://doi.org/10.1038/nature02026

Ito, J., Batth, T. S., Petzold, C. J., Redding-Johanson, A. M., Mukhopadhyay, A., Verboom, R., Meyer, E. H., Millar, A. H., & Heazlewood, J. L. (2011). Analysis of the *Arabidopsis* cytosolic proteome highlights subcellular partitioning of central plant metabolism. Journal of proteome research, *10*(4), 1571–1582. https://doi.org/10.1021/pr1009433

Jain, M., Nijhawan A., Tyagi A. K., Khurana J. P. (2006). Validation of housekeeping genes as internal control for studying gene expression in rice by quantitative real-time PCR. Biochem. Biophys. Res. Commun. 345, 646–651. 10.1016/j.bbrc.2006.04.140

Johann To Berens, P., & Molinier, J. (2020). Formation and Recognition of UV-Induced DNA Damage within Genome Complexity. International journal of molecular sciences, 21(18), 6689. https://doi.org/10.3390/ijms21186689

Kawauchi, J., Inoue, M., Fukuda, M., Uchida, Y., Yasukawa, T., Conaway, R. C., Conaway, J. W, Aso, T., Kitajima, S. (2013). Transcriptional properties of mammalian elongin a and its role in stress response. Journal of Biological Chemistry, 288(34), 24302-24315. doi:10.1074/jbc.M113.496703

Kile, B., Schulman, B., Alexander, W., Nicola, N., Martin, H. & Hilton, D. (2002). The SOCS box: a tale of destruction and degradation. Trends Biochem. Sci., 27, 235-241. doi:10.1016/S0968-0004(02)02085-6

Kilian, J., Whitehead, D., Horak, J., Wanke, D., Weinl, S., Batistic, O., D'Angelo, C., Bornberg-Bauer, E., Kudla, J., Harter, K. (2007). The AtGenExpress global stress expression data set: Protocols, evaluation and model data analysis of UV-B light, drought and cold stress responses. Plant Journal, 50, 347-363. doi:10.1111/j.1365-313X.2007.03052.x

Koth, C. M., Botuyan, M. V., MorELOAnd, R. J., Jansma, D. B., Conaway, J. W., Conaway, R. C., Chazin, W. J., Friesen, J. D., Arrowsmith, C.H., Edwards, A. M. (2000). Elongin from saccharomyces cerevisiae. Journal of Biological Chemistry, 275(15), 11174-11180. doi:10.1074/jbc.275.15.11174

Lahari, T., Lazaro, J., & Schroeder, D. F. (2017). RAD4 and RAD23/HMR Contribute to *Arabidopsis* UV Tolerance. Genes, 9(1), 8. https://doi.org/10.3390/genes9010008

Lahari, T., Lazaro, J., Marcus, J. M., & Schroeder, D. F. (2018). RAD7 homologues contribute to *Arabidopsis* UV tolerance. Plant science: an international journal of experimental plant biology, 277, 267–277. https://doi.org/10.1016/j.plantsci.2018.09.017

Liang, L., Flury, S., Kalck, V., Hohn, B., & Molinier, J. (2006). CENTRIN2 interacts with the *Arabidopsis* homolog of the human XPC protein (AtRAD4) and contributes to efficient synthesis-dependent repair of bulky DNA lesions. Plant molecular biology, 61(1-2), 345–356. https://doi.org/10.1007/s11103-006-0016-9

Lolas, I. B., Himanen, K., Grønlund, J.T., Lynggaard, C., Houben, A., Melzer, M., Van Lijsebettens, M., Grasser, K. D (2010). The transcript elongation factor FACT affects *Arabidopsis* vegetative and reproductive development and genetically interacts with HUB1/2. Plant J. 61, 686-97. doi: 10.1111/j.1365-313X.2009.04096.x.

Lu, Q., Tang, X., Tian, G., Wang, F., Liu, K., Nguyen, V., Kohalmi, S. E., Keller, W. A., Tsang, E. W., Harada, J. J., Rothstein, S. J., & Cui, Y. (2010). *Arabidopsis* homolog of the yeast TREX-2 mRNA export complex: components and anchoring nucleoporin. The Plant journal : for cell and molecular biology, 61(2), 259–270. https://doi.org/10.1111/j.1365-313X.2009.04048.x

Mahrour, N., Redwine, W. B., Florens, L., Swanson, S. K., Martin-Brown, S., Bradford, W. D., Staehling-Hampton, K., Washburn, M. P., Conaway, R. C., and Conaway, J. W. (2008) Characterization of Cullin-box sequences that direct recruitment of Cul2-Rbx1 and Cul5-Rbx2 modules to Elongin BC-based ubiquitin ligases. J. Biol. Chem. 283, 8005–8013

Matsuyama, A., Arai, R., Yashiroda, Y., Shirai, A., Kamata, A., Sekido, S., Kobayashi, Y., Hashimoto, A., Hamamoto, M., Hiraoka, Y., Horinouchi, S., & Yoshida, M. (2006). ORFeome cloning and global analysis of protein localization in the fission yeast Schizosaccharomyces pombe. Nature biotechnology, 24(7), 841–847. https://doi.org/10.1038/nbt1222

Mistry, J., Chuguransky, S., Williams, L., Qureshi, M., Salazar, G. A., Sonnhammer, E. L., ... & Bateman, A. (2021). Pfam: The protein families database in 2021. Nucleic acids research, 49(D1), D412-D419.

Molinier, J., Lechner, E., Dumbliauskas, E., & Genschik, P. (2008). Regulation and role of *Arabidopsis* CUL4-DDB1A-DDB2 in maintaining genome integrity upon UV stress. PLoS genetics, 4(6), e1000093. https://doi.org/10.1371/journal.pgen.1000093

Mullenders, L. H. F. (2018). Solar UV damage to cellular DNA: From mechanisms to biological effects. Photochemical and Photobiological Sciences, 17(12), 1842-1852. doi:10.1039/c8pp00182k

Okumura, F., Matsuzaki, M., Nakatsukasa, K., & Kamura, T. (2012). The Role of Elongin BC-Containing Ubiquitin Ligases. Frontiers in oncology, 2, 10. https://doi.org/10.3389/fonc.2012.00010

Papadopoulos, J. S., & Agarwala, R. (2007). COBALT: constraint-based alignment tool for multiple protein sequences. Bioinformatics *(Oxford, England)*, *23*(9), 1073–1079. https://doi.org/10.1093/bioinformatics/btm076

Pause, A., Peterson, B., Schaffar, G., Stearman, R., & Klausner, R. D. (1999). Studying interactions of four proteins in the yeast two-hybrid system: structural resemblance of the pVHL/elongin BC/hCUL-2 complex with the ubiquitin ligase complex SKP1/cullin/F-box protein. Proceedings of the National Academy of Sciences of the United States of America, 96(17), 9533–9538. https://doi.org/10.1073/pnas.96.17.9533

Rastogi, R. P., Richa, Kumar, A., Tyagi, M. B., & Sinha, R. P. (2010). Molecular mechanisms of ultraviolet radiation-induced DNA damage and repair. Journal of nucleic acids, 2010, 592980. https://doi.org/10.4061/2010/592980

Reed, S. H. (2005). Nucleotide excision repair in chromatin: the shape of things to come. DNA repair, 4(8), 909–918. https://doi.org/10.1016/j.dnarep.2005.04.009

Ribar, B., Prakash, L., & Prakash, S. (2006). Requirement of ELOC1 for RNA polymerase II polyubiquitylation and degradation in response to DNA damage in saccharomyces cerevisiae. Molecular and Cellular Biology, 26(11), 3999-4005. doi:10.1128/MCB.00293-06

Ribar, B., Prakash, L., & Prakash, S. (2007). ELOA1 and CUL3 are required along with ELOC1 for RNA polymerase II polyubiquitylation and degradation in DNA-damaged yeast cells. Molecular and Cellular Biology, 27(8), 3211-3216. doi:10.1128/MCB.00091-0

Ribeiro-Silva, C., Sabatella, M., Helfricht, A., Marteijn, J. A., Theil, A. F., Vermeulen, W., & Lans, H. (2020). Ubiquitin and TFIIH-stimulated DDB2 dissociation drives DNA damage handover in nucleotide excision repair. Nature communications, 11(1), 4868. https://doi.org/10.1038/s41467-020-18705-0

Risseeuw, E. P., Daskalchuk, T. E., Banks, T. W., Liu, E., Cotelesage, J., Hellmann, H., Estelle, M., Somers, D. E., & Crosby, W. L. (2003). Protein interaction analysis of SCF ubiquitin E3 ligase subunits from *Arabidopsis*. The Plant journal : for cell and molecular biology, 34(6), 753–767. https://doi.org/10.1046/j.1365-313x.2003.01768.x

Sarikas, A., Hartmann, T., & Pan, Z. Q. (2011). The cullin protein family. Genome biology, 12(4), 220. https://doi.org/10.1186/gb-2011-12-4-220

Schmid, M, Davison, TS, Henz, SR, Pape, UJ, Demar, M, Vingron, M, Schölkopf, B, Weigel, D, Lohmann, JU. (2005). A gene expression map of *Arabidopsis thaliana* development. Nat Genet37,501-6. doi: 10.1038/ng1543

Schroeder, D. F., Gahrtz, M., Maxwell, B. B., Cook, R. K., Kan, J. M., Alonso, J. M., Ecker, J. R., & Chory, J. (2002). De-etiolated 1 and damaged DNA binding protein 1 interact to regulate Arabidopsis photomorphogenesis. Current biology : CB, 12(17), 1462–1472. https://doi.org/10.1016/s0960-9822(02)01106-5

Sessions, A., Burke, E., Presting, G., Aux, G., McElver, J., Patton, D., Dietrich, B., Ho, P., Bacwaden, J., Ko, C., Clarke, J. D., Cotton, D., Bullis, D., Snell, J., Miguel, T., Hutchison, D., Kimmerly, B., Mitzel, T., Katagiri, F., Glazebrook, J., … Goff, S. A. (2002). A high-throughput *Arabidopsis* reverse genetics system. The Plant cell, 14(12), 2985–2994. https://doi.org/10.1105/tpc.004630

Shu, K., & Yang, W. (2017). E3 Ubiquitin Ligases: Ubiquitous Actors in Plant Development and Abiotic Stress Responses. Plant & cell physiology, 58(9), 1461–1476. https://doi.org/10.1093/pcp/pcx071

Shuck, S. C., Short, E. A., & Turchi, J. J. (2008). Eukaryotic nucleotide excision repair: from understanding mechanisms to influencing biology. Cell research, 18(1), 64–72. https://doi.org/10.1038/cr.2008.2

Sprenger, J., Lynn Fink, J., Karunaratne, S., Hanson, K., Hamilton, N. A., & Teasdale, R. D. (2008). LOCATE: a mammalian protein subcellular localization database. *Nucleic acids research*, *36*(Database issue), D230–D233. https://doi.org/10.1093/nar/gkm950.

Stogios, P. J., Downs, G. S., Jauhal, J. J., Nandra, S. K., & Privé, G. G. (2005). Sequence and structural analysis of BTB domain proteins. Genome biology, 6(10), R82. https://doi.org/10.1186/gb-2005-6-10-r82

Sugasawa, K. (2016). Molecular mechanisms of DNA damage recognition for mammalian nucleotide excision repair. DNA repair, 44, 110–117. https://doi.org/10.1016/j.dnarep.2016.05.015

Tkach, J. M., Yimit, A., Lee, A. Y., Riffle, M., Costanzo, M., Jaschob, D., Hendry, J. A., Ou, J., Moffat, J., Boone, C., Davis, T. N., Nislow, C., & Brown, G. W. (2012). Dissecting DNA damage response pathways by analysing protein localization and

abundance changes during DNA replication stress. Nature cell biology, 14(9), 966–976. https://doi.org/10.1038/ncb2549

Weber, H., Bernhardt, A., Dieterle, M., Hano, P., Mutlu, A., Estelle, M., Genschik, P., & Hellmann, H. (2005). *Arabidopsis* AtCUL3a and AtCUL3b form complexes with members of the BTB/POZ-MATH protein family. Plant physiology, 137(1), 83–93. https://doi.org/10.1104/pp.104.052654

Weems, J. C., Slaughter, B. D., Unruh, J. R., Boeing, S., Hall, S. M., McLaird, M. B., Yasukawa, T., Aso, T., Svejstrup, J. Q., Conaway, J. W., & Conaway, R. C. (2017). Cockayne syndrome B protein regulates recruitment of the Elongin A ubiquitin ligase to sites of DNA damage. The Journal of biological chemistry, 292(16), 6431–6437. https://doi.org/10.1074/jbc.C117.777946

Weems, J. C., Slaughter, B. D., Unruh, J. R., Hall, S. M., McLaird, M. B., Gilmore, J. M., Washburn, M. P., Florens, L., Yasukawa, T., Aso, T., Conaway, J. W., & Conaway, R. C. (2015). Assembly of the Elongin A Ubiquitin Ligase Is Regulated by Genotoxic and Other Stresses. The Journal of biological chemistry, 290(24), 15030–15041. https://doi.org/10.1074/jbc.M114.632794

Winter, D., Vinegar, B., Nahal, H., Ammar, R., Wilson, G. V., & Provart, N. J. (2007). An "Electronic Fluorescent Pictograph" browser for exploring and analyzing large-scale biological data sets. PloS one, 2(8), e718. doi.org/10.1371/journal.pone.0000718

Yamasaki, T., & Ohama, T. (2011). Involvement of Elongin C in the spread of repressive histone modifications. The Plant journal: for cell and molecular biology, 65(1), 51–61. https://doi.org/10.1111/j.1365-313X.2010.04400.x

Yasukawa, T., Bhatt, S., Takeuchi, T., Kawauchi, J., Takahashi, H., Tsutsui, A., Muraoka, T., Inoue, M., Tsuda, M., Kitajima, S., Conaway,R.C., Conaway,J.W., Trainor, P. A., Aso, T. (2012). Transcriptional elongation factor elongin A regulates retinoic acid-induced gene expression during neuronal differentiation. Cell Reports, 2(5), 1129-1136. doi:10.1016/j.celrep.2012.09.031

Yasukawa, T., Kamura, T., Kitajima, S., Conaway, R. C., Conaway, J. W., & Aso, T. (2008). Mammalian Elongin A complex mediates DNA-damage-induced ubiquitylation and degradation of Rpb1. The EMBO journal, 27(24), 3256–3266. https://doi.org/10.1038/emboj.2008.249

Zhai, Y., Deng, Y., Cheng, G., Peng, L., Zheng, Y., Yang, Y., & Xu, J. (2015). Sugarcane elongin C is involved in infection by sugarcane mosaic disease pathogens. Biochemical and Biophysical Research Communications, 466(3), 312-318. doi:10.1016/j.bbrc.2015.09.015

Zhu, M., Chen, Y., Ding, X. S., Webb, S. L., Zhou, T., Nelson, R. S., & Fan, Z. (2014). Maize elongin C interacts with the viral genome-linked protein, VPg, of sugarcane mosaic virus and facilitates virus infection. New Phytologist, 203(4), 1291-1304. doi:10.1111/nph.12890

Chapter 4. General Discussion and Conclusions

The main source of energy for living organisms is sunlight, which consists of beneficial visible light and damaging UV-B radiation. Plants need sunlight for photosynthesis. However, due to their sessile nature, they cannot avoid exposure to the high level of UV-B radiation. UV-B radiation can damage DNA by generating DNA photoproducts such as CPDs and 6-4pps and Dewar isomers. These DNA photoproducts alter DNA chemical structure and in turn inhibit cellular processes such as DNA transcription and replication. To protect themselves from the deleterious effects of the UV-induced DNA photoproducts as well as to prevent mutations and genome instability, plants have to repair these DNA photoproducts.

Plants utilize two different pathways to repair the UV-induced DNA photoproducts: light repair via photolyases and dark repair via NER. NER is a conserved multi-step mechanism that starts with damage recognition, followed by removal of the damaged oligonucleotide and DNA resynthesis repair. Recognition of the UV-induced photoproducts during NER is via two subpathways; TC-NER if the damaged DNA located in the transcribed strand of the active gene, and GG-NER if the damaged DNA located in the non-transcribed regions of the genome (Hanawalt 2002). Following UV damage, the GG-NER components, DDB1/DDB2/CUL4/ RBX1 in mammals and RAD6/RAD16/ELOC/CUL3 in yeast target the damaged DNA in the non-transcribed strand and initiate the repair (Kapetanaki et al. 2006; Yu et al. 2016). The mammalian Eongin A/B/C/ CUL5 /RBX2 and the yeast Eongin A/ C/ CUL3 /RBX1 target the large subunit of the lesion stalled RNAPII on the transcribed strand for ubiquitination and degradation (Yasukawa et al. 2008; Ribar et al. 2007).

In *Arabidopsis* GG-NER, the mammalian-type damage recognition factors DDB1, DDB2, and CUL4 have been demonstrated to be necessary for plant UV tolerance and GG-NER (AlKhateeb & Schroeder 2009; Koga et al. 2006). In the second and third chapters of this thesis, I have demonstrated that *Arabidopsis* RAD16 homologs and ELOC homologs are also implicated in plant UV resistance. In addition, my results indicate that both RAD16 and ELOC homologs also have roles in plant development, since *Atrad16s* mutants exhibit short silique & early flowering phenotypes. Whereas,

ELOC overexpression exhibit growth, silique, and seed production phenotypes (increased plant height, long silique, and more seeds).

Thus, both mammalian and yeast type GG-NER damage recognition modules DDB1/DDB2/RBX1 and RAD7/RAD16/ELOC (RAD7 type-ELOC complex) are implicated in plant UV tolerance. In addition to the RAD7-type Elongin C complex, my results showed that Elongin A-type Elongin C complex is also required for wild-plant UV tolerance and growth. Supporting this are the observations that *Arabidopsis eloc* and *eloa* null mutants are sensitive to UV radiation and ELOA/ELOC overexpression results in increased silique length and seed production.

Why do plants need both the mammalian and yeast GG-NER damage recognition modules? What proteins do the two ELOC complexes (RAD7- and ELOA-containing) pair with in response to both UV and visible light? And what is the basis of the observed developmental trait?

4.1 Hypothesized *Arabidopsis* GG-NER requires the two damage recognition modules: DDB1/2 and RAD7/16

The mammalian and yeast damage recognition factors, DDB1/2 and RAD7/16, share functional similarities including recognition of UV-induced photoproducts, and histone modification via interacting with histone acetyl transferase GCN5 and ubiquitinating conserved components XPC/RAD4. However, the mechanism that these complexes use to recognize the UV-induced photoproducts are different. RAD7/16 complex scans DNA using the RAD16 ATPase as a motor, thus damage recognition by this complex requires ATP (Teng et al. 2008). However, DDB1/2 complex uses jumping as target search mechanism in an ATP-independent manner (Ghodke et al. 2014).

In addition, following damage recognition, RAD7/16 complex forms an E3 ubiquitin ligase complex through interacting with ELOC and CUL3 (Boiteux & Jinks-Robertson 2013). Similarly, the DDB1/2 complex also functions as an E3 ubiquitin ligase complex via interacting with CUL4 and RBX1 (Kapetanaki et al. 2006). The mammalian and yeast E3 ubiquitin ligase complexes are required for XPC and RAD4 ubiquitination, respectively. XPC ubiquitination enhances its binding affinity, whereas RAD4 ubiquitination results in its degradation (Boiteux & Jinks-Robertson 2013; Zhang&

Gong 2016). Therefore, it is possible that DDB1/2 activity complements RAD7/16 activity. In addition, XPA/RAD14 homolog does not exist in plants; XPA/RAD14 binds the damaged site at the single-strand DNA. As a result, it is possible that plants use the mammalian and yeast damage recognition modules to counteract the absence of XPA homolog (Fadda 2015; Sugasawa et al. 2009).

4.2 Suggested ubiquitin ligase activities mediate plant UV tolerance and growth

E3 ubiquitin ligases play a key role in regulating protein turnover. They facilitate protein ubiquitination for proteasome degradation. The E3-based protein ubiquitination process involves three different enzymes: the Ub activating enzyme (E1) transfers the ubiquitin to the Ub conjugating enzyme (E2) which then interacts with E3 the ubiquitin ligase enzyme. Then, E3 ubiquitin ligase ubiquitinates the lysine residue of the target protein. This in turn facilitates target protein degradation by the proteasome (Choi et al. 2014). Cullin-based E3 ubiquitin ligases are a type of E3 ubiquitin ligases that are involved in many developmental and NER processes.

The yeast *S. cerevisiae* E3 ubiquitin ligase complex (ELOC1/RAD7/RAD16/CUL3) is involved in NER (Liu et al. 2019). *Arabidopsis* ELOC is well conserved; it shares more than 70% amino acid identity with ELOC homologs in other plants, and 40% identity with yeast ELOC homolog (Yamasaki & Ohama 2011). AtELOC has a single BTB/POZ domain that mediates CUL3 interaction (Yamasaki & Ohama 2011). In addition, the *Arabidopsis* genome also has two CUL3 proteins: CUL3A and CUL3B. AtCUL3 proteins bring together RING finger domain proteins such as RAD16 and substrate-specific BTB/POZ domains proteins such as ELOC (Hua & Vierstra 2011; Choi et al. 2014). Thus, I speculate that AtELOC could combine with RAD16 & CUL3 to have E3 ligase function. I expect this E3 ligase complex to play a role in plant development and UV tolerance. Since *Atcul3a* loss of function mutant has been reported to show a delayed flowering time (Dieterle et al. 2005). Double loss of function mutant *Atcul3a Atcul3b* is embryo lethal. Whereas, a double mutant *cul3a-3 cul3b-1* which demonstrates a partial *CUL3a* loss of function and complete *CUL3b* loss of function has been reported to show a reduced rosette diameter in addition to delayed flowering time (Thoman et al. 2005). In addition, my results showed that *Atrad16s* loss

of function mutants exhibit early flowering time. Moreover, *Atrad16s* loss of function mutants and *Ateloc* null mutant exhibit UV-sensitive phenotypes.

In addition, *Arabidopsis* ELOC is a divergent member of the BTB family that is closely related to SKP1 proteins which interact with CUL1 (Stogios et al. 2005). AtCUL1 is a member of the CULLIN family of proteins, which act as the molecular scaffold in E3 ubiquitin ligase complexes. CUL1 brings together RING finger domain proteins such as RAD16, F-box proteins such as RAD7, and SKP1-like proteins such as ELOC1 (Choi et al. 2014). In this thesis, AtRAD16 was found to physically interact with AtRAD7. Thus, it is also speculated that RAD7/RAD16/ELOC/CUL1 also functions as an E3 ubiquitin ligase that is involved in UV tolerance and development.

4.3 *Ateloa* and *Ateloc* loss of function increases *Arabidopsis* UV sensitivity and AtELOA or AtELOC overexpression increases fertility

The three mammalian Elongins (A/B/C) form a heterotrimeric complex, which stimulates transcript elongation by RNAP II (Aso et al. 1995). In addition to this transcript elongation activity, the three mammalian Elongins are also involved together in a complex with CUL5 and RBX2 that ubiquitinates the large subunit of RNAP II (Rpb1) following DNA damage, targeting it for degradation (Okumura et al. 2012). In *S. cerevisiae*, ELOA and ELOC homologues have been identified, however, no ELOB homologue has been identified (Aso & Conrad 1997). In *S. cerevisiae*, the Elongin A/C complex has no effect on yeast transcriptional elongation (Koth et al. 2000). However, yeast Elongin A and C, together with CUL3 and RBX1, also ubiquitinate the large subunit of RNAP II following DNA damage, targeting it for degradation (Okumura et al. 2012). *Arabidopsis* Elongin A is also well conserved in the BC-box region, consistent with the elongin C interaction I observed. AtELOA is also well conserved in the cullin 5-interaction domain, despite the lack of a CUL5 homolog in *Arabidopsis* genome, suggesting that perhaps AtELOA utilizes an alternative cullin. Thus, I expect *Arabidopsis* ELOA/ELOC to form an E3 ubiquitin ligase complex that targets RNAPII for degradation following UV damage. This may explain the increased UV sensitivity in both *Ateloa*, and *Ateloc* mutants.

Finally, the ability of AtELOA and AtELOC to complex with each other suggests a possible conserved role in transcript elongation. This may explain the enhanced developmental phenotypes exhibited by AtELOA and AtELOC overexpression lines. I spectulate *Arabidopsis* ELOA/ELOC complex to acts as a transcript elongation factor that enhances the transcription of specific genes involved in silique development, seed production, and stem elongation factors. Thus, ELOA/ELOC overexpression may enhance the transcription of these specific genes either by directly increasing the rate of RNAPII transcription or by interacting with histone and regulates the expression of these specific genes.

4.4 Suggested future research

I have studied the effects of *Arabidopsis RAD16* and *RAD16b* loss of function on plant UV tolerance and growth. I also examined RAD16 cellular localization and the effect of RAD16 overexpression on plant UV tolerance and growth. Then I analyzed the genetic and physical interactions between AtRAD16 and other GG-NER and TC-NER components. I also characterized *Arabidopsis* ELOA and ELOC homologs by generating transgenic plants. Then I studied these mutants through analysis of growth phenotypes, their response to UV treatment, and their cellular localization. Further experiments to illuminate the importance of these genes might include the following:

- I have studied the effects of *Arabidopsis rad16b* loss of function on plant UV tolerance and growth. However, RAD16b overexpression is yet to be studied. Due to the absence of *AtRAD16* cDNA in public collections, I could not study the effect of AtRAD16b overexpression on plant UV tolerance and growth. However, RAD16b cDNA could be generated from wildtype plants. Once I generate it I will clone it into Gateway entry vectors, then transfer it to overexpression vectors pEarleyGate100 (CaMV 35S promoter) and pEarleyGate104 (CaMV 35S promoter with an N-terminal yellow fluorescent protein (YFP) tag). This will enable me to examine AtRAD16b cellular localization, and its ability to rescue *Atrad16b* loss of function mutant phenotypes. I could also examine the ability of AtRAD16 and AtRAD16b to complement the UV sensitivity of their corresponding yeast mutants.

➢Sequence homology lead me to predict that *Arabidopsis* RAD16 and RAD16b to play a role in NER. However, I only examined the UV tolerance and sensitivity. Thus, in order to confirm the involvement of the two genes in NER, I need to perform photoproducts repair experiments using both loss of function and gain of function mutants.

➢In both mammalian and yeast, ELOA and ELOC target the large subunit of RNAPII for degradation following UV damage. The large subunit of *Arabidopsis* RNAPII is encoded by NRPB1 (Nawrath et al.1990). Thus, it will interesting to use the commercially available antibody that detects the C-terminal domain of the NRPB1 (Ream et al. 2009), to examine the NRPB1 levels following exposure to UV radiation. If degradation is observed, I will look at NRPB1 levels in *Ateloa* and *Ateloc* mutants to see if they are necessary.

➢In *S.cerevisea*, physical interaction between ScRAD16 and ScELOC1 was determined by using co-purification techniques (Gillette et al. 2006). I could not detect physical interaction between AtRAD16 and AtELOC using yeast-two hybrid analysis. Nevertheless, I could utilize other methods such as co-immunoprecipitation or bimolecular fluorescence complementation to examine possible physical interaction between the two proteins.

➢Phenotypic analysis of *Atrad16* and *Atrad16b* single mutants showed that both mutants have early flowering time, opposite to that exhibited by *Atcul3* loss of function mutant (late; Dieterle et al. 2005). I expect AtCUL3 to be required for *Atrad16* and *Atrad16b* flowering time phenotype. Generating double loss of function mutant *Atrad16 Atcul3* will help us to test this hypothesis. If AtCUL3 is required, the double loss of function mutant should exhibit late flowering time, similar to *Atcul3* mutant.

➢*Atrad16* and *Atcul3* mutants exhibit developmental and UV sensitive phenotypes. Thus, I expect AtRAD16 and AtCUL3 to be a component of an E3 ligase complex that implicates in plant UV tolerance and development. As I discussed, AtCUL3 proteins bring together RING finger domain proteins such as RAD16 and substrate-specific BTB/POZ domains proteins such as ELOC. Thus, I expect AtRAD16 together with AtCUL3, and AtELOC to form an E3 ubiquitin ligase complex.To examine this hypothesis, I could generate or order *AtCUL3* cDNA, clone it into yeast and examine

possible physical interaction between AtCUL3 and each of AtELOC and AtRAD16 using yeast two hybrid assay. I could also use another protein–protein interaction assays such as co-immunoprecipitation to test this hypothesis.

➢Both the *Arabidopsis* Elongin A-type and RAD7-type Elongin C complexes are expected to be involved in ubiquitination activities, thus biochemical analysis of these two complexes such as ubiquitination assay could be utilized.

4.5 Conclusions

In conclusion, in this thesis, I identified the *Arabidopsis* ELOA homolog, and characterized the role of RAD16, ELOC, and ELOA homologs in plant UV tolerance and growth. *Arabidopsis* RAD16 homologs make a significant contribution to plant UV tolerance compared to TC-NER components such as CSB and UVSSA as well as the mammalian type GG-NER damage recognition components DDB1 and DDB2. *Arabidopsis* RAD16 homologs also play a role in plant growth and development. Similarly, both *Arabidopsis* ELOA and ELOC homologs are involved in plant UV tolerance, and overexpression of ELOA or ELOC increased plant fertility. The results of this research will help us uncover the mechanisms that plants use to protect themselves from UV radiation and gain insight into the interplay between UV protection and light-regulated development in plants.

4.6 References

Al Khateeb, W., & Schroeder, D. F. (2007). DDB2, DDB1A and DET1 Exhibit Complex Interactions During *Arabidopsis* Development. Genetics, 176, 231 – 242

Aso, T., and Conrad, M. N. (1997). Molecular cloning of DNAs encoding the regulatory subunits of elongin from Saccharomyces cerevisiae and Drosophila mELOAnogaster. Biochem. Biophys. Res. Commun. 241: 334-340

Aso, T., Lane, W. S., Conaway, J. W., & Conaway, R. C. (1995). Elongin (SIII): A Multisubunit Regulator of Elongation by RNA Polymerase II. Science, 269(5229), 1439–1443. http://www.jstor.org/stable/2888734

Boiteux, S., & Jinks-Robertson, S. (2013). DNA repair mechanisms and the bypass of DNA damage in Saccharomyces cerevisiae. Genetics, 193(4), 1025–1064. https://doi.org/10.1534/genetics.112.145219

Bourbousse, C., Vegesna, N., & Law, J. A. (2018). SOG1 activator and MYB3R repressors regulate a complex DNA damage network in *Arabidopsis*. *Proceedings*

of the National Academy of Sciences of the United States of America, *115*(52), E12453–E12462. https://doi.org/10.1073/pnas.1810582115
Choi, C. M., Gray, W. M., Mooney, S., & Hellmann, H. (2014). Composition, roles, and regulation of cullin-based ubiquitin e3 ligases. The *Arabidopsis* book, 12, e0175. https://doi.org/10.1199/tab.0175
Dieterle, M., Thomann, A., Renou, J. P., Parmentier, Y., Cognat, V., Lemonnier, G., Müller, R., Shen, W. H., Kretsch, T., & Genschik, P. (2005). Molecular and functional characterization of *Arabidopsis* Cullin 3A. The Plant journal : for cell and molecular biology, 41(3), 386–399. https://doi.org/10.1111/j.1365-313X.2004.02302.x
Fadda, E. (2015). Role of the XPA protein in the NER pathway: A perspective on the function of structural disorder in macromolecular assembly. Computational and structural biotechnology journal, 14, 78–85. https://doi.org/10.1016/j.csbj.2015.11.007
Ghodke, H., Wang, H., Hsieh, C. L., Woldemeskel, S., Watkins, S. C., Rapić-Otrin, V., & Van Houten, B. (2014). Single-molecule analysis reveals human UV-damaged DNA-binding protein (UV-DDB) dimerizes on DNA via multiple kinetic intermediates. Proceedings of the National Academy of Sciences, 111(18), E1862-E1871.
Gillette, T. G., Yu, S., Zhou, Z., Waters, R., Johnston, S. A., & Reed, S. H. (2006). Distinct functions of the ubiquitin-proteasome pathway influence nucleotide excision repair. The EMBO journal, 25(11), 2529–2538. https://doi.org/10.1038/sj.emboj.7601120
Hanawalt, P. C. (2002). Subpathways of nucleotide excision repair and their regulation. Oncogene, 21(58), 8949-8956.
Hua, Z., & Vierstra, R. D. (2011). The cullin-RING ubiquitin-protein ligases doi:10.1146/annurev-arplant-042809-112256 Retrieved from www.scopus.com
Kapetanaki, M. G., Guerrero-Santoro, J., Bisi, D. C., Hsieh, C. L., Rapić-Otrin, V., & Levine, A. S. (2006). The DDB1-CUL4ADDB2 ubiquitin ligase is deficient in xeroderma pigmentosum group E and targets histone H2A at UV-damaged DNA sites. Proceedings of the National Academy of Sciences of the United States of America, 103(8), 2588–2593. https://doi.org/10.1073/pnas.0511160103
Koga, A., Ishibashi, T., Kimura, S., Uchiyama, Y., & Sakaguchi, K. (2006). Characterization of T-DNA insertion mutants and RNAi silenced plants of *Arabidopsis thaliana* UV-damaged DNA binding protein 2 (AtUV-DDB2). Plant molecular biology, 61(1-2), 227–240. https://doi.org/10.1007/s11103-006-6408-z
Koth, C. M., Botuyan, M. V., MorELOAnd, R. J., Jansma, D. B., Conaway, J. W., Conaway, R. C., Chazin, W. J., Friesen, J. D., Arrowsmith, C.H., Edwards, A. M. (2000). Elongin from saccharomyces cerevisiae. Journal of Biological Chemistry, 275(15), 11174-11180. doi:10.1074/jbc.275.15.11174
Liu, L., Huo, Y., Li, J., & Jiang, T. (2019). Crystal structure of the yeast Rad7-ELOC1 complex and assembly of the Rad7-Rad16-ELOC1-Cul3 complex. DNA repair, 77, 1–9. https://doi.org/10.1016/j.dnarep.2019.02.012
Nawrath, C., Schell, J., & Koncz, C. (1990). Homologous domains of the largest subunit of eucaryotic RNA polymerase II are conserved in plants. Molecular and General Genetics MGG, 223(1), 65-75.

Okumura, F., Matsuzaki, M., Nakatsukasa, K., & Kamura, T. (2012). The Role of Elongin BC-Containing Ubiquitin Ligases. Frontiers in oncology, 2, 10. https://doi.org/10.3389/fonc.2012.00010

Ream, T. S., Haag, J. R., Wierzbicki, A. T., Nicora, C. D., Norbeck, A. D., Zhu, J. K., Hagen, G., Guilfoyle, T. J., Pasa-Tolić, L., & Pikaard, C. S. (2009). Subunit compositions of the RNA-silencing enzymes Pol IV and Pol V reveal their origins as specialized forms of RNA polymerase II. Molecular cell, 33(2), 192–203. https://doi.org/10.1016/j.molcel.2008.12.015

Ribar, B., Prakash, L., & Prakash, S. (2007). ELOA1 and CUL3 are required along with ELOC1 for RNA polymerase II polyubiquitylation and degradation in DNA-damaged yeast cells. Molecular and Cellular Biology, 27(8), 3211-3216. doi:10.1128/MCB.00091-0

Stogios, P. J., Downs, G. S., Jauhal, J. J., Nandra, S. K., & Privé, G. G. (2005). Sequence and structural analysis of BTB domain proteins. Genome biology, 6(10), R82. https://doi.org/10.1186/gb-2005-6-10-r82

Sugasawa, K., Akagi, J., Nishi, R., Iwai, S., & Hanaoka, F. (2009). Two-step recognition of DNA damage for mammalian nucleotide excision repair: Directional binding of the XPC complex and DNA strand scanning. *Molecular cell*, *36*(4), 642–653. https://doi.org/10.1016/j.molcel.2009.09.035

Teng, Y., Liu, H., Gill, H. W., Yu, Y., Waters, R., & Reed, S. H. (2008). Saccharomyces cerevisiae Rad16 mediates ultraviolet-dependent histone H3 acetylation required for efficient global genome nucleotide-excision repair. EMBO reports, 9(1), 97–102. https://doi.org/10.1038/sj.embor.7401112

Thomann, A., Brukhin, V., Dieterle, M., Gheyeselinck, J., Vantard, M., Grossniklaus, U., and Genschik, P. (2005). *Arabidopsis* CUL3A and CUL3B genes are essential for normal embryogenesis. Plant J. 43(3): 437–448.

Yamasaki, T., & Ohama, T. (2011). Involvement of Elongin C in the spread of repressive histone modifications. The Plant journal : for cell and molecular biology, 65(1), 51–61. https://doi.org/10.1111/j.1365-313X.2010.04400.x

Yasukawa, T., Kamura, T., Kitajima, S., Conaway, R. C., Conaway, J. W., & Aso, T. (2008). Mammalian Elongin A complex mediates DNA-damage-induced ubiquitylation and degradation of Rpb1. The EMBO journal, 27(24), 3256–3266. https://doi.org/10.1038/emboj.2008.249

Yu, S., Evans, K., van Eijk, P., Bennett, M., Webster, R. M., Leadbitter, M., Teng, Y., Waters, R., Jackson, S. P., & Reed, S. H. (2016). Global genome nucleotide excision repair is organized into domains that promote efficient DNA repair in chromatin. Genome research, 26(10), 1376–1387. https://doi.org/10.1101/gr.209106.116

Zhang, L., & Gong, F. (2016). The emerging role of deubiquitination in nucleotide excision repair. DNA repair, 44, 118–122. https://doi.org/10.1016/j.dnarep.2016.05.035

Appendix

Supplementary information 1

Contents:

Table S1.1

Table S1.1 Core NER components in *Escherichia coli*

Protein	Function in GG-NER	Function in TC-NER
Mfd	Not involved	DNA damage recognition factor. Removes the stalled RNAP and recruits core NER components to the damaged site
NusA	Not involved	Interacts with UvrD at the damaged site and facilitates the stalled RNAP backtracking
UvrA	DNA damage recognition factor. Binds UvrB and damaged DNA	Recruited to the damaged site by Mfd or by NusA/UvrD. Binds UvrB
UvrB	Binds UvrA and UvrC. Damage verification and duplex unwinding.	Binds UvrA and UvrC. Damage verification, and duplex unwinding.
UvrC	3’ and 5’ helicase	3’ and 5’ helicase
UvrD	UvrB/UvrC removal, and excision of the DNA fragment containing the lesion	Interacts with NusA and promotes the stalled RNAP backtracking. UvrB/UvrC removal, and excision of the DNA fragment containing the lesion
DNA POLI	DNA synthesis	DNA synthesis
Ligase I	DNA ligation	DNA ligation

Supplementary information 2

Contents:

Tables S2.1-S2.2

Figures S2.1-S2.17

Table S2.1 List of primers used in this study (sequence (5' to 3'))

Genotyping				
RAD16	RAD16-2F	TTGTTAGTATGTGGCAAGCC	RAD6-2R	GCACATACCAAAGCCTCAATC
RAD16b	RAD1b-1F	TAGAAACGATGCGGTACCTTG	RAD16b-1R	GTCATGTTGGTTGCTTCTTCG
RAD7a	RAD7a-3R	ATCTATAAGTGGTGCATGCC	RAD7a-1R	AAAAAGAAGCAAAGCAGAGGG
RAD7c	RAD7c-521F	GAAGGCCTTGGCTTATGCT	RAD7c-1R	TTCTTCCATCTCCACGTCTTG
DDB2	DDB2.3F	ACGACGTGTTTTGTCGGTGTGGAAGAA	DDB2-3R	ATAGCAGGAGCTTTACCAGGC
CSB	CSB-1L	TACCGTTTCAACAAAACCAGC	CSB-1R	TCTTTGACGAAACCAGTTTCG
UVSSA	UVSSA-2L	GAGCAAGAAGCCATTGAGATG	UVSSA-2R	CTGTCTCTCTCGTTGAATCCG
RAD23b	RAD23b-30	GTCTTACCTGAAGAATTTGAGGGTTGG	RAD23b-31	CCTGTTTCCGCTACCACATCTTCGACT
SALK	LBb1.3	ATTTTGCCGATTTCGGAAC		
Semi-quantitative RT-PCR				
RAD16	RAD16c-1211F	GCTTCTTGCAAATTCGCCCA	RAD16c-2147R	ATGGTCATGCTTCCCACCAG
RAD16b	RAD16Bc-129F	TGTGGGTGTAAGGTCTCGTG	RAD16Bc-346R	TTCACCGCCGACTGAATCATRAD1
ACTIN	ACT- F	CTGGAACAAGACTTCTGGGC	ACT- R	GGTGATGAAGCACAATCCAAG
qPCR				
RAD16	RAD16Q5	TGAGACAGGCCGTTGATCAT	RAD16Q6	CAGAGACCACTTCTTGCTCA
EF1A	EF1AQ3	CTGGAGGTTTTGAGGCTGGT	EF1AQ4	GGTGGTGGCATCCATCTTGT

Table S2.2 Percent of identity between yeast and *Arabidopsis* RAD16 protein sequences

	ScRAD16	SpRHP16	AtRAD16	AtRAD16b
ScRAD16		52%	40%	34%
SpRHP16			40%	35%
AtRAD16				61%


1 50
AtRAD16 (1) ----------
AtRAD16b (1) ----------
ScRAD16 (1) ----------
SpRHP16 (1) MGTSCNKINSNSNKGKENMHFVLDDNGDSKGNASNQQVERDDKLDMETTR
51 100
AtRAD16 (1) ----------
AtRAD16b (1) ----------
ScRAD16 (1) ----------MQEGGFIRRRRTRSTKKSVNYNELSDDDTAVKNSKTLQLK
SpRHP16 (51) WNGKEFEEPLSTNKKLIIQSNNTSSQHSTPPLSISDTSTHTG-SSTDNVE
101 150
AtRAD16 (1) --------------MELRSRNKAIRPSTEVVDLEEGTGINPDEEPYAISS
AtRAD16b (1) --------MAGLRSVHVGSETKVVS-KNECAHVTLWTGTAQGDLGVAMEP
ScRAD16 (41) GN------SENVNDSQDEEYRDDATLVKSPDDDDKDFIIDLTGSDKERTA
SpRHP16 (100) ANPNTGFSSARKRSLRSSNLKKKFVPLSSPEESNESEFIDDDESDEVASI
151 200
AtRAD16 (37) DDDSIGSEFQGDEEEEEELEE-VVANDDLPNPVPVLAIVNLPRASKKRKK
AtRAD16b (42) HSHHKNAILPSSSQDENLKEE-EVPDDDDSVGGEVQGEVNANDYIPNPAA
ScRAD16 (85) TDENTHAIKNDNDEIIEIKEERDVSDDDEPLTK-----KRKTTARKKKKK
SpRHP16 (150) IDIKEDETFDSKVEIPEAAPSSSTESDEESIPLSYQSKRRVSARASSSA
201 250
AtRAD16 (86) --PDARKEKVVLLWETWEKEQNSWIDEHMSEDVDLDQHNAVIAETAEPPS
AtRAD16b (91) --PANTKRKWQIMKEKVQ----------MTEDDDFDEQNAVIAEAAEQPL
ScRAD16 (130) -TSTKKKSPKVTPYERNTLRLYEHHPELRNVFTDLKNAPPYVPQRSKQPD
SpRHP16 (200) SSSSRTQAKSIPSHERTHYRLIRQHPELEHVWEKLEEEAPREVKQIEQPK
251 300
AtRAD16 (134) DLIMPLLRYQKEFLAWATKQEQ-SVAGGILADEMGMGKTIQAISLVLARR
AtRAD16b (129) DLIIPLLKYQKEFLAWATIQELSAVRGGILADEMGMGKTIQAISLVLARR
ScRAD16 (179) GMTIKLLPFQLEGLHWLISQEESIYAGGVLADEMGMGKTIQTIALLMNDL
SpRHP16 (250) ELVLNLLPFQREGVYWLKRQEDSSFGGGILADEMGMGKTIQTIALLLSEP
301 350
AtRAD16 (183) EVDRAQFGEAAGCTLVLCPLVAVSQWLNEIARFTSPGSTKVLVYHGAKRA
AtRAD16b (179) EVDRAKSREAVGHTLVLVPPVALSQWLDEISRLTSPGSTRVLQYHGPKRD
ScRAD16 (229) TKSPS---------LVVAPTVALMQWKNEIEQHTK-GQLKIYIYHGASRT
SpRHP16 (300) RGKPT---------LVVAPVVAIMQWKEEIDTHTN-KALSTYLYYGQARD
351 400
AtRAD16 (233) KNIKEFMNYDFVLTTYSTVESEYRRNIMPSKVQCAYCSKSFYPKKLVIHL
AtRAD16b (229) KNVQKLMNYDFVLTTSPIVENEYR--------------------------
ScRAD16 (269) TDIKDLQGYDVVLTTYAVLESVFR--------------------------
SpRHP16 (340) ISGEELSSYDVVLTSYNVIESVYR--------------------------
401 450
AtRAD16 (283) RYFCGPSAVKTAKQSKQKRKKTSDSSSQQGKEADAGEDKKLKKSKKKTKQ
AtRAD16b (253) -------------------------K----------D---------
ScRAD16 (293) --KQ
SpRHP16 (364) --KE
451 500
AtRAD16 (333) TVEKDQLGSDDKEKSLLHSVKWNRIILDEAHYIKERRSNTARAVFALEAT
AtRAD16b (255) --EG--V---DETMSPLHSIKWNRIIVDEAHDIKNRSSRTAKAVFALEAT
ScRAD16 (295) NYGFRRKNGLFKQPSVLHNIDFYRVILDEAHNIKDRQSNTARAVNNLKTQ
SpRHP16 (366) RSGFRRKNGVVKEKSLLHQMEFYRIILDEAHGIKSRTCNTARAVCGLRTT
501 550
AtRAD16 (383) YRWALSGTPLQNRVGELYSLIRFLQIRPYSYYFCK--DCDCRILDYVAHQ
AtRAD16b (298) YRWALSGTPLQNDVDELYSLVS------YSFLN----FFYSTYASFAFRH
ScRAD16 (345) KRWCLSGTPLQNRIGEMYSLIRFLNINPFTKYFCTKCDCASKDWKFTDRM
SpRHP16 (416) RKICLSGTPLQNRIGELFSLLRFLRADPFAYYYCLQCECKSLHWRFSDRS

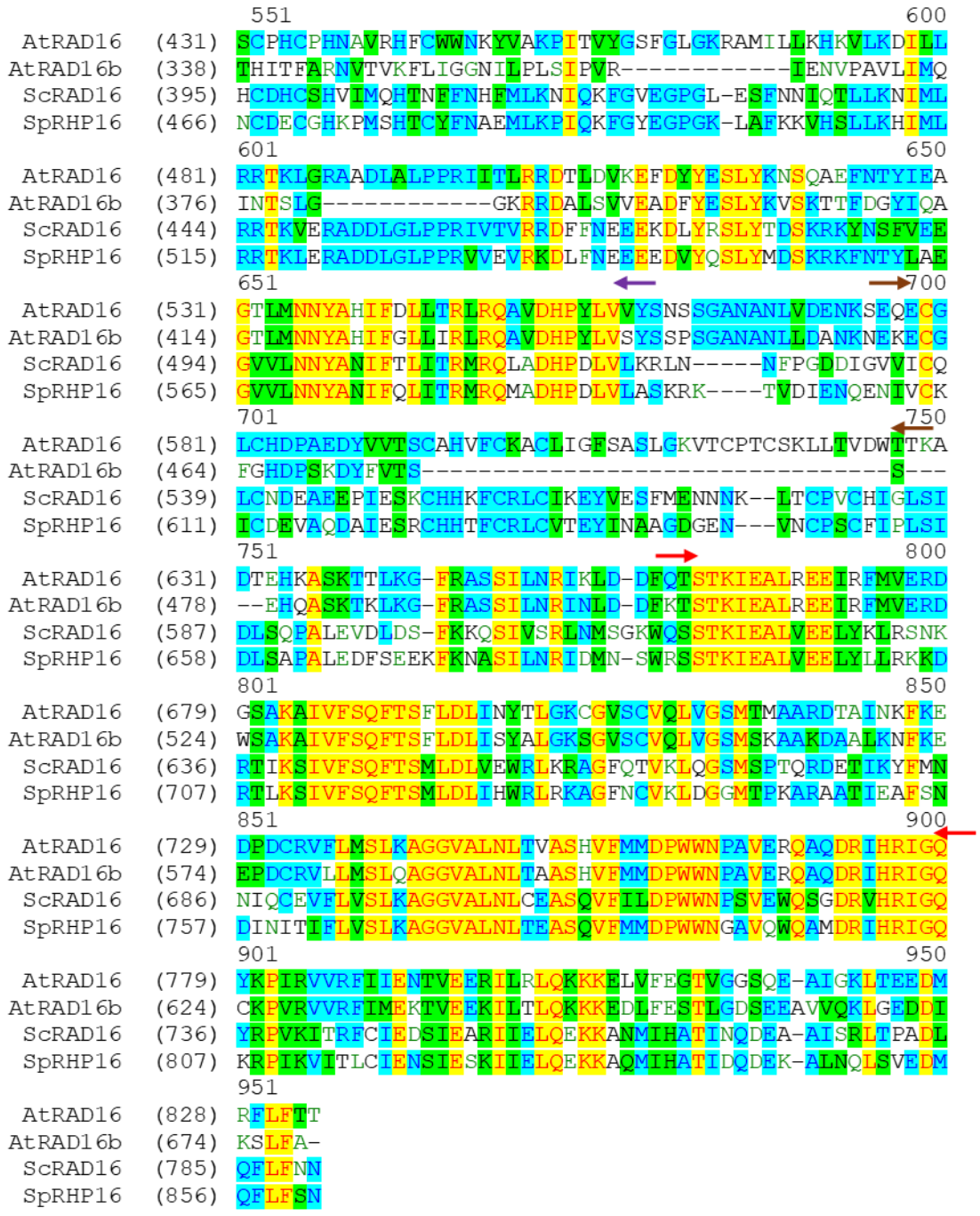

Figure S2.1 Sequence analysis of yeast and *Arabidopsis* RAD16 proteins

RAD16 and RAD16b protein sequences of *Arabidopsis* (NP_172004.1, NP_171767.1), *S. cerevisea* (P31244.1), and *S. pombe* (P79051.1) aligned using AlignX, helicase ATP binding domain is indicated in black, the start and the stop of snf2-N domain is indicated in purple arrows, zinc finger ring-type in brown, and helicase c-terminal domain in red

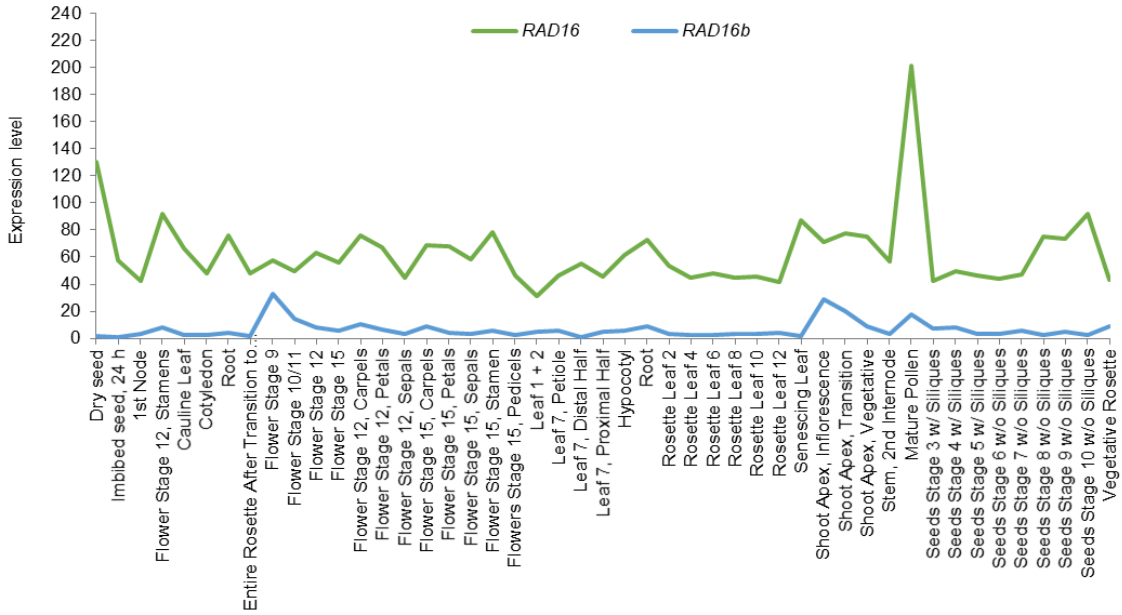

Figure S2.2 Visualization of *Arabidopsis RAD16* and *RAD16b* expression level from AtGenExpress

Expression level of RAD16 (green) and RAD16b (blue) in different tissues during different stages of *Arabidopsis thaliana* development. Expression values were calculated using The Gene Chip OperatingSoftware (GCOS; TGT=100, Bkg=20). Data were obtained from Schmid et al. (2005).

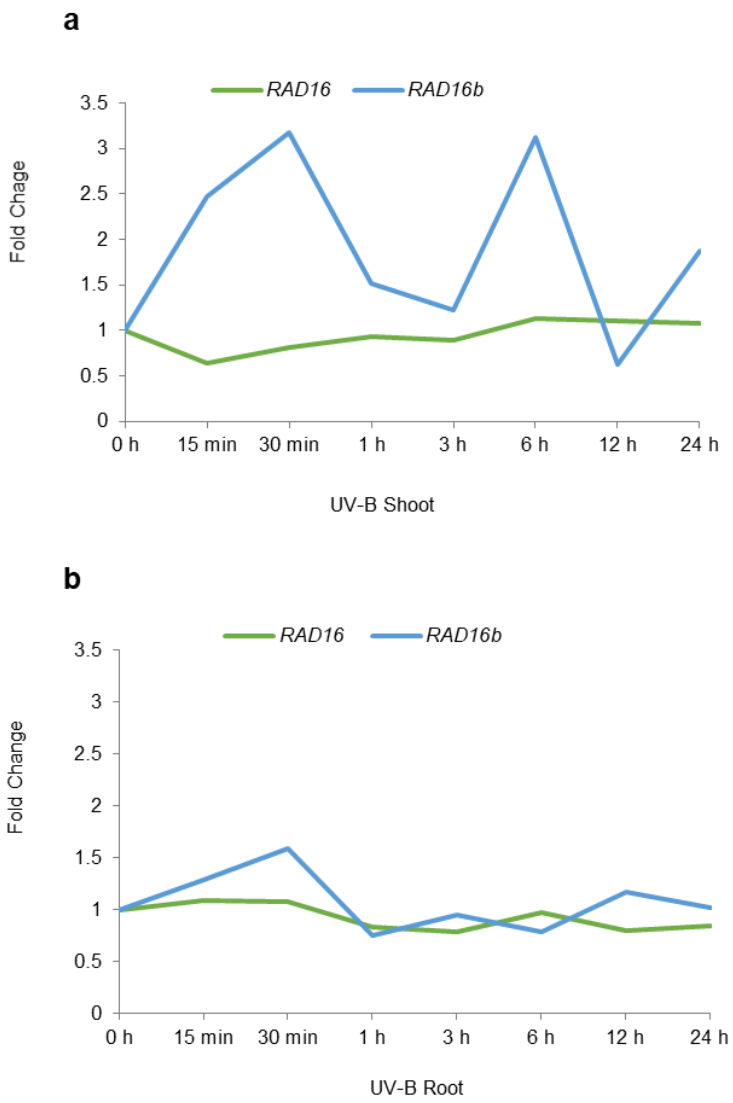

Figure S2.3 Visualization of *Arabidopsis RAD16* and *RAD16b* expression level following UV treatment

Expression level of *RAD16* and *RAD16b* following UV-B treatment in shoot (**a**) and root tissues (**b**) relative to untreated control of the same genotype. Data were obtained from Kilian et al. (2007) visualized by *Arabidopsis* eFP browser (Winter et al., 2007).

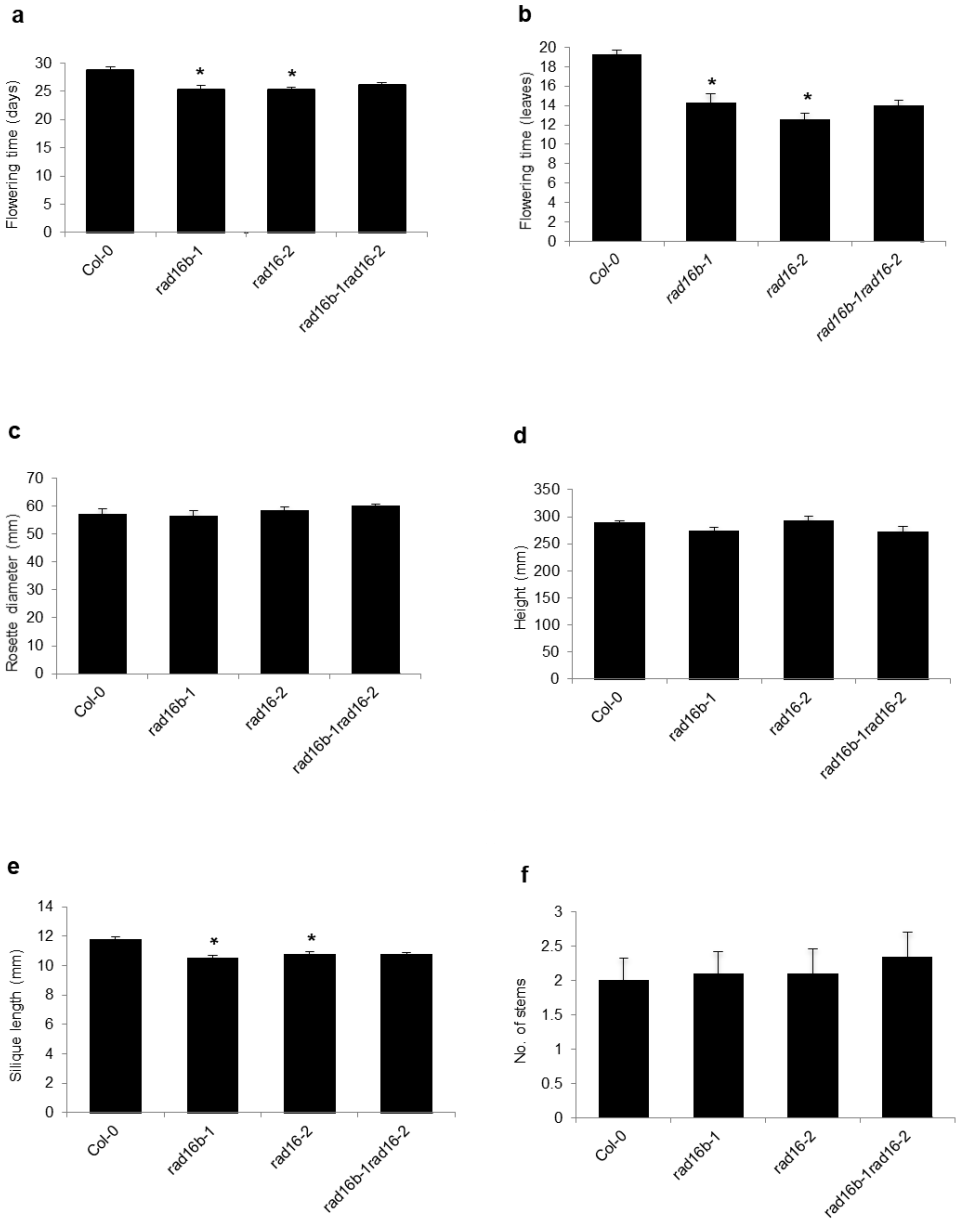

Figure S2.4 Adult developmental phenotypes of *Arabidopsis rad16b* and *rad16* single and double mutants

(**a**) Flowering time, average number of days and (**b**) average number of leaves. (**c**) Average rosette diameter (mm). (**d**) Average height (mm). (**e**) Average slique length. (f) Apical dominance (average number of stems). Values are means ± SE (n= 12), * = $p \leq 0.05$ of single mutant vs wild type, and double mutants vs *rad16-2*.

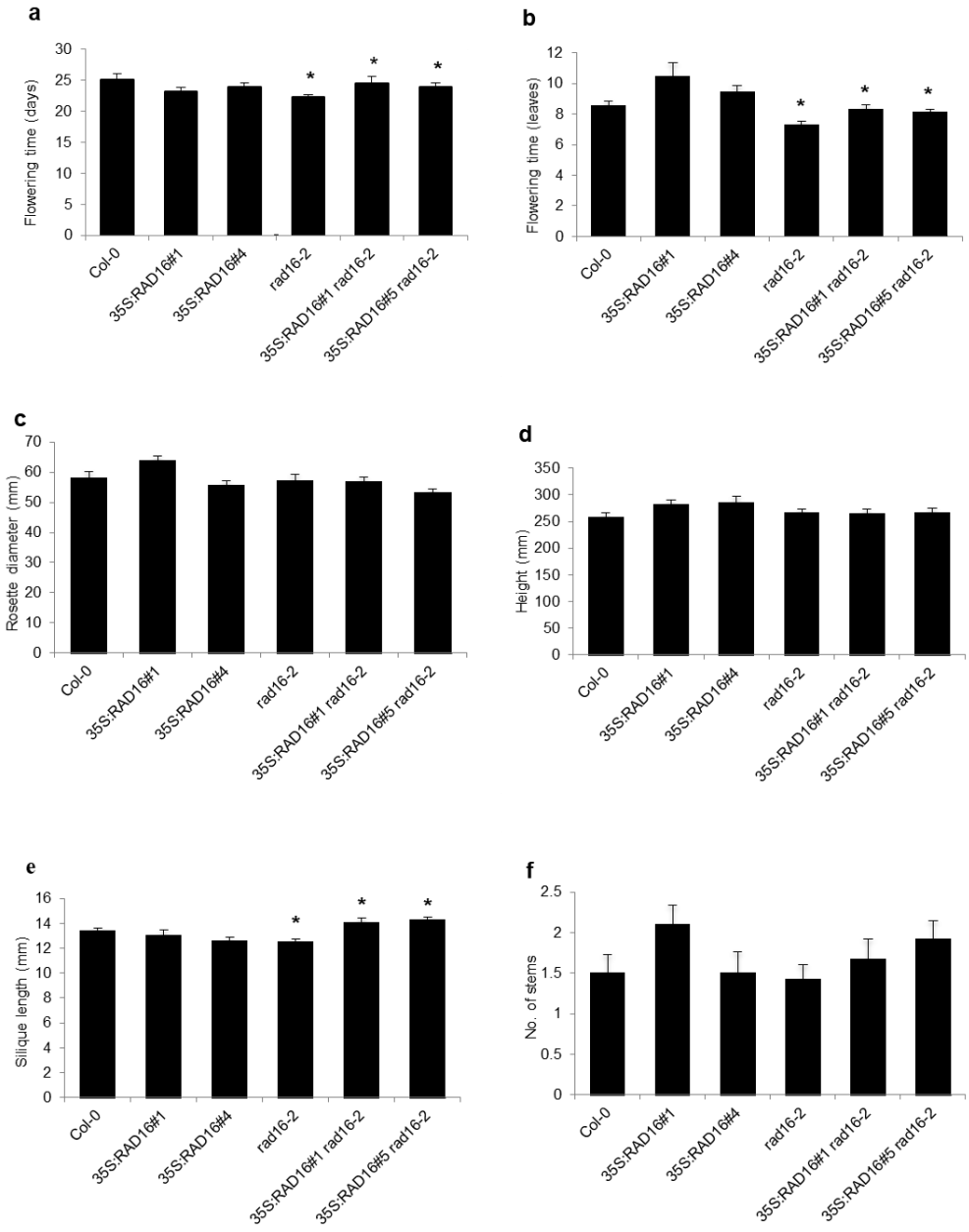

Figure S2.5 *Arabidopsis RAD16* overexpression rescues early flowering time and short silique length phenotypes

(**a**) Flowering time, average number of days and (**b**) average number of leaves. (**c**) Average rosette diameter (mm). (**d**) Average height (mm). (**e**) Average slique length. (f) Apical dominance (average number of stems). Values are means ± SE (n= 12), * = $p \leq 0.05$ of *rad16-2* and *35S: RAD16* vs wild type (Col-0) and *35S: RAD16 rad16-2* vs *rad16-2***.**

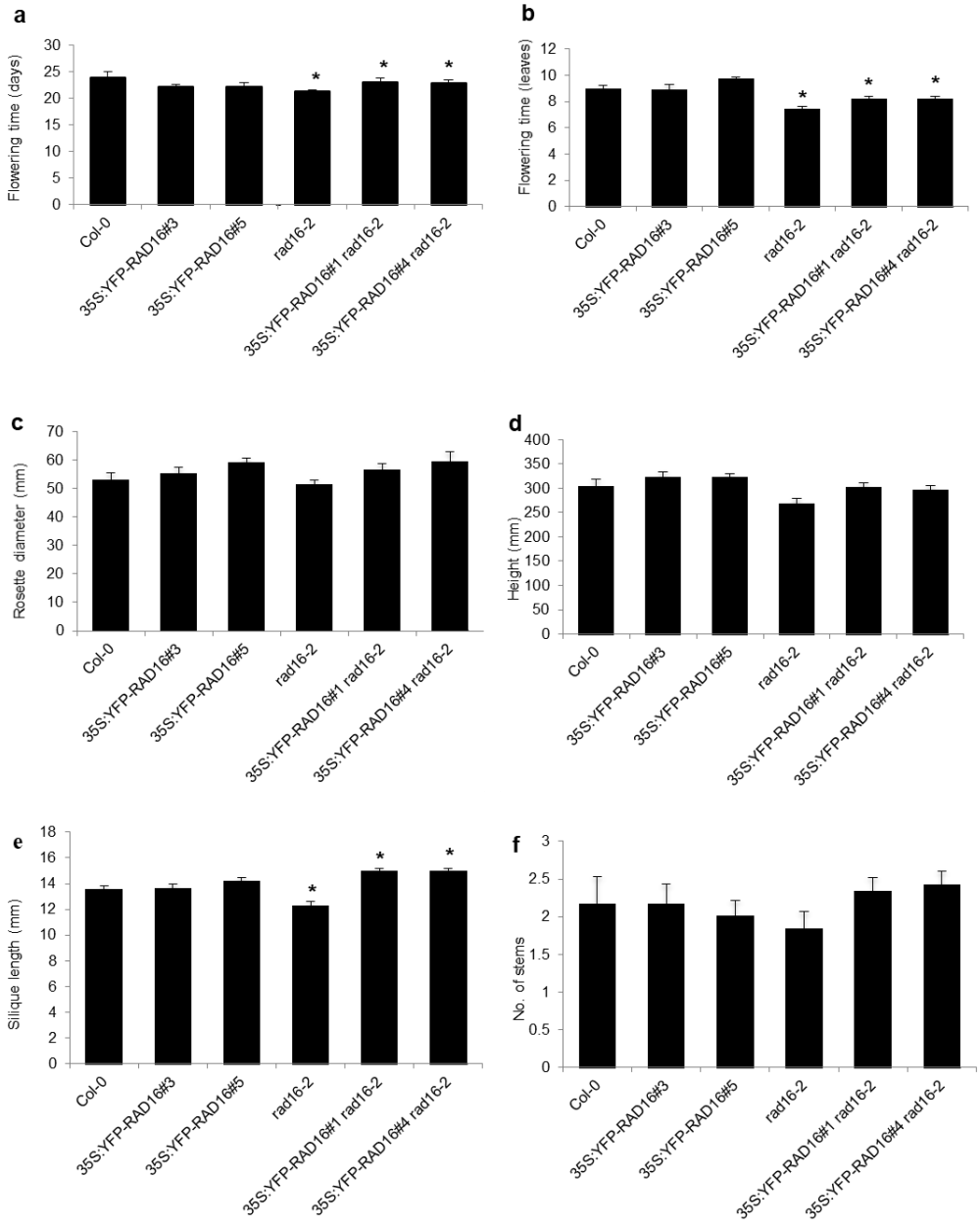

Figure S2.6 *Arabidopsis YFP-RAD16* overexpression rescues the early flowering time and short silique length phenotypes

Flowering time, average number of days (**a**) and average number of leaves (**b**). (**c**) Average rosette diameter (mm). (**d**) Average height (mm). (**e**) Average slique length. (f) Apical dominance (average number of stems). Values are means ± SE (n= 12), * = p ≤ 0.05 of *rad16-2* and *35S: YFP-RAD16* vs wild type (Col-0) and *35S:YFP- RAD16 rad16-2* vs *rad16-2***.**

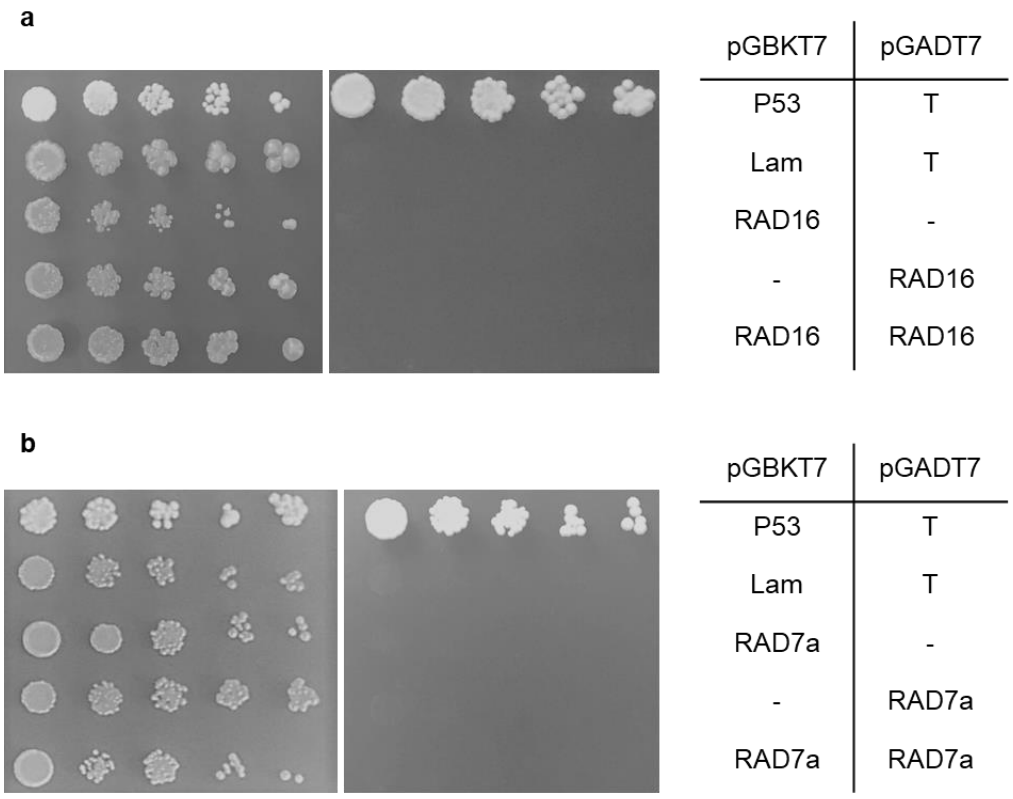

Figure S2.7 Yeast two-hybrid screening for *Arabidopsis* RAD16 and RAD7a self-interaction

Neither RAD16 nor RAD7a interacted with itself. Each of *RAD16* and *RAD7a* were cloned into pGBKT7 (bait) and pGADT7 (prey) vectors and transformed into haploid yeast cells, then mated. Five fold dilutions of the mated diploid strains; RAD16 bait/RAD16 prey (**a**) and RADa bait/RAD7a prey (**b**) were spotted on (-leu -trp) non-selective plates (left) and on selective plates (-leu –trp –ade -his) on the right. P53/T and Lam/T are the positive and negative controls respectively, as P53 interacts with T, whereas Lam does not interact with T.

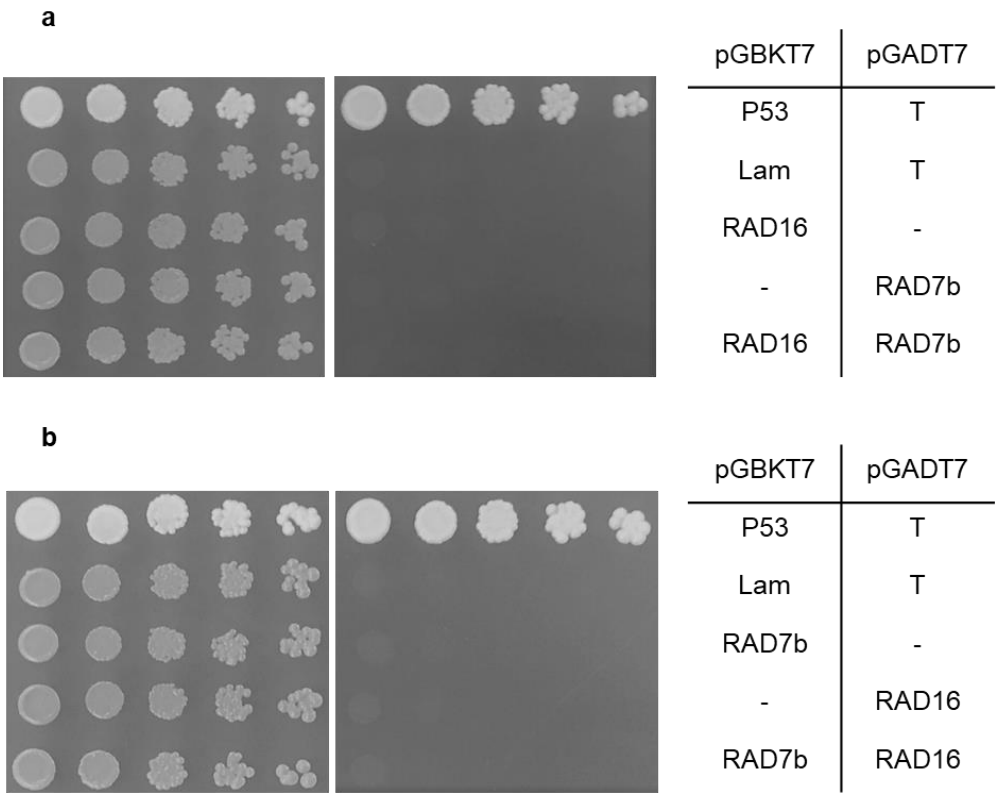

Figure S2.8 Yeast two-hybrid screening for *Arabidopsis* RAD16/RAD7b interaction

RAD16 did not interact with RAD7b. Each of *RAD16* and *RAD7b* were cloned into pGBKT7 (bait) and pGADT7 (prey) vectors and transformed into haploid yeast cells, then mated. Five fold dilutions of the mated diploid strains; RAD16 bait/RAD7b prey (**a**) and RADb bait/RAD16 prey (**b**) were spotted on (-leu -trp) non-selective plates (left) and on selective plates (-leu –trp –ade -his) (right). P53/T and Lam/T are the positive and negative controls respectively, as P53 interacts with T, whereas Lam does not interact with T.

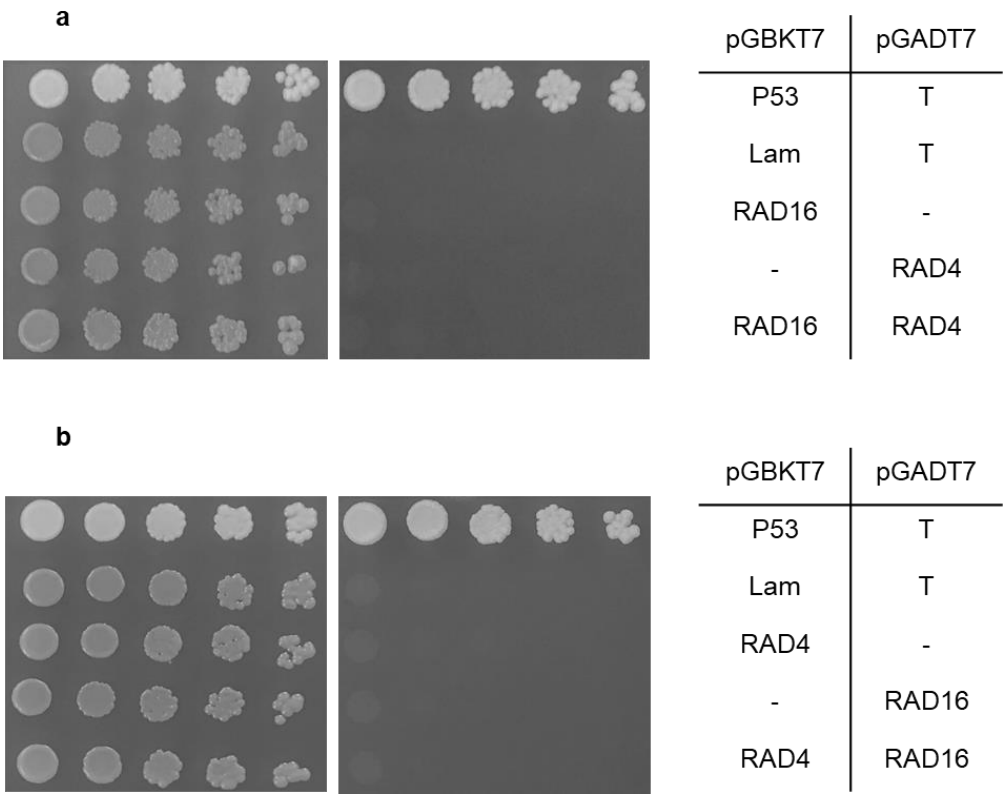

Figure S2.9 Yeast two-hybrid screening for *Arabidopsis* RAD16/RAD4 interaction

RAD16 did not interact with RAD4. Each of *RAD16* and *RAD4* were cloned into pGBKT7 (bait) and pGADT7 (prey) vectors and transformed into haploid yeast cells, then mated. Five fold dilutions of the mated diploid strains; RAD16 bait/RAD4 prey (**a**) and RAD4 bait/RAD16 prey (**b**) were spotted on (-leu -trp) non-selective plates (left) and on selective plates (-leu –trp –ade -his) (right). P53/T and Lam/T are the positive and negative controls respectively, as P53 interacts with T, whereas Lam does not interact with T.

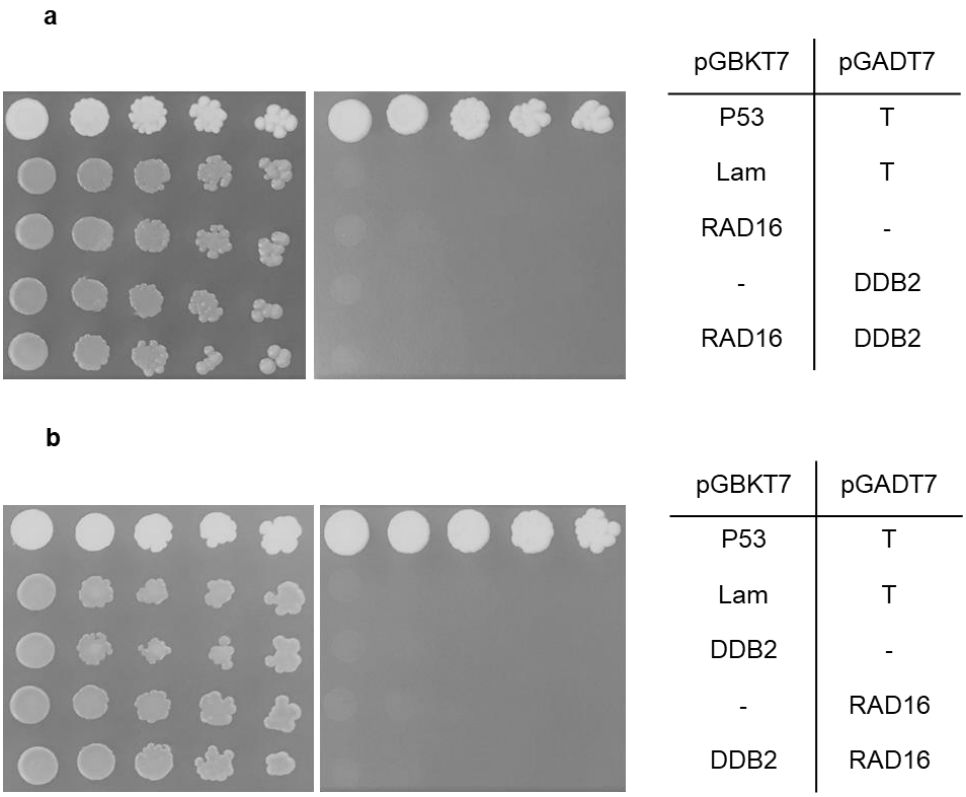

Figure S2.10 Yeast two-hybrid screening for *Arabidopsis* RAD16/DDB2 interaction

RAD16 did not interact withDDB2. Each of *RAD16* and *DDB2* were cloned into pGBKT7 (bait) and pGADT7 (prey) vectors and transformed into haploid yeast cells, then mated. Five fold dilutions of of the mated diploid strains; RAD16 bait/DDB2 prey (**a**) and DDB2 bait/RAD16 prey (**b**) were spotted on (-leu -trp) non-selective plates (left) and on selective plates (-leu –trp –ade -his) right. P53/T and Lam/T are the positive and negative controls respectively, as P53 interacts with T, whereas Lam does not interact with T.

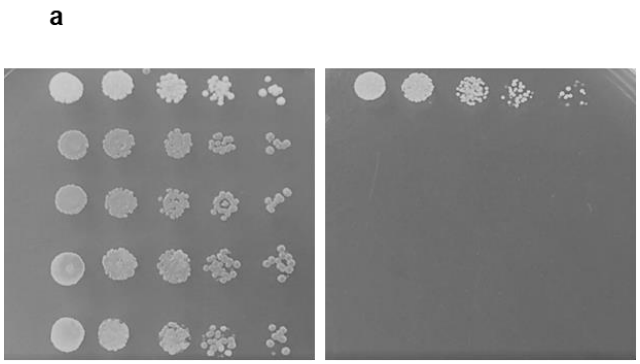

pGBKT7	pGADT7
P53	T
Lam	T
RAD16	-
-	ELOC
RAD16	ELOC

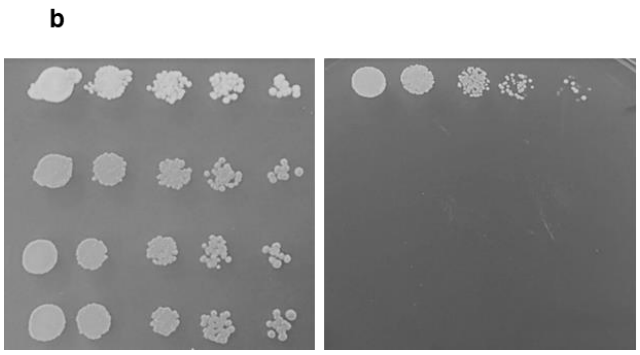

pGBKT7	pGADT7
P53	T
Lam	T
ELOC	-
-	RAD16
ELOC	RAD16

Figure S2.11 Yeast two-hybrid screening for *Arabidopsis* RAD16/ELOC interaction

RAD16 did not interact with ELOC. Each of *RAD16* and *ELOC* were cloned into pGBKT7 (bait) and pGADT7 (prey) vectors and transformed into haploid yeast cells, then mated. Five fold dilutions of the mated diploid strains; RAD16 bait/ELOC prey (**a**) and ELOC bait/RAD16 prey (**b**) were spotted on (-leu -trp) non-selective plates (left) and on selective plates (-leu –trp –ade -his) (right). P53/T and Lam/T are the positive and negative controls respectively, as P53 interacts with T, whereas Lam does not interact with T.

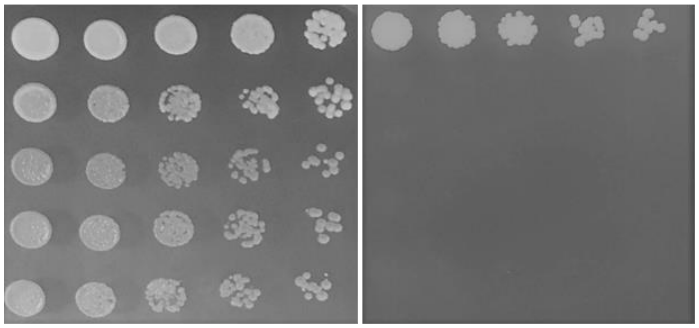

pGBKT7	pGADT7
P53	T
Lam	T
RAD16	-
-	RAD23b
RAD16	RAD23b

Figure S2.12 Yeast two-hybrid screening for *Arabidopsis* RAD16/RAD23b interaction

RAD16 did not interact with RAD23b. Each of *RAD16* and *RAD23b* were cloned into pGBKT7 (bait) and pGADT7 (prey) vectors, respectively, and transformed into haploid yeast cells, then mated. Five fold dilutions of the mated diploid strain; RAD16 bait/RAD23b prey were spotted on (-leu -trp) non-selective plates (left) and on selective plates (-leu –trp –ade -his) (right). P53/T and Lam/T are the positive and negative controls respectively, as P53 interacts with T, whereas Lam does not interact with T.

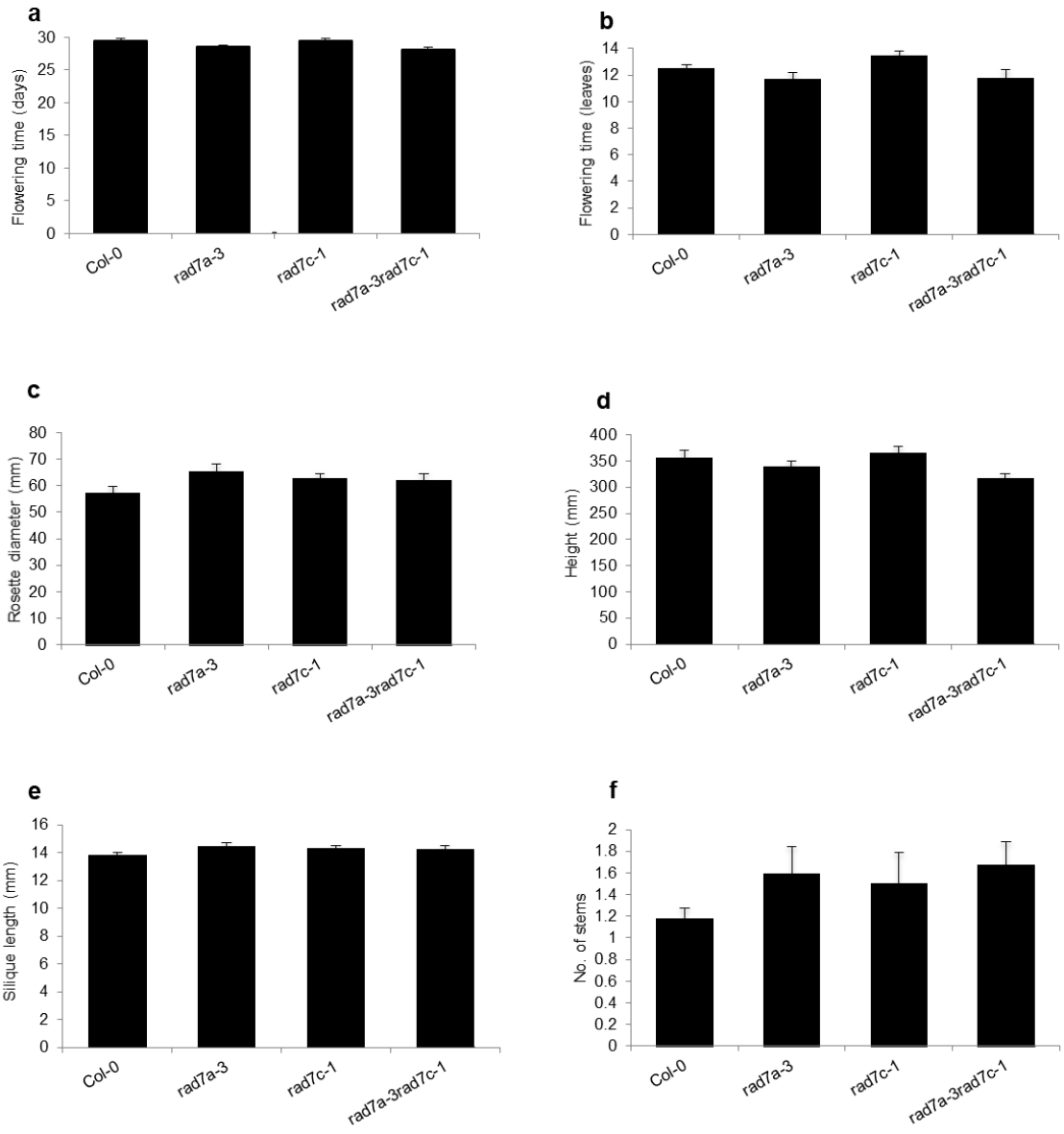

Figure S2.13 Adult developmental phenotypes of *Arabidopsis rad7a* and *rad7c* single and double mutants

(**a**) Flowering time, average number of days and (**b**) average number of leaves. (**c**) Average rosette diameter (mm). (**d**) Average height (mm). (**e**) Average slique length. (f) Apical dominance (average number of stems). Values are means ± SE (n= 12), * = $p \leq 0.05$ of single mutant vs wild type, and double mutants vs *rad16-2*.

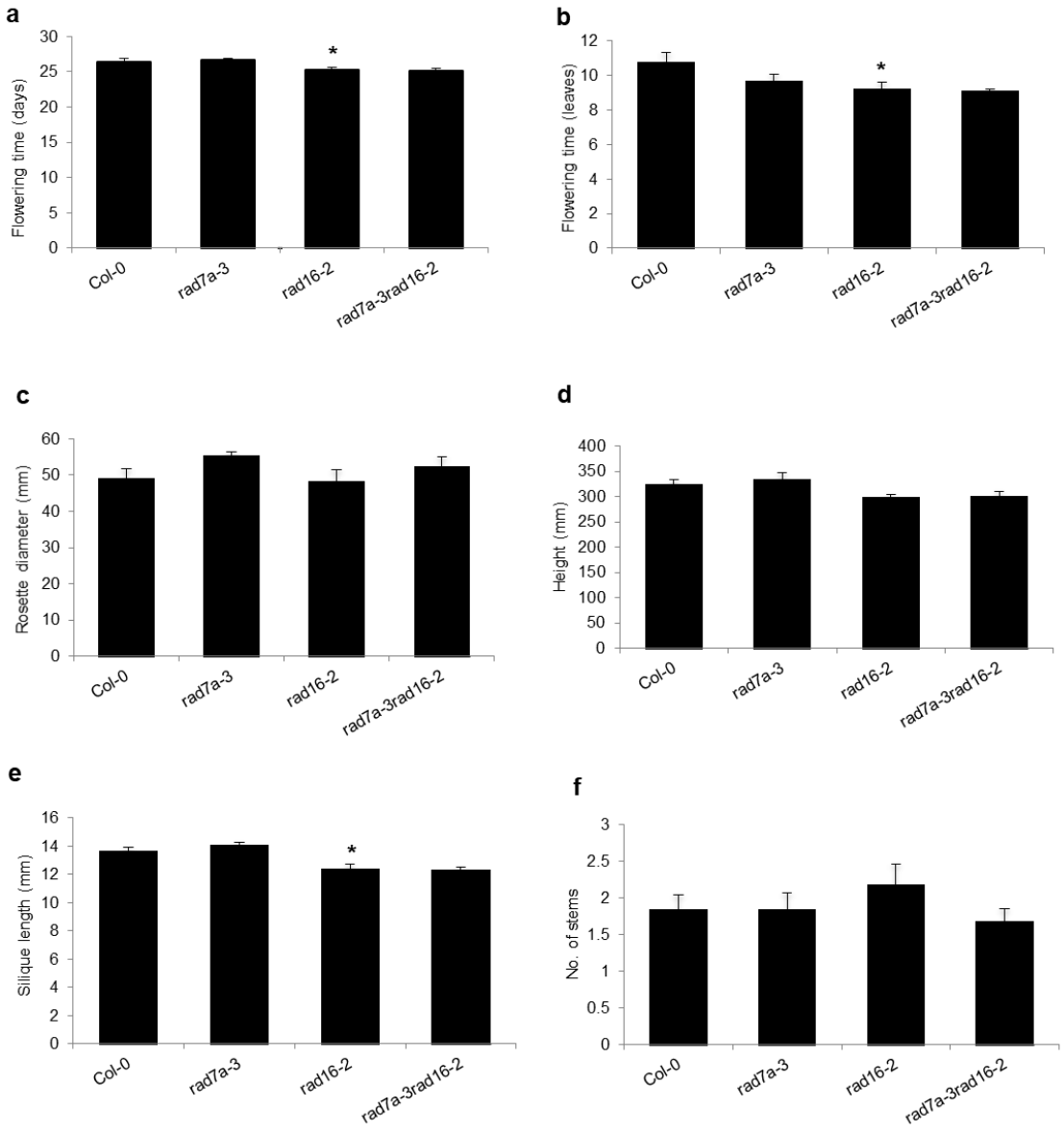

Figure S2.14 Adult developmental phenotypes of *Arabidopsis rad7a* and *rad16* single and double mutants

(**a**) Flowering time, average number of days and (**b**) average number of leaves. (**c**) Average rosette diameter (mm). (**d**) Average height (mm). (**e**) Average slique length. (f) Apical dominance (average number of stems). Values are means ± SE (n= 12), * = $p \leq 0.05$ of single mutant vs wild type, and double mutants vs *rad16-2*.

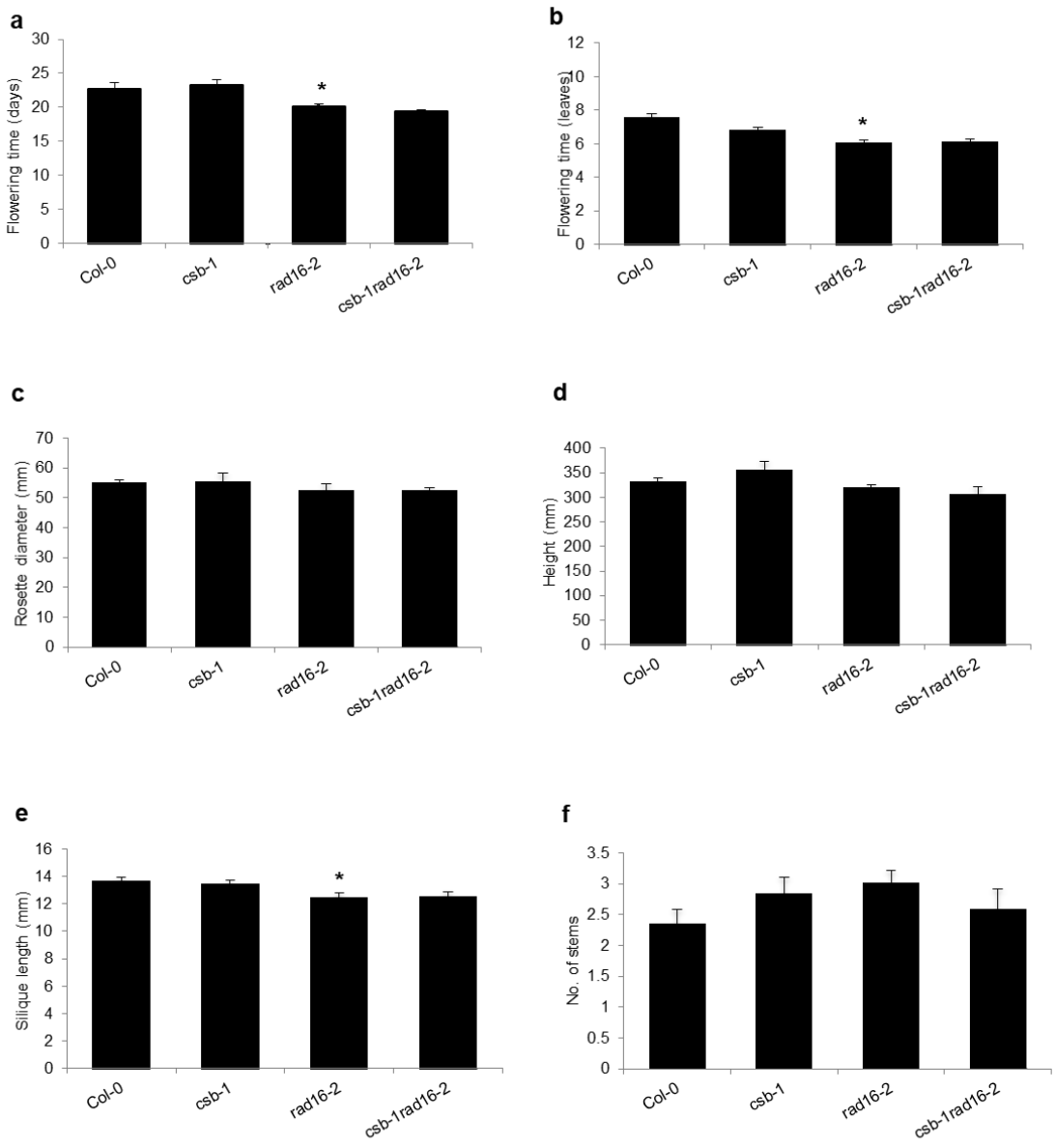

Figure S2.15 Adult developmental phenotypes of *Arabidopsis csb* and *rad16* single and double mutants

(**a**) Flowering time, average number of days and (**b**) average number of leaves. (**c**) Average rosette diameter (mm). (**d**) Average height (mm). (**e**) Average slique length. (f) Apical dominance (average number of stems). Values are means ± SE (n= 12), * = $p \leq 0.05$ of single mutant vs wild type, and double mutants vs *rad16-2*.

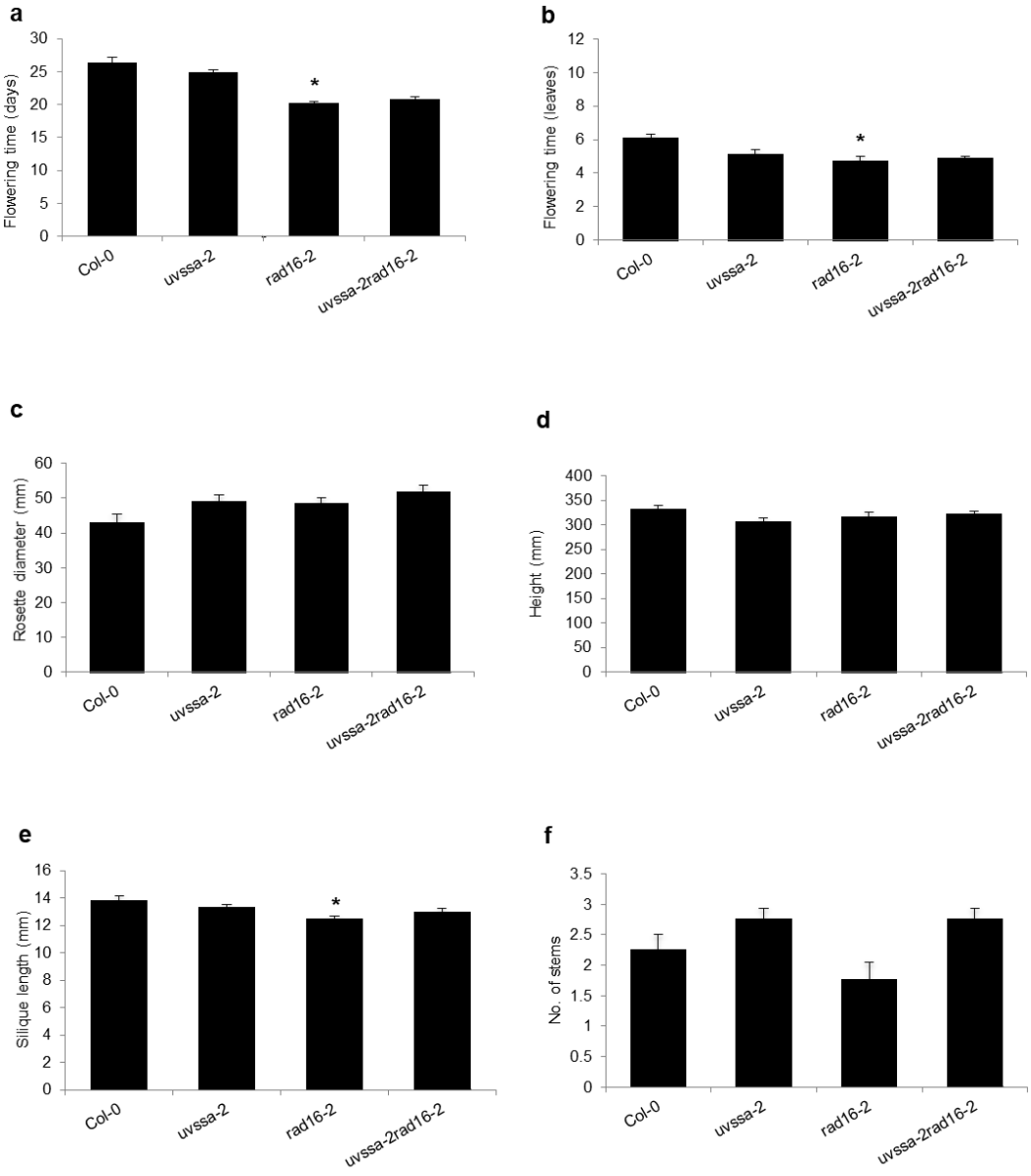

Figure S2.16 Adult developmental phenotypes of *Arabidopsis uvssa* and *rad16* single and double mutants

(**a**) Flowering time, average number of days and (**b**) average number of leaves. (**c**) Average rosette diameter (mm). (**d**) Average height (mm). (**e**) Average slique length. (f) Apical dominance (average number of stems). Values are means ± SE (n= 12), * = $p \leq 0.05$ of single mutant vs wild type, and double mutants vs *rad16-2*.

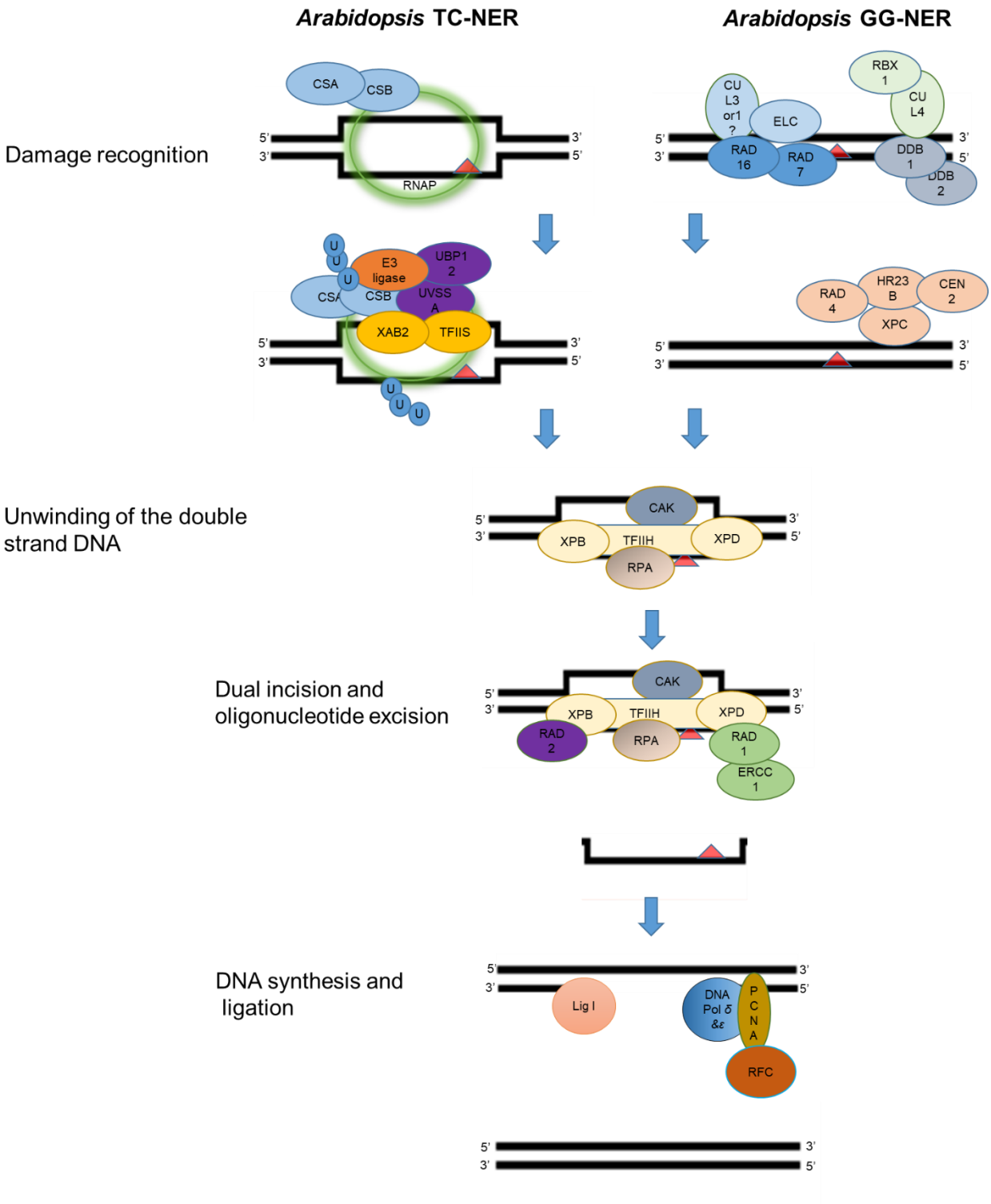

Figure S2.17 A schematic representation of the hypothesized NER pathway in *Arabidopsis thaliana*

See text for details.

Supplementary information 3

Contents:

Table S3.1 List of primers used in this study (sequence (5' to 3'))

Genotyping				
ELOA	ELA-2L	TTGGAATTGAGGGTTTGATTG	ELA-2R	TTACCTGCAACAAAATCGTCC
ELOC	ELC1-1F	CAGGTAAATGGTAGGCAGCTG	ELC1-1R	CGATTGAGCATAATCTCTGC
SALK	LBb1.3	ATTTTGCCGATTTCGGAAC		
SAIL	LB3	ATTTTGCCGATTTCGGAAC		
Semi-quantitative RT-PCR				
ELOA	ELA-c113F	TCCCCTCCTTCCTGGTTCAA	ELA-c863R	TTCAGTAAGATTTCGTCCACCA
EL0C	ELC-q7	AAAGCTTAAGCCGACGACGA	ELC-q4	CAGGGAAAGTCACTACGCCAT
ACTIN	ACT- F	CTGGAACAAGACTTCTGGGC	ACT- R	GGTGATGAAGCACAATCCAAG
qPCR				
ELOA	ELA-q1F	AGGATGCTACTGACGACACAG	ELA-q2R	TCATGTCCTCTTCTCCATAGTGC
ELOC	ELC-q1F	CATCGACAGAGAAGCCGCTA	ELC-q2R	ACGCCATCTTTCGATTCCGA
EF1*α*	EF1A-q3	CTGGAGGTTTTGAGGCTGGT	EF1A-q4	GGTGGTGGCATCCATCTTGT

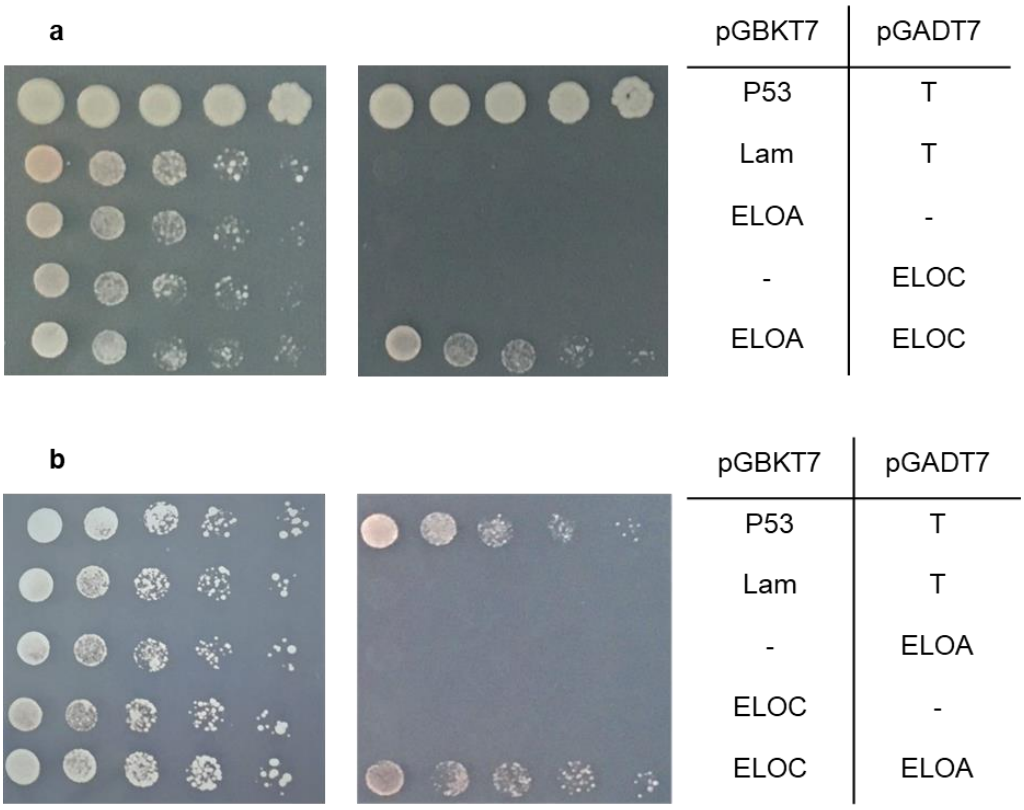

Figure S3.1 Yeast two-hybrid screening of *Arabidopsis* ELOA-ELOC interaction

(**a**) ELOA-pGBKT7 ELOC-pGADT7 interaction. (**b**) ELOC-pGBKT7 ELOA-pGADT7 interaction. Five fold dilutions of ELOA bait/ELOC prey (**a**) and ELOC bait/ELOA prey ELOC bait/ELOA prey (**b**) were spotted on control media (-leu -trp) (left) and on selective media (-leu –trp –ade -his) (right). P53 and Lam are the positive control as p53 bait interacts with T prey allowing the growth on selective media, whereas Lam bait and T prey are the negative control as Lam bait does not interact with T prey.

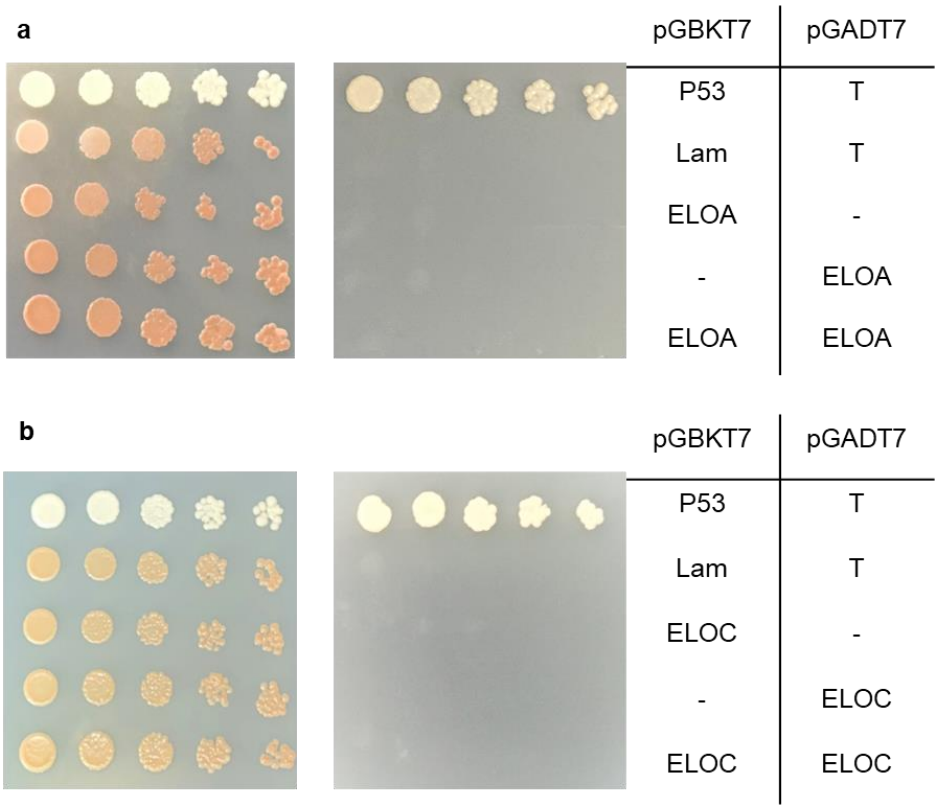

Figure S3.2 Yeast two-hybrid screening of *Arabidopsis* ELOA and ELOC self-interaction

(**a**) ELOA and (**b**) ELOC do not exhibit self-interaction. Five fold dilutions of ELOA bait/ELOA prey (**a**), ELOC bait/ELOC prey (**b**) were spotted on control media (-leu -trp) (left) and on selective media (-leu –trp –ade -his) (right). P53 and Lam are the positive control as p53 bait interacts with T prey allowing the growth on selective media, whereas Lam bait and T prey are the negative control as Lam bait does not interact with T prey.

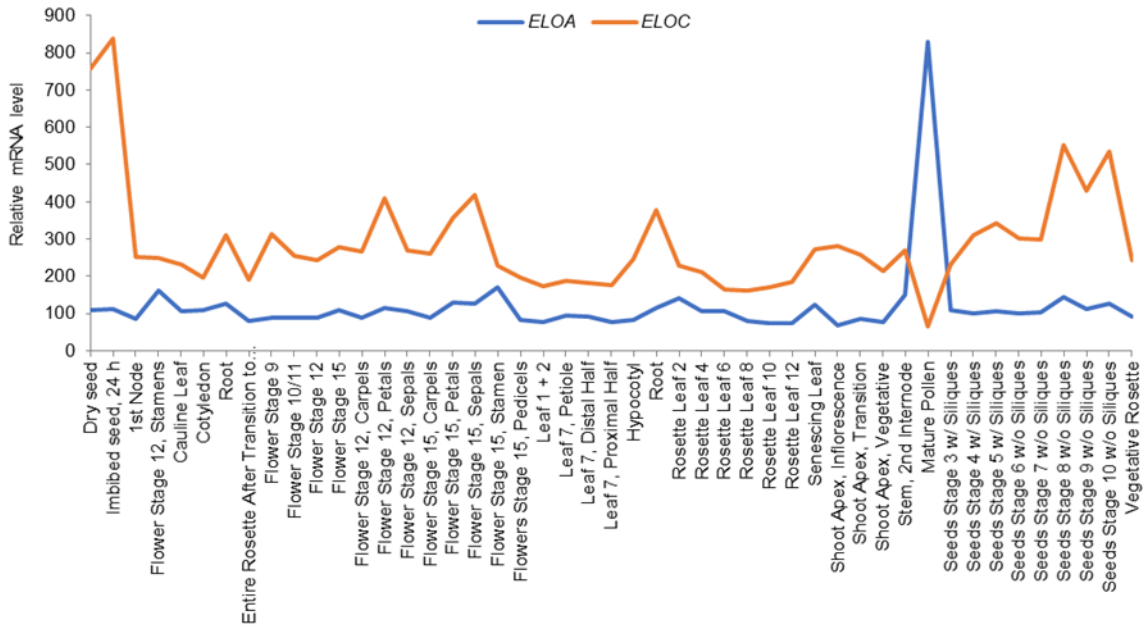

Figure S3.3 Developmental expression of *Arabidopsis ELOA* and *ELOC*

Data from Schmid et al. (2005) accessed via the *Arabidopsis* eFP browser (Winter et al., 2007).

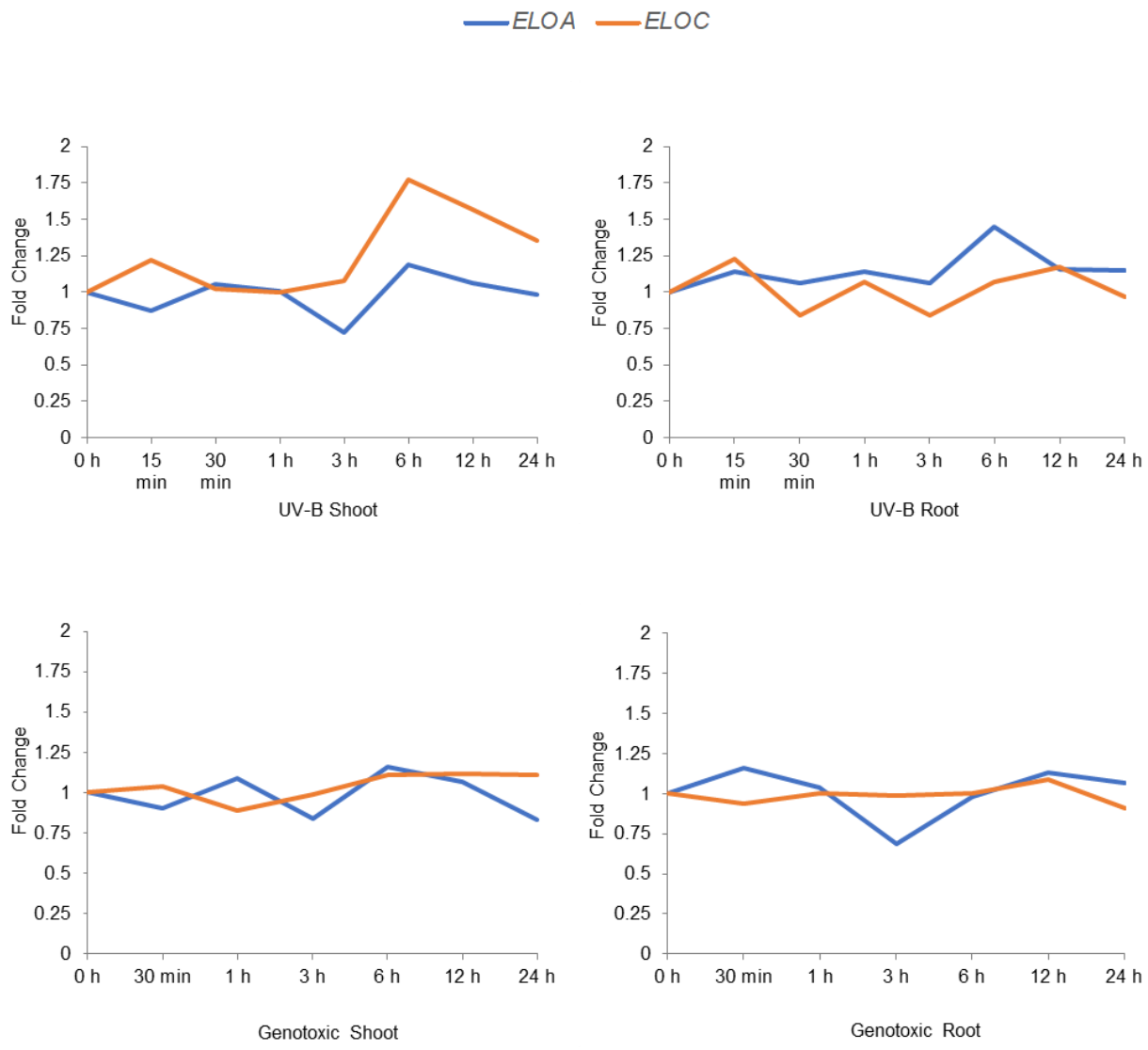

Figure S3.4 Expression of *Arabidopsis ELOA* and *ELOC* following potentially mutagenic stress

Relative expression of *ELOA* and *ELOC* following treatment with UV-B (upper panels) or genotoxic stress (bleomycin plus mitomycin C) (lower panels) in shoot (left panels) and root (right panels) tissues. Data from Kilian et al. (2007) accessed *Arabidopsis* eFP browser (Winter et al., 2007).

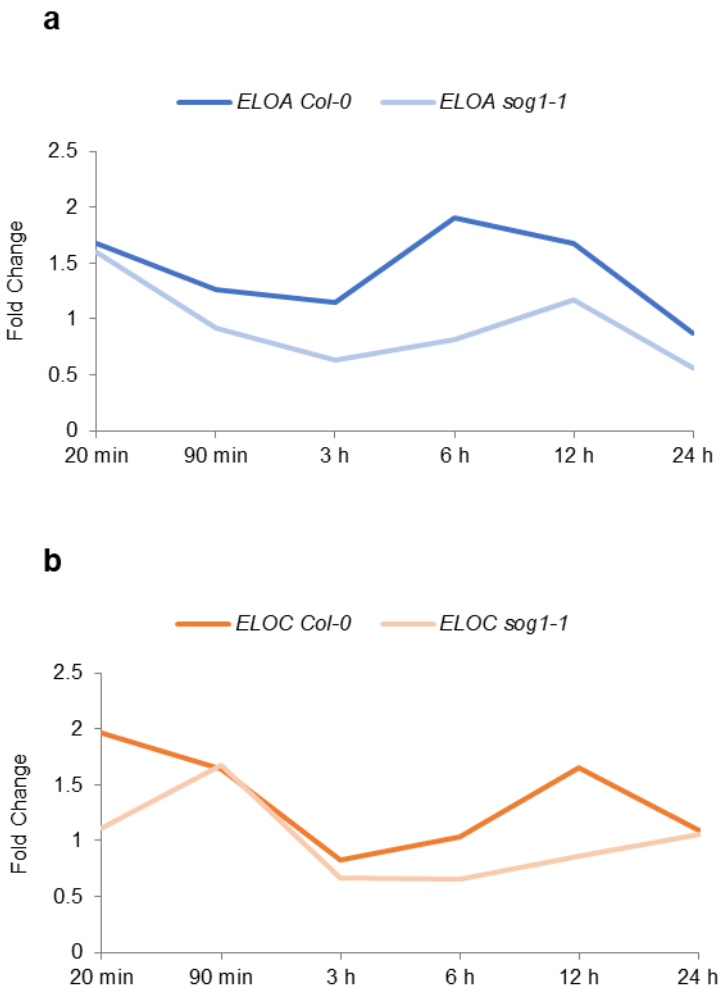

Figure S3.5 Expression of *Arabidopsis ELOA* and *ELOC* following treatment with gamma irradiation

Expression of *ELOA* (**a**) and *ELOC* (**b**) following treatment with gamma radiation relative to unstressed controls of the same genotype, either Col-0 wildtype or *suppressor of gamma 1 (sog1)* mutants. Data from Bourbousse et al. (2018) accessed *Arabidopsis* eFP browser (Winter et al., 2007).

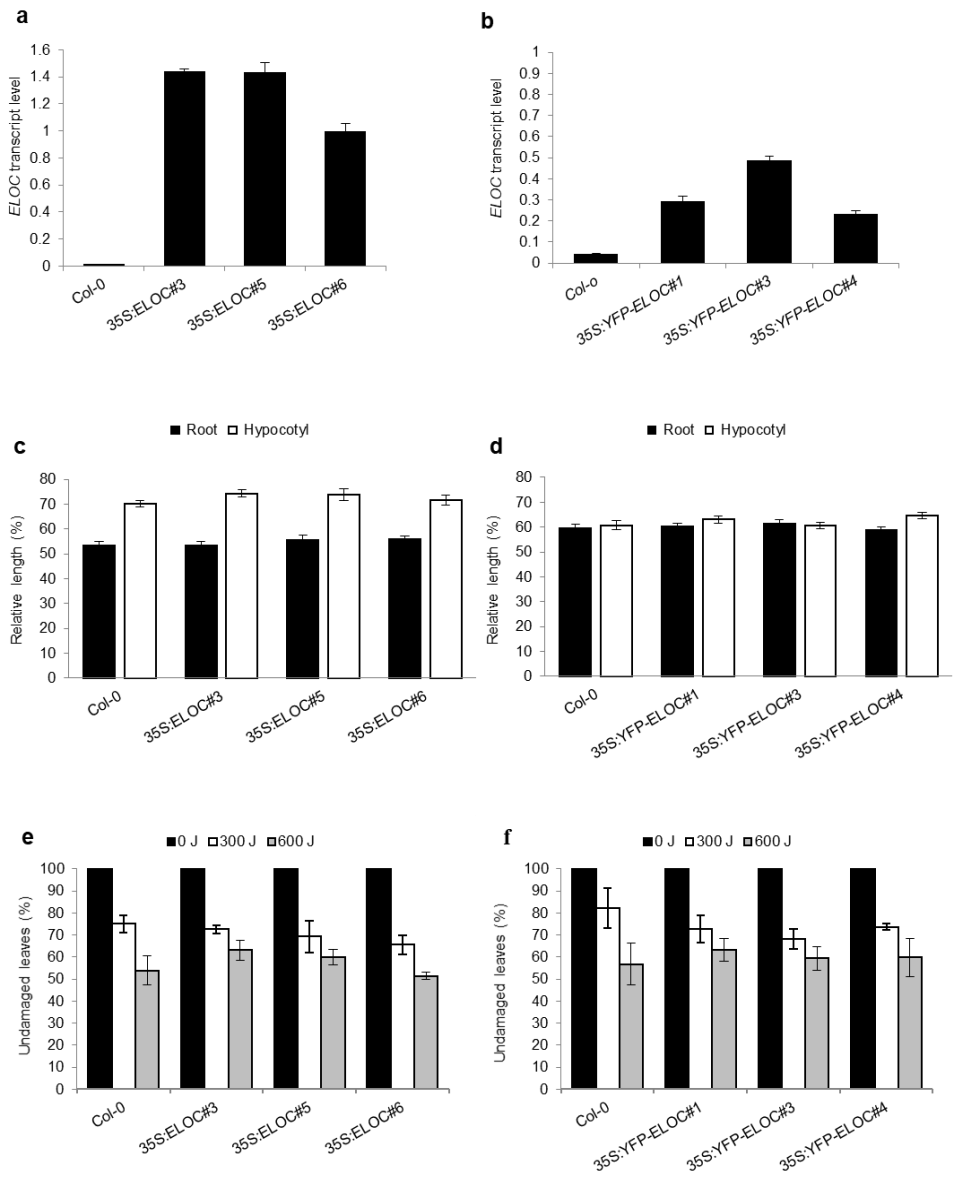

Figure S3.6 *Arabidopsis* ELOC overexpression does not result in enhanced UV tolerance

ELOC transcript level in Col-0 and (**a**) *35S: ELOC* and (**b**) *35S:YFP-ELOC*. *EF1α* gene used as a control to normalize the values. Error bars represent SE of the mean. Hypocotyl and root length in (**c**) Col-0, and *35S: ELOC* (**d**) Col-0 and *35S:YFP-ELOC* seedlings exposed to UV stress (1000 J m^{-2} UV-C) then incubated under dark conditions for72 hours, (n=40). Percentage of undamaged leaves in 3-week- old Col-0 and over expression lines; *35S: ELOC* (**e**) and *35S:YFP-ELOC* (**f**) exposed to UV stress (500 J m^{-2} UV-C), then incubated under dark conditions for 72 hours, (n=12). For (c) and (d), data are represented as relative to unstressed controls of the same genotype. For c-f, values are means ± SE, * = p≤ 0.05 of overexpression line vs wild type (Col-0).

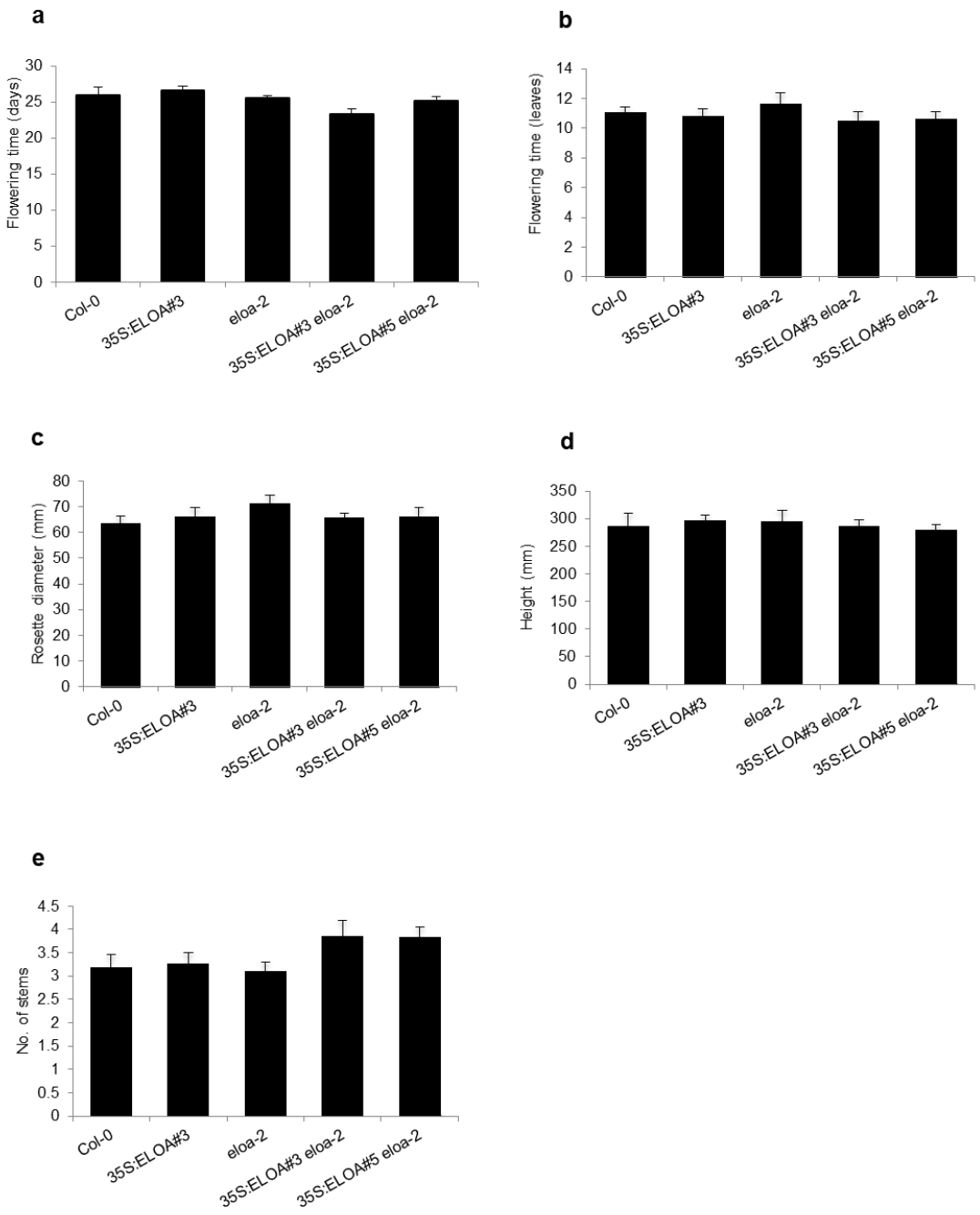

Figure S3.7 Developmental phenotypes of *Arabidopsis* 35S: ELOA overexpression lines

Flowering time (**a**) average number of days and (**b**) average number of leaves. (**c**) Average rosette width (mm). (**d**) Average height (mm). (**e**) Apical dominance (average number of stems).Values are means ± SE (n= 12), * = $p \leq 0.05$ of *elao-2* mutant and *35S: ELOA* vs wild type (Col-0) and *35S: ELOA eloa-2* vs *eloa-2* mutant.

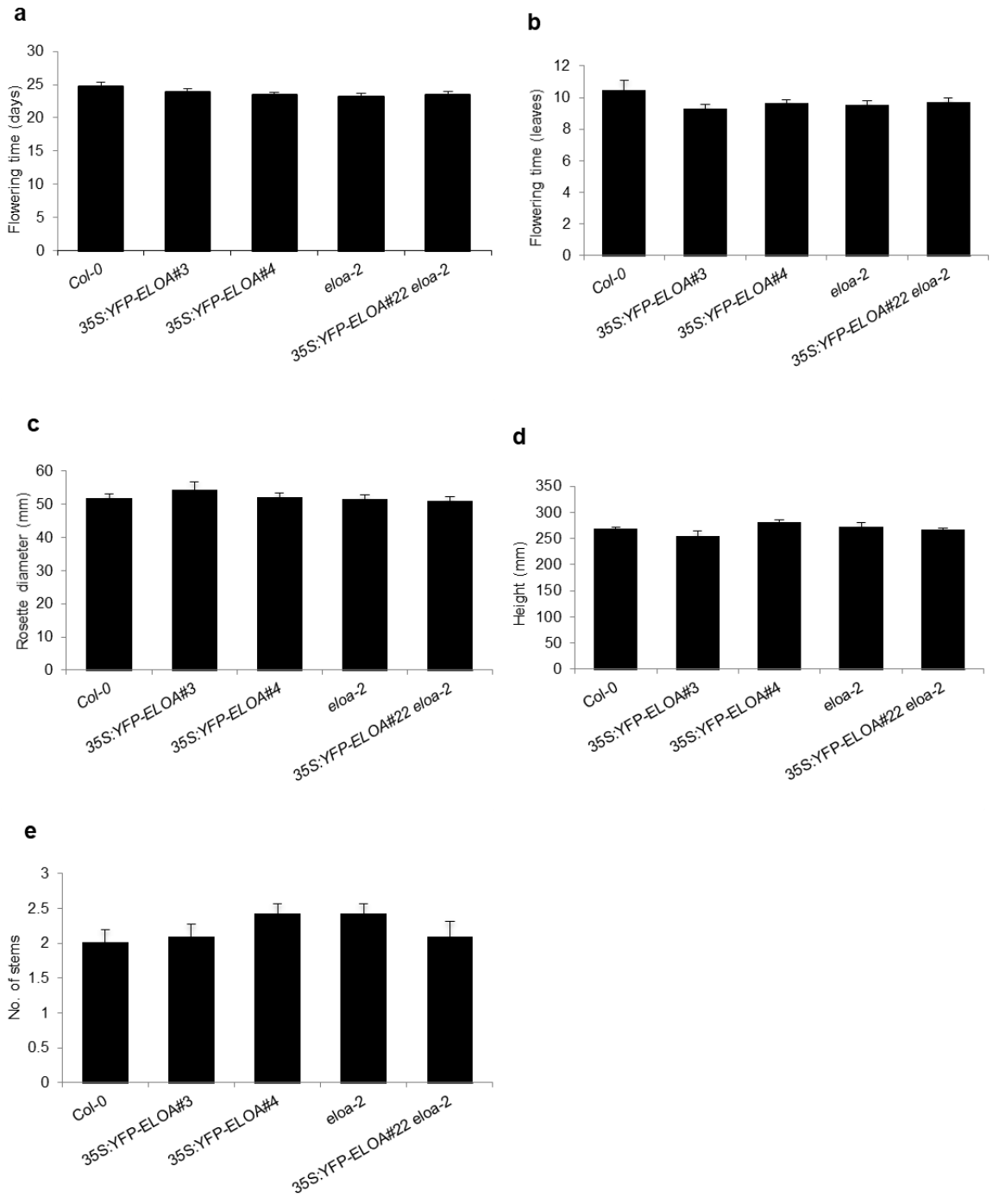

Figure S3.8 Developmental phenotypes of *Arabidopsis* 35S: YFP-ELOA overexpression lines

Flowering time (**a**) average number of days and (**b**) average number of leaves. (**c**) Average rosette width (mm). (**d**) Average height (mm). (**e**) Apical dominance (average number of stems).Values are means ± SE (n= 12), * = $p \leq 0.05$ of *elao-2* mutant and *35S: YFP-ELOA* vs wild type (Col-0) and *35S: ELOA eloa-2* vs *eloa-2*.

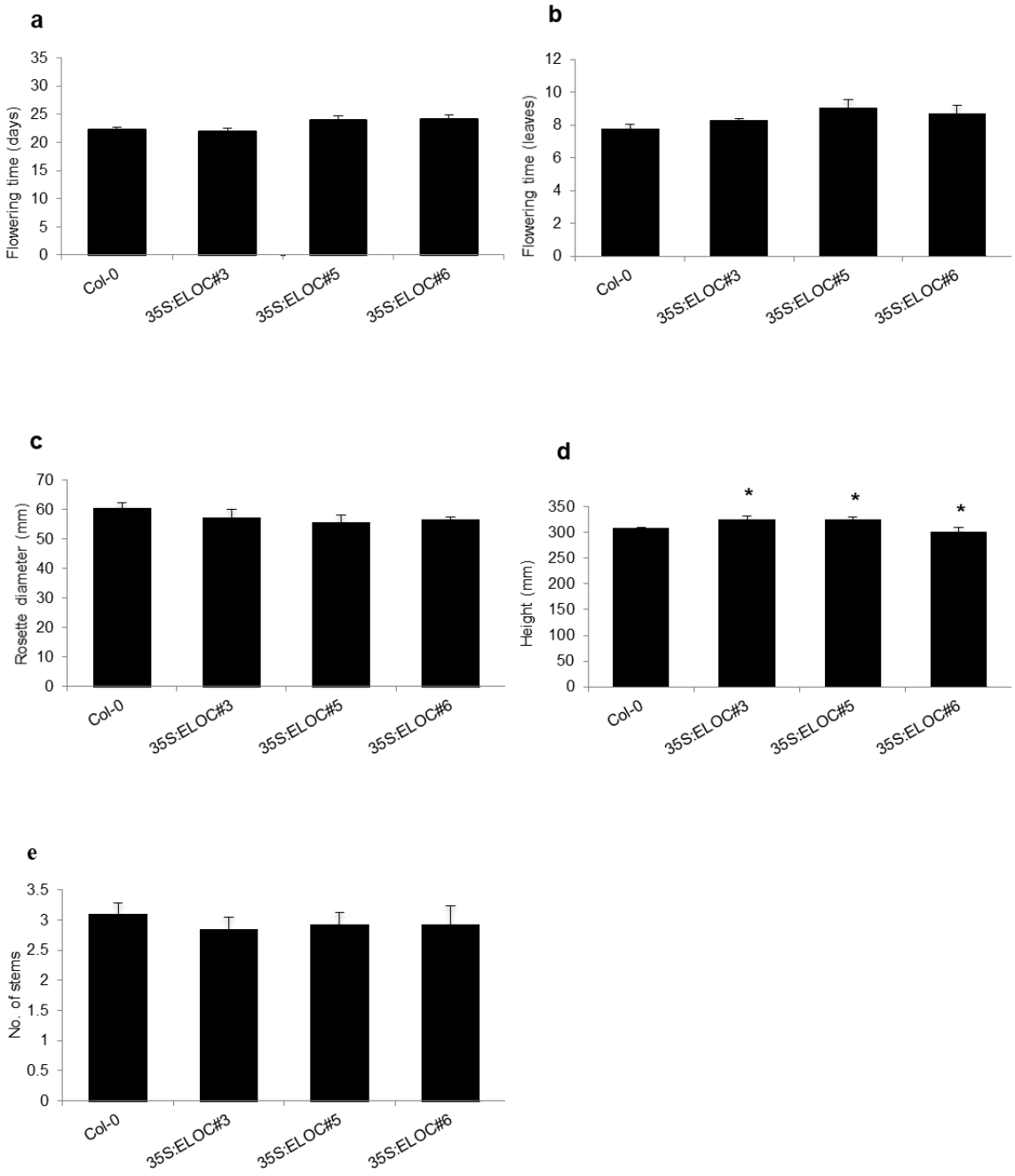

Figure S3.9 Developmental phenotypes of *Arabidopsis* 35S: ELOC overexpression lines

Flowering time (**a**) average number of days and (**b**) average number of leaves. (**c**) Average rosette width (mm). (**d**) Average height (mm). (**e**) Apical dominance (average number of stems).Values are means ± SE (n= 12), * = $p \leq 0.05$ of overexpression lines vs wild type.

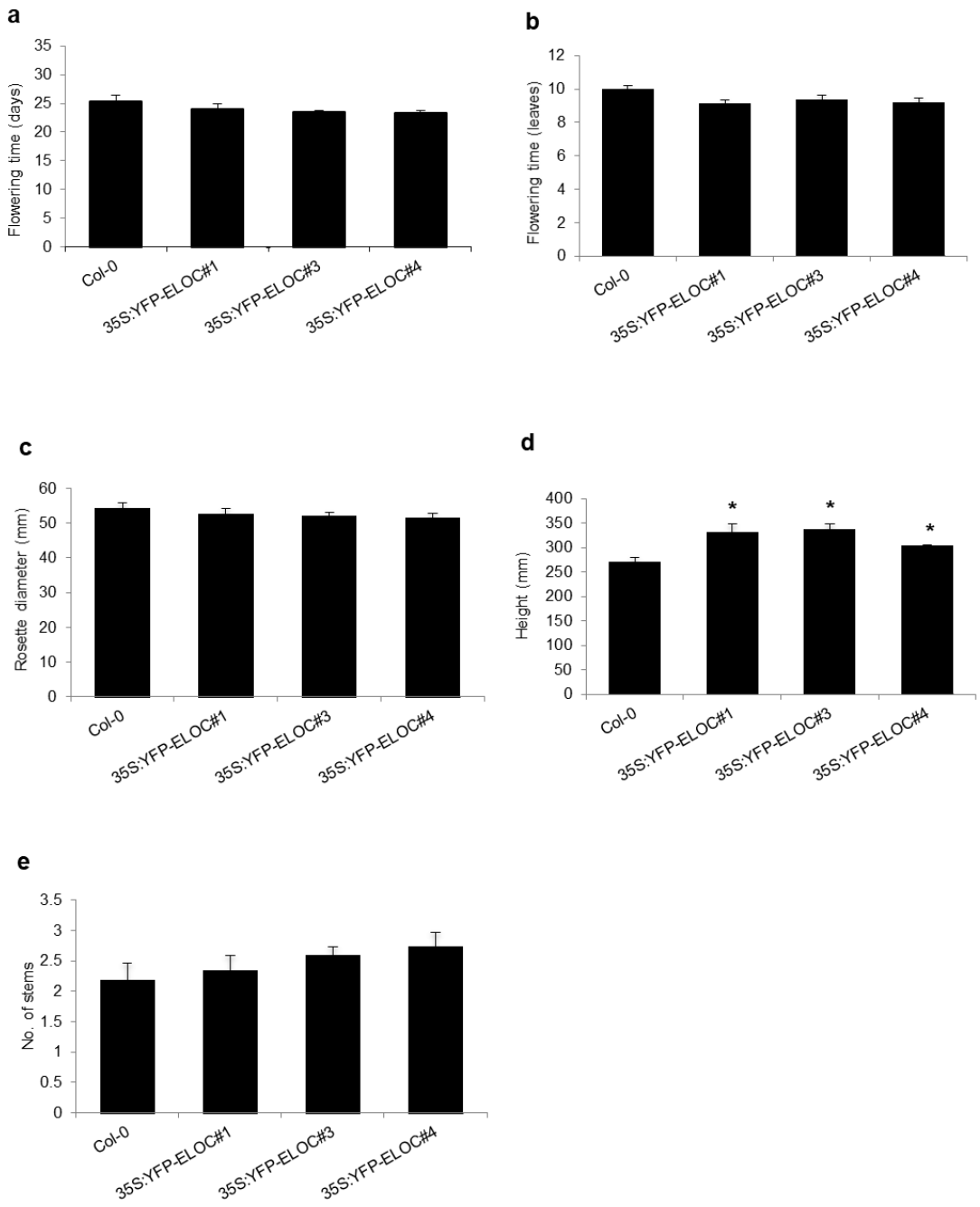

Figure S3.10 Developmental phenotypes of *Arabidopsis* 35S: YFP-ELOC overexpression lines

Flowering time (**a**) average number of days and (**b**) average number of leaves. (**c**) Average rosette width (mm). (**d**) Average height (mm). (**e**) Apical dominance (average number of stems).Values are means ± SE (n= 12), * = $p \leq 0.05$ of overexpression lines vs wild type.

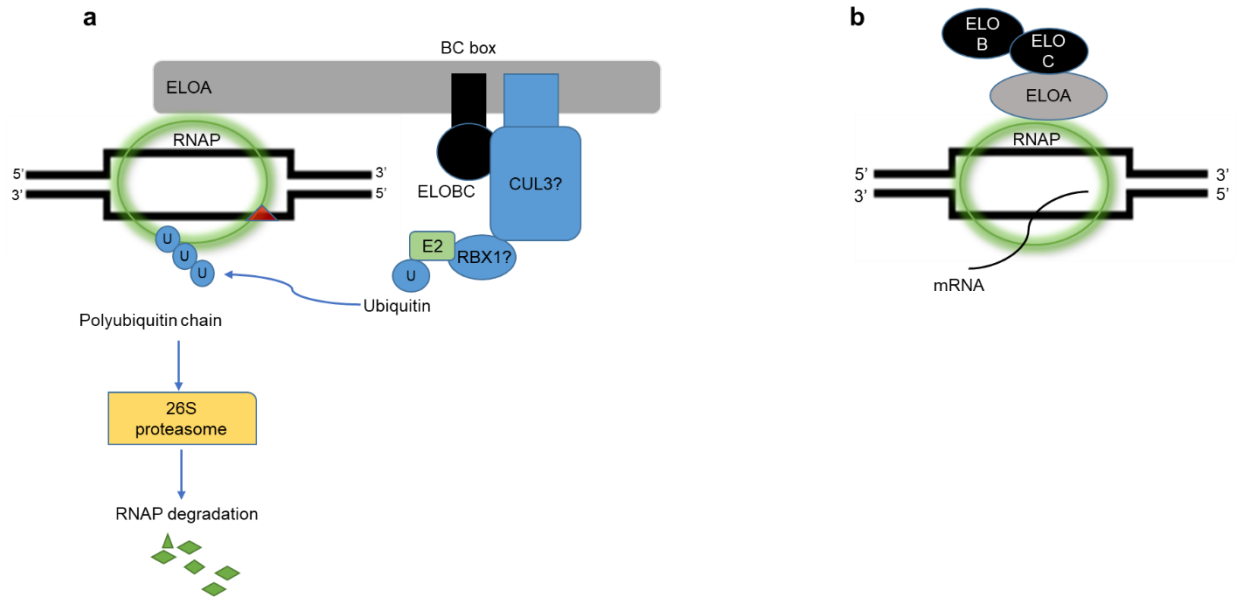

Figure S3.11 A schematic representation of the hypothesized roles of *Arabidopsis* Elongins in (a) ubiquitin ligase in response to UV induced DNA damage and (b) transcript elongation

See text for details.